THÈSE / UNIVERSITÉ DE BRETAGNE OCCIDENTALE

sous le sceau de l'Université européenne de Bretagne

pour obtenir le titre de

DOCTEUR DE L'UNIVERSITÉ DE BRETAGNE OCCIDENTALE

Mention : Océanographie Physique

École Doctorale des Sciences de la Mer

présentée par

Camille Lique

Préparée au sein de l'UMR 6523
CNRS - IFREMER - IRD - UBO
Laboratoire de Physique des Océans

Etude des échanges entre l'Océan Arctique et l'Atlantique Nord : Origine, variabilité et impact sur les mers Nordiques

Thèse soutenue le 8 octobre 2010

devant le jury composé de :

Sabrina SPEICH
Professeur des Universités, UBO, LPO, Brest / *Présidente du jury*

Marie-Nöelle HOUSSAIS
Chargée de Recherche CNRS, LOCEAN, Paris / *Rapporteur*

Cecilie MAURITZEN
Senior Scientist, Met.No, Oslo, Norvège / *Rapporteur*

Frédéric VIVIER
Chargé de Recherche CNRS, LOCEAN, Paris / *Examinateur*

Gilles GARRIC
Cadre de Recherche, Mercator-Océan, Toulouse / *Examinateur*

Anne-Marie TREGUIER
Directrice de Recherche CNRS, LPO, Brest / *Directrice de thèse*

THÈSE / UNIVERSITÉ DE BRETAGNE OCCIDENTALE

sous le sceau de l'Université européenne de Bretagne

pour obtenir le titre de

DOCTEUR DE L'UNIVERSITÉ DE BRETAGNE OCCIDENTALE

Mention : Océanographie Physique

École Doctorale des Sciences de la Mer

Etude des échanges entre l'Océan Arctique et l'Atlantique Nord : Origine, variabilité et impact sur les mers Nordiques

présentée par

Camille Lique

Préparée au sein de l'UMR 6523

CNRS - IFREMER - IRD - UBO

Laboratoire de Physique des Océans

Thèse soutenue le 8 octobre 2010

devant le jury composé de :

Sabrina SPEICH
Professeur des Universités, UBO, LPO, Brest / *Présidente du jury*

Marie-Nöelle HOUSSAIS
Chargée de Recherche CNRS, LOCEAN, Paris / *Rapporteur*

Cecilie MAURITZEN
Senior Scientist, Met.No, Oslo, Norvège / *Rapporteur*

Frédéric VIVIER
Chargé de Recherche CNRS, LOCEAN, Paris / *Examinateur*

Gilles GARRIC
Cadre de Recherche, Mercator-Océan, Toulouse / *Examinateur*

Anne-Marie TREGUIER
Directrice de Recherche CNRS, LPO, Brest / *Directrice de thèse*

Remerciements

Mon père aime à citer Pierre Dac disant que *« celui qui est parti de zéro pour n'arriver à rien n'a de merci à dire à personne »*. J'ai le sentiment aujourd'hui d'avoir tellement de personnes à remercier que c'est peut-être bon signe... Pourtant la tâche n'en est pas moins intimidante : il s'agit de laisser transparaître, le temps de quelques lignes, ce qu'a été cette aventure scientifique sur un plan humain, mais aussi d'en écrire la dernière page. Mais puisqu'il faut bien se lancer, allons-y.

Mes premiers remerciements vont bien évidement à Anne-Marie. Il y a un peu plus de trois ans maintenant, elle m'a accordé une confiance sans failles et sans conditions alors même que je n'avais encore rien fait pour la mériter. Cette confiance là m'a portée, les jours de doute, de remise en question, de découragement, de ras le bol, inhérent à chaque thèse, et m'a permis d'apprivoiser la liberté et l'indépendance que j'ai eu la chance d'avoir durant cette thèse. J'ai énormément appris en travaillant avec elle, et elle m'a transmis un peu de son savoir, mais surtout une façon d'appréhender les choses, un savant mélange entre enthousiasme et tempérance, entre certitudes et questionnements constants. Et puis elle m'a aussi sans cesse encouragée à aller taper à d'autres portes : c'est donc un peu sa faute si ces remerciements risquent d'être un peu long.

Je tiens à remercier toutes les personnes qui ont accepté de juger ce manuscrit : merci à Marie-Noelle Houssais pour ses critiques toujours constructives tout au long de cette thèse, à Cecilie Mauritzen (que j'espère rencontrer un jour !) d'avoir accepté de juger un manuscrit écrit en partie en français, à Sabrina Speich d'avoir endossé le rôle de présidente (ce fut une première pour nous deux !) et merci à Gilles Garric et Frédéric Vivier pour l'intérêt qu'ils ont porté à mon travail, et pour leur gentillesse durant la soutenance. Au passage merci également à Gilles pour son enthousiasme à me laisser jouer avec Glorys.

Au même chapitre mais en remontant un peu plus loin en arrière, je remercie également mon comité de thèse : Christophe Herbaut tout d'abord qui m'a accueillie à maintes reprises au LOCEAN à Paris, toujours avec beaucoup de gentillesse, et avec qui les interactions ont toujours été très constructives pour moi. J'espère que ces interactions continueront dans le futur. Et puis merci aussi à Thierry Penduff qui, de près ou de loin, a finalement souvent été présent, toujours avec beaucoup de bienveillance et un peu d'humour. A Thierry, il me faut aussi associer deux autres branches : la première est celle de Tallahassee. Il y a quelques années déjà, c'est là bas que Nicolas Wienders et Bill Dewar m'ont fait faire mes premiers pas dans le monde merveilleux de la recherche, et m'ont finalement transmis l'essentiel : ce travail, l'océanographie, la vie dans un labo, ça peut et ça doit rester amusant. La seconde branche est celle constituée par ceux du projet Drakkar. Je leur suis extrêmement redevable de m'avoir confié « mon océan » à étudier, et les résultats présentés dans ce manuscrit doivent beaucoup à la qualité des simulations qu'ils produisent. En particulier, merci à Bernard Barnier, qui m'a aidée à trouver ces stages en Floride, puis à Brest, et qui m'a toujours suivie de loin depuis ces

premiers pas. Un merci aussi à tous les Drakkarien, croisés à Grenoble ou ailleurs : Julien Le Sommer, et les plus jeunes, Raph', Mélanie, Jan, Carolina, Laurent, et tous les autres.

Revenant à Brest et à mon quotidien au laboratoire ces trois dernières années, je tiens à remercier tous les membres du LPO. Merci en particulier aux secrétaires (Jocelyne, Françoise, Florence) pour leur accueil toujours souriant, à tous ceux de l'équipe ANIME, et en particulier à Julie Deshayes pour le temps qu'elle a su me consacrer aussi souvent que j'en ai eu besoin, à Bruno Blanke et Nicolas Grima pour toute l'aide qu'ils m'ont apportée sur l'utilisation d'ARIANE, et à tout ceux que j'ai très souvent sollicité et qui ont dû répondre à mes « je ne comprend pas, je n'ai rien fait et ça a planté » : merci à Thierry (qui a le plus souffert), Cathy(s), Sylvie, puis Claude plus récemment. Pas très loin du LPO, merci à Fanny Ardhuin pour toutes les discussions que nous avons pu avoir. J'espère sincèrement que le travail commencé avec David n'est qu'un début, et que, d'une manière ou d'une autre, nous continuerons à travailler ensemble.

Un merci tout particulier à Pascale Lherminier, dont la porte m'a toujours été grande ouverte, pour tout l'enthousiasme qu'elle a montré pour mon travail. Et puis avec Pascale il me faut également remercier les Ovidiens de m'avoir emmenée avec eux pendant la campagne de 2008, Bruno Ferron et Herlé Mercier en tête. Ce fut vraiment une jolie expérience pour moi. Merci à mes camarades de quart, Olivier et Philippe, d'avoir inventé assez de bêtises à faire pour que je ne râle presque pas de devoir me lever à 4h du matin pendant un mois. Et puis, voir les glaces au Groenland, ça reste un moment magique ! Merci à tous pour ces moments si particulier.
Merci aussi à Virginie Thierry, non seulement d'avoir été un G.O. du tonnerre sur Ovide, mais aussi pour sa gentillesse et sa bonne humeur de tous les jours. Et puis, associée à Guillaume Maze lors de la préparation de ma soutenance, elle a été d'une aide plus que précieuse. Merci également à Guillaume pour son soutien ces derniers mois.
Au chapitre des Ovidiens ou presque, merci à Thierry Huck qui s'est révélé être à plusieurs reprises un parfait compagnon de voyage, de Vienne à Bruxelles en passant par ce retour de Portland, épique mais au combien rigolo !

Rigolo c'est aussi le qualificatif parfait pour décrire cette mission en septembre dernier dans le Golfe de Gascogne, sur laquelle Louis m'a emmenée pour que j'oublie qu'un jour il me faudrait soutenir. Merci à lui et à tous les autres pour ces moments ! Et un merci tout particulier à Emilie qui a eu à me supporter 24h sur 24 durant cette mission, mais aussi pour les innombrables pauses café que nous avons partagées ces dernières années, remplies de nos petites et grandes histoires mais surtout de rires et de bonne humeur. Et puis en même temps qu'Emilie, je remercie bien évidement tous mes camarades « petits » que j'ai pu rencontrer au cours de ces trois années, pour tous ces moments qui ponctuent notre quotidien au labo et qui se prolongent parfois en dehors. Une mention spéciale pour ceux avec qui j'ai partagé la dernière ligne droite : Xavier, Arnaud. Et Nicolas aussi qui finira bientôt ! Merci à lui pour les nombreux moments qu'on a passé ensemble cet été, pour toutes ses bonnes et moins bonnes idées, et j'espère que des moments de vie un peu

chouette il y en aura d'autre. Merci aussi à Karina pour le coaching quotidien et pour les moments partagés à l'Ifremer et en dehors, et notamment pour toutes les fois où elle m'a accueillie chez elle, dans sa petite famille qui respire le bonheur. Merci à ceux avec qui j'ai partagé mon bureau : Sébastien au début (qui a démissionné bien vite, mais n'y voyons pas de rapport de cause à effet), puis Claire que j'ai été triste de voir partir, puis Henrick qui m'a supportée pendant la période de rédaction. Merci aux anciens : Catherine pour m'avoir montré le chemin à suivre, Claire, pas partie très loin et revenue depuis, Nico, Jeff, Guillaume ; et à ceux qui sont toujours là : Eric, Flo (entre autre pour tout ses efforts à améliorer ma culture musicale), Damien, Tanguy, Dhouha, Simone, Emanuela, Rui et tous les autres qui sont passés par là... Bonne route à eux !

Je n'oublie pas non plus tout ceux qui font parti de ma vie en dehors, et qui aussi m'ont accompagné dans cette aventure sans toujours bien comprendre de quoi il pouvait en retourner. Une pensée pour ceux rencontrés à Brest, pour ceux qui sont venu m'y rendre visite, et ceux qui m'ont permis de m'en échapper régulièrement. Merci à ma famille, et particulièrement à mon père, ma grand mère, à mon frère et sa petite famille (Florence et maintenant Juliette) d'être venus jusqu'à Brest pour ma soutenance.

Mes derniers mots sont dédiés à la mémoire de ma mère. Elle a montré beaucoup d'enthousiasme à me voir partir faire une thèse à Brest, et m'a encouragé dans cette voie à son commencement. Elle est pour beaucoup dans la personne que je suis aujourd'hui. Elle m'a cruellement manqué le jour de ma soutenance, mais je crois que, l'espace de quelques instants, elle aurait été fière de moi. Et cette pensée là m'est chère.

Enfin merci à tous ceux qui tourneront les prochaines pages. Bonne lecture !

Table des matières

Introduction

« Il est évident que les conditions océanographiques dans le bassin polaire Arctique ont une influence sur le climat, et il est également évident que des changements des conditions de circulation dans ce bassin engendreront des changements pour le climat à l'échelle globale. » C'est avec ces affirmations que *Nansen* (1902) termine la discussion des résultats scientifiques obtenus lors de la mission *Fram* qui se déroula entre 1893 et 1896. Avec un siècle d'avance, Fridtjof Nansen expose ici les raisons majeures qui ont conduit ces dernières années au développement de l'océanographie Arctique. Pourtant, aujourd'hui encore, la communauté scientifique ne semble pas avoir tranché la question de savoir si l'océan Arctique est ou non un élément clé pour l'équilibre du climat, et si les changements que l'on y observe peuvent ou non engendrer des changements à l'échelle du globe.

Le rôle de l'océan Arctique dans l'équilibre du climat.

L'océan Arctique a un rôle dans le maintien de l'équilibre énergétique et thermique du globe. Si le bilan global entre l'énergie solaire reçue et celle ré-émise ou réfléchie est quasiment nul, cette situation d'équilibre ne prévaut cependant pas partout sur la Terre. Ainsi, la somme des flux émis est inférieure à celle des flux reçus aux basses latitudes et supérieure aux hautes latitudes. Ceci s'explique d'abord par le fait que le rayonnement solaire perd un maximum d'énergie pour atteindre les pôles parce que la traversée de l'atmosphère se fait toujours plus en biais, et est donc toujours plus longue au fur et à mesure qu'on se dirige vers les pôles. La quantité d'énergie reçue par unité de surface terrestre est donc moins importante dans les régions polaires que dans les régions équatoriales, et ce d'autant plus que le solde d'énergie se répartit sur une surface toujours plus grande à cause de la rotondité de notre planète et de son inclinaison. Mais ceci s'explique également par la présence de la neige et de la glace, qui vont accentuer la réflexion du flux solaire à proximité des pôles par la blancheur du manteau neigeux, qui renvoie vers l'espace la majeure partie de la lumière incidente (fort albédo).

Afin de rétablir un équilibre énergétique à l'échelle globale, un transport méridien de chaleur se met en place pour refroidir les basses latitudes et réchauffer les hautes la-

titudes. Ainsi, environ la moitié de l'excédent de chaleur reçu par les basses latitudes est transporté vers les pôles par l'atmosphère, et l'autre moitié par l'océan (*Trenberth and Caron*, 2001; *Wunsch*, 2005). Ces contributions relatives varient cependant fortement avec la latitude, comme le montre la figure 1, où sont représentés les transports méridiens de chaleur par l'océan et l'atmosphère en fonction de la latitude. La partie transportée par l'atmosphère est ensuite relâchée aux hautes latitudes, sous forme de rayonnement mais aussi par des phénomènes de condensation, permettant un transfert d'eau douce vers l'océan sous la forme de précipitations et d'apports fluviaux. La seconde partie est transportée par les courants océaniques, principalement de bord ouest : en Atlantique Nord, c'est le Gulf Stream, puis son extension vers le Nord, la dérive Nord Atlantique (North Atlantic Current, noté NAC). Ils transfèrent les eaux chaudes et salées de la Gyre Subtropicale vers la Gyre Subpolaire puis vers les hautes latitudes.

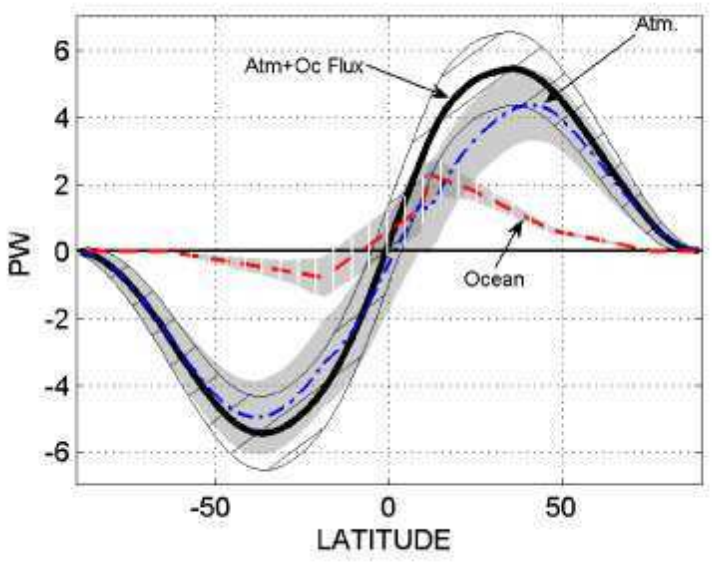

FIG. *1: Adaptée de Wunsch (2005) : Estimation du transport de chaleur méridien (positif vers le nord) par l'océan (rouge) et par l'atmosphère (bleu). Le transport total est aussi indiqué (en noir) ainsi que les barres d'erreur associées à chaque quantité (en gris).*

Cette circulation océanique constitue la branche haute de la cellule méridienne de retournement (MOC pour Meridional Overturning Circulation), pour laquelle l'océan Arctique est une source d'eau douce et un puits de chaleur. La figure 2 synthétise le rôle du bassin Arctique pour la MOC. Une fois transportée aux hautes latitudes, la chaleur est alors transférée vers l'atmosphère, ce qui provoque une densification des eaux de surface qui vont alors plonger, puis s'écouler vers le sud en profondeur avec le courant profond de bord ouest (Deep Western Boundary Current, noté DWBC). Parallèlement à cela, l'océan

Arctique reçoit une quantité importante d'eau douce provenant des précipitations, des rivières et de l'eau Pacifique qui pénètre par le détroit de Bering. Ces apports d'eau douce sont ensuite emportés en surface vers le sud, et vers les zones de convection profonde (mer du Labrador, mers Nordiques et mer d'Irminger).

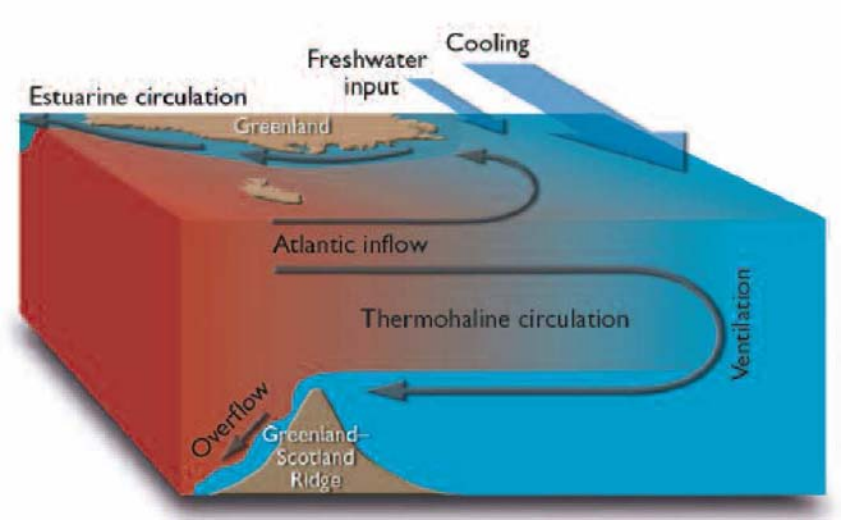

Fig. *2: D'après le rapport de l'ACIA (2005) : Synthèse des systèmes de circulation dans l'océan Arctique.*

Nous avons donc vu ici que le bassin polaire Arctique semble être un élément important pour l'équilibre du climat. Mais on peut également se demander dans quelle mesure des modifications de circulation ou des bilans d'eau douce ou de chaleur dans ce bassin peuvent avoir des répercutions à l'échelle globale.

Des changements attendus et observés en Arctique

Les modèles numériques du type de ceux utilisés pour les scénarios climatiques de l'IPCC (Intergovernmental Panel on Climate Change) prévoient que les régions polaires se réchauffent plus que le reste du globe durant le siècle à venir en réponse à l'augmentation des émissions de gaz à effet de serre dans l'atmosphère. Cette « amplification polaire » du changement climatique est principalement due à la présence de glace aux niveaux des pôles : alors que l'extension de la banquise diminue, l'albédo de la surface varie très fortement (rappelons que la glace de mer a un albédo très supérieur à celui de l'océan) et l'océan emmagasine plus de chaleur, créant ainsi une rétroaction positive qui va accélérer la fonte de la banquise (*Manabe and Stouffer*, 1980; *Holland and Bitz*, 2003). Ainsi, les variations de la température de surface, observées au cours du siècle dernier (Figure 3

(a) d'après *Delworth and Knutson* (2000)) et prédites par les modèles climatiques pour le siècle à venir (Figure 3 (b) d'après le rapport de l'*IPCC* (2007)), ont une amplitude plus importante au niveau des pôles, et l'*IPCC* (2007) prévoit ainsi un réchauffement de la température de surface (SST pour Sea Surface Temperature) en océan Arctique deux à trois fois supérieur à celui prédit pour les zones équatoriales.

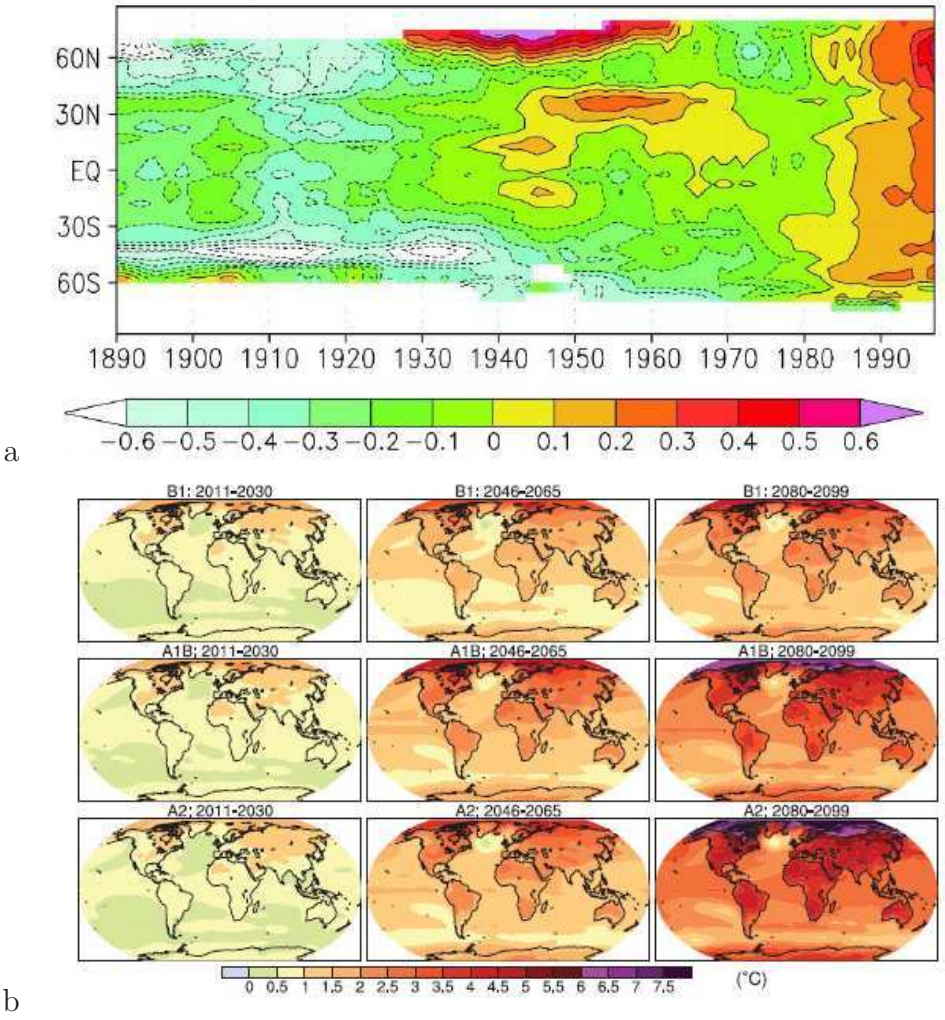

FIG. *3: a) D'après Delworth and Knutson (2000). Moyenne zonale de l'anomalie de la température de surface observée (en K, relatives à la période 1961–1990). b) D'après le rapport de l'IPCC (2007). Moyenne annuelle de l'anomalie de la température de surface (en °C) pour différents scénarios climatiques et pour différentes périodes. Les anomalies sont relatives à la période 1980–1999. Les moyennes des résultats tous les modèles climatiques de l'IPCC (2007) sont représentées.*

Ce réchauffement prévu de l'océan Arctique semble déjà être clairement visible au cours des dernières décennies (e.g., *Polyakov et al.* (2007)). Ainsi, de nombreux auteurs ont observé un réchauffement important affectant les différentes composantes du système Arctique : l'atmosphère (*Rigor et al.*, 2000), les masses d'eau d'origine Atlantique présentes

en Arctique (*Polyakov et al.*, 2005), les eaux Pacifique entrant en Arctique (*Woodgate et al.*, 2006), ou encore les couches supérieures de l'Arctique (*Steele et al.*, 2008).

Mais les modifications observées en Arctique ne se limitent pas à un réchauffement. Le changement le plus visible (et le plus commenté et décrit dans la littérature) reste sans aucun doute la fonte de la banquise. *Cavalieri et al.* (2003) montrent que sur la période où les observations satellitales de l'extension de la glace de mer sont disponibles (depuis 1972), la tendance de diminution n'a cessé de s'accélérer, et un nouveau minimum de l'extension de la banquise a été atteint à la fin de l'été 2007, une surface de 1.5 millions de km^2 ayant été perdue entre 2006 et 2007 à la même période (*Comiso et al.*, 2008). Dans le même temps, *Rothrock et al.* (1999) montrent que l'épaisseur de glace a diminué de plus de 40% entre la période 1958–1976 et les années 90 et la diminution n'a elle aussi cessé de s'accélérer pendant les années 2000 (*Kwok et al.*, 2009). Le déclin de l'extension de glace semble même être plus rapide que ce que prévoient les scénario les plus pessimistes présentés dans le rapport de l'*IPCC* (2007), comme le montre la figure 4 reprise de *Stroeve et al.* (2007) où l'évolution de l'extension observée en septembre de la glace de mer en Arctique est comparée à celle prédite par les différents modèles climatiques. Si l'extension de la banquise semble être remontée à un niveau plus « normal » les étés suivant l'été 2007, il semble que les caractéristiques de la banquise aient été bouleversées par la fonte importante depuis les années 2000, les glaces pérennes ayant pour la plupart été remplacées par des glaces plus jeunes, moins épaisses, et avec des propriétés physiques différentes (salinité, albédo...) (e.g., *Kwok et al.* (2009)).

Ces modifications de la glace de mer ne sont qu'un aspect d'un bilan d'eau douce changeant pour l'océan Arctique, affecté notamment par une intensification importante du cycle hydrologique, avec une augmentation des apports fluviaux, des précipitations et de la fonte de la calotte glacière groenlandaise (voir par exemple *Peterson et al.* (2006)). Des transformations des propriétés hydrologiques de l'Arctique ont également été mises en évidence. Par exemple, *Steele and Boyd* (1998) ont observé une récente diminution de la stratification d'une large partie des couches océaniques de surface en Arctique, alors que *Swift et al.* (2005) notent une importante salinisation des couches de surface après 1976.

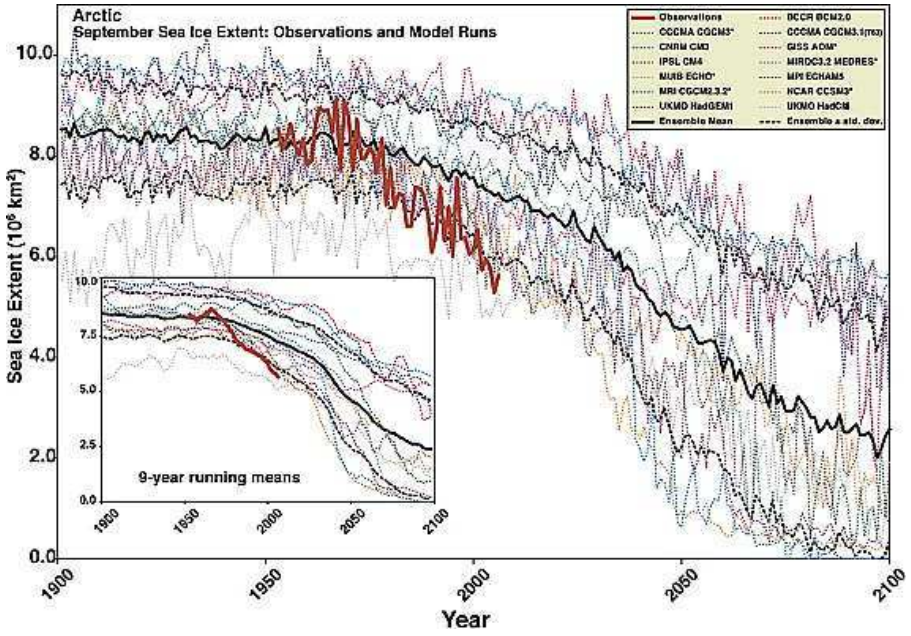

FIG. *4: D'après Stroeve et al. (2007) : Extension de la glace de mer dans l'océan Arctique en septembre (en 10^6 km^2) pour les observations (trait rouge épais) et pour les 13 modèles climatiques de l'IPCC (2007). La moyenne de tous les modèles est donnée en trait noir, ainsi que la déviation standard (traits pointillés).*

L'énumération faite ici des changements observés dans le bassin polaire Arctique est loin d'être exhaustive. Elle a pour but principal de montrer que le système Arctique dans son ensemble semble être en train de se modifier rapidement. Ce constat a conduit à l'émergence de l'idée que l'Arctique aurait peut-être dépassé un point de non retour (« tipping point », e.g., *Lindsay and Zhang* (2005); *Serreze and Francis* (2006)). Mais la question essentielle à laquelle il faut aujourd'hui encore répondre reste cependant : les évolutions observées de l'océan Arctique doivent-elles être considérées comme un indicateur passif ou comme des acteurs efficaces de la variabilité climatique globale ? En d'autre termes, l'océan Arctique subit-il simplement les changements de l'atmosphère aux hautes latitudes, et celles des autres océans qui l'entourent, ou bien est ce que les modifications observées en Arctique sont à l'origine de modifications climatiques à l'échelle du globe ? Mais la réponse ne pourra sans doute pas être si tranchée. Le réchauffement de tout le système arctique évoqué précédemment est un exemple de la complexité du problème. *Polyakov et al.* (2005) et *Schauer et al.* (2008) observent un réchauffement récent des eaux atlantiques qui pénètrent en Arctique, où elles provoquent une élévation des températures. Une autre partie de ce réchauffement est directement imputable au réchauffement de l'atmosphère. Mais à mesure que la température de surface augmente, la glace de mer fond et la quantité d'énergie solaire renvoyée dans l'espace par réflexion diminue, provoquant ainsi un réchauffement plus intense de la surface. Ce sont ces rétroactions entre l'océan, la glace de mer et l'atmosphère qu'il nous reste encore aujourd'hui à comprendre.

Et si la variabilité océanique dans la zone subpolaire induit des changements en Arctique, on s'attend également à ce que le signal d'un changement en Arctique ait son impact climatique le plus important lorsqu'il est exporté vers le sud dans les mers subarctiques, où il va notamment influer sur la circulation thermohaline en Atlantique (*Dickson et al.*, 2008).

Objet de la thèse et plan du manuscrit

C'est l'étude de ces échanges océaniques de masse, d'eau douce et de chaleur, et ces échanges de glace entre l'océan Arctique et les mers subpolaires qui fait l'objet de cette thèse, puisque c'est principalement par ces échanges que les transformations du système Arctique sont susceptibles d'avoir une influence sur le climat global. Plus précisément, on s'attache à documenter et comprendre comment la dynamique moyenne du bassin Arctique, sa variabilité ainsi que celles des propriétés des masses d'eau et de la calotte de glace de mer vont influencer ces échanges. Pour ce faire, nous utilisons différents outils numériques. Principalement, plusieurs simulations de résolution et complexité différentes sont analysées : elles ont pour avantage de proposer un cadre thermodynamiquement cohérent, alors que les observations dans le bassin Arctique et celles des échanges Arctique – Atlantique restent rares et éparses dans le temps et dans l'espace et ne permettent pas à l'heure actuelle d'avoir une vision du système Arctique dans son ensemble.

Ce manuscrit est organisé en cinq parties : un état de l'art des connaissances actuelles sur les échanges Arctique – Atlantique (chapitre 1) précède l'exposé des trois grands chantiers qui ont fait l'objet de ce travail de thèse. Les chapitres 2 à 5 sont basés principalement sur des publications (celle du chapitre 5 est encore en préparation), ce qui implique quelques récurrences entre certains chapitres.

Pour commencer, nous nous intéressons au bilan d'eau douce de l'océan Arctique et aux exports d'eau douce vers la zone subpolaire (chapitres 2 et 3). En analysant une simulation globale couplée glace de mer/océan des 50 dernières années, nous examinons la variabilité du bilan d'eau douce en Arctique, afin de comprendre quelle composante de ce bilan est responsable des variations du contenu halin du bassin Arctique, mais également de déterminer comment est forcée la variabilité des exports d'eau douce vers l'Atlantique Nord (chapitre 2). Dans le chapitre 3, nous nous concentrons sur un autre aspect du bilan d'eau douce de l'océan Arctique et de ses variations et modifications : une réanalyse océanique des années récentes (GLORYS) nous permet d'explorer les conséquences pour le contenu halin de l'Arctique de l'accélération de la fonte de la banquise et plus particulièrement l'impact du minimum d'extension de glace sans précédent qui a eu lieu à la

fin de l'été 2007.

Le chapitre 4 est dédié à une analyse lagrangienne qualitative de la circulation moyenne en Arctique et des transformations des masses d'eau associées. Le but initial de cette étude est de mieux comprendre et quantifier l'origine des eaux exportées de l'Arctique vers l'Atlantique, mais la méthode numérique originale utilisée ici nous permet de proposer un schéma complet de la circulation dans le bassin Arctique.

Dans le chapitre 5, on s'intéresse à l'influence des différents forçages atmosphériques (vent, flux de chaleur et halins) dans le bassin Arctique. Nous avons choisi de focaliser cette étude sur les mécanismes de variabilité du volume de glace contenu dans l'hémisphère nord. Dans ce but, des expériences de sensibilité sont réalisées à l'aide d'un modèle régional de l'Arctique et l'Atlantique Nord, permettant de mieux comprendre et quantifier les distributions spatiales et temporelles des contributions des différents forçages atmosphériques.

Chapitre 1

Etat de l'art

De nos jours, l'océan Arctique et plus particulièrement les échanges océaniques entre l'Arctique et la zone subpolaire sont l'objet de toutes les attentions. D'abord parce que leur rôle fondamental dans la « machine climatique » globale ne semble aujourd'hui plus faire de doute. Mais également car d'importants enjeux économiques et géopolitiques se jouent en Arctique, notamment entre les différents pays frontaliers (États-Unis, Canada, Norvège, Danemark et Russie) qui revendiquent tour à tour la souveraineté sur le fond de l'océan Arctique et sur le Pôle Nord géographique. La compréhension du système Arctique dans son ensemble est donc devenu cruciale, et un effort international semble être fait dans cette direction. Les années 2007–2008 ont été déclarées « Année Polaire Internationale », et de nombreuses campagnes de mesures ont été menées en Arctique à cette occasion, renforçant encore un peu plus les différentes actions visant à intensifier les observations dans le bassin polaire Arctique. Afin d'améliorer notre compréhension de ce bassin, un effort de la communauté scientifique est également en cours pour améliorer les modèles numériques dans les régions polaires. Ce travail de thèse a été réalisé au moment de l'Année Polaire Internationale, et s'est donc appuyé, en partie tout au moins, sur une bibliographie récente qui n'a cessé de s'étoffer durant ces trois années. Avant d'entrer dans le détail des travaux effectués durant cette thèse, nous présentons brièvement dans une première partie l'état de nos connaissances quant aux échanges océaniques entre l'océan Arctique et les mers subpolaires.

1.1 Échanges océaniques entre l'Arctique et l'Atlantique Nord.

FIG. *1.1: Schéma de la circulation en Arctique et des échanges avec l'Atlantique Nord. Source : Woods Hole Oceanographic Institution, http ://www.whoi.edu/page.do ?pid=12317.*

La figure 3.2 décrit schématiquement le fonctionnement du système Arctique et les principaux courants qui constituent les échanges de masses d'eau entre l'océan Arctique et les mers subpolaires.

Les eaux d'origine pacifique, froides et relativement peu salées, pénètrent dans les couches de surface en Arctique par le détroit de Bering. Elles sont majoritairement entraînées dans la gyre de Beaufort, qui occupe le bassin canadien, puis sont exportées vers l'Atlantique Nord : une partie passe à l'Ouest du Groenland à travers l'Archipel Canadien Arctique (Canadian Arctic Archipelago, noté CAA) pour rejoindre ensuite la baie de Baffin puis la mer du Labrador, tandis qu'une partie moins importante passe à l'Est du Groenland, à travers le détroit de Fram puis le long de la côte avec le Courant Est Groenland (East Greenland Current, noté EGC). Une petite partie des eaux pacifiques est entraînée par un courant côtier sur le plateau qui longe l'Alaska puis les nord du CAA, puis est exportée vers l'Atlantique Nord à travers les détroits de Davis et de Fram. Dans le même temps, le NAC amène des eaux chaudes et denses qui pénètrent en Arctique à travers la partie Est du détroit de Fram et la mer de Barents. La partie des eaux entrant par le

détroit de Fram avec le Courant Ouest Spitsberg (West Spitsbergen Current, noté WSC) reste sous une couche de surface plus froide (la halocline) qui agit comme une barrière empêchant les contacts avec la glace de mer mais aussi avec l'atmosphère. L'autre partie des eaux passe par la mer de Barents où, au contact avec l'atmosphère froide, elle perd de la chaleur. Ces deux branches d'eau atlantique se rejoignent ensuite au niveau de la Fosse de Saint-Anna, où elles vont se mélanger pour former une masse d'eau plus homogène. Après avoir circulé dans le bassin Arctique, elles ressortent soit à l'Ouest du Groenland, par le CAA puis le détroit de Davis, soit à l'Est par le détroit de Fram, emportées par l'EGC en surface mais aussi par le DWBC plus en profondeur.

Les échanges Arctique/Atlantique peuvent donc se résumer de la façon suivante :
- Le NAC apporte une quantité importante de chaleur en Arctique, à travers le détroit de Fram et la mer de Barents.
- De l'eau douce, sous forme liquide et de glace de mer, est exportée vers les mers subpolaires des deux côtés du Groenland. A l'Est, l'EGC longe la côte jusqu'au sud du Groenland pour rejoindre la gyre subpolaire. Des décrochements de ce courant alimentent également en eau douce les mers nordiques. Du côté Ouest, les exports se fond à travers le CAA pour rejoindre la baie de Baffin, puis à travers le détroit de Davis pour pénétrer en mer du Labrador.

Bien que l'on soit conscient de l'importance de quantifier à la fois la valeur moyenne mais surtout la variabilité de ces échanges, il n'existe encore aujourd'hui que peu de mesures directes publiées, et pas d'estimation de la variabilité sur une longue période (voir la section 5 de *Lique et al.* (2009) et la section 3 de *Lique et al.* (2010) pour un résumé des mesures publiées). Les simulations numériques semblent donc être actuellement la seule solution pour mieux connaitre et comprendre la variabilité de ces échanges. Cependant, modéliser ces échanges est loin d'être trivial, comme nous allons l'expliquer dans la section suivante.

1.2 Modélisation des échanges entre l'Arctique et l'Atlantique Nord.

Le seul moyen pour évaluer et étudier les tendances et la variabilité naturelle des échanges entre l'Arctique et l'Atlantique Nord reste encore aujourd'hui les modèles numériques. Récemment, *Gerdes et al.* (2008) ont tenté de synthétiser les déficiences communes aux modèles réalistes de l'Arctique, afin de déterminer l'impact de ces déficiences sur la représentation des exports d'eau douce de l'océan Arctique vers l'Atlantique Nord. Ils mettent ainsi en avant trois problèmes majeurs qui expliquent que relativement peu

d'études de modélisation s'intéressant à la variabilité de ces échanges existent dans la littérature.

Tout d'abord, le manque d'observations directes rend difficile la validation des simulations numériques. Les valeurs présentées dans la littérature divergent grandement : on trouve par exemple des estimations des flux de masse et d'eau douce à travers le détroit de Fram variant du simple au triple suivant les études (voir *Lique et al.* (2009)). La situation semble cependant s'être améliorée ces dernières années. *Dickson et al.* (2007) ont présenté un résumé des mesures publiées dans la littérature concernant les flux d'eau douce en l'Arctique et dans la région subarctique, déterminant également la « meilleure » estimation disponible pour chaque flux. Dans le cadre du projet *ASOF (Arctic-Subarctic Ocean Fluxes)*, un effort particulier a été fait pour mesurer avec précision ces échanges Arctique/Atlantique, mais également pour maintenir les systèmes d'observation sur de longues périodes de temps (plusieurs années). Cela devrait donc permettre dans les années à venir de disposer de séries temporelles de mesures auxquelles nous pourrons confronter les solutions données par les modèles numériques.

Dans leur étude, *Dickson et al.* (2007) soulignent également la diversité des solutions données par les modèles concernant les échanges à l'Ouest du Groenland. En effet, le CAA est composé d'un nombre important de petites îles, et la bathymétrie y est donc complexe et peu profonde. Jusqu'à présent, une grande majorité des modèles climatiques (du type de ceux utilisés pour les prédictions de l'IPCC par exemple) ont une résolution spatiale trop faible pour permettre une connexion à travers le CAA, bien que l'export d'eau douce liquide observé semble y être deux fois plus important qu'à travers le détroit de Fram (*Gerdes et al.*, 2008). De plus, plusieurs études (*Goosse et al.*, 1997; *Wadley and Bigg*, 2002; *Lietaer et al.*, 2008) ont montré que le fait de permettre ou non un échange de masse d'eau et de glace à travers le CAA modifie à la fois la circulation en Arctique, mais aussi l'intensité de la MOC en Atlantique Nord. *Wadley and Bigg* (2002) soulignent qu'une mauvaise représentation (ou l'absence de représentation) du CAA engendre également un biais pour la représentation des exports à travers le détroit de Fram, la répartition entre l'Est et l'Ouest du Groenland ne pouvant plus être reproduite correctement. Il semble donc crucial d'être capable de modéliser correctement les échanges à travers les différents passages du CAA. Notons au passage qu'un problème similaire se pose pour le détroit de Bering dans les modèles qui demande également une résolution élevée pour être correctement représenté. Là aussi, l'influence de cette connexion entre l'océan Pacifique et l'Arctique sur l'intensité de la MOC et donc le climat global a été démontrée dans plusieurs études (*Wadley and Bigg*, 2002; *DeBoer and Nof*, 2004).

Enfin, modéliser correctement l'Arctique et les échanges avec Atlantique Nord nécessite

une connaissance des flux de surface (précipitations et apports par les fleuves) bien meilleure qu'elle ne l'est actuellement. *Aagaard and Carmack* (1989) et *Dickson et al.* (2007) soulignent l'incertitude qu'il existe pour ces termes. La plupart des modèles océaniques sont forcés par des flux de surface climatologiques, la variabilité de ces quantités n'étant pas quantifiable à partir des observations. *Gerdes et al.* (2008) montrent que, dans les modèles de l'Arctique, les flux advectifs entrant et sortant vont s'ajuster afin d'atteindre un état d'équilibre. Un biais dans la représentation des flux de surface va donc entraîner à la fois un biais de la quantification des flux advectifs d'eau douce, mais aussi un biais important dans les propriétés des masses d'eau. Pour palier cette déficience sur la connaissance des flux halins en surface, la plupart des modélisateurs ont recours à une source supplémentaire d'eau douce en surface : un rappel vers une salinité de surface climatologique. Cependant, cette méthode est loin d'être parfaite. Ainsi *Steele et al.* (2001b) ont montré que l'ajout de ce terme dans les modèles tel qu'il est fait le plus souvent empêche de simuler correctement les variations de la salinité de surface en Arctique, et par conséquent de reproduire correctement la variabilité de la circulation, et notamment les différents régimes de circulation mis en évidence par *Häkkinen and Proshutinsky* (2004).

On se doute évidemment que les difficultés pour modéliser correctement l'océan Arctique ne concernent pas seulement la représentation du bilan d'eau douce et des exports d'eau douce vers l'Atlantique Nord. La circulation de l'eau Atlantique pose également problème. *Golubeva and Platov* (2007) ou encore *Karcher et al.* (2007) ont par exemple montré que le fait d'avoir une circulation cyclonique ou anticyclonique de l'eau Atlantique à l'intérieur de l'Arctique dépendait uniquement du flux de vorticité potentielle aux frontières du bassin Arctique. La nécessité de reproduire correctement le flux d'eau Atlantique pénétrant en Arctique par le détroit de Fram et la mer de Barents apparaît là encore clairement. Ainsi, les solutions données par les différents modèles numériques diffèrent grandement (*Karcher et al.*, 2007; *Aksenov et al.*, 2010), et là encore le manque d'observations ne permet pas réellement d'estimer quelle solution est la « meilleure ». D'autres processus physiques influent également sur la dynamique des flux entrant d'eau Atlantique. Citons par exemple la marée (*Holloway and Proshutinsky*, 2007b) ou encore l'influence des intéractions entre les tourbillons et la topographie (effet Neptune, e.g. *Nazarenko et al.* (1998) ou *Holloway and Wang* (2009)). La représentation de ces processus dans les modèles, qui est loin d'être triviale, permet d'améliorer significativement la représentation du flux d'eau Atlantique à travers le détroit de Fram et la mer de Barents (*Holloway and Wang*, 2009). De même, la circulation de l'eau Pacifique entre le détroit de Bering et le CAA ou le détroit de Fram est également difficile à simuler correctement. Des observations récentes (*Spall et al.*, 2008) semblent montrer qu'une partie de ce transport d'une section à l'autre se fait par un courant côtier le long de la côte Nord américaine,

mais aussi par des tourbillons qui sont advectés dans le bassin Arctique. Dans ce bassin, le rayon de Rossby est de l'ordre de 10 à 15 km et il faut donc atteindre une résolution spatiale très élevée (de l'ordre du km) pour pouvoir reproduire ces tourbillons, ce qui est le cas de très peu de modèles numériques à l'heure actuelle.

Le projet international *AOMIP (Arctic Ocean Model Intercomparison Project, Proshutinsky et al. (2001))* a pour but d'examiner conjointement différentes simulations de l'Arctique, afin de mettre en évidence puis de combler les déficiences communes à la majorité des modèles numériques actuels. Cette approche semble être aujourd'hui une des voies à suivre pour tenter de combler le manque de connaissance actuel du système Arctique, puisqu'elle permet à la fois d'améliorer notre connaissance des processus océaniques et des interactions avec la glace de mer en déterminant les similarités entre les différents modèles, mais aussi d'évaluer la fiabilité et la robustesse des résultats donnés par les simulations au regard des différences entre les différents modèles.

Au cours de ce travail de thèse, nous avons analysé plusieurs simulations utilisant des configurations différentes du modèle NEMO/LIM (*Madec*, 2008) (globales ou régionales), réalisées dans le cadre des projets DRAKKAR et GLORYS. Ces simulations (en particulier celles globales) n'ont pas été réalisées spécifiquement pour des études sur la région Arctique, mais les résultats donnés par ces simulations dans le bassin Arctique semblent placer notre modèle au moins dans la moyenne des autres modèles participant au projet AOMIP, notamment grâce à sa haute résolution (12 km en moyenne en Arctique pour le modèle au 1/4°). Pour chaque étude, nous nous sommes ainsi attaché à comparer notre simulation à la fois aux observations disponibles, mais également aux autres modèles participant au projet AOMIP. L'état de l'art concernant la variabilité des échanges Arctique/Atlantique Nord et l'impact de ces échanges sur les zones subarctiques est brièvement rappelé dans les deux parties suivantes.

1.3 Variabilité et forçage atmosphérique.

Les difficultés inhérentes à la modélisation et le manque d'observations (dû notamment aux conditions météorologiques rudes dans cette région) rendent l'estimation des échanges Arctique/Atlantique difficiles, et la connaissance de la variabilité temporelle de ces échanges quasiment inconnue. Pourtant, il existe une composante de ces échanges qui déroge à cette règle : il s'agit du flux de glace à travers le détroit de Fram. Chaque année, environ 10% de la masse totale de glace de mer présente en Arctique est exportée à travers ce détroit (*Aagaard and Carmack*, 1989). A partir des mesures satellites, *Vinje* (2001) ou *Kwok et al.* (2004) estiment la série temporelle de la surface de glace exportée sur la période 1978–2002. Le flux de glace est également estimé pour les années 1990–2000

en combinant des mesures sonars de l'épaisseur de glace (*Kwok et al.*, 2004), même si l'incertitude sur cette grandeur reste encore très importante. *Spreen et al.* (2009) complètent cette série temporelle en estimant le volume de glace exporté à travers le détroit de Fram sur la période 2003–2008 à partir des données satellite ICEsat qui donnent accès pour la première fois à l'épaisseur, la surface et la vitesse de dérive de la glace de mer, même si là aussi la barre d'erreur reste grande sur l'estimation de ces quantités.

La connaissance de cette série temporelle longue est importante : elle a permis par la suite de mieux comprendre les mécanismes de la variabilité observée, et en particulier de mettre en évidence le rôle des forçages atmosphériques. Certaines études numériques montrent l'influence des vents locaux sur la variabilité de l'épaisseur de glace et par conséquent sur celle du flux exporté (*Harder et al.*, 1998; *Houssais and Herbaut*, 2003). Dans le même temps, de nombreux auteurs (*Kwok and Rothrock*, 1999; *Vinje*, 2001; *Kwok et al.*, 2004) se concentrent sur l'influence sur ces exports des variations de la circulation atmosphérique à grande échelle, dont les indices AO ou NAO (Oscillation Arctique ou Oscillation Nord Atlantique) sont un bon indicateur. Pourtant, cette influence ne semble pas être triviale à comprendre. *Kwok et al.* (2004) montrent que sur la période 1980–2000, la corrélation entre les variations de l'indice NAO et celles du flux exporté est importante, mais cette corrélation disparaît si on considère une période plus longue (1960–2000) (*Vinje*, 2001). Le lien entre la NAO et le flux de glace à Fram ne semble donc exister que sur des périodes où l'indice NAO est plutôt positif, mais n'est pas robuste sur des plus longues échelles de temps. Dans une étude récente, *Tsukernik et al.* (2010) tentent de réconcilier tous ces différents travaux qui apparaissent comme contradictoires. A partir de champs journaliers du flux de glace à travers le détroit de Fram et de la pression de surface (Sea Level Pressure, noté SLP), ils montrent que la structure atmosphérique prédominante reliée à la variabilité haute fréquence des exports de glace est en fait un dipôle Est/Ouest centré sur le Groenland et la mer de Barents. A des échelles de temps plus longues (saisonnières à annuelles), ce dipôle semble encore être prédominant, même si il est parfois masqué par la structure spatiale de la NAO.

Le lien entre forçage atmosphérique, à échelle locale ou à grande échelle, et variabilité des exports de glace à travers le détroit de Fram est donc bien documenté dans la littérature. Mais qu'en est-il de la variabilité des autres échanges Arctique/Atlantique Nord ? La question est posée explicitement par *Dickson et al.* (2000), qui se demandent dans quelle mesure la NAO contrôle l'export d'eau douce, sous forme liquide et de glace, entre l'Arctique et l'Atlantique Nord. *Cuny et al.* (2005) montrent que, dans la région du CAA et la baie de Baffin, la corrélation entre les vents méridiens et l'indice NAO est très faible, l'influence de la topographie complexe étant prépondérante. Par conséquent, le flux de glace à travers le détroit de Davis ne semble que très peu influencé par les variations de

la NAO, et ses fluctuations semblent plutôt correspondre à des variations très locales des vent au dessus du CAA.

La question reste cependant très ouverte lorsque l'on se tourne vers les échanges océaniques avec les mers subpolaires. L'EGC permet le transfert des eaux polaires arctiques aux mers nordiques et au bassin d'Irminger. Le transport associé à ce courant est très fortement variable, à la fois dans le temps et dans l'espace, et il semble également que les mécanismes responsables de la variabilité temporelle diffèrent selon la latitude. La présence d'un cycle saisonnier à 75°N (*Woodgate et al.*, 1999) que l'on ne retrouve pas au niveau des détroits de Fram et du Danemark suggère que l'influence du forçage local n'est pas la même tout le long du courant, mais la question d'une influence plus systématique des forçages atmosphériques sur la dynamique et la variabilité de l'EGC est encore très largement ouverte. La connaissance de séries temporelles d'observations plus longues devrait aider à répondre à ces questions, comme celles des transports de masse et d'eau douce de l'EGC au détroit de Fram publiées récemment par *De Steur et al.* (2009).

L'autre transfert d'eau douce liquide de l'Arctique vers la zone subpolaire se fait à travers le CAA puis le détroit de Davis. Là encore, les observations sont rares et comme nous l'avons dit précédemment, peu de modèles numériques sont capables de simuler correctement ces échanges qui se font à travers des passages étroits (de l'ordre de 20 km dans le CAA). A l'issue du programme ASOF, *Melling et al.* (2008) ont tenté de synthétiser les différentes mesures existantes pour les différents passages. Ils soulignent également l'influence de la variabilité atmosphérique (à la fois localement et à plus grande échelle) sur la variabilité des transports de masse et d'eau douce. Ils montrent par exemple que les variations du transport à travers Lancaster Sound semblent être corrélées avec un décalage temporel de 8 mois aux variations de l'indice AO. Mais la série temporelle des observations est relativement courte (5 ans) ce qui rend la robustesse de ce lien sujette à caution. Des observations sur des échelles de temps plus longues ainsi que des simulations représentant correctement ces échanges sont nécessaires pour comprendre les mécanismes en jeu pour la variabilité des échanges Arctique/Atlantique à l'Ouest du Groenland.

Concernant le flux entrant d'eau Atlantique à travers le détroit de Fram et la mer de Barents, la situation n'est pas plus simple. *Ingvaldsen et al.* (2004) montrent en utilisant des observations de mouillages dans le Barents Sea Opening (BSO) sur 4 ans que la variabilité du flux d'eau Atlantique entrant en mer de Barents est très largement déterminée par les variations très locales des vents dans cette région. Pourtant, si les mécanismes responsables des variations du transport de masse à travers cette section semblent bien compris, la variabilité de l'apport de chaleur en Arctique semble elle être mal comprise. Une piste pour mieux comprendre les variations de température des eaux atlantiques

pourrait venir d'une étude récente de *Levitus et al.* (2009) qui montre que les variations de température de la couche d'eau atlantique entre 100 et 150 m en mer de Barents sont corrélées avec l'indice AMO (Atlantic Multidecadal Oscillation). Ceci signifie que les variations locales de la température du flux entrant en mer de Barents sont l'expression d'une variabilité climatique à l'échelle du bassin Atlantique. Les mêmes difficultés se posent pour comprendre les variations des flux de masse et de chaleur entrant par le détroit de Fram. *Schauer et al.* (2008) montrent que la distribution de la température à travers la partie Est du détroit de Fram a fortement varié au cours des dix dernières années. De même le transport de masse varie fortement durant cette même période (*Fieg et al.*, 2010), même si les mécanismes responsables de cette variabilité sont encore mal compris. De plus, peu d'études considèrent à la fois les deux branches d'eau atlantique entrants en Arctique, alors qu'il semble que les variations de leur transport de masse et de chaleur pourraient être liées à une répartition des masses d'eau qui varie dans le temps, et qui serait contrôlée plus au sud, au passage des seuils par exemple (*Orvik and Niiler*, 2002). Il apparaît là la nécessité de considérer le flux d'eau Atlantique entrant en Arctique dans son ensemble, non seulement à l'entrée de la mer de Barents et au détroit de Fram, mais également plus au Sud. *Maslowski et al.* (2004) ou plus récemment *Aksenov et al.* (2010) se sont intéressé à ce problème en utilisant des modèles numériques à haute résolution qui semblent montrer des résultats prometteurs au vu des comparaisons avec les observations. Mais ils n'ont dans un premier temps considéré que l'état moyen, et l'analyse de la variabilité et des mécanismes en jeu reste encore à faire.

Enfin, une autre piste pour comprendre le rôle de la variabilité atmosphérique sur celle des échanges Arctique/Atlantique pourrait venir d'une étude récente de *Joyce and Proshutinsky* (2007). En appliquant « la règle des îles » au Groenland (*Godfrey*, 1989), ils montrent qu'il existe une circulation cyclonique forcée par le vent autour du Groenland. Mais cette étude ne présente que des cas de vents climatologiques (neutre, de type AO + ou -). La question de savoir si la variabilité de cette circulation pourrait ou non être reliée à la variabilité des vents reste à traiter, de même que de savoir quelle part de la variabilité totale des échanges Arctique/Atlantique cette circulation cyclonique pourrait expliquer.

1.4 Influences des exports de masses d'eau Arctique sur les mers subpolaires.

De larges incertitudes demeurent donc quant à l'estimation des différentes composantes des échanges Arctique/Atlantique Nord, et plus encore quant à la connaissance de leur variabilité et des mécanismes qui en sont responsables. Mais nous avons également montré

que, dans le cas de l'apport d'eau Atlantique par exemple, il faut sans doute considérer un problème bien plus global que simplement les échanges localisés aux frontières de l'Arctique. Dans le même ordre d'idée, de nombreuses études, à partir d'observations et/ou de modèles, se sont intéressées à l'influence de ces échanges sur les mers subpolaires, voire sur la circulation océanique globale. On en donne ici deux exemples.

Épisodes de « Great Salinity Anomaly »(GSA).

Dickson et al. (1988) sont les premiers à déceler des épisodes où la salinité de la mer du Labrador est anormalement faible, épisodes qui ont eu lieu au début des décennies 1970, 1980 et 1990, et qu'ils désignent sous le nom de « Great Salinity Anomaly ». Mais les auteurs divergent encore quant à l'explication de ces épisodes. Les études numériques de *Köberle and Gerdes* (2003) et *Haak et al.* (2003) semblent montrer que ce sont des anomalies de l'export de glace à Fram, dues à des anomalies de l'épaisseur de glace, qui, en se propageant avec l'EGC jusqu'à la mer du Labrador, sont responsables des GSA. Dans le même temps, *Houghton and Visbeck* (2002) montrent que les anomalies du flux d'eau douce à travers le détroit de Davis ont une amplitude suffisante pour expliquer à elles seules les variations de salinité en mer du Labrador.

Il semble qu'en réalité les GSA n'aient pas systématiquement la même origine. En utilisant toutes les séries temporelles de salinité disponibles pour les mers nordiques et la mer du Labrador, *Belkin et al.* (1998) montrent que l'épisode qui a lieu pendant les années 1970 est causé par une anomalie positive de l'export d'eau douce liquide et de glace de mer à travers le détroit de Fram. Les GSA observées pendant les décennies 80 et 90 peuvent elles être reliées à la fois à des anomalies de l'export d'eau douce venant de l'Arctique par la baie de Baffin, mais aussi à des processus locaux (formation de glace de mer) dus à la sévérité des hivers pendant ces périodes.

Des épisodes similaires ont aussi été observés dans les mers nordiques (par exemple *Curry and Mauritzen* (2005)), et sont souvent reliés à des augmentations des flux d'eau douce et de glace venant de Fram. Cependant, les contributions relatives de ces deux termes, les temps de propagation de ces anomalies et la détermination *a priori* de leurs impacts (certaines anomalies des flux n'entraînent pas de variations de salinité dans les mers subpolaires) sont encore des questions ouvertes.

Liens avec la Cellule Méridienne d'Overturning (MOC).

Les différents scénarios climatiques de l'*IPCC* (2007) qui prennent en compte l'augmentation de l'émission de gaz à effet de serre dans l'atmosphère prédisent pour le siècle à

venir une diminution importante de l'intensité de la MOC. Mais, dans le même temps, les études numériques de *Gent* (2001) et *Latif et al.* (2000) prévoient une stabilisation de la MOC dans le futur. S'il faut donc rester prudent quand à l'interprétation de ces résultats, ils ont cependant permis de mettre en lumière l'importance des liens entre les échanges Arctique/Atlantique Nord et les zones de convection profonde (mers nordiques et mer du Labrador) et donc avec l'intensité de la MOC.

Tout d'abord, l'apport de chaleur pour l'océan Arctique se fait par le NAC, qui est la branche haute de la MOC en Atlantique Nord. Lorsque *Schauer et al.* (2008) observent que les eaux pénétrant en Arctique se sont réchauffées récemment, cela implique aussi que les eaux apportées par le NAC sont plus chaudes (donc moins denses), et qu'elles auront donc moins tendance à plonger. Cet effet est également amplifié par le réchauffement de la température de l'air aux hautes latitudes qui entraîne un réchauffement des couches de surface de l'océan, ce qui va là encore avoir tendance à réduire l'intensité de la convection.

Mais c'est surtout à l'influence des exports d'eau douce dans les mers subpolaires sur l'intensité de la MOC que se sont intéressées récemment de nombreuses études. La question est même posée très clairement par *Jones and Anderson* (2008) : *« Is the global conveyor belt threatened by Arctic Ocean fresh water outflow ? »*. Intuitivement, on pourrait penser que l'atmosphère se réchauffant aux hautes latitudes, la glace de mer va avoir tendance à se morceler et à fondre et les exports d'eau douce vers l'Atlantique (sous forme liquide et de glace) à augmenter. On s'attend alors à ce que la salinité des couches de surface dans les zones de convection diminue, et donc que les plongées d'eaux denses, qui sont les moteurs de la MOC, soient limitées voire inexistantes. Mais est-ce si simple que cela ? L'étude numérique de *Haak et al.* (2003) montre que les épisodes de GSA, où la salinité des couches de surface en mer du Labrador diminue, ne s'accompagnent pas systématiquement d'une réduction de l'intensité de la convection. De même, alors que leurs simulations reproduisent correctement la baisse de salinité récemment observée en Atlantique Nord (*Curry and Mauritzen*, 2005), *Wu et al.* (2004) obtiennent une intensification de la MOC en Atlantique Nord, associée à une augmentation du gradient de densité des couches de surface entre les régions subpolaires et les moyennes latitudes.
Si l'on voit ici que le lien entre les échanges Arctique/Atlantique et l'intensité de la MOC est encore loin d'être compris et expliqué, une des pistes à suivre est sans nulle doute celle proposée par *Jungclaus et al.* (2005), pour qui la variabilité de la convection profonde est expliquée par les interactions entre les mécanismes de stockage et libération de l'eau douce en Arctique d'une part, et ceux responsables des changements de circulation dans les mers nordiques causés par des modifications du transport d'eau douce en Atlantique Nord d'autre part. En d'autres termes, il faut à la fois considérer la variabilité des échanges avec l'Arctique mais aussi de ceux avec la région plus au sud pour pou-

voir expliquer les variations de l'intensité de la convection profonde. Et il faut également ajouter l'influence des phénomènes locaux (vents, échanges avec l'atmosphère) pour que l'explication soit complète.

Ces deux exemples montrent bien l'importance que peut avoir la variabilité des échanges Arctique/Atlantique pour le climat à l'échelle globale, et justifient que, dans la suite de ce travail de thèse, nous nous soyons concentrés sur la compréhension de ces échanges et de leur variabilité.

Chapitre 2

Variabilité des transports d'eau douce et de glace de l'Arctique vers l'Atlantique Nord.

2.1 Préambule

L'océan Arctique est le plus grand réservoir océanique d'eau douce, qui y est stockée à la fois sous la forme de glace de mer mais aussi de masses d'eau très peu salées (en moyenne, environ 84 000 km^3 d'eau douce sont stockés en Arctique (*Serreze et al.*, 2006)). En effet, ce bassin océanique reçoit une quantité importante d'eau douce par les apports fluviaux, les précipitations et les eaux Pacifique pénétrant en Arctique, puis une grande quantité de cette eau douce est exportée vers l'Atlantique Nord. Cette connexion océanique entre les océans Pacifique et Atlantique permet notamment de réduire le contraste de salinité qui existe entre ces deux océans : pour un taux de précipitations comparable, l'évaporation au dessus de l'Atlantique Nord est bien plus importante que celle au dessus du Pacifique Nord, ce qui engendre une différence de salinité moyenne d'environ 0.3 psu entre les deux régions (*Steele et al.*, 1996). Mais surtout, cette connexion océanique, qui conduit à un export net d'une partie de l'eau douce stockée dans le bassin Arctique, a potentiellement un impact climatique important puisque l'intensité de ces exports peut moduler l'intensité de la MOC en Atlantique (*Aagaard and Carmack*, 1989; *Dickson et al.*, 2008).

Construire un bilan d'eau douce pour l'océan Arctique est probablement l'un des exercices les plus classiques en océanographie Arctique. *Aagaard and Carmack* (1989) furent sans doute les premiers à suivre cette approche, à partir d'observations des différents termes du bilan disponibles dans la littérature. Depuis, de nombreux auteurs ont tenté de construire ce bilan à partir d'observations et/ou de résultats de simulations numériques (e.g. ; *Steele et al.* (1996); *Holland et al.* (2006); *Serreze et al.* (2006); *Dickson et al.* (2007); *Gerdes*

et al. (2008)). Pourtant, si le fonctionnement général du stockage moyen d'eau douce dans le bassin Arctique semble aujourd'hui connu, il n'en n'est pas de même ni pour la variabilité de ce bilan, ni pour des mécanismes qui contrôlent cette variabilité.

Dans ce chapitre, nous construisons à notre tour un bilan d'eau douce pour le bassin Arctique à partir d'une simulation numérique des cinquante dernières années, réalisée avec un modèle global au 1/4° dans le cadre du projet DRAKKAR. Une comparaison avec les études antérieures permet d'évaluer les performances de notre simulation qui, à l'origine, n'est pas dédiée à des études Arctique. Nos deux principales motivations sont de mieux comprendre les mécanismes à l'origine des variations du contenu halin en Arctique, mais surtout de déterminer comment est forcée la variabilité des échanges d'eau douce océanique de l'Arctique vers l'Atlantique, des deux côtés du Groenland. Les résultats de cette étude ont abouti à la publication d'un article publié en 2009 dans *Climate Dynamics*, dont la version finale est retranscrite dans la section suivante.

2.2 Article : A Model-based Study of Ice and Freshwater Transport Variability Along Both Sides of Greenland (C. Lique, A.M. Tréguier, M. Scheinert et T. Penduff, *Climate Dynamics*, 2009)

Abstract : We investigate some aspects of the variability of the Arctic freshwater content during the 1965–2002 period using the DRAKKAR eddy admitting global ocean/sea ice model (12 km resolution in the Arctic). A comparison with recent mooring sections shows that the model realistically represents the major advective exchanges with the Arctic basin, through Bering, Fram and Davis Straits, and the Barents Sea. This allows the separate contributions of the inflows and outflows across each section to be quantified.
In the model, the Arctic freshwater content variability is explained by the sea-ice flux at Fram and the combined variations of ocean freshwater inflow (at Bering) and outflow (at Fram and Davis). At all routes, except trough Fram Strait, the freshwater transport variability is mainly accounted for by the liquid component, with small contributions from the sea-ice flux. The ocean freshwater transport variability through both Davis and Fram is controlled by the variability of the export branch (Baffin Island Current and East Greenland Current, respectively), the variability of the inflow branches playing a minor role.
We examine the respective role of velocity and salinity fluctuations in the variability of the ocean freshwater transport. Fram and Davis Straits offer a striking contrast in this regard. Freshwater transport variations across Davis Strait are completely determined by the variations of the total volume flux (0.91 correlation). On the other hand, the freshwater transport through Fram Strait depends both on variations of volume transport and salinity. As a result, there is no significant correlation between the variability of freshwater flux at Fram and Davis, although the volume transports on each side of Greenland are strongly anti-correlated (-0.84). Contrary to Davis Strait, the salinity of water carried by the East Greenland Current through Fram Strait varies strongly due to the ice-ocean flux north of Greenland.

2.2.1 Introduction.

Changes in the Arctic freshwater budget have gained a renewed interest since it is today well admitted that just a small change of one of its components could strongly affect the World Ocean circulation and thus the climate dynamics. For instance, the Bering Strait freshwater flux may influence the Atlantic Ocean overturning circulation and the Deep Western Boundary Current (*Woodgate et al.*, 2005), and possibly the whole world climate, as suggested by *DeBoer and Nof* (2004). The freshwater fluxes exiting the Arctic

Ocean through Davis Strait and Fram Strait potentially influence the intensity and the timing of the deep convection in the Nordic Seas and the Labrador Sea and then the global thermohaline circulation (e.g., *Aagaard and Carmack* (1989), *Jones and Anderson* (2008)).

Many recent studies report drastic changes in the Arctic Ocean during the last decades. For example, *Cavalieri et al.* (2003) reported from satellite records a large decrease in the sea-ice extent since the early 1980's, while *Rothrock et al.* (1999) used observations made with submarine-based sonars to document a 40% decrease in the sea-ice thickness, comparing data during the 1958–1976 period and the 1990's period. At the same time, monitoring of the river discharge from the six major Eurasian rivers revealed a 7% increase from 1936 to 1999 (*Peterson et al.*, 2002). Changes in the Arctic hydrographic proprieties have also been emphasized. *Swift et al.* (2005) reported that most of the upper Arctic Ocean became significantly saltier since 1976, although these conclusions suffer from the lack of long term recordings. Some of these changes seem to be closely linked with variability in the atmospheric circulation, whose leading mode of variability is the Arctic/North Atlantic Oscillation (AO/NAO) (e.g., *Dickson et al.* (2000)). The link between the NAO and the variability of the different components of the Arctic freshwater supply has been investigated in numerous studies. For instance, the NAO influences the sea-ice export through Fram Strait, even though the link may not be robust when we consider long time scales (*Vinje*, 2001; *Kwok and Rothrock*, 1999). The NAO could also influence the freshwater storage in the Beaufort Gyre, depending on whether the wind circulation regime is cyclonic or anticyclonic (*Proshutinsky and Johnson*, 1997; *Proshutinsky et al.*, 2002).

Aagaard and Carmack (1989) were the first to provide a complete freshwater budget for the Arctic Ocean. Numerous authors follow this approach, investigating the different components of the budget, including river runoff, exchanges with atmosphere, and the different advective flows of ocean waters and sea-ice through the four pathways (ie, Bering Strait, Fram Strait, the Canadian Arctic Archipelago (CAA) and to the Barents Sea) (e.g., *Serreze et al.* (2006)). But all these observational works meet the same limitations : the lack of direct observations in the area, due to the harsh winter climatic conditions. Some components of the balance are becoming better observed and estimated, like the sea-ice export through Fram Strait, but most of them remain largely untouched, and their seasonal and interannual variability is still unknown.

Coupled climate models or coupled ocean/sea-ice models have been used to overcome the sparseness of observations. Such models are really useful in that they provide a complete self consistent dataset for analysis. *Holland et al.* (2006) examined the Arctic freshwa-

ter budget in climate model integrations of the twentieth and twenty-first century. They found a important freshening of the Arctic over the two centuries, along with an increase of the ocean freshwater exports to the North Atlantic. *Steele et al.* (1996) used a simple coarse resolution ocean/sea-ice model of the Arctic Ocean to investigate the freshwater budget over the 1979–1985 period, and found that the ocean freshwater flux through Fram Strait may be out of phase with the flux through the CAA. *Maslowski et al.* (2004) studied the relative importance of the volume, salt and heat exchanges through Fram Strait and the Barents sea, based on a pan-Arctic ocean/sea-ice 1/12° resolution model. They emphasize the role of the Barents Sea in the import of Atlantic Waters into the Arctic Ocean. *Köberle and Gerdes* (2003) performed an ocean/sea-ice model simulation over the 1948–1998 period, in order to study the variations of the Arctic sea-ice content. They underline the wind effects on this variability, and on the sea-ice exports into the North Atlantic. Following an original approach, *Proshutinsky et al.* (2002) and then *Häkkinen and Proshutinsky* (2004) were probably the first to analyze the variability of the freshwater content in the Arctic. The role of the Beaufort Gyre on the freshwater storage has been investigated in detail, using both observations and ocean/sea-ice model. But their conclusions suffered from the absence of Bering Strait in their coarse resolution model. Moreover, they do not consider Fram Strait and Davis Strait separately, as they focused on the freshwater exports into the North Atlantic. The diversity of model results concerning the Arctic freshwater balance can be seen for instance in *Steiner et al.* (2004). They compare among other things the freshwater content simulated by the different models of AOMIP (Arctic Ocean Model Intercomparison Project ; *Proshutinsky et al.* (2005)). *Gerdes et al.* (2008) investigate the Arctic freshwater budget in one of these models, and review the defaults and uncertainties commonly found in Arctic models, as well as their causes and consequences for the representation of the freshwater supply. They underline the critical role of surface conditions and the representation of the different boundaries enclosing the Arctic (the CAA and Bering Strait).

The present study aims at increasing our understanding of the Arctic freshwater budget variability during the last half century. We want to understand the major mechanisms responsible of variations in the Arctic freshwater content. We focus on the ocean freshwater exchanges through the CAA and through Fram Strait, in order to contrast the variability that occurs on both sides of Greenland, both in term of volume and freshwater fluxes. Moreover, the liquid flux and the sea-ice transport are contrasted across these two pathways. To do so, we use a global coupled ocean/sea-ice model. Compared to previous studies, our higher resolution model (between 10 and 13 km in the Arctic ocean) allows us to represent with an acceptable accuracy the hydrography and the dynamics of the Arctic Ocean, and especially the ocean and sea-ice circulation through the various passages enclosing the Arctic Ocean.

The remainder of this paper is organized as follows. The model and the simulations used for the study are briefly described in section 2. We validate the model in section 3, as we consider the mean freshwater balance for the Arctic Ocean. The variability of this budget is examined in section 4 in order to determine which components best explain the Arctic freshwater content variability. Circulation and freshwater fluxes across the openings of the Arctic Ocean are described in section 5. In section 6, mechanisms responsible of the interannual variability of the ocean freshwater exports to the subpolar area along both sides of Greenland are investigated. A conclusion is given in section 7.

2.2.2 The Numerical Experiment.

The global ORCA025 coupled ocean/sea-ice model configuration developped in the DRAKKAR project (*The DRAKKAR group*, 2007) is used to perform the different simulations. An overall description of the model and its numerical details are given in *Barnier et al.* (2006). This model configuration uses a global tripolar grid with 1442x1021 grid points and 46 vertical levels. Vertical grid spacing is finer near the surface (6 m) and increases with depth to 250 m at the bottom. Horizontal resolution is 27.75 km at the equator, 13.8 km at 60°N , and gets to 10 km in the Arctic Ocean. The ocean/sea-ice code is based on the NEMO framework version 1.9. (*Madec et al.*, 1998). It uses a partial step representation of the bottom topography and a momentum advection scheme which both yielded significant improvements (*Penduff et al.*, 2007). Parameterizations include a laplacian mixing of temperature and salinity along isopycnals, a horizontal biharmonic viscosity, and a turbulence closure scheme (TKE) for vertical mixing. The bathymetry is derived from the 2-minute resolution Etopo2 bathymetry file of NGDC (National Geophysical Data Center). The sea-ice model is the Louvain-la-Neuve model (LIM), which is a dynamic-thermodynamic model specifically designed for climate studies. A detailed description is given in *Timmermann et al.* (2005).

Our experiment hereinafter referred to as EXP1 is interannual and runs from 1958 to 2002 with no spin-up. Initialization is done using data from the Polar Science Center Hydrographic T/S Climatology (PHC; see *Steele et al.* (2001a) for details). The forcing dataset is a blend of data from various origins at different frequencies (*Brodeau et al.*, 2010). Precipitation and radiation come from the CORE dataset assembled by W. Large (*Large and Yeager*, 2004), at monthly and daily frequency respectively, based on satellite observations when available. A climatology of the same satellite dataset is used for the early years. Air temperature, humidity and wind speed are six-hourly fields from the ECMWF reanalysis ERA40. Turbulent fluxes (wind stress, latent and sensible heat flux) are estimated using the CORE bulk formulae (*Large and Yeager*, 2004). River runoff rates are prescribed using the *Dai and Trenberth* (2002) climatological dataset. To avoid

an excessive model drift, we add a relaxation of sea surface salinity to the PHC climatology. The coefficient (0.167 m/day) amounts to a decay time of 60 days for 10 m of water depth ; under the ice cover restoring is five times stronger. We add extra restoring at the exit of the Red Sea and Mediterranean Sea because those overflows are not adequately represented at that model resolution. A complete description of the experiment is found in *Molines et al.* (2006). We have chosen to study a 38 year period from 1965 to 2002, excluding this way the first seven years of the simulation when the model adjustment is the most important. For instance, a freshening of the Arctic ocean occurs between 1958 and 1965 (the freshwater content increases by 1.3 10^4 km^3 between 1958 and 1965). After that, the Arctic properties are more stable even though a model drift still exists (see the evolution of the salinity described in the following section).

In section 6, we use a second experiment (hereinafter referred to as EXP2) run at IFM-GEOMAR (Kiel). This simulation is exactly the same as EXP1 but for three things. The run is forced with pure CORE forcing, which means that air temperature, humidity and wind speed are taken from NCEP rather than ERA 40. The applied relaxation to the PHC climatology of sea surface salinity is weaker, with a coefficient of 300 days for 10 m of water depth, both at the sea surface and under sea-ice. Finally, a three dimensional restoring to the PHC climatology of salinity and temperature (with coefficient of 180 days) is applied in the polar areas, north of 80°N and south of 50°S . This simulation has been performed for studies of the Tropics and Sub-Tropics areas : therefore, a weak surface relaxation was wanted in these regions while a weaker variability in the polar area was not a problem. The two simulations yield different mean states and different variability of the circulation and properties in the Arctic Ocean : this allows us to use EXP2 in section 6 to add robustness to the identified mechanisms of the variability.

2.2.3 The mean simulated Arctic Ocean.

The aim of this section is to assess the model performances in the Arctic Ocean. We define the Arctic Ocean as the area enclosed by the following transects across ocean straits (Fig. 2.1) : the Bering Strait, a section across the Barents Sea between Norway and Svalbard Island (following the 20 °E meridian), Fram Strait and Davis Strait. Because of the model resolution, there is no link between the CAA and Hudson Bay. We decide to take into account the Arctic Ocean south of the CAA to allow comparison with available data of freshwater transport in Davis Strait (*Cuny et al.*, 2005), the fluxes through the CAA remaining largely unknown and difficult to monitor because of the complex geography (*Holland et al.*, 2006).

FIG. *2.1: Map showing the bathymetry (in meters as a unit) of the Arctic Ocean. The domain is enclosed by four sections : the Bering Strait (1), the Davis Strait (2), the Fram Strait (3), and the Barents Section (4). The isobaths shown are 500, 1000, 2000, 3000, 4000 and 5000 m.*

As calculations of the freshwater budget depend on two terms (salinity and velocity), we look at the mean salinity profile and the mean circulation over our domain. The averaged salinity profile for our domain is shown in Fig. 2.2, and compared to the same profile calculated from the PHC climatology data (*Steele et al.*, 2001a). The EXP1 profile is very similar to the PHC profile. The strong observed halocline is well represented, although waters between 300 and 1500 meters get slightly fresher throughout the 38-years integration (around 0.1 psu, see Fig. 2.2). From 1965 to 2002, the 34.8 psu isohaline gets about 200 m deeper. This is consistent with the corresponding calculated drift of the salinity (-1,8 mSv). Using this salinity as a reference, this small drift represents a gain of 1.1 10^3 km^3 of liquid freshwater (see appendix for definition), i.e. less than 2% of the mean freshwater content over the period considered.

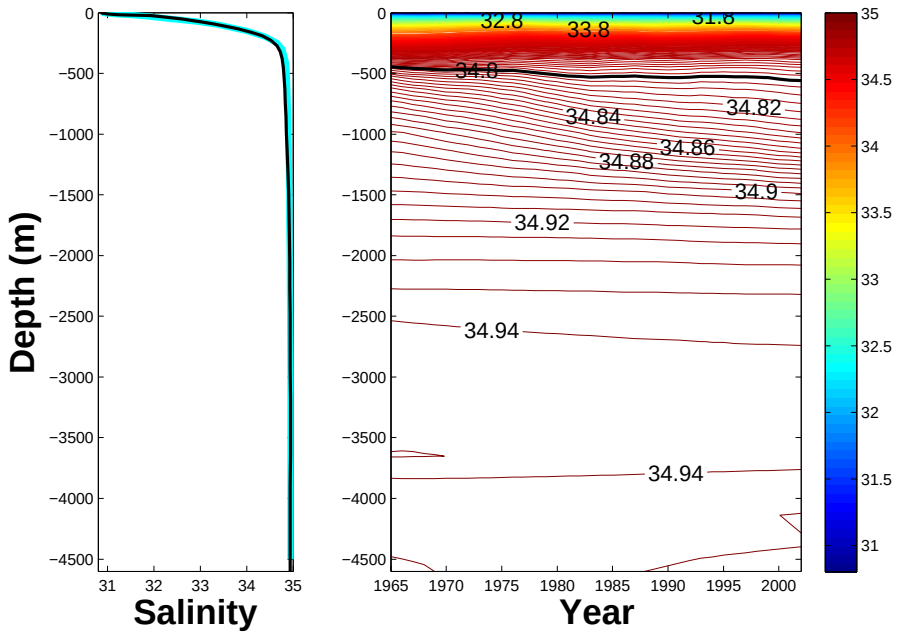

FIG. *2.2: Left : Annual average salinity profile (in psu) for the 1965–2002 period over the Arctic domain (see text for domain definition). The simulated salinity profile (thin black line) and the PHC climatology salinity profile (cyan line) are indicated. Right : Time–Depth section of annual mean salinity profile (in psu) over the Arctic domain.*

The mean surface circulation and ice velocity field are shown in Fig. 2.3 and 2.4 respectively. The model reproduces the observed circulation in the Arctic Ocean, as described for instance by *Pickard and Emery* (1990). A clockwise circulation is visible in the Canadian Basin (the Beaufort Gyre), and, on the other side of the Lomonosov Ridge, the surface and the sea-ice velocity fields exhibit the Transpolar Drift that crosses the Arctic Basin. It seems however that the simulated Beaufort Gyre is displaced closer to the Canadian coast compared to its observed location. Sea-ice velocities are stronger than surface current velocities, but both fields have similar structures. The time series of the Arctic sea-ice extent is shown in Fig. 2.5. Calculations are done considering the total northern hemisphere as a domain. Model results are in remarkable agreement with NSIDC observations (*Fetterer et al.*, 2002, updated 2009), both in terms of interannual variability and long-term trend, despite a slight underestimation of the time-averaged value.

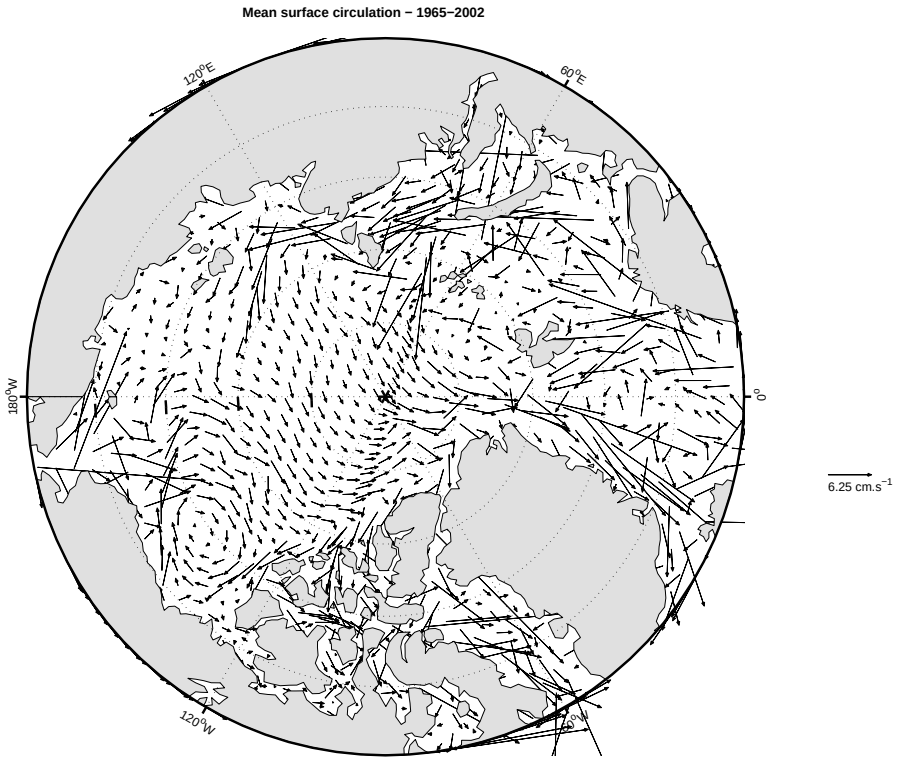

FIG. *2.3: The annual averaged surface circulation over the Arctic Ocean for the EXP1.*

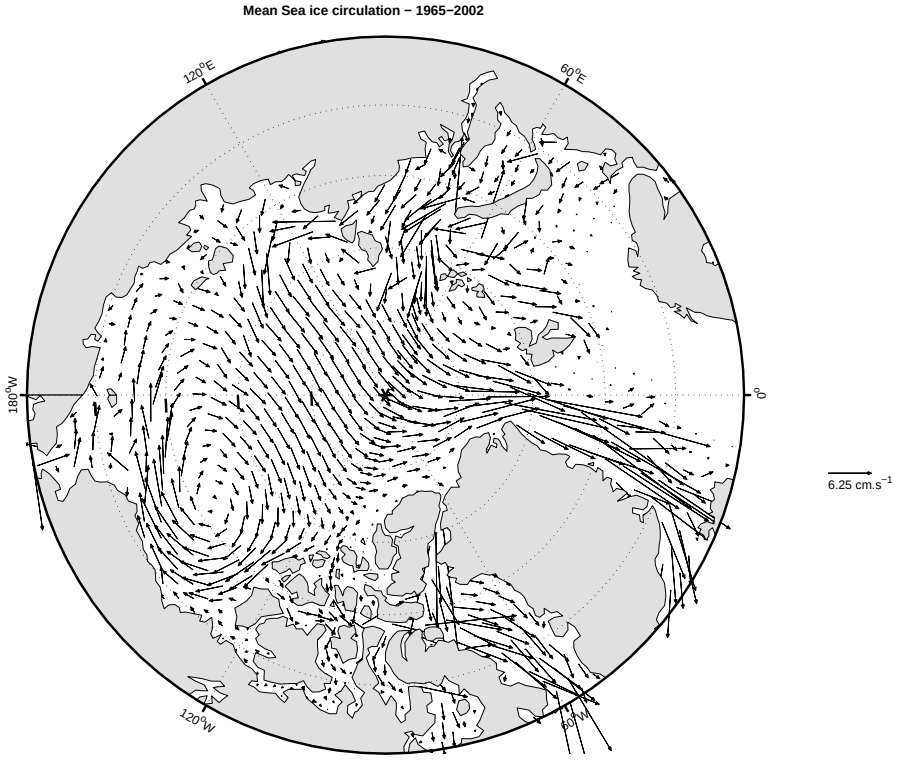

FIG. *2.4: The annual averaged sea-ice velocity over the Arctic Ocean for the EXP1.*

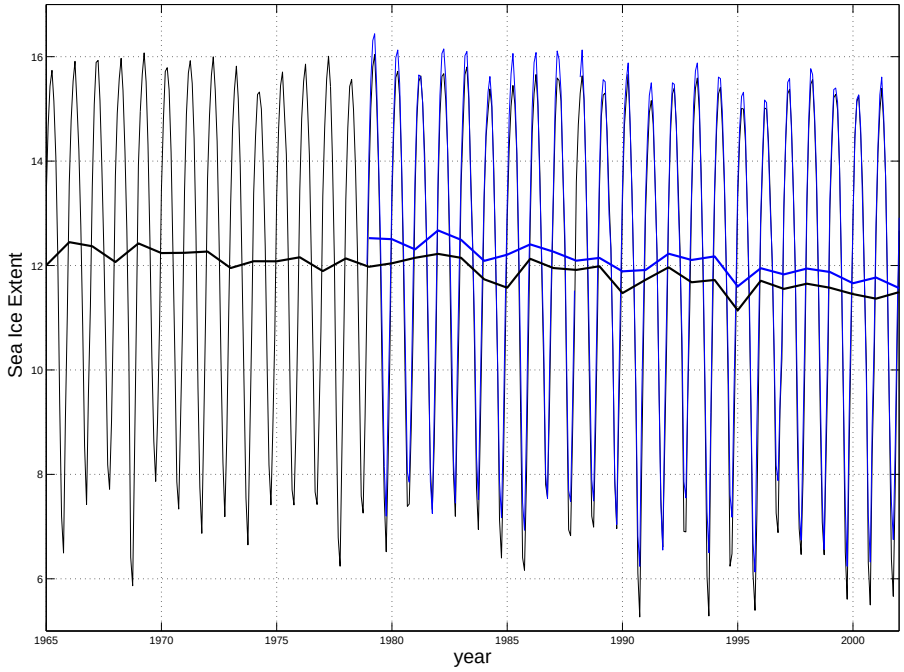

FIG. *2.5: Time series of the Arctic sea-ice extent monthly (thin line) and annual (thick line) mean ($\times 10^6$ km^2)from EXP1 (black line) and observations (blue line). See text for definition of the domain considered and data description.*

Our definition of freshwater budget is standard, based on a reference salinity $S_0 = 34.8$ psu (see Appendix for details). The mean values and standard deviations of the components of the Arctic freshwater balance over the 1965–2002 period are listed in Table 2.1.

Budget Term $S_{ref} = 34.8psu$ (mSv)	**Mean**	**Std Dev**	**Previous Estimates and References**
P-E	**69.5**	3.4	65 : *Serreze et al.* (2006) – 31 : A&C89
Runoffs	**108**	–	94 : *Lammers et al.* (2001) 102 : *Serreze et al.* (2006)
Damping	**29.4**	33.2	–
Ocean Transport			
Bering Strait	95.8	10.7	79 : *Woodgate and Aagaard* (2005) – 57 : A&C89
Davis Strait	-121.9	15.9	-92 : *Cuny et al.* (2005) – 57 : *Loder et al.* (1998)
Fram Strait	-63.1	16.4	-63/-95 : *Meredith et al.* (2001) – -28 : A&C89
Barents Section	-8.1	2.2	-9.6 : *Maslowski et al.* (2004) – -18 : A&C89
TOTAL	**-97.4**	28.4	
Ice Transport			
Bering Strait	4.2	2.7	3 : *Woodgate and Aagaard* (2005)
Davis Strait	-17.1	3.8	-12.9 : *Cuny et al.* (2005)
Fram Strait	-69.1	22.2	-56 : *Kwok and Rothrock* (1999) -88 : *Dickson et al.* (2007)
Barents Section	-6.4	2.3	-3.9 : *Kwok et al.* (2005b)
TOTAL	**-88.4**	22.3	

TAB. *2.1: Average Arctic Ocean freshwater budget over the period 1965-2002. Means are calculated from monthly output. Standard deviations are calculated from annual means. Previous estimates of the means are also shown. The sign convention is such that a source of freshwater into the Arctic Ocean is a positive value. A&C89 refer to Aagaard and Carmack (1989). Note that the sum of the budget terms, 21 mSv, is larger than the freshwater content change between january 1965 and december 2002, due to inaccuracies of the budget terms and the contribution of isopycnal diffusion, which is not taken into account. The freshwater content change is -2.9 mSv, resulting from salinity change (-1.8 mSv), sea surface height increase (3.5 mSv) and sea ice volume change (-4.6 mSv).*

Runoffs represent the most important freshwater source to the Arctic Ocean. This is due to the presence of many river discharges, chiefly from the drainage of the Ob, Yenesei, Lena and Mackensie. The runoff value used for our simulation (108 mSv) compares well with previous estimates (e.g., *Serreze et al.* (2006)), but also with values commonly found in numerical experiments (see e.g. *Steele et al.* (2001b) for the run-off values used in AOMIP models.). *Aagaard and Carmack* (1989) underline the considerable uncertainty regarding the source of freshwater that the precipitation minus the evaporation represents, and estimate a range of values from 14 to 48 mSv. Our model is forced with the precipitation values from the Serreze-Hurst-Yang precipitation climatology (*Serreze et al.*, 2006). In our simulation, precipitation over the Arctic Ocean exceeds evaporation by 69.5 mSv of freshwater in a typical year, and thus the net precipitation represents

an important source of freshwater. This value seems to be realistic regarding the area considered and the values published recently (e.g., *Dickson et al.* (2007)). An extra numerical term has to be taken into account in our freshwater budget : the damping to the climatological sea surface salinity. It represents a mean source of 29.4 mSv, i.e. about half the net precipitation term.

The freshwater transport includes contributions through four pathways, and each contribution is composed of two parts : liquid water and sea-ice. Moreover, we analyze at the same time the volume transport and the liquid and sea-ice freshwater fluxes in order to validate our mean simulated Arctic Ocean. The flux across Bering Strait is a freshwater source for the Arctic Ocean, but the mean value calculated in our simulation is 20% larger than the observations of 79 mSv from *Woodgate and Aagaard* (2005). They also estimate the Bering Strait volume throughflow as 0.8 Sv northward in the annual mean, which is 61% less than our simulated transport, despite the fact that the two boundary currents are seasonally present in the model as they are observed. The over estimate of the freshwater exchange is thus due to too high velocities across the Strait. The ice transport across Bering Strait is quite small and agrees well with recent measurements by *Woodgate and Aagaard* (2005).

Observations from *Loeng et al.* (1997) suggest that 3.3 Sv enter into the Barents Sea while 1.4 Sv are flowing outside, resulting in a net volume transport of 1.9 Sv. The simulated mean net transport through the Svalbard-Norway section is 2.9 Sv, with 4.1 Sv entering the Barents Sea and 1.2 Sv recirculating back to the Greenland Sea. This means that the flow entering the Arctic Ocean through this section is somewhat larger than observed. *Maslowski et al.* (2004) obtain similar values and they suggest as an explanation that the discrepancy may be due to the absence of tides in their model, which could be also true in our model. This flux across the Barents Section represents a salt source, i.e. a small sink of freshwater for the Arctic Ocean and its value is yet similar to the -9.6 mSv considered as representative by *Maslowski et al.* (2004). The sea-ice transport is somehow larger than the estimate of *Kwok et al.* (2005b), but the difference could be explained by the different periods considered, as they observe a large range of sea-ice fluxes (e.g., -7.4 mSv in 1995 and -1.0 mSv in 2003), depending on the year considered.

Ocean and sea-ice net transports across Fram Strait and Davis Strait, flowing southward along both sides of Greenland, represent the most important sinks of freshwater for the Arctic Ocean. The ranges of estimates for these contributions are really large and diverse in the literature, as well as the volume transport estimates. Our simulation results lie within the range of previous estimates (see Table 2.1) concerning the mean freshwater and sea-ice fluxes. The mean simulated net transports of -2.5 Sv through Davis Strait

and -1.8 Sv through Fram Strait are also coherent with observational estimates : *Schauer et al.* (2008) calculate a 2 Sv southward net transport using 14-16 moorings covering Fram Strait from 1997 to 2006, and *Cuny et al.* (2005) estimate the net volume transport in Davis Strait between 1987 and 1990 to -2.6 Sv. A more detailed study of the different branches composing the volume transport through these two pathways is done is section 5.

Although the simulated Arctic exhibits a few biases as discussed above, the model reasonably represents the large scale circulation, the hydrographic properties and the exchanges with the atmosphere and the subarctic area. The model values compare favorably with previous estimates from direct measurements. This suggests that the model can provide interesting indications on the interannual variability of the Arctic freshwater budget, and insight into the mechanisms that drive this variability.

2.2.4 The interannual variability of the freshwater content and its origins.

The aim of this section is to analyze the interannual variability of the Arctic Ocean freshwater content over the 1965–2002 period and to determine which components of the Arctic freshwater budget account for this variability.

2.2.4.1 The freshwater content of the Arctic Ocean.

Häkkinen and Proshutinsky (2004) present one of the few studies of the evolutions of the liquid freshwater content of the Arctic Ocean. They use their model of the Arctic and North Atlantic domain to provide a time series of the Arctic freshwater anomaly for the same period as our study (1950–2000). *Köberle and Gerdes* (2007) also calculate in their model the times series of the liquid freshwater content in the upper 350m. These two studies are used for comparison with our own model results. The time series of the Arctic Ocean freshwater content anomaly for the EXP1 run is shown in Fig. 2.6, along with its liquid and sea-ice components. Mean values, standard deviations and linear trends are given in Table 2.2.

Freshwater Content	**Mean (km^3)**	**Std Dev (km^3)**	**Trend (km^3/yr)**
Liquid	$5.86.10^4$	2480	15.4
Ice	$1.50.10^4$	2140	-31.6
Total	$7.46.10^4$	2840	-16.2

TAB. *2.2: Liquid and Ice freshwater content. Mean value, standard deviation and linear trend are calculated for each component for the 1965–2002 period. Means are calculated from monthly output. Standard deviations and linear trends are calculated from annual mean. Note that a mistake from the published version of the paper has been corrected here as the linear trend is indicated in km^3/yr.*

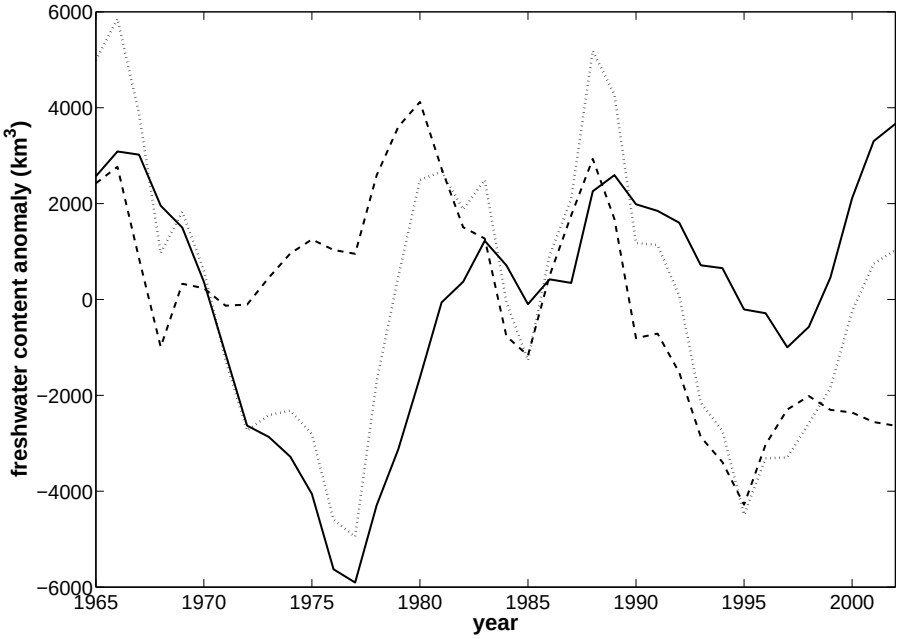

FIG. *2.6: Time series of Arctic Ocean freshwater content anomaly. Reference salinity is 34.8 psu. The liquid freshwater anomaly (solid lines), the sea-ice anomaly (dashed lines) and the total freshwater anomaly (dotted lines) are indicated.*

The ice part represents around 25% of the Arctic freshwater content. The annual means show large variability about the mean state, with a standard deviation of 2140 km^3, i.e. 14% of the long-term mean. In addition to these fluctuations, there is a linear decrease of the Arctic sea-ice volume of 2%/decade, relative to the long term mean over the 1965–2002 period. These results are consistent with those from previous modeling studies (for instance *Hilmer and Lemke* (2000) obtain a decreasing linear trend of 4%/decade over the 1958–1998 period, or 1.8%/decade over the 1958–1999 period in *Fichefet et al.* (2003)). A similar trend is also reported in the different papers using satellite based data to study the Arctic sea-ice evolution : e.g., *Parkinson et al.* (1999) observe a 2.8%/decade decrease of the Arctic sea-ice extent over the 1978–1996 period when our modeled sea ice extent

time series decreases with a 3.4%/decade trend.

Our time series of ocean freshwater content is qualitatively similar to the one of *Häkkinen and Proshutinsky* (2004), with the same maxima (in 1981 and 1988) and minima (in 1977, 1985 and 1995). We also found that our minima are close to ones of *Köberle and Gerdes* (2007) (around 1977, 1986 and 1997 in their model), but their time series shows a persistent decreasing trend that is not present in our model results. However, this trend is only present for their integration with a constant flux adjustment and not for the similar integration with surface salinity restoring. The ocean freshwater content mean is equal to 5.96 10^4 km^3 of freshwater, with a standard deviation of 2.48 10^3 km^3, that is about 4% of the long term mean. The variations are mostly due to time-variations of the different freshwater sinks and sources. An increasing trend is also superimposed to the interannual variability. However, available salinity data in the Arctic ocean are insufficient to determine if this could reveal a natural trend of the liquid freshwater content or if it is totally due to the model drift.

2.2.4.2 The origins of the freshwater content variability.

We now examine the interannual variability of the freshwater sources and sinks involved in the freshwater content variability. *Häkkinen and Proshutinsky* (2004) propose three major processes responsible for variations in the Arctic freshwater storage. The first process they consider is Ekman pumping in the Beaufort Gyre as a cause for the accumulation and release of freshwater. The mechanism is strongly dependent on whether the atmospheric wind is cyclonic or anticyclonic. The second process presented by *Häkkinen and Proshutinsky* (2004) is the variability of sea-ice growth and melt. But they find that these first two processes have in fact a very weak impact on freshwater content anomalies. The only significant process is the third one : the advective exchanges of water masses between the Arctic Ocean and the subpolar seas.
Time series of anomalies of the different components of the Arctic freshwater budget over the 1965–2002 period for the EXP1 run are shown in Fig. 2.7. The time series of the freshwater content derivative anomalies are superimposed on each plot for direct comparison. Fig. 2.8 provides a graphic synthesis of the various terms : their mean value, their standard deviation and their correlation with the time derivative of the freshwater content. Significance level for nonzero correlation are computed from the effective degrees of freedom based on the integral timescales (*Sciremammano*, 1979). Significance levels as well as effective degrees of freedom (hereinafter referred to as n) are given in the text and in the different tables.

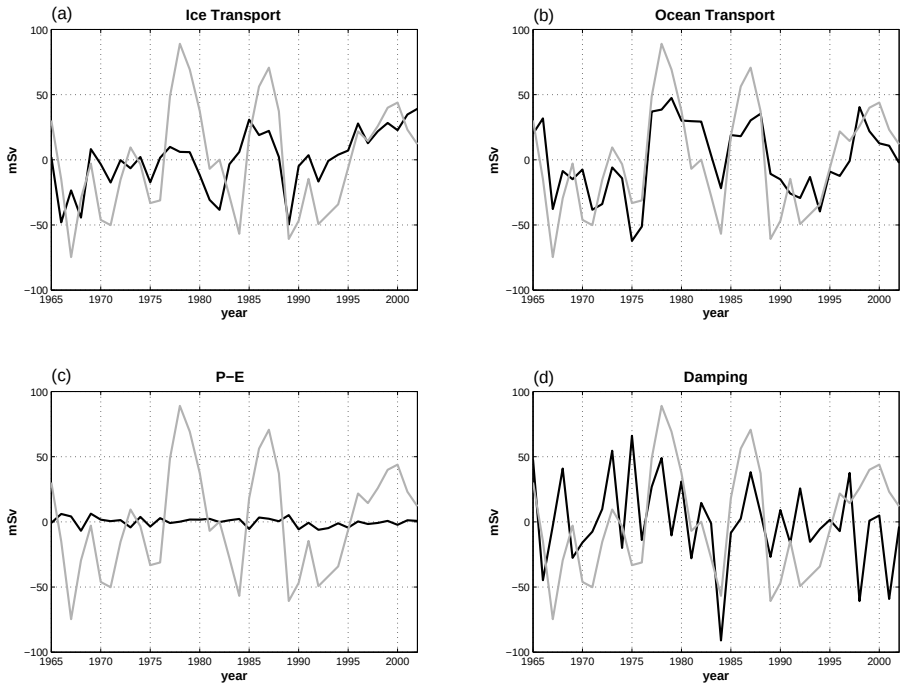

FIG. *2.7: Time series of the anomalies of : (a) sea-ice transport, (b) ocean transport, (c) net precipitation , and (d) damping over the period 1965–2002 for the EXP1 run. The time series of the anomalies of the freshwater content derivative is also stacked on each plot (gray line).*

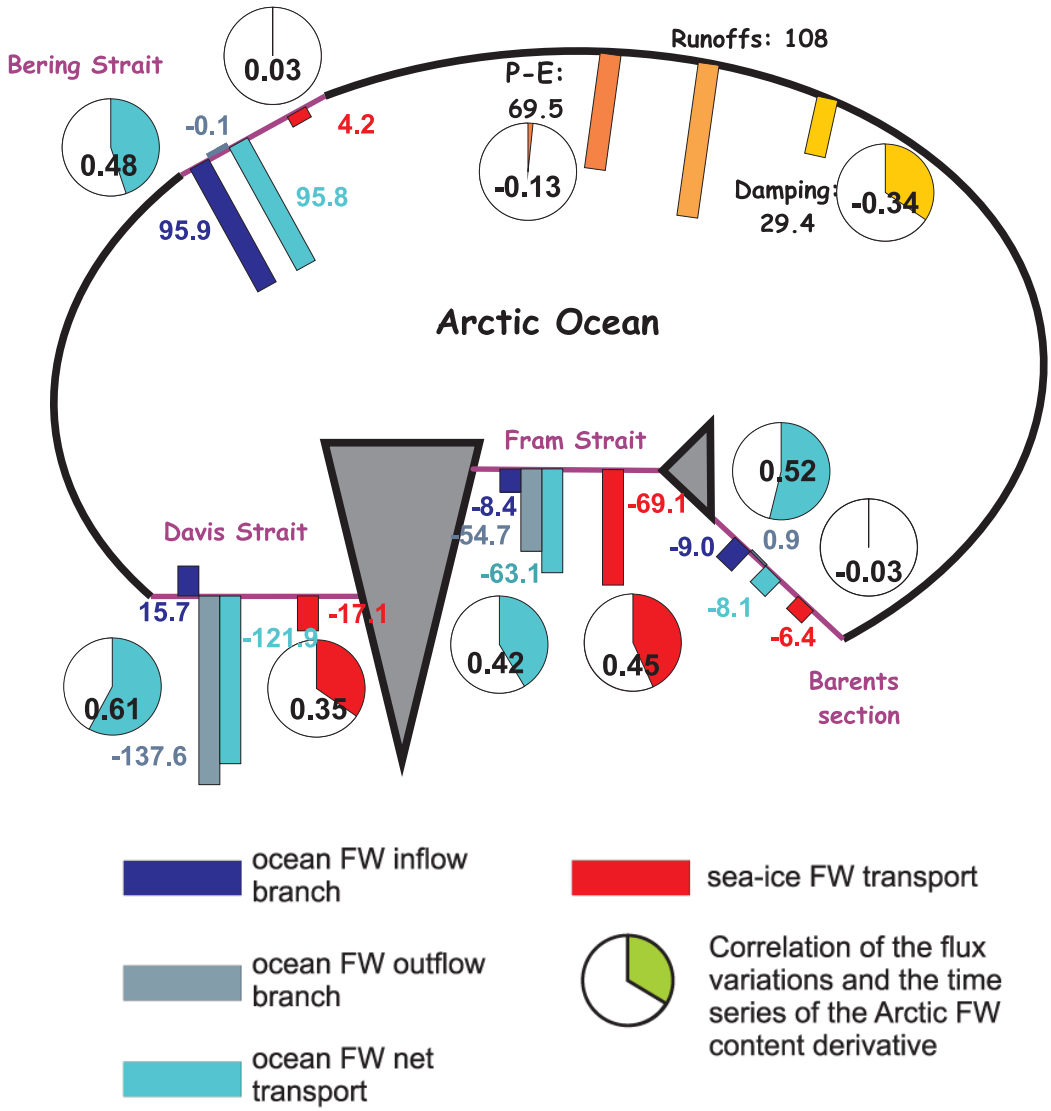

FIG. *2.8: Schematic view of the Arctic freshwater balance. Mean value of each source and sink is represented (bar, in mSv), as well as the correlation of its variations with the times series of the Arctic freshwater content derivative (circular diagrams). The sign of the freshwater fluxes indicates if the flux represents a sink or a source of freshwater for the Arctic Ocean, regardless the direction of the volume fluxes (For instance, the inflow branch through Fram Strait brings waters with salinity higher than 34.8, and thus has a negative sign).*

Surface fluxes : The Arctic river runoff exhibits some interannual variability (*Holland et al.*, 2006) and long-term trend (+7% over 1936–1999, *Peterson et al.* (2002)), but their impact on the Arctic freshwater budget was shown to be small compare to changes in sea-ice and liquid freshwater contents (*Proshutinsky et al.*, 2001). The simulation was forced with monthly climatological runoff : its interannual variability has been ignored and this term does not appear in Fig. 2.7. In the studied area, the model is forced

with the precipitation values from the Serreze-Hurst-Yang climatology (*Serreze et al.*, 2006), without interannual variability. The variability in $P - E$ is thus totally due to the variations of the evaporation term. $P - E$ only exhibits a weak linear trend of about 0.02 mSv/decade. The standard deviation of this term is small (3.3 mSv), and its time variations are not significantly correlated with the variations of the freshwater content derivative. The relaxation to climatological sea surface salinity represents a source of freshwater for the Arctic Ocean. No trend is visible on this component, in agreement with the fact that the model does not drift too much over the considered period (see Fig. 2.2). But this term is also highly variable, with a standard deviation (std=33.2 mSv) stronger than the mean value (29.4 mSv). The negative correlation of its variations with the variations of the freshwater content derivative (correlation -0.34, significance 90%, n=22) indicate that this term damps the variability as expected. Interannual variations of the Arctic freshwater content are thus not caused mainly by surface fluxes, i.e. net precipitations, runoffs and relaxation. We thus turn our attention to the advective fluxes.

The advective fluxes : From 1965 to 2002, the divergence of ocean freshwater fluxes represents an important sink for the Arctic freshwater content variability. No long-term trend is visible over the considered period for this term, but its interannual variations are substantial (std=28.6 mSv, Fig. 2.7(b)). The variations of this term are highly correlated with the variations of the freshwater content derivative (correlation 0.75, significance 95%, n=16), showing that the ocean freshwater flux has a leading role in the freshwater content variability. The sea-ice transport divergence (see Fig. 2.7(a)) exhibits almost the same behavior as the ocean freshwater transport, with no visible trend over the 1965–2002 period, and comparable interannual variability (std = 22.3 mSv). The correlation between its variations and those of the freshwater content derivative is significant as well (correlation 0.52, significance 95%, n=22).
The variability of the Arctic freshwater content is thus largely controlled by the divergence of advective fluxes, as found by *Häkkinen and Proshutinsky* (2004) in their model. As the ocean transport and the sea-ice transport are the sum of four contributions, the exchanges across the four sections need to be examined in order to determine their relative importance.

2.2.5 Advective fluxes.

The freshwater balance of the Arctic Ocean has been already calculated from model simulations (e.g., *Holland et al.* (2006), *Köberle and Gerdes* (2007), *Steele et al.* (1996)). However, to our knowledge, this kind of study has never been done using a model with such high resolution (around 12 km at these latitudes). The most important improvement of our study is probably the better representation of the oceanic circulation across the different sections enclosing the Arctic Basin, and thus of the freshwater exchanges

with the North Atlantic and the North Pacific. The contribution across each transect is composed of an inflow and an outflow, this makes the study more complicated since we want to analyze each branch of current separately. The aim of this section is to describe in detail these freshwater exchanges and to determine which contribution has the bigger impact on the Arctic freshwater content variability. Of course our analysis is dependent on the choice of a reference salinity (Appendix 1) and the decomposition of the total advective transport into various branches depends on the volume transport of each branch. For this reason, we will consider both the freshwater and the volume transports. The times series of the ocean and sea-ice freshwater exchanges across the four pathways are shown in Fig. 2.9. The mean values are also given in Table 2.3. Correlations between the time series of each component and of the freshwater content derivative are given in Table 2.4.

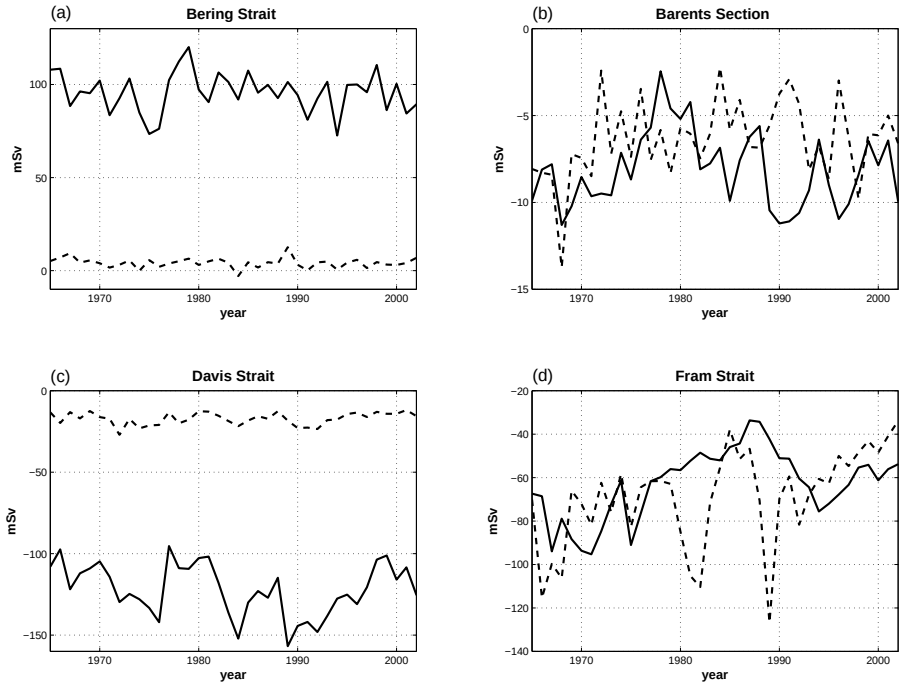

FIG. *2.9: Times series of the ocean freshwater transport (solid line) and sea-ice freshwater transport (dashed line) through (a) Bering Strait, (b) Barents section, (c) Davis Strait, and (d) Fram Strait. The reference salinity is 34.8 psu. The sign convention is such that a source of freshwater for the Arctic Ocean is a positive value.*

		Bering Strait	**Barents Section**	**Davis Strait**	**Fram Strait**
Transport (Sv)	*inflow*	1.3	4.1	1.2	6.5
	outflow	0	-1.2	-3.7	-8.3
	net	1.3	2.9	-2.5	-1.8
Ocean FW Transport (mSv)	*inflow*	95.9	-9.0	15.7	-8.4
	outflow	-0.1	0.9	-137.6	-54.7
	net	95.8	-8.1	-121.9	-63.1
Sea-ice FW Transport (mSv)	*net*	4.2	-6.4	-17.1	-69.1

TAB. *2.3: Averages of the volume, ocean freshwater and sea-ice exchanges across the four transects enclosing the Arctic Basin (see text for definition of the domain). Means are calculated from monthly output. The sign convention is such that a source of freshwater for the Arctic Ocean is a positive value.*

	Ocean freshwater transport	**Sea-ice freshwater transport**
Bering Strait	**0.48** (n=29, 95%)	0.03
Barents Section	**0.52** (n=18, 95%)	-0.03
Davis Strait	**0.61** (n=20, 95%)	**0.35** (n=27, 90%)
Fram Strait	**0.42** (n=15, 90%)	**0.45** (n=21, 95%)

TAB. *2.4: Correlations between the time series of the ocean freshwater and sea-ice exchanges across the four transects enclosing the Arctic Basin and the time series of the freshwater content derivative. Effective degrees of freedom (n) and statistical significance level are indicated (in brackets) for correlation coefficients that are significant (shown in bold font). Only significant correlations are referred to in the text.*

		DAVIS STRAIT		**FRAM STRAIT**	
		EXP1	*EXP2*	*EXP1*	*EXP2*
$T_{FW}(v, S_1)$	*Mean (mSv)*	-121.9	-61.2	-62.4	-33.8
	Std (mSv)	15.9	14.6	16.1	11.4
$T_{FW}(v', S_1')$	*Mean (mSv)*	-10.4	-6.2	-1.4	-1.9
	Std (mSv)	2.3	2.1	2.1	1.6
	r	0.09	0.30	0.25	-0.17
$T_{FW}(\overline{v}, S_1')$	*Mean (mSv)*	0	0	0	0
	Std (mSv)	4.7	2.9	9.9	6.8
	r	**0.52** (n=23)	0.34	**0.70** (n=9)	**0.76** (n=14)
$T_{FW}(v', \overline{S}_1)$	*Mean (mSv)*	0	0	0	0
	Std (mSv)	1.4	13.1	9.7	7.7
	r	**0.95**(n=15)	**0.97**(n=17)	**0.80** (n=6)	**0.81**(n=17)
$T_{FW}(\overline{v}, \overline{S}_1)$	*Mean (mSv)*	-111.6	-55.0	-61.0	-32.0
	Std (mSv)	0	0	0	0

TAB. *2.5: Mean, Standard deviation (std) and correlation (r) with the ocean freshwater flux of each contribution to the transport as defined by Eq. 2.1 across Davis Strait and Fram Strait, for the two experiments (EXP1 and EXP2). Means are calculated from monthly output. Standard deviations are calculated from annual mean. For the correlation coefficients, bold font indicates statistical significance at 95% confidence level or higher and effective degrees of freedom (n) are indicated in bracket. Only significant correlations are referred to in the text.*

2.2.5.1 Bering Strait.

The flux through Bering Strait is a source of freshwater for the Arctic Ocean. The throughflow has strong seasonal and interannual variations, because of the seasonally present boundary currents : the warm and fresh Alaskan Coastal Current (ACC) present in the eastern strait every year at least in summer or in autumn, and the cold and fresh Siberian Coastal Current (SCC) occasionally present in the western Bering Strait. Velocities across the whole strait are highly correlated with the local wind (*Woodgate et al.*, 2005).

Aagaard and Carmack (1989) estimate the Bering Strait freshwater flux relative to 34.8 psu as 53 mSv, and *Woodgate and Aagaard* (2005) use long term moorings and ship surveys, from 1990 to 2004, to improve this estimate, adding three contributions : the freshwater advected by the Alaskan Coastal Current (about 7 to 14 mSv), general stratification of the water column within the strait (about 10 mSv), and sea-ice advection (3.2 ± 2.2 mSv). This leads to a new estimate of the freshwater transport : 74 mSv and 3.2 mSv of sea-ice. In the model, the simulated ocean freshwater transport is 28% larger than observed (see Fig. 2.9(a) and Table 2.3), even though the salinity of the Pacific

Waters entering into the Arctic Ocean is consistent with the salinity across Bering Strait described by *Woodgate et al.* (2005) (S seasonally varies from 31.9 to 33 psu). The simulated sea-ice flux is also larger than the estimate but still within the uncertainty range. The variability of the sea-ice transport is very small (std = 2.7 mSv) and thus does not influence the variability of the freshwater storage. The ocean freshwater transport has a larger variability (std = 10.7 mSv), significantly correlated with the Arctic freshwater content derivative (r = 0.48, significance 95%, n=29). In our model, this latter flux is the source that has the most important influence on the variability of the freshwater storage, compared with other sources.

2.2.5.2 Barents Section.

Freshwater exchanges are evaluated across the 'Barents Section' (20°E), between Norway and Svalbard Island. The main inflow of Atlantic Water into the Barents Sea (and thus the Arctic Basin) takes place in the warm, salty Norwegian Atlantic Current entering through the Barents Sea Opening. A percentage of this branch of current recirculates with the cold, Arctic originated, Bear Island Current, and then exiting the Barents Sea. Another source of water to the Barents Sea is the colder and fresher Norwegian Coastal Current, which carries waters originating from the Baltic Sea and Scandinavian runoff eastward. Finally, the last output of water is the cold, fresh East Spitsbergen Current, flowing eastward of Spitsbergen Bank and then with the Bear Island Current.
The simulated transport across the Barents Section provides a sink of freshwater to the Arctic Ocean. Our simulation results differ from those obtained by *Maslowski et al.* (2004) with their model as our sea-ice outflow and ocean freshwater outflow have the same order of magnitude, while *Maslowski et al.* (2004) find a liquid flux about four times higher than the sea-ice flux. Both components of the freshwater flux represent sinks of freshwater for the Arctic Ocean (see Fig. 2.9(b)), even though the net volume flux brings Atlantic Waters into the Arctic Ocean. But these two sinks of freshwater are negligible regarding the other components of the freshwater budget. No direct measurements of the ocean freshwater input has been done across this section, but our simulated ocean freshwater outflow of 8.1 mSv with a standard deviation of 2.2 mSv seems to agree well with the one obtained by *Maslowski et al.* (2004) with their model (9.6 mSv). *Kwok et al.* (2005b) estimate the sea-ice flow across the section using a 10-year record of satellite ice motion and thickness. They show that the flux exhibits a strong interannual variability : the outflow varies from 7.4 mSv in 1994–1995 to 1.0 mSv in 2002–2003. Our simulated sea-ice outflow exhibits important fluctuations as well, with a standard deviation of about 36% of the long-term mean. No long term trend are visible for those two fluxes over the considered period. Time series of freshwater transport is significantly correlated with the Arctic freshwater content derivative (see Table. 2.4), but neither the ocean transport nor the ice transport across the Barents section has large enough variations to influence the

Arctic freshwater storage, compared to the other components of the freshwater balance.

2.2.5.3 Fram Strait.

Fram Strait is the only deep-water connection between the Arctic Ocean and the world ocean. It is an important site for the exchange of mass, heat, and salt (*Fahrbach et al.*, 2001). The warm West Spitsbergen Current (WSC) and the ice-infested East Greenland Current (EGC) are the two major currents in Fram Strait. While the WSC carries warm Atlantic waters northward into the Arctic Ocean, the EGC transports cold, fresh water and sea-ice southward out of the Arctic basin (*Schlichtholz and Houssais*, 1999). At around 79°N the WSC splits into two branches, because of the complex topography : the first branch flows northward and enters the Arctic Ocean, while the second branch recirculates and then flows southward along the eastern edge of the EGC. The mean circulation and salinity sections are remarkably well represented in the model (see Fig. 2.10 (c) and (d)), as we compare with observations collected between September 1997 and September 1999 (*Fahrbach et al.*, 2001). The water mass repartition is very similar, with very fresh waters (S between 31 and 34 psu) visible in the upper western part of the section, while the remainder of the transect is more homogeneous (S between 34.9 and 34.98 psu). Simulated velocities are also very coherent with observations. The two branches of current are visible, even though the modeled WSC is slower in the model than in *Fahrbach et al.* (2001) data (12 cm/s versus 24 cm/s), and the EGC is stronger than the observed one (15 cm/s versus 9 cm/s).
Fram Strait is the major exit for the Arctic sea-ice. The budget of *Aagaard and Carmack* (1989) for the Arctic ocean features a freshwater flux through Fram Strait that is dominated by sea-ice : they estimate that 90% of the total Arctic sea-ice export exits here, advected by the EGC, and continuously fed by melting along the Greenland Coast. Many authors have estimated the sea-ice contribution to the freshwater transport and its interannual variations (e.g., *Vinje* (2001), *Kwok and Rothrock* (1999)), but the ocean contribution remains largely unknown. *Meredith et al.* (2001) estimated the liquid freshwater flux using sections of oxygen isotopes and the ratio of the meteoric water flux to sea-ice melt. Our simulation provides us with both contributions at the same time, with their interannual variations.

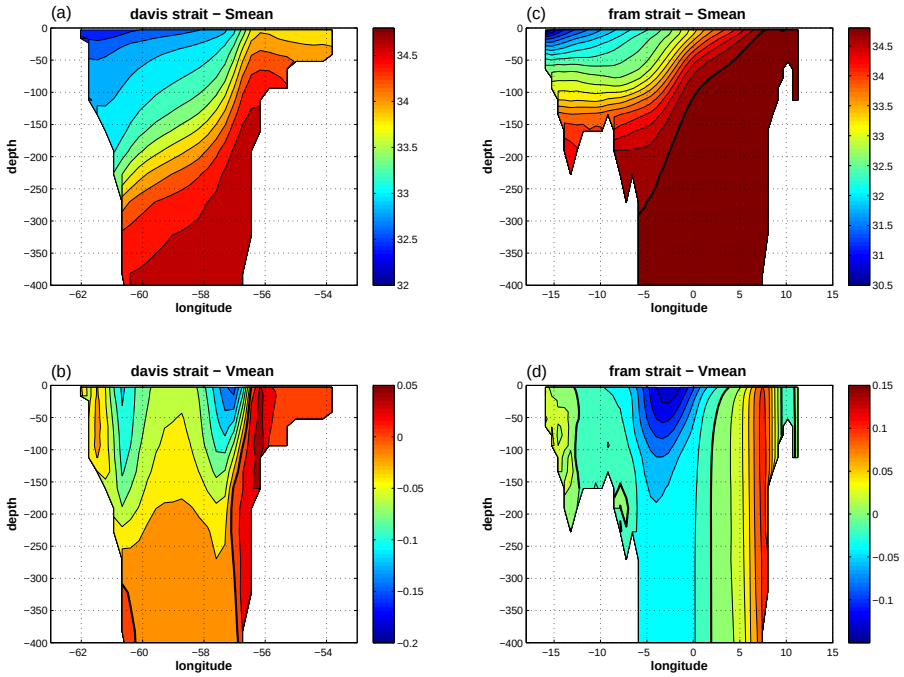

FIG. *2.10: Section of mean salinity (in psu) and speed (in m/s) of the 400 upper meters across Davis Strait (a and b) and across Fram Strait (c and d). Calculations are done over the 1965–2002 period for the EXP1 run. The 34.8 isohaline and the null speed contour are indicated in bold. We just represent the upper part of the two sections where the transport and the freshwater transport have significant contributions.*

The time series of the simulated sea-ice export across Fram Strait is shown in Fig. 2.9(d). Over the 1965–2002 period, 69.1 mSv is exported in the mean from the Arctic, with an important interannual variability (std = 22.2 mSv). *Rothrock et al.* (2000) summarize estimates of the Fram Strait ice flux available through the late 1990's. These range from 42 mSv to 128 mSv, depending on record length and measurement techniques. Our value lies roughly in the middle of this range. No trend is visible in our time series, but the value is highly variable. Three maxima in 1968, 1981–1982 and 1989, and a minimum in 1985 are noticeable, and we remark that these extrema are also present in the simulated time series of *Haak et al.* (2003). They analyze the 1968 maximum as the cause of the observed 70's Great Salinity Anomalies in the Labrador Sea. Nevertheless, our model does not reproduce some of the observed events described for instance by *Vinje* (2001), such as the large positive export anomaly that occured during the winter 1994/1995.
The time series of volume and ocean freshwater transport anomalies at Fram Strait are shown in Fig. 2.11. The northward and southward contributions are also indicated. *Fahrbach et al.* (2001), *Schauer et al.* (2004) and *Schauer et al.* (2008) give estimate of the volume transport there, based on current meter moorings, deployed from 1997 to 2006. They refer for their calculations to the total northward transport as WSC and to the total southward transport as EGC. We take the same convention. *Schauer et al.* (2008)

calculate a volume transport of 12 Sv to the north and 14 Sv to the south, the net transport being about 2 Sv to the south. Simulated volume transports are weaker than these estimates, with a northward component oscillating around 6.5 Sv and a southward component around 8.3 Sv. The mean net transport is 1.8 Sv southward, with a range of variations weaker than 2 Sv. *Schauer et al.* (2008) estimates are however significantly larger than earlier estimates given in the literature. For instance, *Schlichtholz and Houssais* (1999) estimate a transport of 1.1 Sv for the WSC and 6.2 for the EGC, which is this time lower than our values.

Due to the lack of measurements across Fram Strait, direct estimates of the ocean freshwater transport are sparse in the literature, and its variability has not been studied before. *Meredith et al.* (2001) estimate the EGC average freshwater export of -45 mSv, which is much larger than the previous estimate by *Aagaard and Carmack* (1989) of -28 mSv. Estimate of the WSC contribution is even more uncertain, with observed values ranging from -5 mSv (*Aagaard and Carmack*, 1989) to -24 mSv (*Dickson et al.*, 2007). Our simulation exhibits a weak mean WSC contribution (-8.3 mSv), the negative sign being explained by waters saltier than 34.8 psu within the WSC. The EGC contribution has an important interannual variability. The mean value (-54.7 mSv) is consistent with *Meredith et al.* (2001) estimate, and two periods are clearly pronounced : a first one between 1965 and 1975 when the freshwater flux is important (around -90 mSv), and a second period between 1985 and 1990 when the flux is weaker (around -40 mSv). No estimates of the long term variability has been done before, so it is difficult to determinate if this contrast between the two periods is realistic or just a model artifact. The variability of the net freshwater flux through Fram Strait is clearly controlled by the export branch, as the inflow has a weaker influence on the variability (see Fig. 2.11 (d)).

Fram Strait is the only pathway where the mean ocean freshwater transport and sea-ice transport have the same order of magnitudes (respectively -63.1 mSv and -69.1 mSv), the same amplitude of variation (respectively std = 16.2 mSv and std = 22.2 mSv), and the variations of the two terms are as much correlated with the variations of the freshwater content derivative (respectively r = 0.42, significance 90%, n=15 and r =0.45, significance 95%, n=21). This shows that both terms strongly influence the variations of the Arctic freshwater storage. However, the variations of the two terms are not significantly correlated with one another.

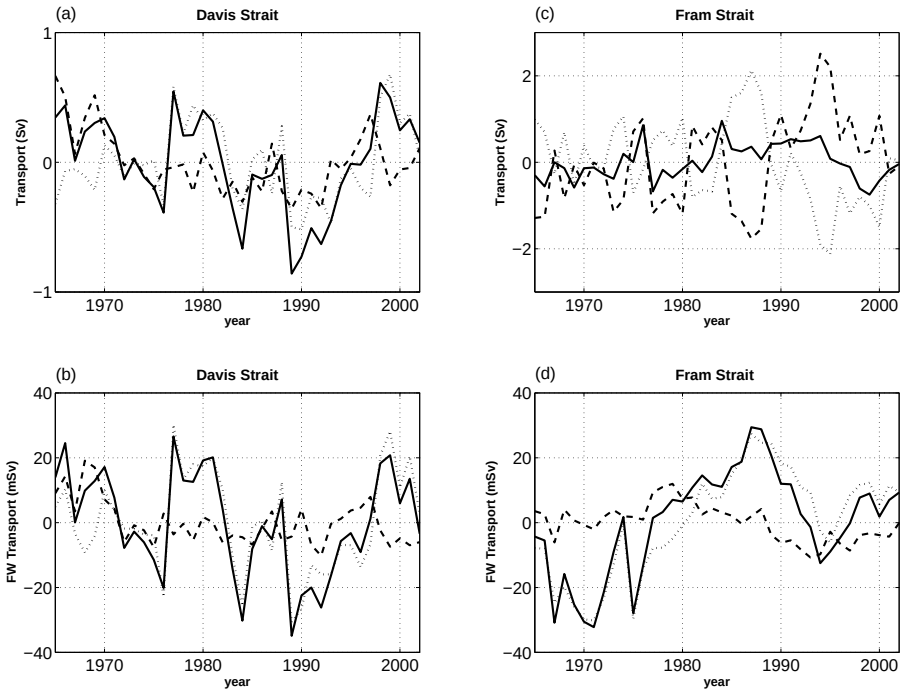

FIG. *2.11: Times series of the volume transport anomalies ((a) and (c)) and the liquid freshwater transport anomalies ((b) and (d)) across Davis Strait and Fram Strait. The net fluxes (solid lines), the northward fluxes (dashed lines) and the southward fluxes (dotted lines) are indicated. Mean values are given in Table 2.3.*

2.2.5.4 Davis Strait.

The Canadian Arctic Archipelago is a large and complex system of channels through which an important part of the Arctic freshwater export flows. Because of our limited model resolution, there is no link between the CAA and Hudson Bay, so all the freshwater flux exiting the Arctic Ocean will enter in the Labrador Sea through Davis Strait, where direct measurements of the freshwater transport exist (*Cuny et al.*, 2005). The mean flow across Davis Strait is similar to the mean flow across Fram Strait, with two branches of current flowing in opposite directions. As it enters into the Labrador Sea near Cape Farewell in the South of Greenland, the EGC becomes the West Greenland Current (WGC) and flows northward along the Greenland Coast. When it crosses the 670 meters deep Davis Strait, it splits into two branches : the main one recirculates westward with the Labrador Current, while another branch enters the Baffin Bay. On the west part of the Strait, cold and fresh water flows south from Baffin Bay with the Baffin Island Current (BIC). *Cuny et al.* (2005) studied hydrographic proprieties, volume and freshwater transport across Davis Strait, based on ship surveys and moorings deployed across the section from September 1987 to August 1990. The mean simulated salinity section (Fig. 2.10 (a)) agrees well with the observations of *Cuny et al.* (2005) : we find low salinity layers in the upper part of the section. The most important difference with observations is that

the waters in the eastern part of the strait are slightly saltier in the model. The mean circulation across Davis Strait is correctly represented as well (Fig. 2.10 (b)). Indeed, the two current veins exist in our simulation and the vertical structures are realistic. On the WGC, model velocities reach 10 cm/s, i.e. slightly less than observed (15 cm/s). It is also true in the BIC, where the maximum simulated speeds are 5 cm/s weaker than observed (15 cm/s against 20 cm/s).

The time series of the simulated sea-ice export across Davis Strait is shown in Fig. 2.9(d). *Cuny et al.* (2005) assumed that the sea-ice transport through the Canadian Archipelago and then Davis Strait is negligible, because the sea-ice is mostly land-fast. They estimated the sea-ice freshwater transport to -12.9 mSv. Our simulated ice flux is a bit larger, with a mean value of -17.1 mSv, and weak variations (std = 3.8 mSv).

As we did for Fram Strait, we decide to attribute the total northward transport to the WGC, and the southward transport to the BIC. The time series of volume and ocean freshwater transport anomalies across Davis Strait are shown in Fig. 2.11. The northward and southward contributions are also indicated. The net volume and ocean freshwater fluxes are dominated by the southward contributions, the mean WGC fluxes and their variations being negligible. Mean values agree well with estimates from *Cuny et al.* (2005) (a transport of 1.2 Sv and a freshwater transport of 38 mSv). The weaker freshwater transport is explained by higher salinity due to a salty bias in the upper Labrador Sea, also found in many other models (*Treguier et al.*, 2005). The volume and ocean freshwater transported by the Baffin Island Current (respectively -3.7 Sv and 137.6 mSv) exhibit important and similar interannual variability. These transports agree well with estimates of *Cuny et al.* (2005) and *Loder et al.* (1998), who respectively measure volume transport of -4.6 Sv and -3.3 Sv, and freshwater transport of 152 mSv and 120 mSv. The differences between the observations and our simulation are due to slower currents across the section. No long-term trend is seen on these fluxes, but the interannual variations are important, reaching 30 mSv. As for Fram Strait, the variability of the net freshwater flux is also controlled by the variations of the freshwater export by the BIC (see Fig. 2.11 (b)).

Unlike at Fram Strait, the total freshwater export through Davis Strait is due to the ocean freshwater flux, the sea-ice transport being negligible. The ocean freshwater flux has a comparable influence on the Arctic freshwater content as the ocean flux through Fram Strait, as their amplitude of variations and their correlation with the freshwater content derivative are similar.

2.2.5.5 Discussion.

Finally, the advective flux that drives the variability of the Arctic freshwater content is dominated by four single components (see Fig. 2.8). In our model, the ocean transport through Bering Strait is the only source of freshwater with an important interannual variability. The freshwater stored in the Arctic Ocean is then mostly exported to the Nordic

and Labrador Seas, across Fram Strait (as liquid freshwater and sea-ice) and Davis Strait (mostly as liquid freshwater). As we compare the times series of the liquid freshwater fluxes across the four sections (see Fig. 2.12 (b)), it seems that the most important variability is found across Fram and Davis Straits. Nevertheless, no significant correlation exists between the freshwater fluxes across the two sections. Furthermore, variations of the Pacific freshwater import through Bering Strait are not correlated with variations of the total freshwater flux exiting to the North Atlantic (through Davis and Fram Straits and the Barents section). Explanation of this absence of correlation could be then that the waters entering the Arctic Ocean are modified (become fresher) before they exit the Atlantic. To confirm this idea, we look at the time series of the volume flux anomaly across the four sections (Fig. 2.12 (a)). As expected from mass conservation, variations of the total flux exiting toward the North Atlantic are highly correlated with those at Bering Strait (correlation -0.97, significance 95%, n=23. The minus sign is explained by our transport sign convention, where a source of water for the Arctic Ocean is a positive value.). This reflects a rapid adjustment by fast surface waves rather than an advective process, since no significant lag is found when the correlation is calculated using monthly time series.

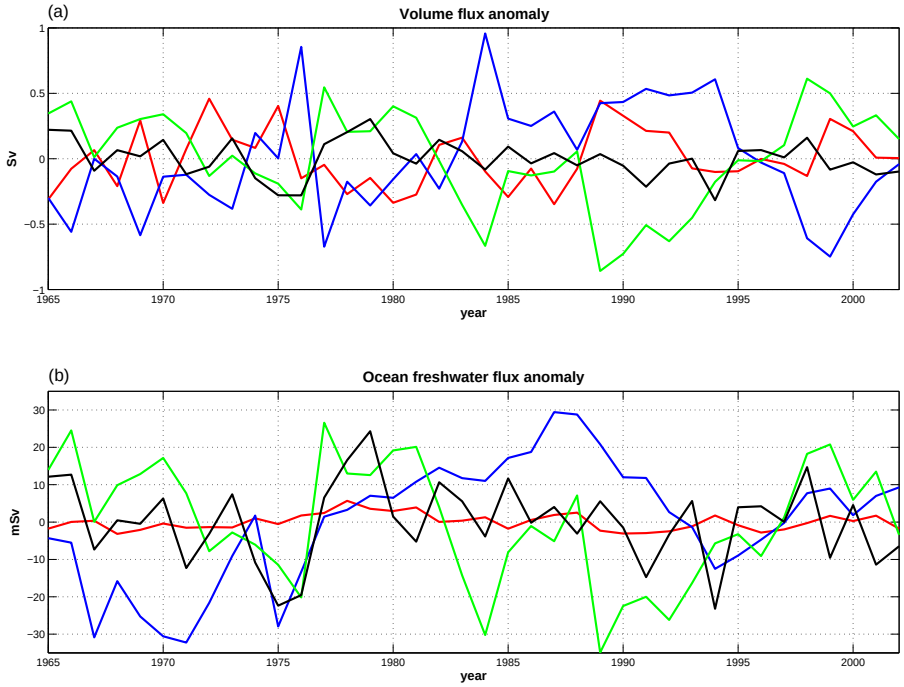

FIG. *2.12: Anomaly of the volume flux (a) and the freshwater flux (b) across the four sections enclosing the Arctic Basin : the Barents section is plotted in red, Fram Strait in blue, Davis Strait in green and Bering Strait in black.*

2.2.6 Mechanisms driving the interannual variability of the Arctic ocean freshwater export.

The remainder of the study will be focused on the freshwater export along both sides of Greenland, i.e. across Fram and Davis Straits, as they are the two most important sinks of freshwater for the Arctic Ocean. As the sea-ice transport is negligible across Davis Strait and well known and observed across Fram Strait, we will concentrate on the liquid part of the freshwater flux. We will try to identify the mechanisms responsible of the interannual variability of these two fluxes.

2.2.6.1 Davis versus Fram.

Steele et al. (1996) investigated the freshwater balance of the Arctic Ocean over a short period (1979–1985) with an ocean/sea-ice model. They found that the freshwater outflow through the CAA tends to compensate for the ocean freshwater outflow across Fram Strait, with a one year lag. Since this result is obtained for a very short period, concern about the model dependency is probably legitimate. No significant correlation or anti-correlation can be found between monthly ocean freshwater fluxes through Davis Strait and Fram Strait in our simulation for lags ranging from -5 to 5 years. However volume transport variations along both Greenland sides are strongly anti-correlated (r= -0.84, significance 95%, n=14) at zero lag. Moreover, since these two fluxes exhibit similar variations (std = 0.37 Sv for Davis Strait and std = 0.42 Sv for Fram Strait), the total volume export from the Arctic Ocean along both sides of Greenland remains almost constant in time. This anti-correlation could find its origin in the large-scale wind-forced cyclonic circulation around Greenland calculated by *Joyce and Proshutinsky* (2007), as they apply Godfrey's Island Rule to Greenland. It thus seems that the total ocean freshwater export and the total volume export are not strongly linked, unlike at Davis Strait where a high correlation was found between both fluxes (r=0.97, significance 95%, n=13). To check whether this result is model dependent, we use the EXP2 run presented in section 2. The correlation between the ocean freshwater flux and the volume flux across Davis Strait is also very high in this simulation (r=0.90, significance 95%, n=17). The fact that the Davis Strait transports of the two experiments are correlated (r=0.90, significance 95%, n=16) suggests furthermore that the variability is forced by the atmosphere and does not result from purely oceanic nonlinear instabilities or modes of variability, which would be uncorrelated between the two experiments. In contrast, the ocean freshwater flux and the volume flux across Fram Strait are not significantly correlated in both runs. The ocean freshwater flux variability across Davis Strait thus seems to be controlled by the variability of the volume transport, i.e. the velocity across the section, while the ocean freshwater flux variability at Fram Strait seems to be controlled by variations in the salinity distribution. This hypothesis is tested in the following.

2.2.6.2 Analysis of freshwater fluxes.

Freshwater fluxes depend on salinity and velocity fields. We want to determine which one of the two terms control the time variability of the freshwater transport. The fluxes across the different pathways can be broken down into different components.
We write velocity and salinity as :

$$\begin{cases} v = \overline{v} + v' \\ S = \overline{S} + S' \end{cases}$$

with $\overline{v}$ and $\overline{S}$ being the time-averaged velocity and salinity, and v' and S' being respectively the deviations from these averages. The freshwater flux can be separated into four terms as follows :

$$\begin{aligned} T_{FW} &= \iint (\overline{v} + v') \frac{S_0 - (\overline{S} + S')}{S_0} dA \\ &= \iint \overline{v} \frac{S_0 - \overline{S}}{S_0} dA - \iint \overline{v} \frac{S'}{S_0} dA + \iint v' \frac{S_0 - \overline{S}}{S_0} dA - \iint v' \frac{S'}{S_0} dA \end{aligned}$$

As we note

$$S_1 = \frac{S_0 - S}{S_0}$$

we have

$$\begin{cases} \overline{S_1} = \dfrac{S_0 - \overline{S}}{S_0} \\ S_1' = -\dfrac{S'}{S_0} \end{cases}$$

and then obtain :

$$T_{FW}(v, S_1) = T_{FW}(\overline{v}, \overline{S}_1) + T_{FW}(\overline{v}, S_1') + T_{FW}(v', \overline{S}_1) + T_{FW}(v', S_1') \tag{2.1}$$

Fig. 2.13 shows the anomalies of the various contributions to the ocean freshwater transport across Davis Strait and Fram Strait, in both runs. Means and standard deviations of each term are given in Table 2.5, as well as correlations of each contribution with the ocean freshwater flux.

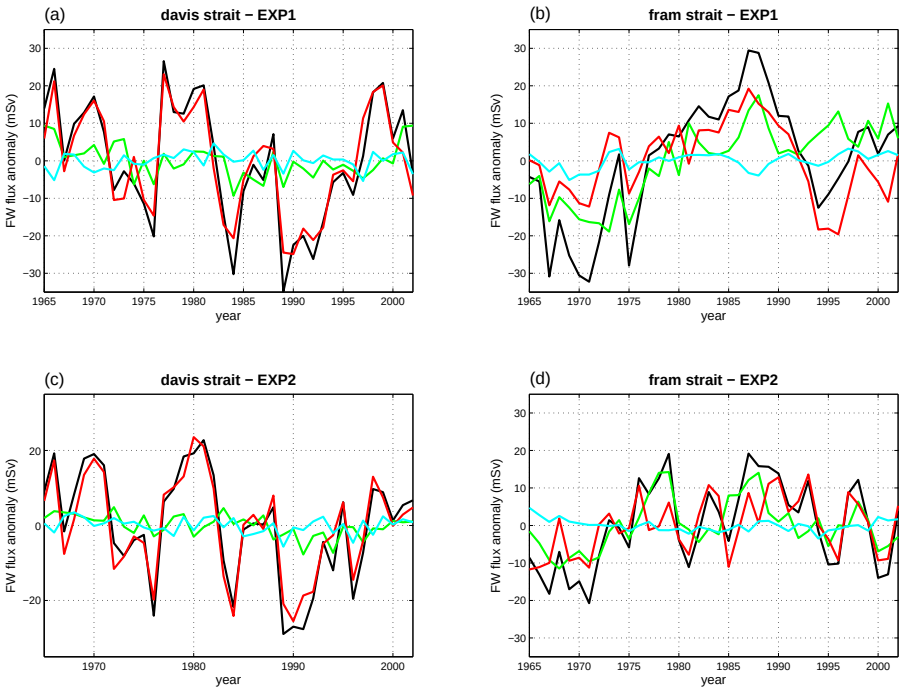

FIG. *2.13: Analysis of the ocean freshwater transport across Davis Strait (a and c) and Fram Strait (b and d) for the two runs (EXP1 for a and b, and EXP2 for c and d). Time Series of the four terms anomalies of the analysis are shown :* $T_{FW}(v, S_1)$ *in black,* $T_{FW}(v', S_1')$ *in cyan,* $T_{FW}(\overline{v}, S_1')$ *in green and* $T_{FW}(v', \overline{S}_1)$ *in red.*

Fig. 2.13 shows that the quadratic term $T_{FW}(v', S_1')$, calculated from monthly output, is stronger across Davis Strait than across Fram Strait (meanly -10,4 mSv and -1,4 mSv for the EXP1 run) but with similar standard deviations (below 3 mSv). In both runs and at both straits, quadratic components thus have a negligible contribution to the freshwater flux mean and variability.

A contrast between Fram Strait and Davis Strait appears clearly. Across Davis Strait, $T_{FW}(v', \overline{S}_1)$ anomalies are two times stronger than $T_{FW}(\overline{v}, S_1')$ anomalies in EXP1, and more than four times in EXP2 run. Across Fram Strait, both anomalies have the same order of magnitude (std around 9,8 mSv for the EXP1 run). $T_{FW}(v', \overline{S}_1)$ anomalies are correlated at 0.95 with the total ocean freshwater flux anomalies at Davis Strait, and only at 0.8 across Fram Strait (see Table 2.5). This analysis confirms that freshwater flux anomalies are mainly controlled by velocity anomalies at Davis Strait and by the variations of both salinity and velocity distributions at Fram Strait.

2.2.6.3 Origins of the exported waters.

Proshutinsky et al. (2002) suggested that the Beaufort Gyre could accumulate an important part of the freshwater content anomaly. The variability of the Sea Surface Height (SSH) anomaly in the Beaufort Gyre would thus be linked with the ocean freshwater

export from the Arctic Ocean. *Steele et al.* (1996) and *Thomas et al.* (1996) also suggest that the Beaufort Gyre has a major role in the Arctic freshwater balance. They distinguish between the Bering Strait ocean freshwater input and the runoff that would be stored on the Siberian side of the Beaufort Gyre, and the sea-ice component mostly visible in the Canadian edge of the gyre. Could the contrast between the freshwater flux variability along both sides of Greenland find its origin in the way the ocean freshwater is stored in the Arctic Ocean, especially in the Beaufort gyre ?

In the model, the correlation between the Beaufort Gyre SSH variability and the times series of the freshwater flux across Fram Strait or Davis Strait remains unsignificant at every lag. Moreover, we find a significant zero-lag correlation between the freshwater flux entering through Bering Strait and the fluxes exiting into Fram Strait and Davis Strait (respectively r=-0.52, significance 95%, n=30 and r=0.40, significance 95%, n=26). This seems to contradict the idea of *Proshutinsky et al.* (2002), who see the gyre as a 'Flywheel', where the freshwater is stored and then released trough the CAA, and Fram Strait. Our model results suggest that any storage and release happens in less than one year. A complete study of the Arctic Ocean dynamics and the characteristic time scales of the circulation remains beyond the scope of the present paper.

We now investigate why the waters exported through Davis Strait into the Labrador Sea have almost constant salinity, while it varies on the eastern side of Greenland. Fig. 2.14 shows the time-correlations between the ocean-ice flux variability and the variability of the freshwater flux trough Fram Strait. As the sea-ice melts, salinity in the upper layer of the ocean decreases and thus the freshwater export through Fram Strait increases. The area where the correlations are the strongest is also the one where the variability of the ocean-ice flux is highly correlated with the variability of the salinity in the 500 upper meters of the ocean (not shown). Moreover, the sea-ice drift pattern also shows that the most important part of the exported sea-ice through Fram Strait have get passed through this area in the North of Greenland. Salinity of waters exported through Fram Strait is then strongly dependent of their interactions with sea-ice exported by the same pathway and the way it melts on surface, while waters exiting through Davis Strait are less influenced by this and their salinity is roughly constant.

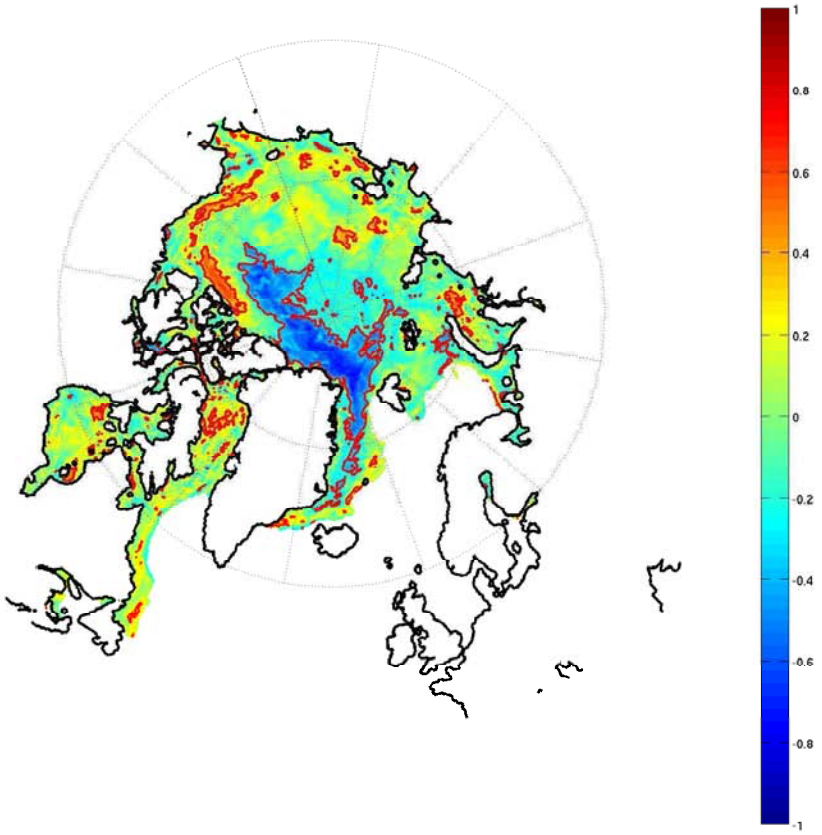

FIG. *2.14: Correlation between the ocean freshwater flux through Fram Strait and the ocean-ice flux over the Arctic domain. Calculations are done over the 1965–2002 period for the EXP1 run. The 95% significance level is indicated in red (based upon 36 degrees of freedom, which is an upper limit).*

2.2.7 Conclusions.

Direct observations of the Arctic Ocean hydrographic properties and circulation are still limited and insufficient to understand the mechanisms responsible for their variability. Here we have used a global ocean/sea-ice coupled model to investigate the freshwater budget of the Arctic Ocean and analyze the variations of its different components. A validation of the hindcast simulation has been done, examining the mean state of the Arctic Ocean proprieties and circulation, and comparing the mean freshwater budget over the 1965–2002 period, with previous estimates from direct observations of the various sources and sinks. As the model reproduces the already observed components of the Arctic freshwater and mass budgets with reasonable accuracy, we focus on the interannual variability of the different components. A limitation of our model however is the fact that the interannual variability in river runoff and precipitation is excluded.

Sea-ice and ocean freshwater advective contributions have been quantified across the four

sections enclosing our domain : Bering Strait, Davis Strait, Fram Strait and a section across the Barents Sea. The mean circulation across these four transects is reproduced remarkably well, thanks to the fine model resolution. The freshwater inflow through Bering Strait is the only source that drives an important part of the simulated Arctic freshwater content variability. Ocean and sea-ice freshwater transports at Fram Strait have similar magnitudes.

A special interest has been given to the Arctic freshwater exports along both sides of Greenland, where time varying volume fluxes are highly anti-correlated. The net ocean freshwater flux variability is controlled by the variability of the freshwater export through Fram and Davis Straits. Freshwater flux variations are controlled by velocity variations at Davis Strait, and by both salinity and velocity variations across Fram Strait.

Our study provides a synthesis of the freshwater storage and export of the Arctic Ocean. Liquid freshwater enters the Arctic through Bering Strait, runoffs and precipitation. As the liquid freshwater flux entering through Bering Strait is only partly correlated with the total freshwater flux exiting into the North Atlantic (r=0.44, significance 95%, n=27), it seems that the waters are modified while they cross the Arctic Ocean. It is clearly the case for the waters exported through Fram Strait. Their salinity is strongly influenced by the melt and the formation of sea-ice along the northern side of Greenland. The role of the Beaufort Gyre does not appear clearly in the present study, but this was also noted by *Häkkinen and Proshutinsky* (2004) in a coarser resolution model. A more detailed analysis of the dynamics of the Arctic Ocean and the time scales associated with freshwater storage will be the subject of a forthcoming paper.

Acknowledgement This study uses numerical experiments carried out within the DRAKKAR project. EXP1 has been run at the IDRIS CNRS computer centre in Orsay, France, by J.M. Molines. The integration of the experiment EXP2 has been performed at the Höchstleistungsrechenzentrum Stuttgart (HLRS) by A. Biastoch. C. Lique is supported by CNES and IFREMER. A.M. Treguier and T. Penduff are supported by CNRS. The model integration and the analysis by M. Scheinert was supported by the BMBF Nordatlantik project 03F0443B AP3.2. We also thank C. Herbaut and M.N. Houssais for useful discussions.

2.2.8 Appendix : Details on the freshwater balance.

The liquid freshwater stored in our domain is computed as :

$$FW_{liq} = \iiint \frac{S_0 - S}{S_0} dV$$

where V is the volume of the domain, S is the salinity calculated by the model, and S_0 is a reference salinity, here equal to a value of 34.8 psu (this choice will be discussed later). As we assume a constant sea-ice salinity S_{ice} of 6 psu, the sea-ice freshwater content is defined as :

$$FW_{ice} = \frac{S_0 - S_{ice}}{S_0} V_{ice} \times \frac{\rho_{ice}}{\rho_{water}}$$

where V_{ice} is the sea-ice volume, ρ_{ice} the sea-ice density (900 kg.m^{-3}) and ρ_{water} the density of water (1000 kg.m^{-3}).. The freshwater transport across a section is defined as the sum of two contributions, the ice part and the liquid part :

$$T_{FW} = T_{FWliq} + T_{FWice}$$

$$T_{FW} = \iint U \frac{S_0 - S}{S_0} dA + \int \frac{(S_0 - S_{ice})}{S_0} \times \frac{C_{ice}}{100} \times \frac{\rho_{ice}}{\rho_{water}} \times U_{ice} \times dh$$

with U being the speed across the section of area A, U_{ice} the ice velocity, h the ice thickness, C_{ice} the sea-ice concentration.
The freshwater balance of the area can be expressed as follows :

$$FW(t) = \int \delta t \left\{ T_{FW}(Bering) + T_{FW}(Barents) + T_{FW}(Fram) + T_{FW}(Davis) \right\} + \int \delta t \left\{ (E - P - R) + DP \right\}$$

with $E - P$ representing the surface evaporation rate minus the precipitation rate over the whole surface of the domain, R being the runoff and DP being the surface damping.

The definition of the freshwater fluxes and contents are strongly dependent on a reference salinity, S_0. For this study, we choose 34.8 psu as the reference salinity, mostly as to follow *Aagaard and Carmack* (1989). This salinity is considered as being a reasonable estimate of the mean Arctic salinity and is the most commonly adopted in the literature. In this way, when we will consider the exchanges between the Arctic Ocean and the subpolar area, the sign of the freshwater fluxes will indicate if the flux represents a sink or a source of freshwater for the Arctic Ocean, regardless the direction of the volume fluxes.

Chapitre 3

Évolutions récentes du bilan d'eau douce du Bassin Arctique.

3.1 Préambule

A la fin de l'été 2007, l'extension de la banquise a atteint un niveau minimum jamais vu depuis le début des observations satellites (*Comiso et al.*, 2008). Les causes de cet événement sont multiples, et ont été très largement décrites dans la littérature ces trois dernières années. En particulier, les rôles du vent (*Ogi et al.*, 2008), du flux radiatif solaire absorbé par les couches de surface de l'océan (*Perovich et al.*, 2008), de la couverture nuageuse (*Schweiger et al.*, 2008), mais aussi du préconditionnement de la banquise (diminution de l'épaisseur et remplacement des glaces pérennes par des glaces saisonnières (*Drobot et al.*, 2008; *Zhang et al.*, 2008)) ont été documentés. Il semble en fait que ce soit la concomitance de plusieurs phénomènes indépendants qui ait entraîné cet événement spectaculaire.

Si les causes du minimum de glace en 2007 sont donc bien comprises, les conséquences de cet épisode, en particulier pour l'océan, sont elles encore largement méconnues. Ce sont les répercussions éventuelles pour le contenu halin du bassin arctique que nous examinons dans ce chapitre. On tente en particulier de répondre aux questions suivantes :

– Peut on mettre en évidence un signal dans le bilan d'eau douce de l'océan Arctique consécutif à la fonte importante de glace de mer de l'été 2007 ? En d'autres termes, l'équilibre du bilan d'eau douce de l'océan Arctique que nous avons décrit dans le chapitre précédent a-t-il ou peut-il être perturbé par un événement de ce type ?
– Y'a-t-il eu une modification des exports d'eau douce ou de glaces de mer vers l'Atlantique Nord après cet épisode ? On cherche ici à voir si le signal d'une fonte importante de la banquise en Arctique peut, en étant exporté vers le sud, avoir des répercussions sur l'océan à l'échelle globale et sur le climat.

Les publications citées précédemment sur les causes du minimum de glace de 2007 sont principalement basées sur des observations. Au moment où nous avons débuté cette étude, très peu de modélisateurs parviennent à reproduire convenablement l'événement de 2007, et les données océaniques publiées des années post 2007 sont rares. Ceci explique donc qu'il n'existe que peu d'études sur les conséquences du minimum de glace de 2007 pour l'océan. Ici, nous analysons une réanalyse océanique des années 2002–2008 réalisée dans le cadre du projet GLORYS (GLobal Ocean ReanalYsis and Simulations). Une première évaluation de la simulation nous a permis d'évaluer la capacité du modèle à reproduire correctement l'événement de 2007, et nous avons donc pu continuer notre analyse. De plus, les grandes similarités entre le modèle utilisé ici et celui analysé au chapitre précédent nous permet de replacer l'événement de 2007 dans un contexte temporel plus large.

L'étude est présentée sous la forme d'un article resoumis après révisions à *Journal of Climate* en septembre 2010.

3.2 Article : Evolution of the Arctic Ocean salinity, 2007–2008 : Contrast between the Canadian and the Eurasian basins (C. Lique, G. Garric, A.M. Tréguier, B. Barnier, N. Ferry, C. E. Testut et F. Girard-Ardhuin, *En révision pour Journal of Climate*, 2010b)

Abstract : We investigate the variability of the salinity in the Arctic Ocean and in the Nordic and Labrador Seas over recent years, to see how the freshwater balance in the Arctic and the exchanges with the North Atlantic have been affected by the recent important sea ice melting, especially during the 2007 sea ice extent minimum.
The GLORYS1 global ocean reanalysis based on a global coupled ocean/sea ice model with an average resolution of 12 km grid in the Arctic Ocean is used in this regard. Although no sea-ice data and no data under sea-ice are assimilated, our simulation over the 2001-2009 period is shown to represent fairly well the 2007 sea ice event and the different components accounting for the ocean and sea ice freshwater budget, compared to available observations. In the reanalysis, the 2007 sea ice minimum is due to an increase of the sea ice export through Fram Strait (25%) and a important sea ice melt in the Arctic (75%).
Liquid freshwater is accumulated in the Beaufort Gyre after 2002, in agreement with recent observations, and we show that this accumulation is due to both the sea ice melt and a spatial redistribution of the freshwater content in the Canadian Basin.
In the Eurasian Basin, we find a very contrasted situation with an increase of the salinity. The effect of the sea ice melt is counterbalanced by an increase of the Atlantic inflow, and a modification of the circulation north of Fram Strait after 2007. We suggest that a strong anomaly of the atmospheric conditions was responsible for this change of the circulation.

3.2.1 Introduction.

The Arctic Ocean is the main reservoir of freshwater on the world ocean, as it collects and stores large amount of freshwater received mainly from large river discharge, inflow of low salinity water from the Pacific Ocean through Bering Strait and net precipitation over the Arctic Basin. The freshwater is then released to the North Atlantic, as sea ice and low salinity water export along both sides of Greenland, through Davis Strait and Fram Strait. This freshwater balance of the Arctic Ocean has received much attention in recent years, as we expect that just a small change of one component of the freshwa-

ter budget could affect the strength of the Atlantic meridional overturning circulation (e.g., *Aagaard and Carmack* (1989); *Jones and Anderson* (2008)) and therefore possibly modulate the global climate. *Serreze et al.* (2006) have recently presented a summary of the current estimations from observations (or from model results when observations were not available) of the different sources and sinks of freshwater for the Arctic Ocean. In this paper, they underline the lack of long term measurements for most of the freshwater budget components, that makes difficult to know the variability of the different terms, or to detect their possible long term trend. However, substantial changes seems to have recently affected different components of the Arctic freshwater system, such as an intensification of the hydrological cycle (increases of river discharge, Greenland ice melting and precipitation, see for instance *Peterson et al.* (2006)) or changes in the Arctic hydrographic properties (e.g., *Steele and Boyd* (1998); *Swift et al.* (2005)). A synthesis of the observed changes in the Arctic freshwater system over the last century can be found in *White et al.* (2007).

The only well-observed component of the Arctic freshwater system is probably the sea ice cover. From satellite records, *Cavalieri et al.* (2003) reported on a large decline of the sea ice extent since the late 1970's, that strongly accelerates over the last decade. At the end of the summer in 2007, the Arctic sea ice has retreated to an unprecedented minimum during the nearly 30 years of satellite observations (*Comiso et al.*, 2008), the sea ice extent being 25% lower than during the previous minimum record in September 2005 (Fig. 3.1 (a)). This new record is related to a number of factors, including atmospheric conditions as well as a preconditioning of the sea ice, due to the thinning of multi-year sea ice or the replacement of multi-year ice by first-year ice in previous years (*Drobot et al.*, 2008; *Zhang et al.*, 2008). Over the same period, the sea ice thickness has also strongly decreased (*Rothrock et al.*, 1999; *Kwok et al.*, 2009), even though this quantity remains poorly observed, what makes difficult to evaluate from observations the variability of the sea ice volume in the Arctic.

In the present study, we use the GLORYS1 global ocean reanalysis (*Ferry et al.*, 2010) which covers the period 2002–2008 to map changes in Arctic salinity, to quantify the amount of freshwater corresponding to the 2007 sea ice melt, and to compare the state of the Arctic freshwater balance before and after this event, in order to emphasize its possible impact for the Arctic Ocean or the subarctic region.

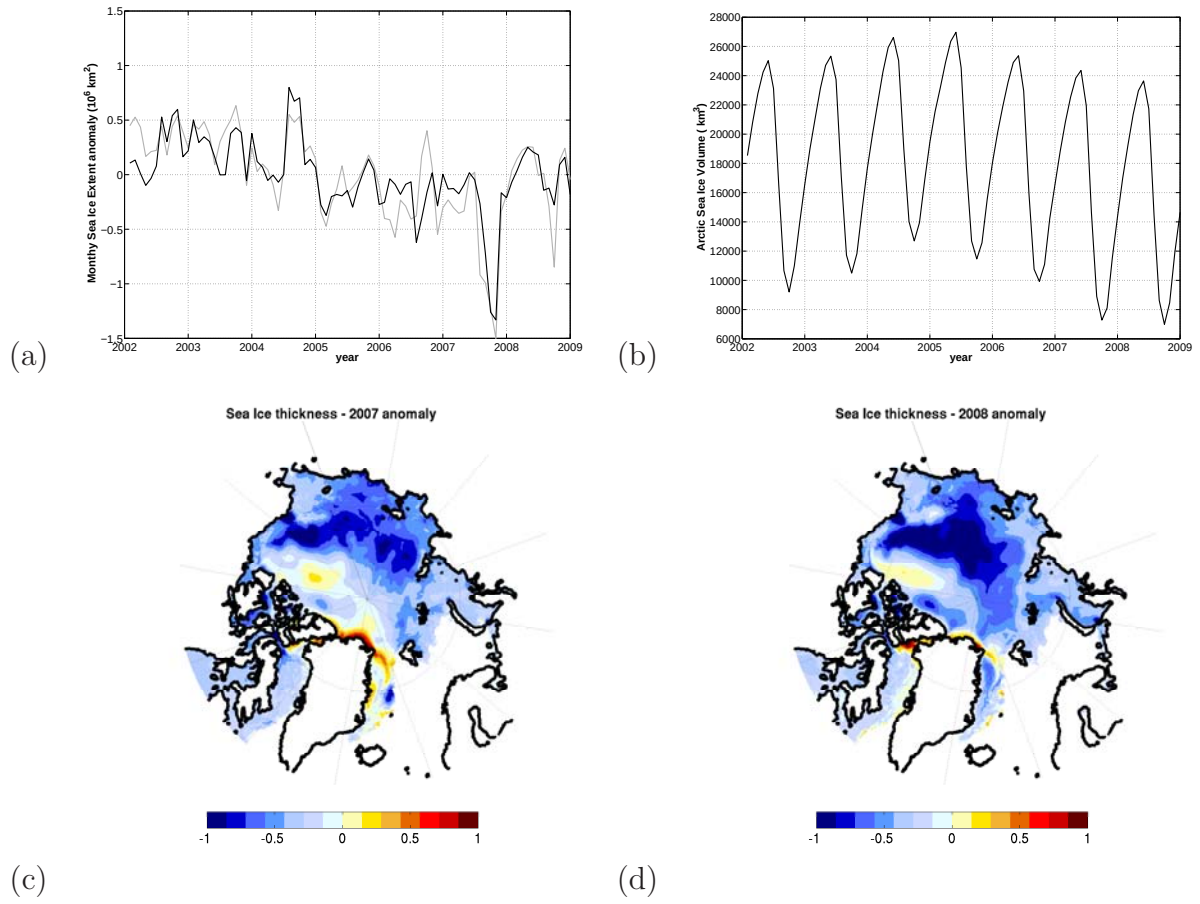

FIG. *3.1: GLORYS1 monthly Arctic Sea Ice Extent anomaly (a) and Volume (b). NSIDC observed Sea Ice Extent is superimposed in gray for direct comparison (Fetterer et al., 2002, updated 2009). The sea ice volume can be compared to Kwok et al. (2009) (Fig.5). Sea ice thickness anomalies (meters) in 2007 (c) and 2008 (d). "Anomaly" refers to the difference with the average over 2002–2006.*

3.2.2 GLORYS1 : 2002–2008 global ocean reanalysis.

In this study we use GLORYS1 global ocean reanalysis (*Ferry et al.*, 2010) which is a global ocean eddy permitting model simulation constrained by data assimilation produced in the framework of the French GLobal Ocean ReanalYsis and Simulations (GLORYS) project and MyOcean European FP7 project. We present in the following the main features of the model and data assimilation scheme used in GLORYS1V1 reanalysis.

The global ORCA025 coupled ocean/sea-ice model configuration described in *Barnier et al.* (2006) is used to perform the reanalysis. It is based on the NEMO numerical framework version 1.09. (*Madec*, 2008), including the LIM2 sea ice model. Note that the standard LIM2 version described in *Fichefet and Morales Maqueda* (1997) has been improved here by including the Elastic Viscous Plastic (EVP) dynamics of the ice (*Hunke*

and Dukowicz, 1997), and computing the ocean-ice stress at each time step. This model configuration uses a global tripolar grid with 1442x1021 grid points and 50 vertical levels. Vertical grid spacing is finer near the surface (1 m) and increases with depth to 450 m at the bottom. Horizontal resolution is 27.75 km at the equator, 13.8 km at 60°N , and gets to 10 km in the Arctic Ocean.

The simulation runs from October 2001 to February 2009 with assimilation of oceanic data. The ocean is initialized from rest with temperature and salinity distributions from the ARIVO 2005 climatology (*Gaillard and Charraudeau*, 2008). The sea ice is initialized from a snapshot (2nd of October 2001) of a longer simulation performed by the DRAKKAR project (ORCA025-G70, *Lique et al.* (2009)). The surface forcing is based on daily atmospheric fields from the operational ECMWF analysis and forecasts (1-day averages) with corrections of tropical rainfalls (*Troccoli and Kallberg*, 2004; *Garric*, 2006). The CLIO bulk formulation (*Goosse et al.*, 2001) is used to evaluate the atmosphere/ocean and atmosphere/sea ice fluxes as in *Barnier et al.* (2006). In particular, details about the coupling between ocean and sea ice could be found in (*Goosse et al.*, 2001). River runoff rates are prescribed using the *Dai and Trenberth* (2002) climatological dataset. A relaxation of sea surface salinity to the PHC monthly climatology (*Steele et al.*, 2001a) is added under sea ice, and the coefficient (0.25 m/day) amounts to a decay time of 40 days for 10 m of water depth.

The ocean model is constrained by the Mercator-Océan data assimilation system version 2 which is a reduced order Kalman filter following the SEEK formulation (*Pham et al.*, 1998) used in numerous ocean eddy permitting simulations (e.g. *Testut et al.* (2003); *Tranchant et al.* (2008)). This approach has been used for several years at Mercator-Océan and has been implemented in different ocean model configurations like the PSY3V2 1/4° global ocean operational analysis forecasting system. The SEEK formulation requires knowledge of the forecast error covariance of the control vector. In GLORYS1, this vector is composed of the barotropic height field and the 3-dimensional temperature, salinity, zonal and meridional velocity fields. The forecast error covariance is based on the statistics of a collection of ocean state anomalies (typically 300) and is seasonally dependent. The length of the assimilation cycle is 7 days and the data assimilation produces, after each analysis, global increments for the ocean barotropic height, temperature, salinity, zonal and meridional velocity. An Incremental Analysis Update (IAU) method (*Bloom et al.*, 1996) is used to apply the increment in order to reduce the spin up effects after the analysis time. The reader is referred to (*Ferry et al.*, 2010) for a more detailed description of the simulation, data assimilation method and validation.

The assimilated observations are Sea Surface Temperature (SST) maps from the daily

NCEP RTG 1/2° product (*Thiebaux et al.*, 2003), along track altimetric data provided by SSALTO/DUACS originating from Topex/Poseidon, ERS-2, GFO, Envisat and Jason-1 satellites, and in situ temperature and salinity profiles (including XBTs, CTDs, Argo data, TOGA/TAO and PIRATA moorings, etc...) from the CORA02 in situ database distributed by Coriolis Global Data Assembly Center (http ://www.coriolis.eu.org/cdc/).

It is worth noting that under sea ice and or when the observed SST is below -1°C , no data is assimilated at all. So, no in situ profile is assimilated within the Arctic domain studied, except near the Alaskan Arctic coast during summer 2008 where a few XBTs are assimilated during summer. However, we checked that the salinity increments are weak and do not contribute significantly to the Arctic freshwater budget. Thus the Arctic region in GLORYS1 reanalysis can be considered as a "free" regional model forced with reanalyzed boundary conditions, in which the only constraint by the observations in the sea surface salinity restoring under sea ice.

We first evaluate the capacity of GLORYS1 global ocean reanalysis at reproducing the observed Arctic sea ice extent and especially the 2007 minimum (Fig. 3.1(a) and the following section), as well as its performance at simulating the Arctic freshwater system (Table 3.1). We define the Arctic Ocean as the area enclosed by the following transects across ocean straits : the Bering Strait, a section across the Barents Sea between Norway and Svalbard Island (following the 20°E meridian), Fram Strait and Davis Strait (Fig. 3.2).

FIG. *3.2: Arctic Ocean and localization of the main place names used in the text. The domain is enclosed by four sections : the Bering Strait, the Davis Strait, the Fram Strait, and the Barents Sea Opening. The dotted line indicated the separation between the Canadian and the Eurasian Basins, alo,g the Lomonosov Ridge. Bathymetry contours 500, 1000, 2000, 3000, 4000 and 5000 m are drawn with a thin line. The 500 m contour delimits the shelves from the interior of the Basins.*

TAB. *3.1: Arctic Ocean freshwater budget from different sources. All FW fluxes are given in km^3/yr. Means are calculated from monthly output, with 34.8 as a reference salinity. The sign convention is such that a source of freshwater for the Arctic Ocean is a positive value. Atmospheric forcing is the sum of the two terms : P-E (2744 km^3/yr) and the damping (410 km^3/yr). Results from Lique et al. (2009) and from observations are also shown for comparison. All observational values are taken from Serreze et al. (2006) who provide a 'best' estimates among the different values given in the literature, except for flux through Davis Strait, which are based on Cuny et al. (2005). Note that the value indicated here for model estimation of the freshwater flux through Davis Strait differs from the value given in Lique et al. (2009) as we include in this term the contribution of the connection with Hudson Bay which is open by one grid point (contrary to what was said in Lique et al. (2009) (Table 1). Over a long period (1965-2002) the sum of the budgets terms (168 km^3/yr) roughly equals the freshwater content change between January 1965 and December 2002 (95 km^3/yr).*

Budget Term $S_{ref} = 34.8psu$ (km^3/yr)	**2002–2006 average**	**1965–2002 average from *Lique et al.* (2009)**	**Observations**
Atmospheric forcing	3154	3119	2000
Runoffs	3688	3406	3200
Ocean Transport			
Bering Strait	2889	3021	2500
Davis Strait	-4390	-4345	-3500
Fram Strait	-1230	-1990	-2400
Barents Sea Opening	-719	-255	-90
TOTAL	**-3450**	**-3569**	**-3490**
Ice Transport			
Bering Strait	205	132	100
Davis Strait	-341	-539	-410
Fram Strait	-940	-2179	-2300
Barents Sea Opening	-47	-201	–
TOTAL	**-1123**	**-2788**	**-2810**

The definitions used in this study for the freshwater content and the freshwater fluxes are similar to the one used in *Lique et al.* (2009), with the same reference salinity of 34.8. The total freshwater content stored in our domain is thus computed as :

$$FWC = FWC_{liq} + FWC_{ice} = \iiint \frac{S_{ref} - S}{S_{ref}} dV + \frac{S_{ref} - S_{ice}}{S_{ref}} \times V_{ice} \times \frac{\rho_{ice}}{\rho_{water}}$$

where V is the volume of the domain, S is the salinity calculated by GLORYS1, and S_{ref} is the reference salinity, S_{ice} is the sea-ice salinity (constant and equal to 6 psu) and V_{ice} is the sea-ice volume.

The values for the 2002–2006 average of the different components accounting for the Arctic freshwater balance are listed in Table 3.1. In a previous paper, we have analyzed the variability of the Arctic freshwater budget over the period from 1965 to 2002 in a simulation run with a similar set-up of the same model without assimilation of observations and a different atmospheric forcing (*Lique et al.*, 2009). Results from observations and from this previous study are also shown for comparison. The simulated Arctic freshwater budget of the GLORYS1 reanalysis for the recent period is in general agreement with the observational budget of *Serreze et al.* (2006), and comparable with the mean budget calculated by *Lique et al.* (2009). The main difference between the GLORYS1 results and the observational budget by *Serreze et al.* (2006) is the smaller simulated liquid and sea ice freshwater export through Fram Strait. However, this could be explained, at least partly, by the different periods used to average the fluxes. The time series of the sea ice and liquid freshwater exports through Fram Strait presented in *Lique et al.* (2009) shows periods when the sea ice and liquid freshwater contributions are as low as the GLORYS1 values. The freshwater flux through the Barents Sea Opening given by the GLORYS1 reanalysis represents a larger sink of freshwater than in the observations and in the budget presented in *Lique et al.* (2009). The difference with the latter study is due to an overestimation of the Atlantic inflow intensity (by about 1 Sv more) through the section. We examine the contribution to the surface forcing from the salinity restoring to the climatology. At a seasonal time scale, its variations are anticorrelated with the fluctuations of the sea ice /ocean flux, but its maximum remains smaller by about a factor of five. As the restoring acts as a damping, the variability for the freshwater content in the reanalysis is somehow smaller than it would be without restoring. Thus this term is not driving an important part of the Arctic freshwater content variability in the reanalysis, even though its amplitude can be locally large, especially where and when the sea ice /ocean flux is large. The freshwater budget averaged over 2002-2006 is largely unbalanced contrary to the budgets from *Lique et al.* (2009) and from observations. As the period considered here is short, we do not expect that the freshwater content (as liquid and sea ice forms) would remain constant. The accumulation sustained over 2002-2006 is of the order of magnitude of what could be seen in some years in Fig. 6 of *Lique et al.* (2009). However, as the run starts in October 2001, we also acknowledge that part of this trend could be unrealistic and consists of the model initial adjustment.

3.2.3 Quantification of the 2007 sea ice melt.

In September 2007, satellite observations of the sea ice extent have revealed that the Arctic sea ice extent has reached a record minimum of 4.1 million km^2 (*Comiso et al.*, 2008). GLORYS1 reproduces fairly well the 2007 sea ice minimum, as well as the variability of the sea ice extent (Fig. 3.1(a)). The simulated monthly ice extent anomalies are highly correlated with satellite observations over 2002–2008 (r=0.84), even though the

TAB. *3.2: Liquid and sea ice freshwater contents, and contribution from the Canadian and Eurasian Basin. In the Canadian Basin, contributions from the shelves and the interior are also indicated, the interior being defined by the area deeper then 500m. Means are calculated from monthly output, with a reference salinity of 34.8, and for the whole water column from the surface to the bottom (negative contributions the the liquid FW content are allowed). See Fig. 3.2 for the definitions of the two basins.*

Freshwater Content (km^3)	**2002–2006 average**	**2007**	**2007 anomaly**	**2008**	**2008 anomaly**
Ice : Canadian Basin	10398	9552	-846	9241	-1057
Interior	6394	5806	-588	5395	-999
Shelves	4004	3746	-258	3846	-58
Ice : Eurasian Basin	3984	3212	-772	3173	-811
Ice : Total	14382	12764	-1618	12414	-1968
Liquid : Canadian Basin	50424	51123	+699	51464	+1040
Interior	26336	27693	1357	28244	+1908
Shelves	24088	23430	-658	23220	-868
Liquid : Eurasian Basin	1057	-314	-1371	-738	-1795
Liquid : Total	51481	50809	-672	50726	-755
Total	65863	63573	-2290	63140	-2723

reanalysis globally overestimates the Arctic Sea ice extent by 7% on average.

Until now, there were only sparse observations both in time and space of the sea ice thickness, and it was thus difficult to validate the sea ice thickness and volume computed in numerical models. Recently, *Kwok et al.* (2009) provide us with one of the first estimate of the spatial distribution of sea ice thickness from 10 campaigns of the ICEsat satellite, and thus with an estimation of the Arctic Sea ice volume over the recent period, even though the uncertainty remains huge on this quantity. When compared to satellite observations from *Kwok et al.* (2009) (their Fig. 7), the reanalysis seems to capture well both the spatial pattern and the amplitude of the sea ice thickness, as well as their variability (not shown here).

We thus use the GLORYS1 outputs to estimate the Arctic sea ice volume and its variability (Fig. 3.1(b)). The values and the tendency calculated from GLORYS1 are again similar to those found by *Kwok et al.* (2009) (their Fig. 5(f)). From 2006 to 2007, the sea ice volume in the Arctic has decreased by 1566 km^3 on a year average, and 471 additional km^3 of sea ice volume has been lost between 2007 and 2008. It corresponds to an equivalent of 1248 and 375 km^3 of freshwater respectively, the conversion from sea ice volume to freshwater content being done following the definition given in the previous section. This is due to both a decrease of the sea ice extent (Fig. 3.1(a)) and of the sea ice thickness (Fig. 3.1(c)&(d)).

To have an idea of the freshwater signal magnitude due to the sea ice volume decrease (a loss of 1623 km^3 of freshwater from 2006 to 2008), one can compare this quantity to the 2000 km^3 anomaly of freshwater exported through Fram Strait in two years, that was estimated to be on the origin of the episode of Great Salinity Anomaly (GSA) observed during the 1970's in the North Atlantic (*Dickson et al.*, 1988). Hence, one could imagine that, if the total of the 2006–2008 freshwater anomaly were exported or were about to be exported to the North Atlantic, we could expect to observe a GSA-like signal in the subpolar region. We thus examine the Arctic freshwater budget for the year 2007 and 2008 relative to the 2002–2006 period, to track the freshwater signal corresponding to the sea ice melt and find out whether this anomaly has been absorbed into the Arctic Ocean or possibly exported to the subpolar region.

First of all, we determine the area where we can expect the most important impact for the sea ice melt. In GLORYS1, the export of sea ice increases in 2007 (compared to the 2002–2006 average shown in Table 3.1) by 25% through Fram Strait and 20% through Davis Strait and thus 315 and 66 additional km^3 of freshwater are respectively exported in this year. As the 2007 anomaly of freshwater content corresponding to sea ice is 1618 km^3 lower than the 2002–2006 average (Table 3.2), the increase of the sea ice export is responsible of about 25% of the sea ice freshwater content decrease, and thus sea ice melt accounts for the remaining 75%. This is consistent with the result of *Zhang et al.* (2008) who find in their model that atmospheric conditions in 2007 lead to an increase of the ice volume export at Fram Strait, that is responsible for 30% of the 2007 sea ice volume decrease over the Arctic. The spatial pattern of the sea ice extent in September 2007 (both from satellite observations and from GLORYS1) suggests that the sea ice melt might have mostly occurred in the Canadian Basin. This is confirmed in our reanalysis as the ocean/sea ice flux increases mostly in the Canadian Basin whilst the sea ice is melting (not shown). This is also consistent with the sea ice thickness decrease in this part of the Arctic Basin (Fig. 3.1(c)&(d)). In the following section, we look for the possible changes in salinity and freshwater content in this basin. We consider that the Canadian part of the Arctic Ocean is delimited by the Lomonosov Ridge, Bering Strait and Davis Strait.

3.2.4 Freshwater content changes in the Canadian Basin.

In two recent papers, *Proshutinsky et al.* (2009) and *McPhee et al.* (2009) provide unprecedented description of spatial and temporal variability of the salinity in the Beaufort Gyre from observations during the 2000's. They find an important accumulation of freshwater in the very recent years (from 2003 to 2007 (*Proshutinsky et al.*, 2009) and in 2008 (*McPhee et al.*, 2009)). One could expect that the freshwater increase in the Beaufort Gyre would be related to the sea ice melt. However, both studies underline the predominant role of the atmospheric circulation for this freshwater accumulation : Ekman

pumping process is enhanced during these years due to the persistence of Arctic High anticyclonic circulation.

Fig. 3.3 shows the 2002–2006 average freshwater content (a) and the 2007 (c) and 2008 (d) anomalies. To allow direct comparison with *Proshutinsky et al.* (2009) and *McPhee et al.* (2009), freshwater content is computed from the surface to the uppermost level where the salinity equals the reference salinity (S_{ref} = 34.8). The freshwater content calculated from the PHC climatology (*Steele et al.*, 2001a) is also shown for comparison (Fig. 3.3(b)).

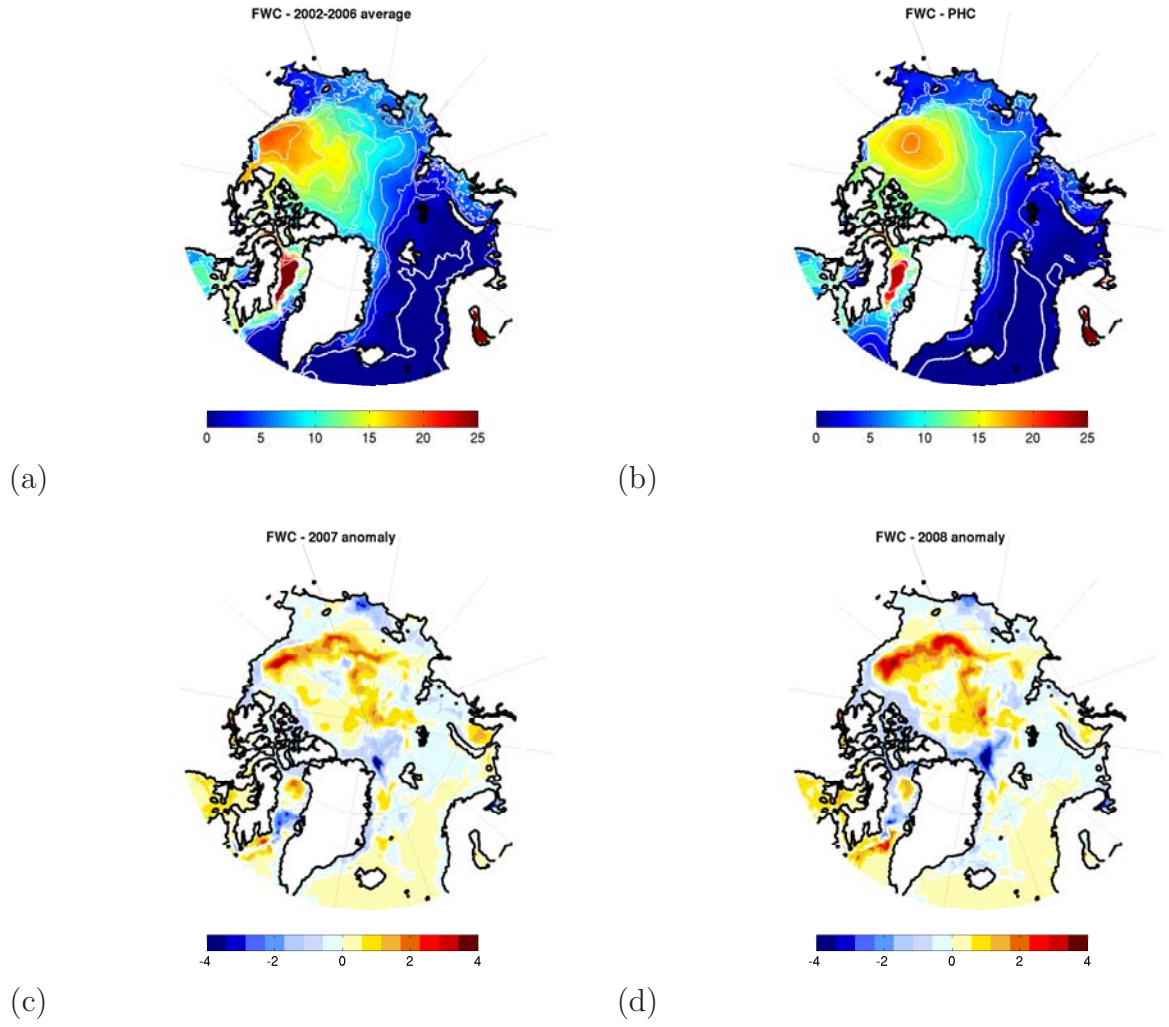

FIG. *3.3: (a) and (b) – mean freshwater content (FWC, meters) from 2002 to 2006 model results and from PHC climatology, respectively. (c) and (d) – FWC anomalies (meters) from model results (relative to 2002-2006) for 2007 and 2008, respectively.*

Compared to the PHC climatology, the GLORYS1 average (Fig. 3.3(a)) presents similar spatial pattern (Fig. 3.3(b)), but the freshwater content in the Beaufort Gyre is higher

for the GLORYS1 average than in PHC. The difference could be explained by the fact that the climatology is heavily weighted toward the decade of the 1970s and 1980s, when the freshwater content in the Beaufort Gyre was shown to be smaller than in the 2000's, as it has been previously underline by *Proshutinsky et al.* (2009). Despite the different period represented by GLORYS1 and PHC, mean freshwater content calculated from both GLORYS1 and PHC shows that most of the freshwater in the Arctic is stored in the Beaufort Gyre in the Canadian Basin.

Compared to the 2002-2006 average, the freshwater content in the Beaufort Gyre increases up to 3 and 4 meters in 2007 and 2008, respectively (Fig. 3.3(c)&(d)). *Proshutinsky et al.* (2009) and *McPhee et al.* (2009) observed very similar increases of the freshwater content in the Beaufort Gyre in 2007 and 2008 respectively (see Fig. 9 in *Proshutinsky et al.* (2009) and Fig. 1 in *McPhee et al.* (2009)). If we consider the whole water column (and thus allow negative contribution to the liquid freshwater content), the Canadian Basin gains 699 km^3 of liquid freshwater in 2007 compared to the average, and 341 km^3 more of freshwater in 2008 (Table 3.2, these amounts are 573 and 307 km^3 of freshwater if we choose to take the same definition as the one used for the Fig. 3.3 and in *Proshutinsky et al.* (2009)).

Hence, the variability of the total freshwater content is very small in the Canadian Basin, as the loss of freshwater from sea ice in this basin in 2008 compared to the 2002–2006 average (-1057 km^3) is balanced by the gain of liquid freshwater in 2008 compared to the 2002–2006 average (+1040 km^3). The spatial patterns of the 2007 and 2008 freshwater content anomalies (Fig. 3.3(c)&(d)), as well as the quantification of the freshwater anomalies on the shelves and in the interior of teh Canadian Basin (Table 3.2) are also consistent with the hypothesis of *Proshutinsky et al.* (2009) regarding the role of an increasing Ekman pumping for the accumulation of freshwater in the Beaufort Gyre. In the reanalysis, the accumulation of freshwater in the Beaufort Gyre occurs meanwhile a salinisation of the coastal area along the shelves. A strong negative anomaly (4 meters decrease) is visible in the East Siberian Sea. *Polyakov et al.* (2008) also find an out-of-phase variability in the central Arctic Basin and on the shelves as they analyze the freshwater content variations over the last 100 years, and they conclude that freshwater anomalies generated on the shelves, and particularly in the East Siberian Sea, will be exported to the Central Basin where they tend to moderate the freshwater content changes. The pattern of the freshwater anomalies in 2007 and 2008 (Fig. 3.3) are consistent with their finding. Moreover, the salinisation in the East Siberian Sea occurs meanwhile a westward intensification of the wind stress along the coast (see the right column of Fig. 3.4). Following the scenario proposed by *Steele and Ermold* (2004), this westward intensification of the wind could have pushed relatively salty Pacific Water along the coast in

the East Siberian Sea and the Laptev Sea and have caused the salinisation. In GLORYS1, the Ekman pumping calculated from the wind stress fields increases in 2007 and 2008 in the Beaufort Gyre (not shown) and this leads to a spatial redistribution of the freshwater in the Canadian Basin due to the enhanced intensity of the Beaufort Gyre. We also find in our reanalysis a completely similar spatial distribution between the SSH fields and the freshwater content fields, as it was previously suggested by *Häkkinen and Proshutinsky* (2004) to show the link between the freshwater content distribution in the Canadian Basin and the atmospheric conditions. Over a longer time period (1965-2002), we could not find any robust correlation between the freshwater content variations in the Arctic and the SSH ones in the Beaufort Gyre (*Lique et al.*, 2009), what suggests that the mechanisms of an accumulation of freshwater in the gyre that behaves as a flywheel could be only intermittent. Note also that we are able to reproduce the amplitude of the freshwater accumulation in the Beaufort Gyre without any interannual variability of the river runoff, which make this source of freshwater for the Arctic an unlikely candidate to explain the freshwater increase.However, *Polyakov et al.* (2008) suggest that the variability of the river runoff inputs on the Arctic shelves could be responsible at least for a part of freshwater content anomalies observed along the shelves that will be afterward exported to the central Arctic. Thus, the lack of interannual variability for the river runoff might lead to an overestimation of the freshening simulated in the Beaufort Gyre. Last, as also suggested by *Polyakov et al.* (2008), we find that the net precipitation (precipitation minus evaporation) variations are by an order of magnitude too small (compared for instance to the sea ice/ocean flux) to lead to important changes of salinity in the Arctic. For instance, we find a negative anomaly for this term in 2007 in the Canadian Basin (relative to 2002-2006 average).

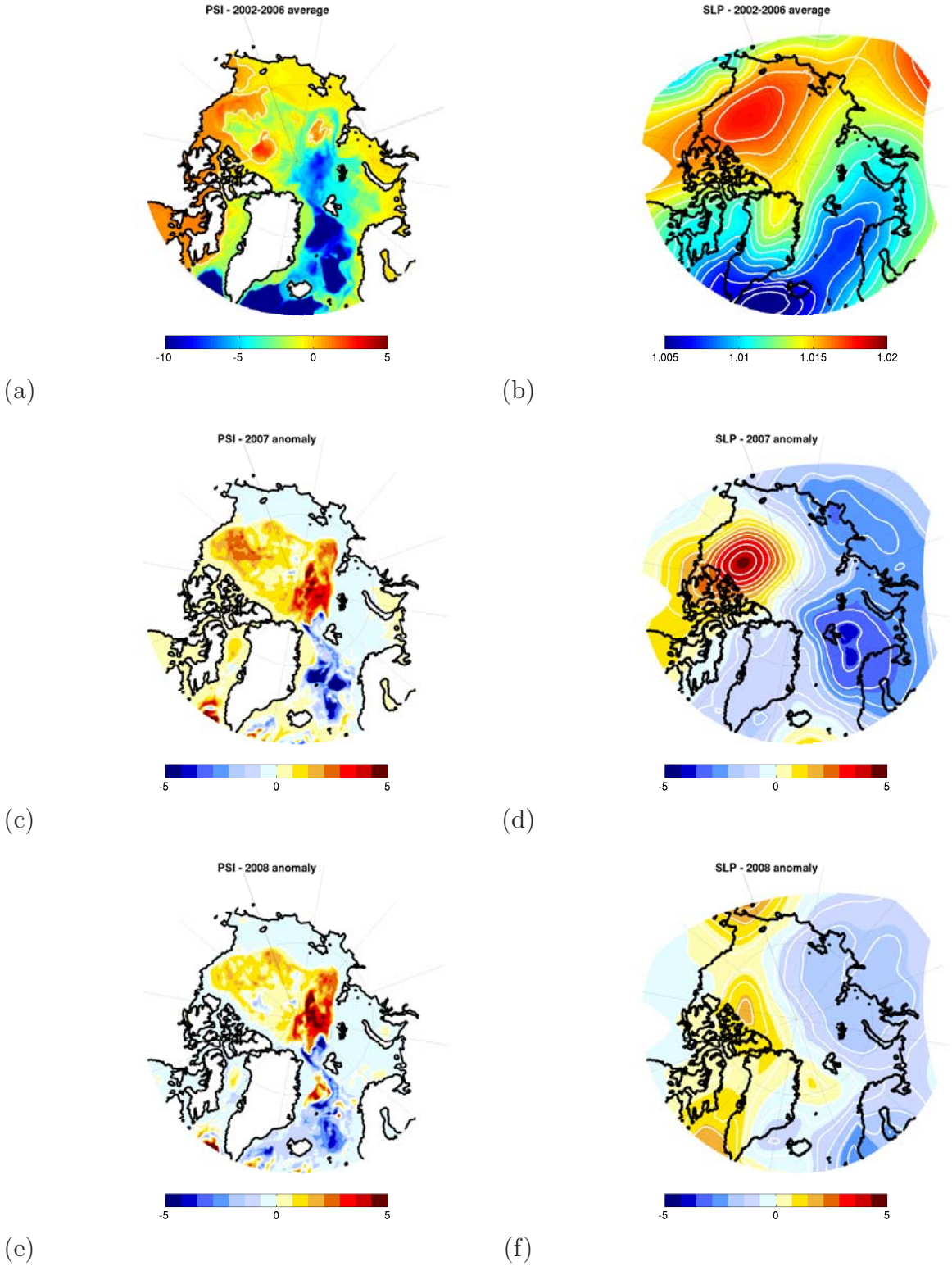

FIG. *3.4: Average over 2002–2006 of the barotropic streamfunction (Ψ, in Sv, a) and the Sea Level Pressure (SLP, in hPa, b). 2007 (c & d) and 2008 (e & f) anomalies of Ψ and SLP. "Anomaly" refers to the difference with the average over 2002–2006. The contours interval is 1 hPa for the SLP.*

We also examine the variability of the advective exchanges of freshwater with the sub-polar region to detect possible changes linked with the freshening of the Arctic Ocean in the Canadian Basin. As the sea ice is mostly melting in the Canadian Basin, one could logically expect an increase of the freshwater export through the Canadian Arctic Archipelagos and through Davis Strait. However, the GLORYS1 2007 and 2008 anomalies of the liquid freshwater transport through Davis Strait are negative in 2007 (-57 km^3/yr) and very small in 2008 (98 km^3/yr). This is consistent with the study of *Våge et al.* (2009) that shows that the observed freshwater transport through Davis Strait just slightly increases from 2004 to 2007, as it does in our simulation. Note that the constant freshwater export is consistent with the sustained wintertime convection in the Labrador Sea (the convection in the Labrador Sea is found to be deeper in GLORYS1 during the winter 2007–2008 than previous winter, in agreement with the observations collected by *Yashayaev and Loder* (2009)). In *Lique et al.* (2009), the variability of the liquid freshwater transport through Davis Strait was found to be driven by velocity fluctuations, the role of the salinity fluctuations being negligible. Similarly, *Polyakov et al.* (2008) conclude from the analysis of a large dataset of observations that the strength of the export of Arctic water controls the supply of Arctic fresh water to sub-polar basins while the intensity of the Arctic Ocean salinity anomalies is of less importance. Thus, possible changes of salinity of the surface water in the Canadian Basin due to the sea ice melting might not strongly modulate the liquid freshwater transport through Davis Strait. However, as a very important quantity of freshwater is accumulating and stocked in the Beaufort Gyre, one might expect that a change in the atmospheric circulation (a change to a positive state of the AO) could lead to a fast release of the freshwater and thus an increase of the freshwater export to the North Atlantic during the coming years, as suggested by *Proshutinsky et al.* (2009).

3.2.5 Salinisation of the Eurasian Basin.

Fig. 3.1(c)&(d) show that the sea ice thickness has also decreased in the Eurasian Basin in 2007 and 2008, suggesting a loss of sea ice in this basin and thus a transfer of freshwater from the sea ice to the ocean (as the sea ice export through Fram Strait does not increase substantially). When we quantify the sea ice loss, the sea ice melt represents a loss of 772 km^3 of freshwater in 2007 and 39 km^3 more in 2008 for the Eurasian Basin compared to the 2002–2006 average (we consider the Eurasian Basin as the part of the Arctic Ocean that is in the east of the Lomonosov Ridge and closed by Fram Strait and the Barents Sea Opening). However, contrary to the Canadian Basin, the liquid contribution of the freshwater content in this basin decreases as well in 2007 and 2008, the liquid freshwater content anomaly in 2008 being equal to -1795 km^3 of freshwater, i.e. roughly twice larger than the decrease due to sea ice melt. *McPhee et al.* (2009) have observed a negative freshwater content anomaly in the Eurasian Basin in 2008 compared

to the PHC climatology, but they conclude that this signal is negligible compared to the freshening of the Canadian Basin. However, this conclusion suffer from a very limited number of observations in the Eurasian Basin. In particular, they do not have any observations north of Fram Strait, where our reanalysis results show the stronger signal of a salinisation (Fig. 3.3(c)&(d)). We thus try to understand the origin of this signal, that appears from the surface to about 800 m.

Fig. 3.4 shows the 2002-2006 average and the 2007 and 2008 anomalies of the barotropic streamfunction (Ψ) and the sea level pressure (SLP, calculated from ERA-Interim reanalysis). In the Eurasian Basin, we have a strong positive anomaly of Ψ due to an important decrease of the intensity of the gyre composed by the Atlantic Inflow and the Transpolar Drift in the Arctic Ocean. In contrast, the strong negative anomaly in the Greenland Sea reveals an intensification of the gyre circulation in this basin, probably linked with the similar anomaly visible in the atmospheric fields. Hence, the water masses that flow with the Atlantic Inflow through Fram Strait preferentially recirculate shortly just north of the strait, instead of penetrating further in the Eurasian Basin. This strong anomaly of circulation is also coherent with Fig. 3.5(Top), as we have in GLORYS1 an increase of both the northward and the southward volume transports through Fram Strait after 2005, the net transport remaining roughly constant.

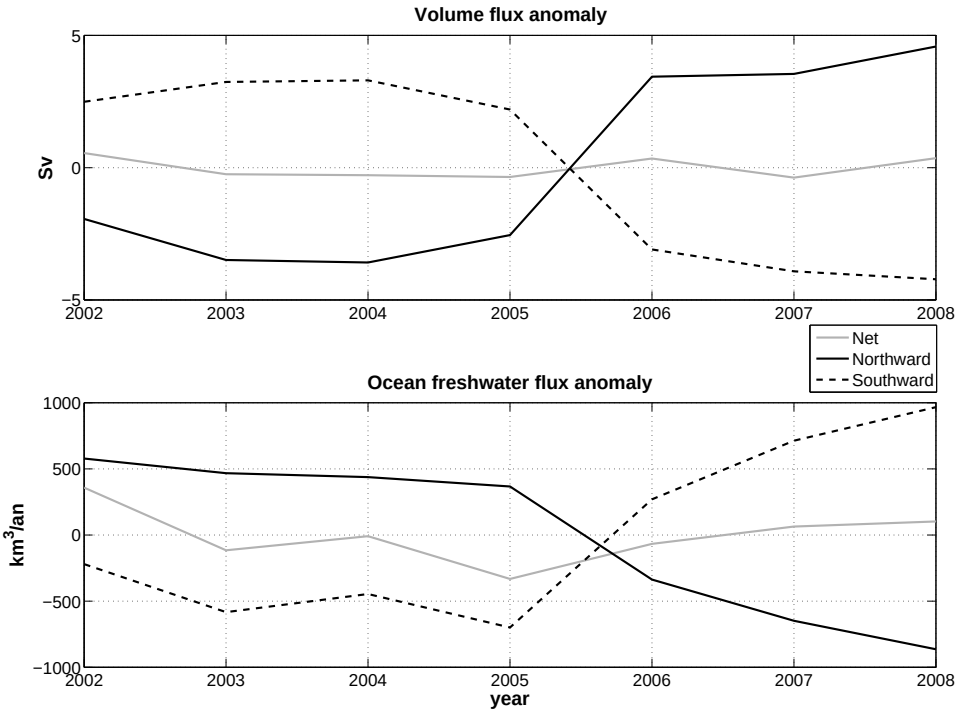

FIG. *3.5: Anomaly (relative to 2002-2008) of the mass flux (Top) and the freshwater flux (Bottom) through Fram Strait. The net fluxes as well as the northward and southward contributions are indicated. A positive mass flux goes northward, and a positive freshwater flux is a source of FW for the Arctic.*

We then investigate the link between this anomaly of circulation and the signal of a negative freshwater content anomaly in the Eurasian Basin. In GLORYS1, the decrease of the freshwater flux corresponding to the saline Atlantic Inflow through Fram Strait (Fig. 3.5) is completely due to an increase of the volume transport, the salinity remaining constant, which is qualitatively consistent with the very slight salinity decrease observed and reported in *Holliday et al.* (2009). On the other hand, the modeled southward freshwater flux through Fram Strait increases after 2005. In the reanalysis, as the short recirculation north of Fram Strait is enhanced, the water masses exiting at Fram Strait are directly coming from the Atlantic Inflow, and thus these water masses do not undergo important modifications as they do not travel long inside the Arctic Basin. Thus, both the salinity and the volume transport of the outflowing branch increase, the resultant being a decrease of the freshwater export. With respect to that issue, GLORYS1 results seems to be inconsistent with the observational results of *De Steur et al.* (2009) (their Fig. 2), who find an slight increase of the freshwater export through Fram Strait after 2005. However, they notice that freshwater anomalies were rather small when compared to the volume transport anomalies after 2005, the different behavior being due to deep volume transports increasing, where the freshwater signal is negligible. In GLORYS1, both the surface and the deeper volume transport increase (their contributions to the total volume

transport anomaly are roughly equal) and this lead to a overestimation of the freshwater signal. Moreover, *De Steur et al.* (2009) use model output to estimate the contribution of the freshwater export on the shelves, and find that this contribution increase after 2006 and thus counterbalanced the decrease of the contribution of the freshwater export in the core of the East Greenland Current (EGC). We have found in a previous paper *Lique et al.* (2010) that the resolution of our model was not sufficient to represent properly the current on the shelves from the Bering Strait to Fram Strait, and on the eastern coast of Greenland. Hence we are not able to reproduce the contribution of the freshwater export on the shelves that could be important as well to moderate the freshwater transport signal.

The increasing Atlantic inflow through Fram Strait (and the associated anomaly of circulation) leads to a very local salinisation North of Fram Strait, while the freshwater content in the central Arctic remains constant : this is consistent with the results of *Polyakov et al.* (2008) as they find that the freshwater anomalies in the central Arctic can not be explained by the variations of the Atlantic inflow.

3.2.6 Concluding discussion

On the overall, in the GLORYS1 reanalysis, the Arctic Ocean is getting saltier in 2007 and 2008 compared to the 2002–2006 average. However the two basins present very contrasted situations. In the Canadian Basin, the total freshwater content remains roughly constant as the quantity of freshwater equivalent to sea ice melt is transferred to the ocean through a gain of liquid freshwater. We also find a spatial redistribution of the freshwater in this basin, as atmospheric conditions lead to an enhanced Beaufort Gyre where the freshwater is accumulated, which is fully consistent with recent observations in this region (*Proshutinsky et al.*, 2009; *McPhee et al.*, 2009). At the same time, the coastal regions in the Canadian Basin undergo salinisation and the liquid and sea ice freshwater export on the western side of Greenland remains constant in 2007 and 2008. This out-of-phase variability of the freshwater content in the central Arctic and along the shelves was reported by *Polyakov et al.* (2008) as they analyze a large dataset of observations over the last 100 years.

On the other side of the Lomonosov Ridge, the picture is different. Both the sea ice and the liquid contributions of the freshwater content decrease in 2007 and 2008. In GLORYS1, we have a strong signal of a salinisation north of Fram Strait (where no measurements where done recently). We show that this signal is due to an anomaly of the circulation, as the short recirculation of the Atlantic Inflow north of Fram Strait is enhanced after 2006, possibly due to an intensification of the cyclonic gyre in the Greenland Sea linked with a similar anomaly in the atmospheric circulation. Hence both the net inflow and

outflow though Fram Strait are intensified. More salty water enters the Arctic through Fram Strait, and as these water masses recirculate shortly without being modified, the export of liquid freshwater decreases as well. However, the GLORYS1 reanalysis does not reproduce the very fresh coastal current on the Greenland shelves, which contribution has been observed to increase after 2006 and hence counterbalances the decrease of liquid freshwater export within the EGC core (*De Steur et al.*, 2009).

We thus suggest that special atmospheric conditions in 2007 and 2008 (with strong anomaly over both the Beaufort Gyre and the Greenland Sea) could have caused a spatial redistribution of the liquid freshwater in the Arctic Ocean. The current observation system in the Beaufort Gyre designed to monitor changes of the freshwater storage in the Arctic seems to be able to capture a part of the freshwater content variability in the Arctic (the accumulation of freshwater in the Beaufort Gyre). However, our results show that this observation system does not capture an important part of the freshwater content change signal, and thus the current monitoring system should be extended to the Eurasian Basin where we found the larger signal and where no measurement is currently done. Moreover, our results back up the idea suggested by *Proshutinsky et al.* (2009) that a return to more neutral atmospheric conditions could lead to a release of the freshwater accumulated in the Beaufort Gyre to the North Atlantic, and thus possibly causes a new GSA in the future. The monitoring of the freshwater storage in the Beaufort Gyre seems to be a good way to possibly predict such a signal in the future, as GSA needs several years to propagate into the North Atlantic (e.g., *Belkin* (2004)).

Acknowledgement The realization of GLORYS1 global ocean reanalysis had the benefit of the grants that Groupe Mission Mercator Coriolis, Mercator-Ocean, and INSU-CNRS attributed to the GLORYS project, and the support of the European Union FP7 via the MYOCEAN project. Computations were performed with the support of Météo-France HPC Center. C. Lique is supported by a PhD grant from CNES and IFREMER. A.M. Treguier and B. Barnier are supported by CNRS.

Chapitre 4

Origine des masses d'eau exportées de l'Arctique vers l'Atlantique Nord.

4.1 Préambule

Dans le chapitre 2, nous avons analysé le bilan d'eau douce de l'Arctique et sa variabilité, en considérant le bassin Arctique comme une sorte de "boîte noire" pour laquelle nous n'avons pris en compte que les sources et puits d'eau douce extérieurs (advection océanique et flux de surface). Dans le chapitre 3 par contre, nous avons montré que la répartition spatiale de l'eau douce peut elle aussi varier à l'intérieur du bassin. Le fait de ne pas pouvoir trouver de corrélation temporelle claire entre les flux d'eau douce en entrée et en sortie de notre bassin (chapitre 2), ainsi que l'analyse du contenu halin du chapitre 3 nous montrent l'insuffisance de notre méthode, qui ne nous permet pas de comprendre comment et où les masses d'eau se transforment à l'intérieur du bassin, ces transformations étant pourtant cruciales pour la compréhension du système d'eau douce du bassin Arctique.

Ce problème est en fait plus général que le simple cadre de nos travaux. Au cours des dernières décennies, un attention particulière a été portée au monitoring des échanges océaniques entre l'Arctique et l'Atlantique d'une part et le Pacifique d'autre part. Des mouillages ont ainsi été déployés et des campagnes de mesures ont été effectuées sur ces sections, permettant une quantification des transports de masses, d'eau douce et de chaleur à travers les différentes frontières (e.g., *Schauer et al.* (2008) pour le détroit de Fram, *Cuny et al.* (2005) pour le détroit de Davis, *Skagseth* (2008) pour le Barents Sea Opening et *Woodgate et al.* (2006) pour le détroit de Bering). Le maintien de ces systèmes d'observations nous donne accès à une quantification de la variabilité temporelle des échanges à travers ces sections, et la compréhension de cette variabilité devrait s'améliorer encore au fur et à mesure que les séries temporelles s'allongent. Dans le même temps, les progrès

concernant la connaissance et la compréhension de la circulation à l'intérieur de l'Arctique sont eux probablement moindres. Contrairement au reste des océans, les mesures satellites donnent accès à des informations sur les glaces de mer (concentration, dérives et dans une moindre mesure épaisseur), mais pas sur la circulation de surface (altimétrie). A partir de mesures *in situ*, certains auteurs ont pu estimer un schéma qualitatif de la circulation en Arctique. C'est par exemple le cas de l'étude de *Rudels et al.* (1994) dans laquelle la circulation de l'eau atlantique contenue dans les couches intermédiaires (entre 200m et 1700m) est estimée à partir des mesures récoltées durant la mission *Oden 91*. La même stratégie d'étude a également été appliquée à l'eau Pacifique (*Steele et al.*, 2004). Mais les schémas de circulation proposés dans ces études restent très qualitatifs et probablement dépendants de la période à laquelle sont faites les mesures.

Et malgré tous ces progrès, il est encore aujourd'hui très difficile de faire le lien entre les échanges entre l'Arctique et les océans adjacents, et ce qu'il se passe à l'intérieur du bassin Arctique. En d'autres termes, il nous reste encore à déterminer comment les différentes "entrées" et "sorties" de l'océan Arctique sont connectées entre elles. C'est donc bien une perspective lagrangienne de la circulation qu'il nous faut avoir pour pouvoir répondre à cette question.

Différentes pistes ont déjà été suivies dans des études précédentes, utilisant soit des observations de traceurs chimiques (nutriment, concentration en O_2) pour distinguer l'origine des différentes masses d'eau (e.g., *Jones and Anderson* (2008)), soit des méthodes numériques telles que l'implémentation de traceurs passifs dans des simulations (e.g., *Gerdes and Schauer* (1997); *Karcher and Oberhuber* (2002)). Mais ces deux approches sont elles aussi limitées : le manque d'observations ne permet pas d'avoir une vue complète de la circulation dans le bassin, tandis que la seconde approche ne permet d'avoir accès qu'à un schéma de circulation qualitatif.

Dans ce chapitre, nous proposons une troisième approche pour répondre à ce problème, en effectuant une analyse lagrangienne de la circulation dans le bassin Arctique, ainsi que des transformations des masses d'eau associées aux différentes branches de circulation. Dans cette optique, nous utilisons l'outil ARIANE développé au LPO par Bruno Blanke et Nicolas Grima (*http ://www.univ-brest.fr/lpo/ariane/*), que nous appliquons au champs 3D moyens de la simulation numérique également utilisée au chapitre 1.

L'étude est présentée sous la forme d'un article publié en 2010 dans *Journal of Geophysical Research*. Nous avons choisi pour présenter nos résultats de nous focaliser sur la détermination de l'origine des masses d'eau exportées de l'Océan Arctique vers l'Atlantique Nord, même si les résultats présentés ici couvrent un plus large spectre.

4.2 Article : On the origins of water masses exported along both sides of Greenland : A Lagrangian Model Analysis. (C. Lique, A.M. Tréguier, B. Blanke et N. Grima, *JGR*, 2010a)

Abstract : The origin of the water masses exported from the Arctic to the North Atlantic along both sides of Greenland are investigated, using an original numerical method. A quantitative Lagrangian analysis is applied to the monthly climatological 3D output of a global ocean/sea-ice high resolution model. It allows quantification of the different branches of the export to the North Atlantic, as well as related timescales and water mass transformations.

In the model, the outflow through Davis Strait consists in equal part of Pacific and Atlantic Water, whilst the export through Fram Strait consists almost fully of Atlantic Water (contrary to observations). Pacific Water is transferred quickly (O(10 years)) to the North Atlantic, through the Beaufort Gyre, where gradual warming and salinification occur. Atlantic Water exiting in the surface layer along both sides of Greenland remains about 10 years in the Arctic Basin, and undergoes cooling and significant freshening. Below the surface water, Atlantic water exiting through the intermediate and deep layers in Fram Strait follows different pathways in the Arctic, with trajectories being subject to topography constraints. The travel time depends strongly on the pathway (from 1 to 1000 years). The intermediate outflow consists mainly of water entering the Arctic at Fram Strait, while half the deep outflow is composed of water from the Barents sea. We find that the Barents Sea Branch, which contributes to both the outflows at Fram and Davis straits, is almost fully transformed after a year due to heat exchanges with the very cold atmosphere.

4.2.1 Introduction

The large scale circulation of the Arctic Ocean has been known for a long time (*Nansen*, 1902; *Coachman and Aagaard*, 1974). Cold and relatively fresh Pacific Water enters the Arctic Ocean through Bering Strait. A part is swept into the Beaufort Gyre, in the Canadian Basin, and exits into the North Atlantic Ocean on the western side of Greenland, through the Canadian Arctic Archipelagos (CAA) and then through Davis Strait, whilst a second part follows the shelf break along the Canadian Coast and eventually exits along both sides of Greenland through Davis Strait and Fram Strait. At the same time, warm and dense water enters the Arctic Ocean from the Atlantic Ocean along two main pathways : Fram Strait and the Barents Sea. However, the fate of these two branches of Atlantic Water is different. The part crossing Fram Strait with the West Spitsbergen

Current (hereafter called the Fram Strait Branch) remains beneath colder and fresher water layers. This prevents the heat in the Atlantic layer from melting sea ice as well as from contact with the atmosphere. On the other hand, Atlantic Water taking a route through the Barents Sea (hereafter called the Barents Sea Branch) loses a part of its heat by contact with the colder atmosphere, and undergoes strong modifications. As the two branches join in the St. Anna Trough, they carry on waters with contrasting properties, that will thus follow different pathways in the Arctic Basin, and eventually come back to the North Atlantic mainly through Fram Strait, and, to some extent, through Davis Strait.

However, our understanding of the Arctic dynamics remains crude and fragmented, and several major questions are in abeyance in the literature. Some studies provide us with a partial or qualitative circulation scheme (*Rudels et al.*, 1994; *Jones et al.*, 1995; *Steele et al.*, 2004; *Karcher et al.*, 2007), but the relative contributions of the different circulation branches, their associated water mass modifications as well as the order of magnitude of their residence times still needs to be determined. The role of the Barents Sea in modifying the Atlantic inflow has been pointed out by *Gerdes and Schauer* (1997) but the mechanisms at play there are still not clearly established. These questions seem hard to address with the few available observations or a classical modeling approach using Eulerian fields. A recent effort has focused on overcoming the lack of knowledge regarding the Arctic circulation, through international observational and modeling programs, such as AOMIP (Arctic Ocean Model Intercomparison Project ; *Proshutinsky et al.* (2005)) or DAMOCLES (Developing Arctic Modeling and Observing Capabilities for Long-term Environmental Studies ; *http ://www.damocles-eu.org*). A chemical observational approach has also been recently used to try to distinguish and follow the journey of the different water masses exported to the North Atlantic (runoff, Pacific Water, Atlantic Water), since their chemical composition makes them clearly recognizable (*Jones et al.*, 1998, 2003; *Taylor et al.*, 2003; *Falck et al.*, 2005). However, direct measurements are still too sparse both in time and space to allow a quantification of the origin of the Arctic outflow to the North Atlantic. At the same time, an important effort has also been made to monitor and model the exchanges between the Arctic Ocean and the Nordic Seas, as "*the signal of Arctic change is expected to have its major climatic impact by reaching south through subarctic seas, either side of Greenland, to modulate the Atlantic thermohaline conveyor*" (*Dickson et al.*, 2008). It has been suggested (*Mauritzen*, 1996; *Holloway and Proshutinsky*, 2007b) that the Arctic/North Atlantic exchanges could have a more important role in the global 'conveyor' than just influencing it. The Arctic circulation and related water mass transformations are an important component of the global 'conveyor' that fully invades the Arctic.

In the present study, we use an original approach that allows us to connect these very important Arctic/North Atlantic exchanges with the circulation inside the Arctic, taking advantage of recent progress in numerical modeling. Here we aim at determining the origins of the Arctic waters exported along both sides of Greenland, and at quantifying the water mass modifications that occur in the Arctic Ocean in a numerical model. Lagrangian diagnoses are derived from the velocity and the temperature and salinity fields of a high resolution global sea-ice/ocean simulation in order to track the motion of selected water masses. The same simulation was used in a companion paper (*Lique et al.*, 2009) to study the variability of the freshwater exchanges from the Arctic to the North Atlantic. For this latter issue, the model behavior was shown to be close to observations, even though more model validation is needed and will be presented here. Our Lagrangian analysis provides a quantitative picture of the mean large scale circulation scheme for the Arctic Ocean, and allows to separate the different branches of circulation as well as their associated water mass transformations and time scales. This study will help to understand the mean state of the Arctic Ocean, which is a key point before understanding variability and trends in the region.

Such a Lagrangian analysis has already been carried out successfully in different Ocean General Circulation Models (OGCM). The method is presented in details and discussed in *Blanke and Raynaud* (1997) and *Blanke et al.* (1999). It has been already used to describe the general organization of the global ocean circulation (*Blanke et al.*, 2001; *Speich et al.*, 2001) or to study the salinity modifications associated with the circulation in the Atlantic (*Blanke et al.*, 2002, 2006). A recent study (*Koch-Larrouy et al.*, 2008) used the same model setup (but in a regional configuration) to study the circulation and the water mass transformations in the Indonesian Seas. Our work is based on these previous studies for which the Lagrangian method has shown credible consistency and efficiency.

The remainder of this paper is organized as follows. The numerical tools are briefly presented in section 2. Model performance in the Arctic area is evaluated in section 3, as we validate the mean simulated Arctic with in-situ observations and indications given by other modeling studies. The two following sections deal with the Lagrangian results on Arctic dynamics (section 4) and the water mass transformations in the Arctic (section 5). The influence of the Arctic Oscillation (AO) on the circulation scheme we propose is discussed in section 6. A conclusion is given in section 7.

4.2.2 The Numerical Tools.

4.2.2.1 Ocean model.

The global ORCA025 coupled ocean/sea-ice model configuration developed for the DRAKKAR project (*The DRAKKAR group*, 2007) is used to perform the simulation. An overall description of the model and its numerical details are given in *Barnier et al.* (2006). This model configuration uses a global tripolar grid with 1442x1021 grid points on the horizontal and 46 vertical levels. Vertical grid spacing is finer near the surface (6 m) and increases with depth to 250 m at the bottom. Horizontal resolution is 27.75 km at the equator, 13.8 km at 60°N , and gets to 10 km in the Arctic Ocean. The ocean/sea-ice code is based on the NEMO framework version 1.9. (*Madec*, 2008). It uses a partial step representation of the bottom topography and a momentum advection scheme that both yielded a better representation of the ocean dynamics (*Le Sommer et al.*, 2009). Parameterizations include a Laplacian mixing of temperature and salinity along isopycnals, a horizontal biharmonic viscosity, and a turbulence closure scheme (TKE) for vertical mixing. The bathymetry is derived from the 2-minute resolution Etopo2 bathymetry file of NGDC (National Geophysical Data Center). The sea-ice model is the Louvain-la-Neuve model (LIM), which is a dynamic-thermodynamic model specifically designed for climate studies. A detailed description is given in *Timmermann et al.* (2005).

A complete description of our simulation can be found in *Molines et al.* (2006). It is interannual and runs from 1958 to 2001 with no spin-up. Initialization uses data from the Polar Science Center Hydrographic T/S Climatology (PHC ; *Steele et al.* (2001a)). The forcing dataset is a blend of data from various origins at different frequencies referenced as DFS3 in *Brodeau et al.* (2010). Precipitation and radiation come from the CORE dataset assembled by W. Large (*Large and Yeager*, 2004), at monthly and daily frequency respectively, based on satellite observations when available. A climatology of the same satellite dataset is used for the early years up to 1979 and 1984 respectively. Air temperature, humidity and wind speed are six-hour fields from the ECMWF ERA40 reanalysis. Turbulent fluxes (wind stress, latent and sensible heat fluxes) are estimated using the CORE bulk formula (*Large and Yeager*, 2004). River runoff rates are prescribed using the *Dai and Trenberth* (2002) climatological dataset. To avoid an excessive model drift, we add a relaxation of sea surface salinity to the PHC climatology. The coefficient (0.167 m/day) amounts to a decay time of 60 days for 10 m of water depth ; under the ice cover, the restoring coefficient is five times stronger. This choice was made within the DRAKKAR consortium because of problems encountered with earlier versions of the forcing data, especially in the Weddell Sea. We acknowledge that this restoring is a strong constraint on our model solution and thus the analysis presented in this paper is affected by this constraint. We have considered using a twin experiment that has been carried

out with no relaxation under sea ice (W. Hazeleger and S. Drijfhout, personal communication), but the drift of water mass properties in the Arctic was found unacceptable for the purpose of the present paper.

To run our Lagrangian diagnoses, a climatological year has been built by averaging month by month the monthly means of the simulation from 1980 to 2001. The first twenty two years of the simulation have been excluded, when the model adjustment is larger in the Arctic Ocean (see *Lique et al.* (2009) for a quantification of the model drift). Interannual variability as well as high frequency variability (finer than one month) are thus excluded from our analysis.

4.2.2.2 Lagrangian method.

The off-line mass preserving Lagrangian ARIANE scheme is used for this study (*http ://www.univ-brest.fr/lpo/ariane/*). A description of the algorithm can be found in *Döös* (1995) and *Blanke and Raynaud* (1997). Water masses are represented by numerous small water parcels (particles) carrying an infinitesimal transport and seeded on given geographical sections. As the algorithm respects water mass incompressibility, each particle conserves its infinitesimal volume along its trajectory. It is integrated with time until it reaches geographical interception sections. The mass transfer between two given sections can thus be determined. The idea is more to describe the large scale circulation, for instance by computing horizontal streamlines (*Blanke et al.*, 1999), than to compute the most realistic individual trajectories. In all our experiments, the maximum transport carried by a particle is fixed to 10^{-3} Sv. This allows us to define our Lagrangian transports with accuracy better than 10^{-3} Sv (*Valdivieso Da Costa and Blanke*, 2004).

Along its trajectory, a given particle will show changing properties (salinity and temperature), as given by the local Eulerian fields of the ocean model. The Lagrangian scheme does not consider turbulent motions in the trajectory calculations, but, as the ocean model parametrizes such effects, the signature of T/S evolutions along the computed trajectories can be found and the water mass transformations can be quantified. Since we compute our Lagrangian diagnoses from monthly mean fields, we assume that velocity and tracer fluctuations, and their correlations, are small over periods shorter than monthly climatological means. Variations of temperature and salinity along a trajectory then correspond mostly to the mean effect of direct warming by the solar heat flux, run-off, precipitation and evaporation processes, and to the mean lateral and vertical turbulent diffusion in the model. The access of the information for each individual particles (their infinitesimal transport as well as their T/S property) at their entrance and exit sections allows the calculation of heat and freshwater fluxes.

4.2.3 The simulated Arctic Ocean.

As already shown by studies based on the same Lagrangian method (*Koch-Larrouy et al.*, 2008; *Friocourt et al.*, 2005), the degree of confidence one can grant to the Lagrangian interpretation depends on the overall credibility of the Eulerian fields. Three specific issues will be addressed in this section, in order to assess the model performance in the Arctic Ocean : the exchanges by advection with the subpolar area, the circulation and the representation of the water masses in the Arctic Ocean. We define the Arctic Ocean as the area enclosed by the following transects across ocean straits (Fig. 4.1) : the Bering Strait, a section across the Barents Sea between Norway and Svalbard Island (following the 20 °E meridian), the Fram Strait and the Davis Strait. These four sections will be used as intercepting sections in our Lagrangian experiments.

FIG. *4.1: Arctic Ocean and localization of the main place names used in the text. The four sections enclosing the domain of the Lagrangian experiments are shown as thick lines. The additional section used in section 5 is drawn as a dotted line. Bathymetry contours 500, 1000, 2000, 3000, 4000 and 5000 m are drawn with a thin line.*

4.2.3.1 Exchanges.

The mean values of the simulated exchanges of mass, liquid freshwater, sea-ice and heat across the four sections enclosing the Arctic Basin over the period 1980–2001 are given in

		Bering Strait	**Barents Section**	**Davis Strait**	**Fram Strait**
Mass	net	1.3	2.9	-2.6	-1.6
transport	inflow	1.3	4.1	0.6	3.9
(Sv)	outflow	0	-1.2	-3.2	-5.5
Freshwater	net	95.2	-8.1	-123.8	-47.6
transport	inflow	95.2	-9.1	4.4	-7.5
(mSv)	outflow	0	1.0	-127.2	-40.1
Heat	net	5.4	71.6	12.6	24.4
transport	inflow	5.4	85.5	10.4	30.0
(10^{12} W)	outflow	0	-13.9	2.2	-5.6
Sea-ice volume *(10^3 km^3/yr)*		0.043	-0.25	-0.29	-3.0

TAB. *4.1: Mean volume, freshwater, heat and sea ice exchanges from the Arctic Ocean to the Subpolar Area over the period 1980–2001. Inflow and outflow directions refer to the Arctic Ocean. See text for the definition of freshwater and heat transports.*

Table 4.1. The freshwater transport is computed with 34.8 psu as a reference according to *Aagaard and Carmack* (1989), and the heat transport is referenced to -0.1°C according to *Aagaard and Greisman* (1975). Model values of the transports of mass and freshwater (as liquid and sea-ice) have been discussed by *Lique et al.* (2009). Note that the model estimates in Table 4.1 may differ from those given in *Lique et al.* (2009) because the period considered is a different (1980–2001 here versus 1965–2002 in *Lique et al.* (2009)) and the control sections considered may be shifted by a few grid points.

The circulation across the different sections matches fairly well some available observations, despite a 20% overestimate of the transport (and thus of the liquid freshwater transport) through Bering Strait, compared to the estimate of *Woodgate et al.* (2006). The heat flux through this strait is also consequently too large : 4.9×10^{20} J/yr versus 1–3.10^{20} J/yr in *Woodgate et al.* (2006), with a reference temperature equal to -1.9°C in both calculations. Exchanges through Davis Strait are consistent with direct estimations given by *Cuny et al.* (2005) (net volume, freshwater and heat transport are estimated to -2.6 $\pm$ 1.0 Sv, -92 $\pm$ 34 mSv and $18 \pm 17 \times 10^{12}$ W relative to 0°C respectively, our modeled heat net transport being 13.7×10^{12} W with the same reference). Across Fram Strait, the southward flowing East Greenland Current (EGC) exports a large amount of freshwater. Concurrently, heat is brought northward by the West Spitsbergen Current (WSC) in the eastern part of the strait. Modeled volume and freshwater exchanges have been shown to be in the range of uncertainty of the different observational estimates, although weaker than the estimation by *Schauer et al.* (2004) (*Lique et al.*, 2009), and the heat flux is also consistent with the estimate of *Schauer et al.* (2004) (between 16 and 41.10^{12} W, depending on the year considered). Relative to our chosen reference temperature and salinity,

the simulated transport across the Barents section represents a sink of freshwater and a source of heat for the Arctic Ocean. Our simulation results are close to those obtained by *Maslowski et al.* (2004) with their model and within the range of values given in the review of observations by *Simonsen and Haugan* (1996).

4.2.3.2 Mean circulation.

No direct measurement of Sea Surface Height (SSH) variations can be done in the Arctic Ocean because of sea-ice and the sea ice drift gives only qualitative information about the surface circulation (see *Lique et al.* (2009) for plots of the mean surface circulation and sea ice drift in the model). It is therefore difficult to determine the surface circulation, and even more difficult to sketch a general picture of the dynamics in the basin from direct observations.

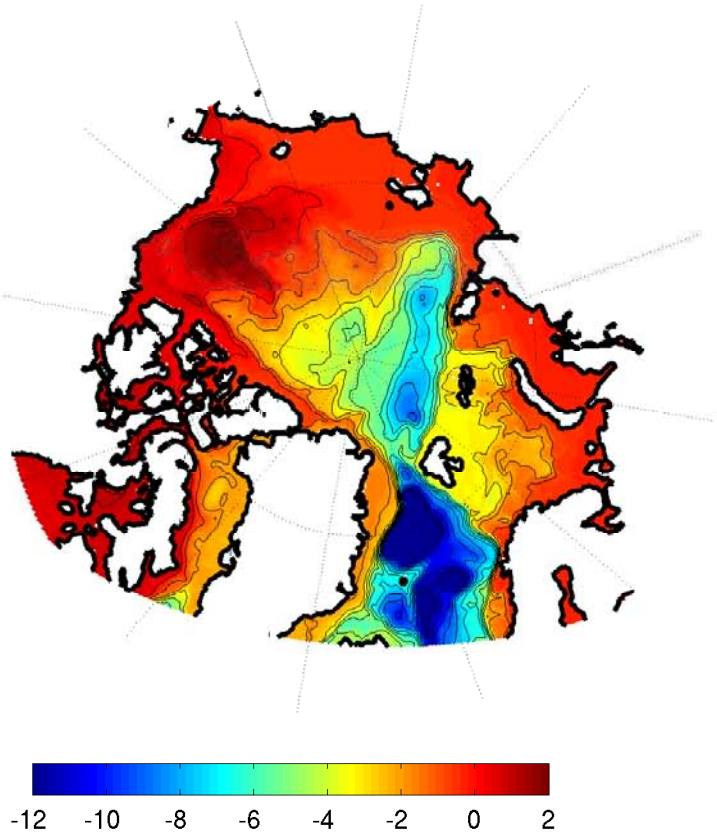

FIG. *4.2: Model annual mean barotropic streamfunction in Sv. The contour interval is 1 Sv.*

Fig. 4.2 shows the mean barotropic streamfunction in the Arctic Ocean calculated in our

simulation. A classical pattern stands out, with two distinct structures in the two main basins. A cyclonic circulation can be seen in the Eurasian basin, with a maximum of 9 Sv, whereas an anticyclonic structure dominates the Canadian side, with a weaker maximum intensity around 2 Sv.

The diversity of model results for the barotropic streamfunction in the Arctic Ocean can be seen for instance in *Steiner et al.* (2004), as they compare the mean streamfunctions from several models having taken part in the AOMIP project (see their Fig. 2). They show that the choice of a parametrization for the eddy-topography interactions as well as the system of coordinates lead to important differences in the simulated Arctic dynamics by the different models. In our model, the circulation in the Eurasian Basin has a higher intensity than any of the models presented in *Steiner et al.* (2004). The most important difference between the model results is the circulation found in the Canadian basin, where the streamfunction has positive or negative sign depending on the model. As a matter of fact, in this basin, the Beaufort Gyre is dominating the surface clockwise circulation, whilst the deeper circulation is counterclockwise, due to the influence of topography (*Holloway et al.*, 2007). The sign of the streamfunction for the flow integrated from the bottom to the surface then depends on the relative intensity of the Beaufort Gyre and of the deep circulation, and also on the depth of the circulation inversion, which takes place around 300 meters in our simulation. This is consistent with the observation of an about 300 meter vertical expansion of the Beaufort Gyre (*Proshutinsky et al.*, 2002).

4.2.3.3 Water mass representation.

Fig. 4.3 compares the annual mean freshwater and heat contents integrated over the upper 1000m for the model and the PHC climatology (*Steele et al.*, 2001a). The same comparison is done in *Steiner et al.* (2004) for a few AOMIP models.

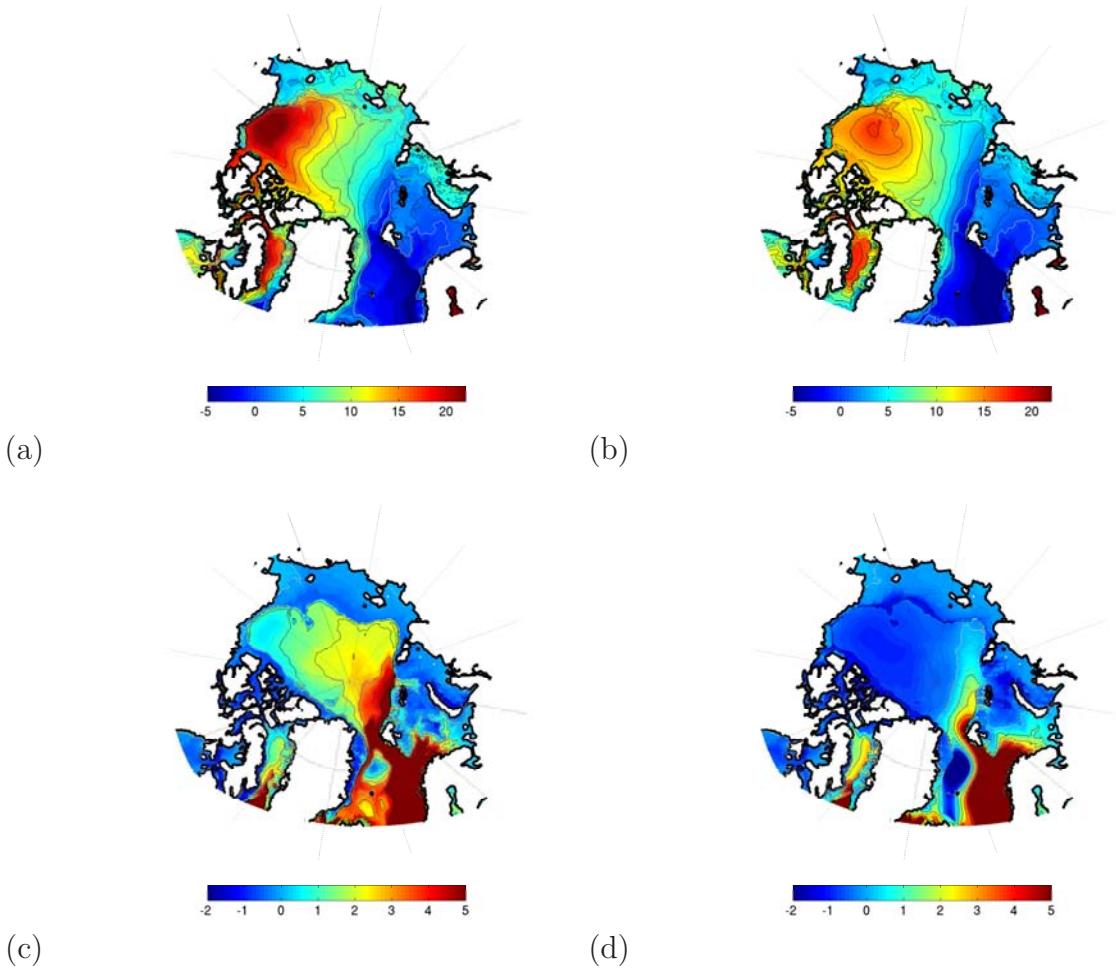

FIG. *4.3: Left : Model annual mean freshwater content ((a), in m.) and heat content ((c), in GJ.m*$^{-2}$*) over the upper 1000 m. Right : Same as Left, but for the PHC climatology. The freshwater content and the heat content are referenced to 34.8 psu and 0°C .*

The model and the climatology both show warm and salty Atlantic water entering the Arctic Ocean via Fram Strait and the Barents Sea. However, the simulated waters in the Nansen Basin seem warmer and slightly fresher than in the climatology, suggesting an overestimation in our model of the part of the inflow through Fram Strait that reaches the interior of the Arctic. This is supported by the large values of the streamfunction found in this basin. In the Canadian Basin, a large amount of freshwater is stored in the Beaufort Gyre, as predicted and discussed by *Proshutinsky et al.* (2002). The general pattern of the modeled freshwater content matches well the climatology, even though the maximum present in the Beaufort Gyre is higher in the model. At the same time, modeled water properties in the Canadian Basin are warmer than in the climatology, with differences ranging from 1 to 3 GJ.m^{-2}. The overestimation of the simulated freshwater and heat contents in the Canadian Basin are logically linked to the overestimation of the freshwater and heat fluxes through Bering Strait, as Pacific Water spreads over the

Beaufort Gyre.

The modeled distribution of heat and freshwater does not show a clear front that would correspond to the Lomonosov Ridge, as in the climatology. Some part of the difference could be explained by an underestimated flow along the Lomonosov Ridge in our model, due to underestimation of the interaction between eddies and bottom topography (the so-called 'Neptune effect' of *Holloway* (1992) whose parametrization by *Nazarenko et al.* (1998) leads to an intensification of the returning flow along the Lomonosov Ridge). In the model, the front is thus too weak compared to observations. Moreover, *Ekwurzel et al.* (2001) show that the front of temperature and salinity between Atlantic Water and Pacific Water shifted from the Lomonosov Ridge in 1991 to the Mendeleyev Ridge in 1994, and this shift is linked to the North Atlantic Oscillation. Annual mean plots of heat and freshwater content (not shown) reveal that the front displacement between 1991 and 1994 is fairly well represented in the model, and that the position of the front is highly variable at interannual scale. This could explain another part of the difference between the patterns of heat and freshwater contents, as the mean front position strongly depends on the period considered.

4.2.3.4 Definition of the different layers.

Fig. 4.4 shows the averaged profiles of salinity, temperature and density referenced to the surface across Davis Strait and Fram Strait. The water masses in both straits are qualitatively well represented by the model, as discussed in *Lique et al.* (2009). These profiles may be qualitatively compared with in-situ profiles presented in *Cuny et al.* (2005) (Davis Strait) and *Fahrbach et al.* (2001) (Fram Strait).

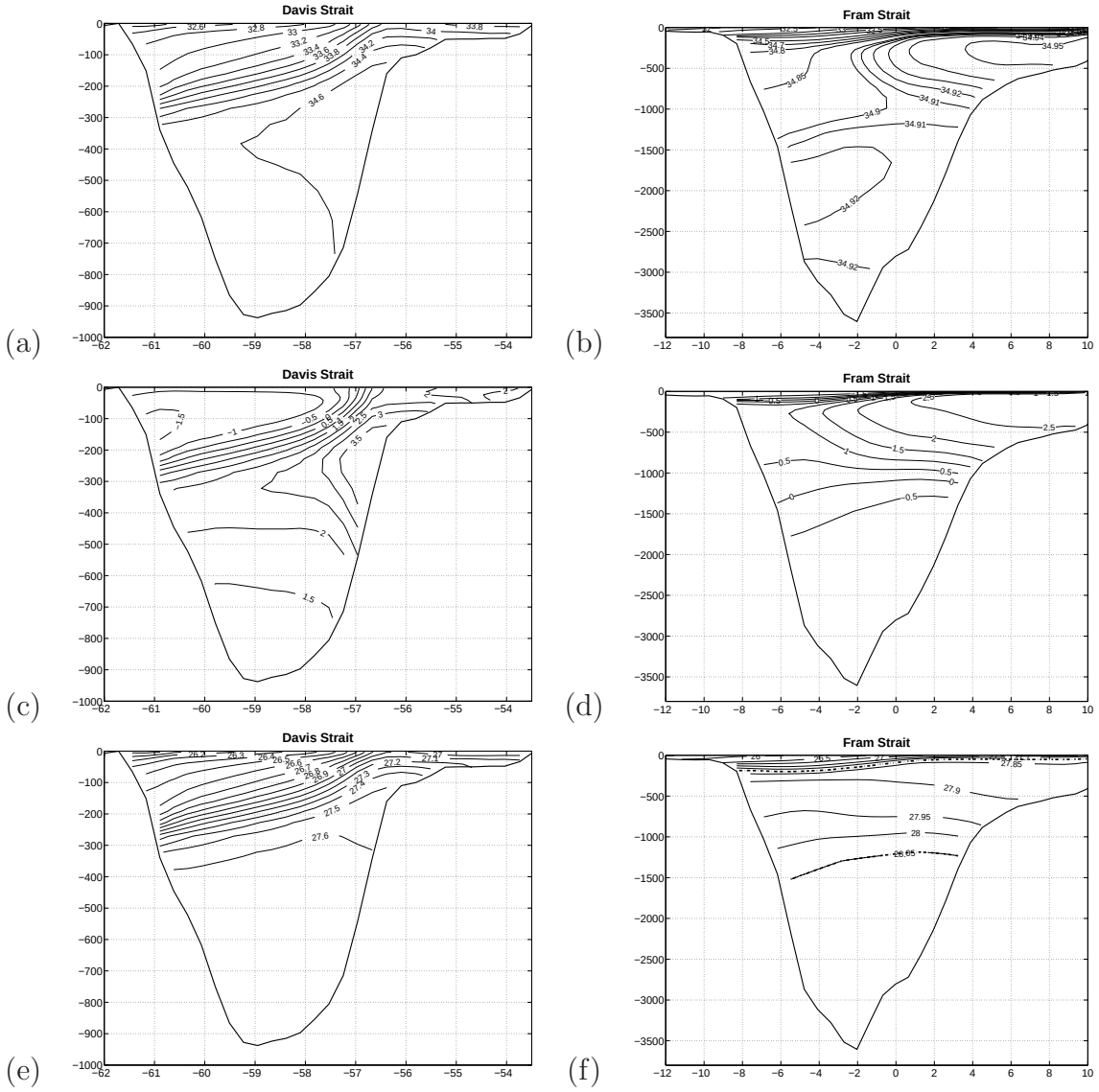

FIG. *4.4: Model vertical section of mean salinity (in psu) (a and b), mean temperature (in °C) (c and d) and mean density (referenced to the surface) (e and f) across Davis Strait (left) and Fram Strait (right). Isopycnal contours 27.8 and 28.05 are superimposed as dotted lines (f).*

We decided to split up the total export across Fram Strait into three density classes, the separation being done by the 27.8 and 28.05 isopycnals. This choice respects the usual distinction made in the literature between the circulation of the upper (*Karcher and Oberhuber*, 2002; *Steele et al.*, 2004), intermediate (*Rudels et al.*, 1994; *Smethie et al.*, 2000) and deep layers (*Jones et al.*, 1995). We assume that the 27.8 isopycnal is a reasonable lower limit of the halocline, as we find it between depths 200 and 400 meters. The 28.05 isopycnal is around 1500 meters depth, which is close to the upper limit of the Lomonosov Ridge and often used to distinguish between the intermediate and deep waters (*Smethie et al.*, 2000). We also consider that the water exported through Davis

Strait does not need to be separated into different density classes, as Davis Strait is only 400 meters deep, and thus we will consider all exports as surface water, their density being under 27.8.

4.2.4 Circulation scheme of the Arctic Ocean.

This section aims at establishing a quantitative scheme of the circulation in the Arctic Ocean, as well as related time scales. We inseminate particles at Fram Strait and Davis Strait during one full year. Initial positions are regularly distributed both in time (still within the same 30-day interval and then repeated for all months) and space (along the vertical and lateral extend of each gridcell). The number of particles in each cell is defined by the constraint about the maximum transport imposed on one single particle (in our case, 10^{-3} Sv). Each particle is allotted a weight equal to a fraction of the local outflow, and keeps its infinitesimal transport all along its trajectory. Particles are integrated backward in time until they reach one of the four sections enclosing our Arctic Basin (see Fig. 4.1). Trajectory calculations are carried out by repeating the same monthly 'climatological year' until the slowest particle comes out the domain. About 100000 particles are introduced at Davis Strait, and twice more at Fram Strait.

Equivalent backward experiments with particles inseminated at Bering Strait and over Barents section have shown that no particle exits the Arctic Ocean through Bering Strait, and that all the particles exiting through the Barents section originate from the very same section and remain in the Barents Sea for a short residence time. Such circulations will then be excluded from our analysis.

4.2.4.1 Origins of the Arctic exports.

Fig. 4.5 and Table 4.2 show the different origins of the exports along both sides of Greenland and quantify their relative contributions.

	DAVIS	**FRAM STRAIT**			
	STRAIT	$\sigma_0 < 27.8$	$27.8 \leq \sigma_0 < 28.05$	$\sigma_0 \geq 28.05$	*Total*
BERING STRAIT	1.11	0	0.01	0	0.01
DAVIS STRAIT	0.62	0	0	0	0
FRAM STRAIT	0.36	0.65	2.14	0.92	3.71
BARENTS SEA	1.03	0.61	0.57	0.81	1.99
TOTAL	3.12	1.26	2.72	1.73	5.71

TAB. *4.2: Transport (in Sv) of the different branches that contribute to the southward transport through Davis Strait and through Fram Strait in three different density layers. Values smaller than 10^{-2} are set to 0.*

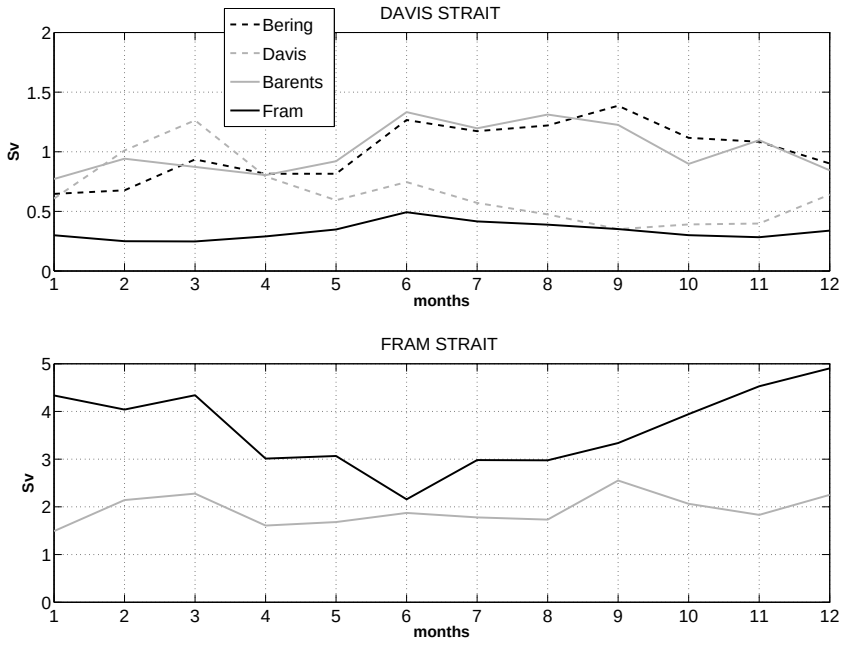

FIG. *4.5: Monthly time series (in Sv) of the relative contributions accounting for the transport passing through Davis Strait (top) and Fram Strait (bottom). The transport accounted for by the water masses that enter the Arctic through Bering Strait, Davis Strait, Fram Strait and the Barents Sea is drawn with a black dashed line, a gray dashed line, a solid black line and a solid gray line, respectively.*

Davis Strait : At Davis Strait, the exports are composed of water masses originating from the four sections enclosing the Arctic Ocean. In the model, Pacific Water from Bering Strait represents 36% of the total annual mean export, but this contribution becomes larger during summer and autumn. *Proshutinsky et al.* (2002) found that the strength of the Beaufort Gyre decreases during this period of the year, and thus an important amount of freshwater is released at that time. This seasonal cycle of the Beaufort Gyre intensity is well represented in the model, and, as in the model the transfer of Pacific Water occurs through the Beaufort Gyre in the upper layers, the increase of Pacific Water export through Davis Strait during summer and autumn is thus due to the increasing release of water by the gyre during these seasons.

Almost 20% of the export at Davis Strait enters the Arctic through this same section. It is however important to make the difference between the fraction of these waters that crosses the Baffin Bay and enters the Arctic further north, the fraction that just recirculates in the Baffin Bay, and the fraction that is caught in a short recirculation around the section. This will be discussed in the next section. Atlantic Water entering the Arctic through Fram Strait or the Barents Sea represents a fraction of the exports (around 40%) similar to that of the Pacific Water, with a clear seasonal cycle as it increases during summer (especially the part originating in the Barents Sea).

Fram Strait : In the model, almost all the water masses exported through Fram Strait are Atlantic Water originating from Fram Strait or the Barents Sea. We only find small traces of Pacific Water. The amount of Pacific Water exiting through Fram Strait is too small compared to observations and estimates using dissolved nutrients (*Jones et al.*, 1998, 2003; *Taylor et al.*, 2003) and this model deficiency will be discussed in section 4.3.

Waters exported near the surface or near the bottom are composed in equal part of water coming from Fram Strait and the Barents Sea. At the same time, the intermediate density class ($27.8 \leq \sigma_0 < 28.05$) is mainly composed of waters entering the Arctic through Fram Strait (80 %). A seasonal cycle is clearly noticeable, as the export through Fram Strait increases during fall and winter. This is especially obvious for the water masses that recirculate from and to Fram Strait. This cycle is in opposition of phase with the transfer of Atlantic Water to Davis Strait. The total amount of exported Atlantic Water is thus roughly constant. This suggests spatial variability of the circulation rather than temporal variability.

4.2.4.2 Streamlines, circulation and residence times.

This part aims at diagnosing the pathways within the Arctic Ocean of the water that eventually exits along either sides of Greenland. The Lagrangian method allows visualization of streamfunctions obtained by vertical integration of the 3D transport field accounted for the particles displacement from an entrance to an exit section (*Blanke et al.*, 1999). Fig. 4.6 and 4.7 show the streamfunctions of the transfers to Davis Strait and Fram Strait (in the three different layers) respectively. Fig. 4.8 shows the accumulated transport at the exit sections (in percentages) as a function of time and for each possible pathway.

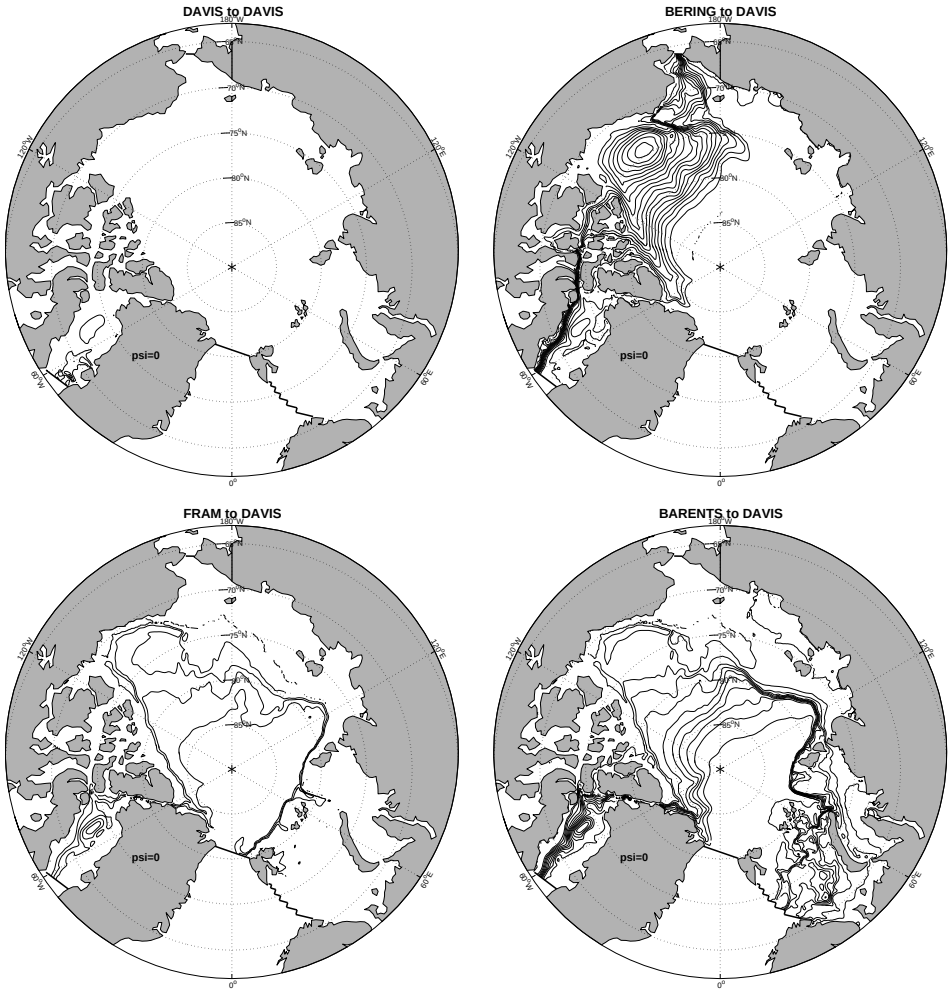

FIG. *4.6: Horizontal mass streamfunction ψ related to the vertically-integrated transport of the water transfers to Davis Strait, from Davis Strait (top left), Bering Strait (top right), Fram Strait (bottom left) and the Barents Sea (bottom right). The contour interval is 0.1 Sv and PSI is set to 0 over Greenland.*

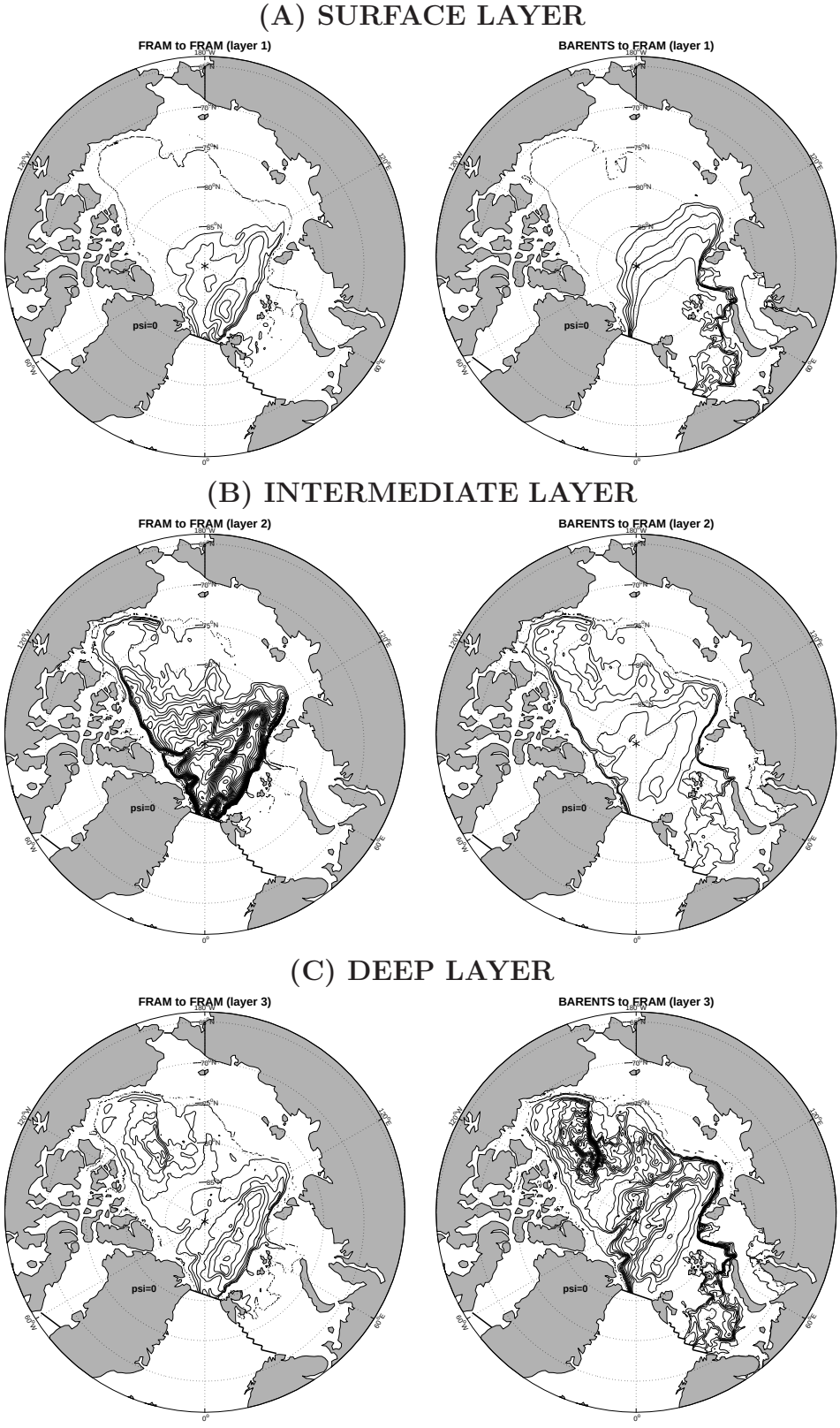

FIG. *4.7: Horizontal mass streamfunction (ψ) related to the vertically-integrated transport of the water transfers to three different layers in Fram Strait, from Fram Strait (left) and the Barents Sea (right). The contour interval is 0.1 Sv and ψ is set to 0 over Greenland.*

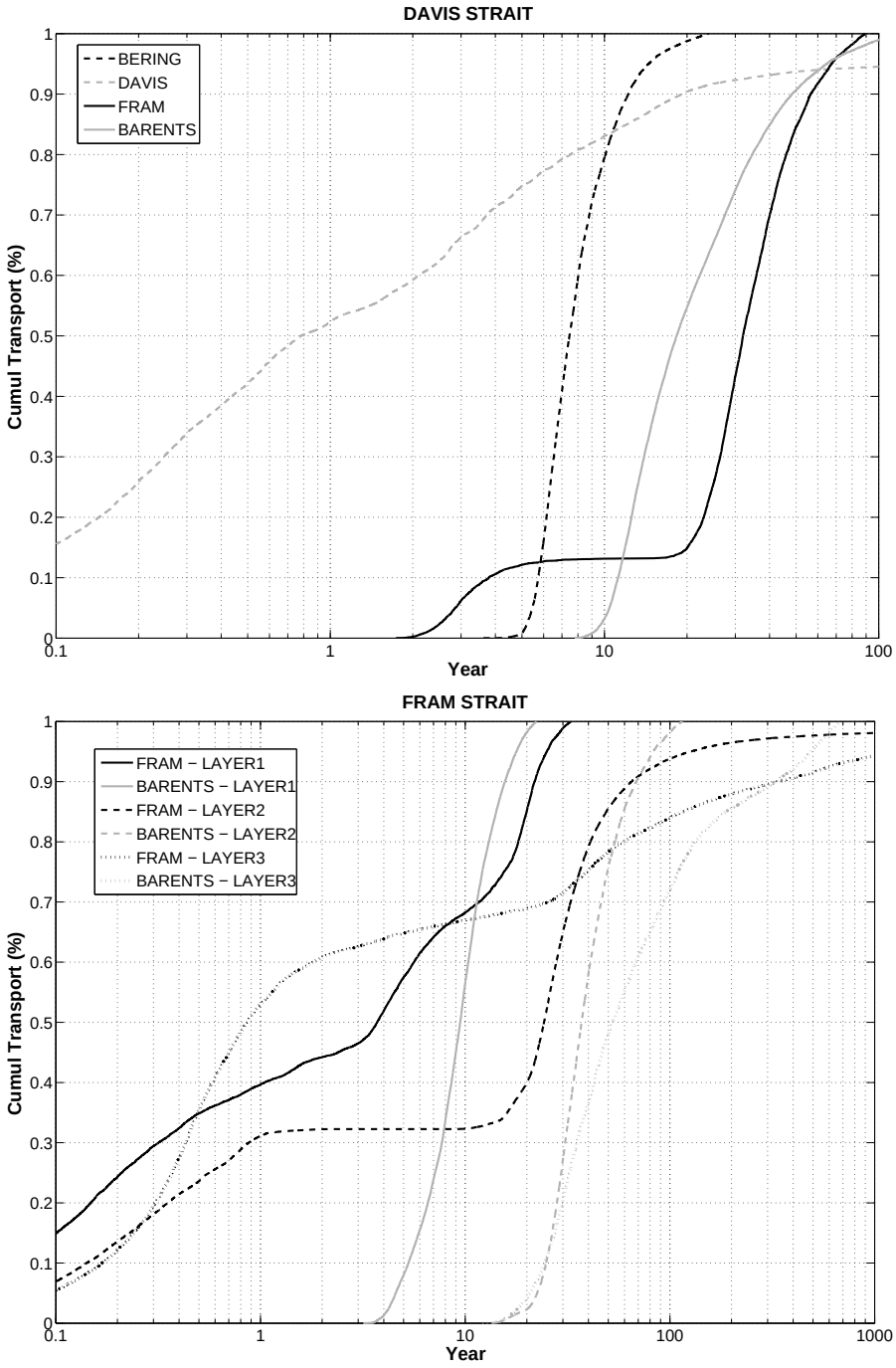

FIG. *4.8: Normalized time-integrated transport as a function of travel times for the different connections under consideration. (Top) To Davis Strait, from Bering Strait, Davis Strait, Fram Strait and the Barents Sea with a black dashed line, a gray dashed line, a solid black line and a solid gray line, respectively. (Bottom) To Fram Strait, from Fram Strait and the Barents Sea with a black line and a gray line, respectively. Individual layers are shown with the different line styles.)*

Davis Strait : On their journey from the Pacific Ocean to the North Atlantic via Davis Strait, the water masses entering the Arctic through Bering Strait are swept into the

anticyclonic Beaufort gyre. In the model, this transfer occurs completely in the upper layer of the Arctic (down to 300 meters), and the waters following this pathway remain in the Canadian Basin. This is consistent with the description of the lateral extent of the Pacific halocline presented by *Steele et al.* (2004), with an eastern limit being roughly the Mendeleyev Ridge. Fig. 4.6 also shows that these waters mostly cross the CAA from M'Clure Strait to Lancaster Sound. One has to remember that the pathway through the CAA strongly depends on the model resolution, but these results are in good agreement with observations presented in *Jones et al.* (2003). They report that *'only pacific water appears to have exited from the Arctic Ocean through the CAA except via Nares Strait, where Atlantic water of Arctic origin (rather than having arrived from the south via the WGC) is encountered at depths of 75 m and greater'*. The transfer from Bering Strait to Davis Strait is fast (between 4 and 25 years), half of it being done in less than 8 years. This is coherent with the residence times for the upper Arctic Ocean calculated in previous studies using transient anthropogenic tracers : *Ostlund and Hut* (1984) estimated a range between 8 to 10 years and *Schlosser et al.* (1994) found a range between 9 to 20 years, with a general increasing trend of age with depth.

Our Lagrangian analysis reveals that, in the model, the water that crosses Davis Strait northward within the West Greenland Current (WGC) is not entering the Arctic Ocean. It recirculates within Baffin Bay, and exits quickly southward through Davis Strait (half of the transfer is done in less than 10 months). The streamlines follow the isobaths, suggesting that the recirculation is subject to topographic constraints.

We now focus on the part of the export at Davis Strait that is composed of Atlantic Water entering the Arctic through Fram Strait or the Barents Sea. Streamlines that represent the transfer from Fram Strait to Davis Strait follow roughly the isobaths. In the model, water masses follow the Nansen Basin slope, and enter to the northern part of the Laptev Sea. Then a branching occurs : one branch flows down along the Lomonosov Ridge in the Makarov Basin, whilst the other branch enters the Canadian Basin and joins the Beaufort Gyre. To get to Davis Strait, Atlantic Water crosses the CAA mostly trough Nares Strait and then Smith Sound, which is also consistent with *Jones et al.* (2003). The whole transfer occurs mainly in the surface and intermediate layers (down to 400 m) and travel times are between 20 and 90 years.

A similar circulation scheme is found for waters entering through the Barents Sea. It first recirculates in the Barents Sea and then follows the same pathways. A part of these waters travels faster, as the first particles inseminated in the Barents Sea reach Davis Strait 8 years later, and 50 % of the transfer occurs in less than 17 years. Transit times are consistent with the times scale related to the circulation scheme proposed by *Smethie*

et al. (2000), in which waters entering the Barents Sea reach the North of Greenland about 23 years later.

Concerning the Atlantic Water pathways, *Nazarenko et al.* (1998) use a passive tracer integration in their model and find a more direct and intense return flow along the Amundsen side of the Lomonosov Ridge, a process that our model fails to reproduce. *Nazarenko et al.* (1998) use an eddy parametrization (the so-called Neptune effect) and show that the eddy-topography interactions are important to properly reproduce this branch of the circulation. As we do not use such a parametrization in our model and as our resolution is too coarse to resolve eddies in the Arctic, our global model may underestimate this branch of circulation for the Atlantic Water.

Atlantic Water exiting through Fram Strait : In the model, most of the water flowing northward within the North Atlantic Drift Current exits the Arctic Ocean through Fram Strait. The circulation scheme and related times scale are strongly dependent on the density classes considered. The water masses that form the surface layer of the export are making a short travel in the Arctic Ocean, both for time and distance. They stay in the Nansen Basin and flow southward within the Transpolar Drift to Fram Strait. These waters need less than 30 years to leave the Arctic, half of the transfer being done in 4–9 years, depending on whether they enter through Fram Strait or Barents Sea.

The intermediate waters that exit through Fram Strait are originating from Fram Strait (80 %) and the Barents Sea (20 %). Fig. 4.7 (B) shows three structures corresponding to the different possible pathways. A part of the water stays in the Nansen Basin, and then flows southward along the Lomonosov Ridge with the transpolar drift before it exits through Fram Strait (this returning flow along the ridge is probably underestimated in the model as explained in the previous paragraph). The remaining water masses cross the Lomonosov Ridge. One branch flows around the Makarov Basin along the East Siberian Sea slope and the Alpha/Mendeleyev Ridge, whilst a second branch enters the Canadian Basin and follows the other side of the Alpha/Mendeleyev Ridge. These latter two branches of circulation converge to the north of the CAA and follow the continental slope until they leave the Arctic through Fram Strait. This circulation scheme for the intermediate water is fully consistent with the one predicted by *Rudels et al.* (1994) and also described by *Smethie et al.* (2000) : the scheme consists of three large cyclonic cells in the three different basins. Half of the transfer from Fram Strait to Fram Strait is done in less than 25 years in the model, even though part of the water can remain more than 1000 years in the basin. The first plateau for this transfer visible in Fig. 4.8 corresponds to the part of the water that just recirculates near the strait. The particles that follow the pathway from the Barents Sea to Fram Strait need 10 to 100 years to exit, half of

them exiting after 40 years. The time scales obtained for intermediate Atlantic Water are similar to the ones usually found in the literature, with an order of magnitude around 20 years (*Schlosser et al.*, 1995; *Smethie et al.*, 2000; *Karcher and Oberhuber*, 2002).

The deep layer ($\sigma_0 \geq 28.05$) of the export through Fram Strait is roughly composed in equal part of water entering the Arctic through Fram Strait and through the Barents Sea. Fig. 4.7 (C) shows that the circulation schemes for both transfers are similar, and also similar to the pathway followed by the waters exiting in the intermediate layer. However, half of the water coming from Fram Strait exits the Arctic after 11 months, whereas this time increases to 50 years for the water flowing from the Barents Sea. The time scales related to the pathway from the Barents Sea to Fram Strait are consistent with the study of *Ostlund et al.* (1987) in which the renewal time for the deep water by the Barents Sea Branch is estimated around 100 years.

Lack of Pacific Water at Fram Strait : a model deficiency ? Our Lagrangian analysis shows that, in the model, almost all the Pacific Water entering the Arctic through Bering Strait exits through the CAA and then Davis Strait, whilst we can only find small traces of Pacific Water at Fram Strait. However, many recent studies (*Jones et al.*, 1998, 2003; *Taylor et al.*, 2003; *Falck et al.*, 2005) used concentrations of dissolved nutrients to trace Pacific Water into the North Atlantic, and showed that a substantial fraction of Pacific Water exits on the eastern side of Greenland, through Fram Strait. As our study aims at determining the origins of the exports along both sides of Greenland, it is crucial to analyze the model deficiency and to quantify its impact on our results.

Jones et al. (1998) used nitrate and phosphate concentration relationships to distinguish Atlantic from Pacific waters and estimated their relative amounts in the first 30 meters in the Arctic Ocean. They showed that Pacific Water exits the Arctic in the western part of Fram Strait within this layer. Afterward, *Jones et al.* (2003) used the same method to show that the exports done in the first 100 meters and within 100 km of the Greenland coast at Fram Strait were mainly composed of Pacific Water between 1997 and 1999, even though interannual variability can lead to large changes in the amount of Pacific Water (*Taylor et al.*, 2003), with complete disappearance of the strongest part of the signal (above the shelf and slope northeast of Greenland) in some years (*Falck et al.*, 2005). Note that in our model, the area across the Fram Strait section where Pacific Water should be found is small relative to the area covered by the outflowing branch. If the same is true in the real ocean, it implies that, in term of transport, the contribution of this water mass remains quite small compared to the Atlantic water contribution, even though the Pacific Water probably contributes significantly to the freshwater export.

What could be, in our model or in our methodology, the explanation for the lack of Pacific Water ? First, the Lagrangian analysis has been run over a climatological year built over monthly mean model outputs from 1980 to 2001. This mean state of the Arctic might not be representative of any instantaneous state of the Arctic dynamics. We have run a sensitivity Lagrangian experiment, using 5 years made of successive 5-day model outputs, to calculate forward trajectories of particles inseminated at Bering Strait. We repeated those 5 years until the slowest particle exited the domain of integration. The transport transmitted to Fram Strait is still negligible (0.02 vs 0.01 in Table 4.2), the transport to Davis is similar (1.07 vs 1.11 Sv in Table 4.2, with half of the particles exiting in less than 8 years with an age distribution similar to Fig. 4.8). It is not possible to redo all our calculations with the 5-day outputs for practical (prohibitive computer time requirements) as well as methodological reasons ("looping over" a given time period to compute long trajectories is questionable). Nevertheless, this single sensitivity experiment suggests that the lack of Pacific water at Fram Strait is not an artifact of the Lagrangian method but rather a shortcoming of the Eulerian fields.

A second explanation could be the fact that in the model all the simulated Pacific Water is swept into the Beaufort Gyre. Fig. 4.6 shows that the simulated Pacific Water is completely transferred to the North Atlantic through the Beaufort Gyre. *Steele et al.* (2004) used observations of the halocline in the Arctic and showed that some Pacific Water enters the Arctic within a coastal current on the eastern side of Bering Strait, and continues along the shelf break, as also previously suggested by *Jones et al.* (1998). As mentioned in *Lique et al.* (2009), our simulated Beaufort Gyre is probably displaced too close to the Canadian coast compared to its observed location, and the coastal current along the shelf is not properly simulated. This model deficiency might be due to a too coarse spatial resolution, or the underestimation of eddy-topography interactions that would help to simulate the coastal current following the shelf north of the CAA (*Nazarenko et al.*, 1998). It can also been seen in the study of *Holloway and Wang* (2009) where simulation with a coarse model but with a parametrization of the Neptune effect simulates properly a narrow current on the shelf along the Canadian Coast.

Third, the model grid (12 km) is too coarse to resolve most of the mesoscale activity. *Spall et al.* (2008) highlight the presence of eddies along the southern Beaufort Sea, and show their ability to transport Pacific Water properties to the interior of the basin. This suggests that a fraction of the Pacific Water entering the Arctic through Bering Strait could be transported via eddies with typical diameters of 30 km. We can logically infer that if a part of the transfer of Pacific Water to Fram Strait occurs in such eddies, it is not represented in our Lagrangian trajectories but rather appears as a transformation of the Atlantic branch due to the model isopycnal diffusion.

4.2.5 Water mass transformations in the Arctic Ocean.

4.2.5.1 Pacific Water.

Modification of Pacific Water in the Arctic Ocean is a key point for the freshwater storage and release in the Arctic Ocean (*Häkkinen and Proshutinsky*, 2004). Its quantification as well as the mechanisms at play are the focus of this section.

In order to quantify the modifications, we compute the freshwater and heat fluxes corresponding to the different water masses at their entrance and exit sections in the Arctic. The freshwater flux is computed as :

$$T_{FW} = \sum_{part} \frac{S_0 - S_{part}}{S_0} Tr_{part}$$

where S_0 is a reference salinity, here equal to 34.8 psu to be consistent with the estimations given in section 3, S_{part} is the salinity of each particle at the entrance (or exit) section and Tr_{part} is the infinitesimal transport associated with the same particle. The heat flux is defined in an equivalent way as :

$$T_H = \sum_{part} \rho_0 C_p (T_{part} - T_0) Tr_{part}$$

T_{part} being the temperature of a given particle at the entrance (or exit) section and T_0 a reference temperature chosen as -0.1°C to be consistent with results given in section 3.

Results for the pathway from Bering Strait to Davis Strait are given in Table 4.3 (A). A comparison with the values given in Table 4.1 shows that, in our simulation, the outflow of Pacific Water through Davis Strait accounts for 40% of the total freshwater export and 100% of the total heat export through this exit. Pacific Water is the most important advective source of freshwater for the Arctic Ocean. Fig. 4.9 shows the transport distribution binned into salinity and temperature classes at the entrance and exit sections for this water mass. During its travel into the Arctic Basin, Pacific Water becomes saltier, while its temperature only slightly warms. This water mass is thus contributing to a freshening and a cooling of the Arctic Ocean. As the Pacific Water is transferred in the surface layer, one has to remember that the quantification of this water mass transformation is affected by the strong restoring used in the simulation, which results in a large surface flux correction as shown in *Lique et al.* (2009).

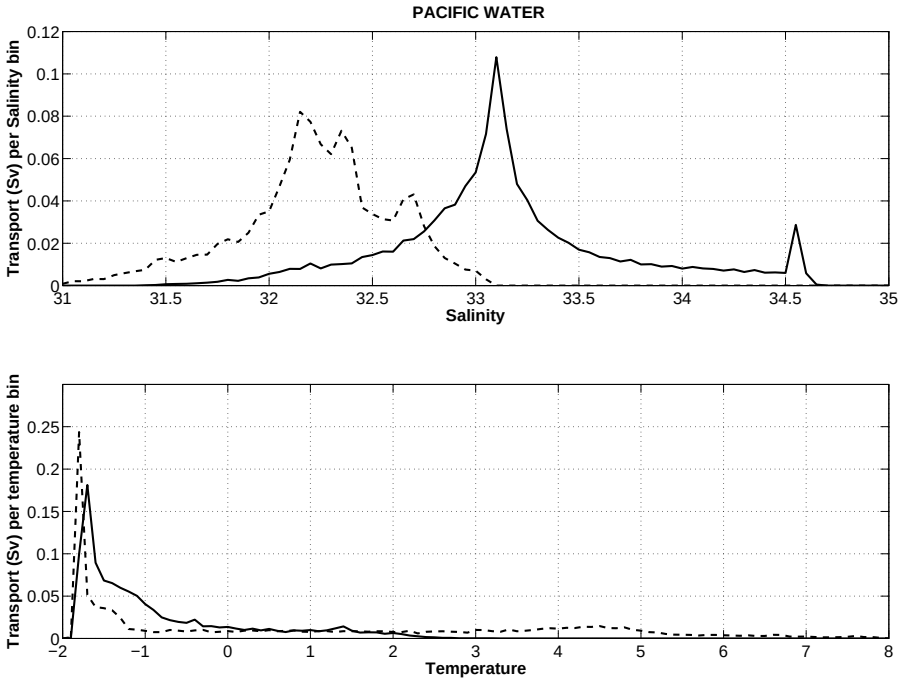

FIG. *4.9: Top : Transport binned as a function of salinity at the entrance and exit sections for the Pacific Water. The bin interval is 0.05 psu.*
Bottom : Same as Top, but as a function of temperature. The bin interval is 0.1°C .

A : Bering to Davis		**Bering Strait (entrance)**	**Davis Strait (exit)**
Freshwater transport		81.2 mSv	51.6 mSv
Heat transport		5.0 TW	-3.2 TW
B : Fram to Davis		**Fram Strait (entrance)**	**Davis Strait (exit)**
Freshwater transport		1.1 mSv	11.4 mSv
Heat transport		3.4 TW	0.2 TW
C : Barents to Davis		**Barents Sea (entrance)**	**Davis Strait (exit)**
Freshwater transport		-1.9 mSv	42.7 mSv
Heat transport		21.5 TW	-1.9 TW
D : Fram to Fram		**Fram Strait (entrance)**	**Fram Strait (exit)**
Freshwater transport	LAYER 1	0.5 mSv	16.9 mSv
	LAYER 2	-8.6 mSv	-3.7 mSv
	LAYER 3	-3.3 mSv	-3.0 mSv
Heat transport	LAYER 1	6.8 TW	-0.6 TW
	LAYER 2	20.0 TW	9.5 TW
	LAYER 3	1.6 TW	-1.2 TW
E : Barents to Fram		**Barents Sea (entrance)**	**Fram Strait (exit)**
Freshwater transport	LAYER 1	-1.4 mSv	31.5 mSv
	LAYER 2	-1.5 mSv	-0.9 mSv
	LAYER 3	-2.2 mSv	-2.5 mSv
Heat transport	LAYER 1	12.8 TW	-2.8 TW
	LAYER 2	10.9 TW	1.6 TW
	LAYER 3	15.5 TW	-0.3 TW

TAB. *4.3: Freshwater and heat transports at the entrance (column 3) and exit (column 4) sections for the different possible pathways. Two secondary pathways('Davis to Davis' and 'Barents to Barents') are deliberately omitted.*

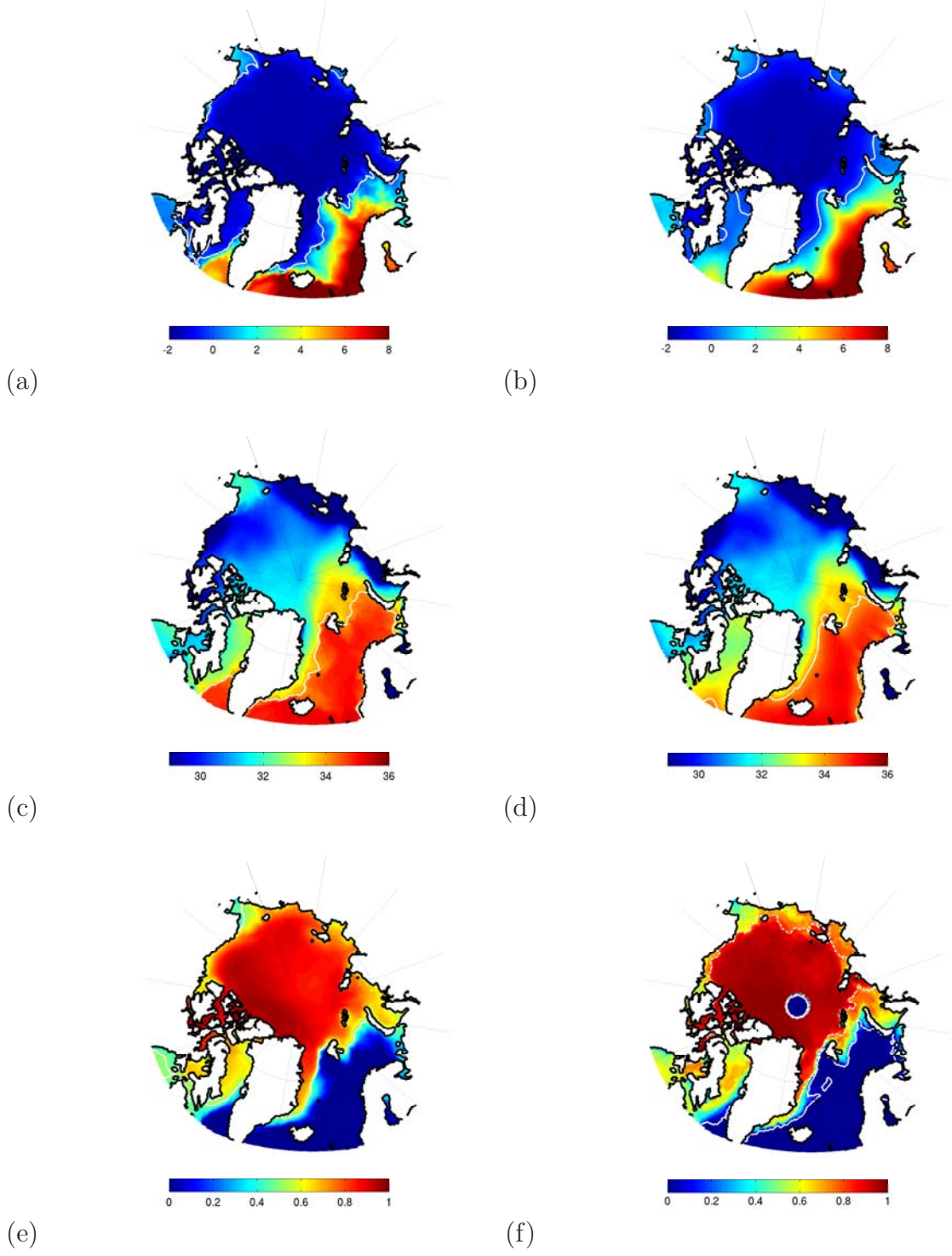

FIG. *4.10: Left : Mean model fields over the Arctic Ocean. (a) Sea Surface Temperature (in °C). The 0° C contour is superimposed in white. (c) Sea Surface Salinity (in psu). The 34 psu contour is superimposed in white. (e) Sea-ice concentration, with the September (dotted line) and March (plain line) extents superimposed with a dotted and a plain white line, respectively.Right : Same as Left, but for the PHC climatology ((b) and (d)) and Sea Ice observations averaged over 1992–2001 (Ezraty et al., February 2007).*

Fig 4.10 (a) and (b) suggests that Pacific Water does not cross any temperature or salinity front before being swept in the Beaufort Gyre. In the model, the limit of the sea ice extent moves seasonally in the Beaufort Sea. The yearly mean sea ice extent as well the September and March mean sea ice extent seem to be consistent with observations (Fig 4.10 (e) and (f)). However, when we follow the T/S properties of Pacific Water along its pathway, the limit of sea ice extent does not correspond to any important and abrupt water mass transformation. It thus suggests that modifications of Pacific Water are done gradually along its travel in the Arctic by turbulent mixing with the water masses already present in the Beaufort Gyre.

4.2.5.2 Atlantic Water.

Quantification of the water mass transformations : Atlantic Water exiting the Arctic through Davis Strait or within the upper layer in Fram Strait undergoes strong freshening and cooling in the Arctic Basin. Its T/S properties are qualitatively similar at the entrance and exit sections for the Fram Strait Branch and the Barents Sea Branch (Fig. 4.11, Davis Strait and layer 1). However, the Barents Sea Branch is saltier as it exits through Davis Strait than through Fram Strait. The part of Fram Strait Branch that eventually exits through Davis Strait is colder at the entrance section than the part exiting through Fram Strait. Thus, the Barents Sea Branch undergoes stronger modifications than the Fram Strait Branch. This is also shown by freshwater and heat fluxes calculated at the entrance and exit sections (Table 4.3). As its upper layer salinity and temperature decrease during the transit, the Atlantic Water carries more freshwater and less heat, and thus contributes to a salinification and a warming of the Arctic Ocean. From its entrance in the Arctic to its exit trough Davis Strait or through the upper part of Fram Strait, the Barents Sea Branch gains around 80 mSv of freshwater and loses around 40 TW of heat. The figures are only about 25 mSv and 10 TW for the Fram Strait Branch.

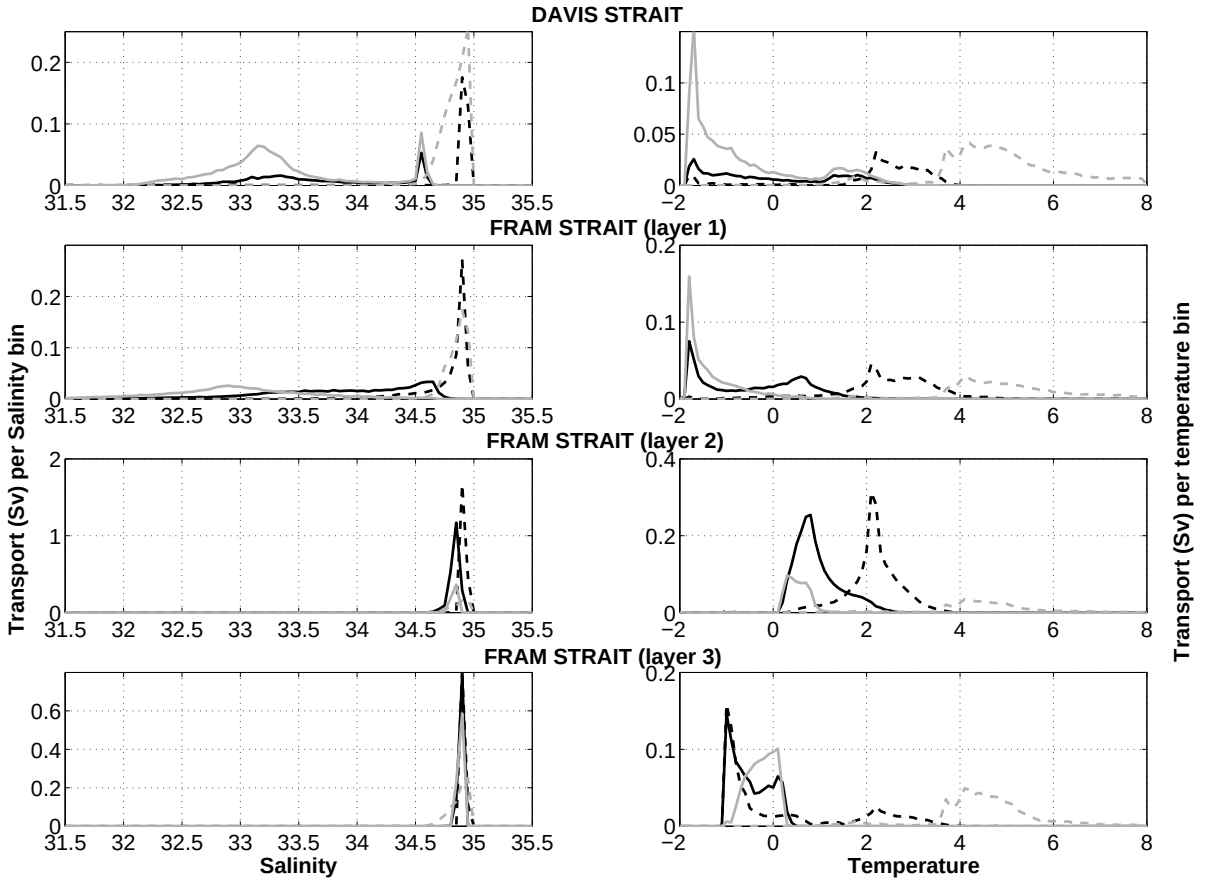

FIG. *4.11: Left : Transport binned as a function of salinity at the entrance and exit sections for the Atlantic Water. The bin interval is 0.05 psu.*
Right : Same as Left, but as a function of temperature. The bin interval is 0.1°C .
The Barents Sea Branch is in gray, the Fram Strait Branch is in black. Distributions on entrance and exit sections are shown as dashed and solid lines, respectively.

The picture is different for the water masses exiting within the intermediate and deep layers through Fram Strait (Fig. 4.11, layers 2 and 3). During its transit within the Arctic Basin, Atlantic Water undergoes a slight modification of salinity whilst its temperature strongly decreases. For water masses exiting in the intermediate density class, salinity decreases from 34.9 to 34.8 psu whilst the peak of temperature goes from 4°C to 0.2°C for the Barents Sea Branch and from 2°C to 0.8°C for the Fram Strait Branch. Modifications of the water masses composing this layer thus contribute to a salinification and a significant warming of the Arctic Ocean, mainly due to modifications of the Fram Strait Branch (see Table. 4.3). In the deeper layer, the Fram Strait Branch undergoes a slight freshening and cooling, whilst the Barents Sea Branch undergoes a slight salinification, together with an important cooling.

To summarize the Atlantic Water modifications, the Atlantic Water undergoes a general cooling and a freshening during its transit in the Arctic Ocean. One must not forget

however that all the figures given in this section might be strongly model dependent, especially because of the surface salinity restoring used in the simulation. Atlantic Water transformations represent a gain of salt and heat for the Arctic Ocean, but the gain does not come from the same water mass. The main part of the salinification is due to transformations of water exiting in the surface layers, and the contribution of the Barents Sea Branch is more than twice larger than the contribution of the Fram Strait Branch. On the other hand, the warming of the Arctic Ocean is due to modifications of the whole Atlantic Water composing the three density classes, even though the fraction of the Barents Sea Branch that exits in the upper layer on both sides of Greenland has a dominant influence.

The role of the Barents Sea : Now that water mass modifications have been quantified in our model, we determine the places where these modifications occur and try to understand the mechanisms responsible for them.
We calculate freshwater and heat fluxes carried by the Barents Sea Branch as it exits the Barents Sea, across a section from Spitsbergen to Russia, following the 500 m isobath (that roughly corresponds to the 80°N parallel). Results are given in Table 4.4.

		Barents Sea (entrance)	**Barents Sea (exit)**	**Exit Section**
Freshwater transport	LAYER 1	-1.4 mSv	21.2 mSv	31.5 mSv
	LAYER 2	-1.5 mSv	0.6 mSv	-0.9 mSv
	LAYER 3	-2.2 mSv	1.1 mSv	-2.5 mSv
	DAVIS	-1.9 mSv	37.2 mSv	42.7 mSv
Heat transport	LAYER 1	12.8 TW	-3.1 TW	-2.8 TW
	LAYER 2	10.9 TW	1.9 TW	1.6 TW
	LAYER 3	15.5 TW	0.2 TW	-0.3 TW
	DAVIS	21.5 TW	-1.1 TW	-1.9 TW

TAB. *4.4: Freshwater and heat transports at three passages along the Barents Sea Branch (see text for detail).*

The transit in the Barents Sea takes roughly 1 year. As they exit, water masses have undergone an important freshening and cooling, whatever the final section they reach in the Arctic. The Barents Sea is only 400 meters deep, so the modifications are due to exchanges with the colder atmosphere, river runoff and precipitation over the Barents Sea (*Schauer et al.*, 2002), as the Barents Sea is seasonally ice-free (see Fig 4.10 (e) and (f)). Table 4.4 shows that the heat flux transported by the Barents Sea Branch at its exit from the Barents Sea is roughly equal to the heat flux transported at its exit from the Arctic through Fram Strait or Davis Strait. This means that this branch undergoes its temperature modifications almost completely in the Barents Sea. For the

salinity modifications, the picture appears more complex. Water masses that exit in the upper layer (through Davis Strait and the upper layer through Fram Strait) have also roughly reached their final salinity as soon as they leave the Barents Sea. The water masses that compose intermediate and deep layers when they leave the Arctic Ocean through Fram Strait undergo a freshening in the Barents Sea and a salinification during the rest of their travel in the Arctic Basin. Fig 4.10 shows that a strong temperature and salinity front exists over the Barents Sea. The front moves seasonally with the limit of the sea-ice extent (not shown). Therefore, important water mass modifications (freshening and cooling) occur in the Barents Sea when the Barents Sea Branch crosses the front perpendicularly.
As it leaves the Barents Sea in St. Anna Trough (*Schauer et al.*, 2002), the modified Atlantic Water meets the Fram Strait Branch that has roughly kept its initial T/S properties. The mixing of the two branches is then responsible for a part of the transformations of the Fram Strait Branch, as predicted by *Smethie et al.* (2000).

4.2.6 Influence of the AO state on the circulation scheme.

The existence of two regimes of circulation for the sea-ice and the ocean surface layer has long been discussed in the literature (*Proshutinsky and Johnson*, 1997; *Häkkinen and Proshutinsky*, 2004). *Rigor et al.* (2002) showed that the switch from one of these regimes to the other is closely linked to a change in the Arctic Oscillation (AO) state, whose index is defined as the leading principal component of the Northern Hemisphere Sea Level Pressure (SLP) (*Thompson and Wallace*, 1998). To give some insight into how our Arctic circulation scheme would change under these two distinct regimes, we perform two additional Lagrangian experiments, using two contrasted new climatological years. These years are intended to represent the circulation during a positive or a negative AO state. They are referred to as 'AO+ year' and 'AO- year' in the following. We build them in the following way : the time series of the annual AO index (the yearly average of all months of the monthly AO index) from 1980 to 2001 is normalized to a zero mean and unit variance. Years with a normalized index larger than 1 are selected and averaged to build the AO+ year (1989, 1990, 1992, 1993, 1995, 1997 and 2000). Years with a normalized index smaller than -1 are used to build the AO- year (1980, 1981, 1984, 1985, 1986, 1987, 1996, 1998 and 2001). In reality, however, positive and negative phases of the AO alternate over a decadal timescale. Thus, one has to remember that our Lagrangian calculations are based here on an idealization, in which a given AO phase is assumed to last long enough for water masses to transit fully in the Arctic Basin under the same AO conditions. Nevertheless, these experiments allow comparison of our results with previous observational studies in which the circulation of sea ice is contrasted during the two regimes (e.g., *Rigor et al.* (2002)), or with modeling studies in which an OGCM is forced by typical AO+/AO- composite atmospheric conditions in order to determinate

the ocean and sea-ice canonical answer to a given AO phase (*Zhang et al.*, 2003; *Brauch and Gerdes*, 2005; *Condron et al.*, 2009).

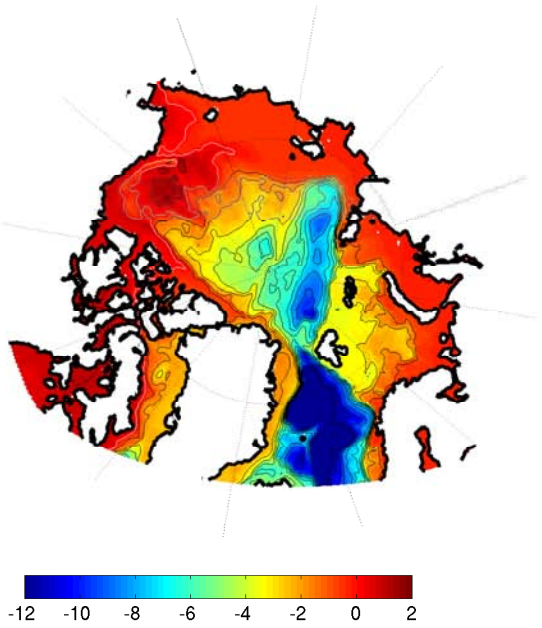

(a)

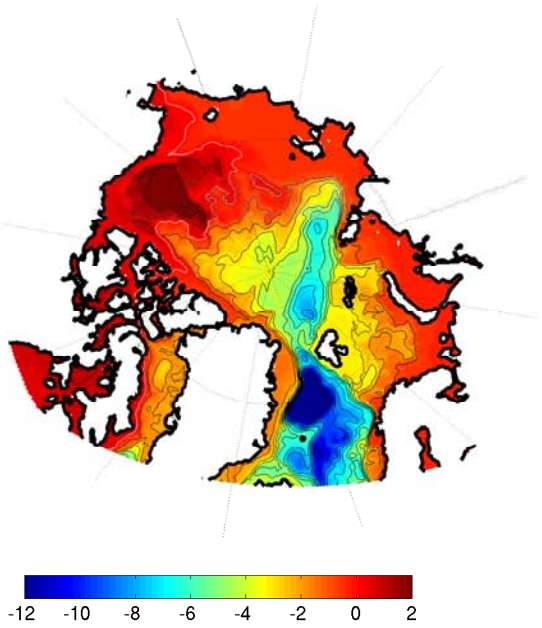

(b)

FIG. *4.12: Model of annual mean barotropic streamfunction in Sv for the AO+ year (a) and the AO- year (b). The contour interval is 1 Sv.*

Fig. 4.12 shows the mean Eulerian barotropic streamfunction for the AO+ and AO- years. The difference between the two regimes matches what one might expect according to results of *Proshutinsky and Johnson* (1997) or *Zhang et al.* (2003). During the positive phase of AO (Fig. 4.12(a)), the Beaufort Gyre contracts remarkably, and the Transpolar Drift structure shifts to the Canadian Basin and becomes predominant in the Arctic Basin. During a negative AO phase (Fig. 4.12(b)), the intensity of the Beaufort Gyre is strongly enhanced whilst the Atlantic inflow and the Transpolar Drift remain in the Eurasian Basin.

The results of our new Lagrangian experiments are given in Table 4.5. Using hydrographic data, *Steele et al.* (2004) showed that the circulation of Pacific halocline water is strongly influenced by the surface wind stress. Thus, the direct transfer of Pacific Water from Bering Strait to Davis Strait is enhanced during the negative phase of AO. Our results are consistent with those conclusions. The export of Pacific Water through Davis Strait is larger for the AO- year. The transfer of Pacific Water to Fram Strait is twice larger for the AO+ year than for the AO- year, as suggested by *Steele et al.* (2004). However, the export on the eastern side of Greenland remains small, and does not agree with direct observations (e.g., *Falck et al.* (2005)).

	DAVIS STRAIT		**FRAM STRAIT**					
			LAYER1		**LAYER2**		**LAYER3**	
	AO+	*AO-*	*AO+*	*AO-*	*AO+*	*AO-*	*AO+*	*AO-*
BERING STRAIT	1.10	1.16	0	0	0.02	0.01	0	0
DAVIS STRAIT	0.60	0.67	0	0	0	0	0	0
FRAM STRAIT	0.50	0.31	0.68	0.58	2.46	1.88	1.08	0.86
BARENTS SEA	1.13	0.88	0.62	0.63	0.70	0.54	0.72	0.79
TOTAL	3.33	3.02	1.30	1.21	3.18	2.43	1.80	1.65

TAB. *4.5: Relative contributions of the different branches that contribute to the southward transport through Davis Strait and Fram Strait, for AO+ and AO- years. Transports are given in Sv. Values smaller than 10^{-2} are set to 0.*

As also expected from the results of *Proshutinsky and Johnson* (1997), the Fram Strait Branch is intensified when the AO is positive and the Transpolar Drift is then predominant. This leads to an increase of the export along both sides of Greenland, and in the three density layers in Fram Strait. The picture seems to be more complicated for the Barents Sea Branch. The export of water originating from Barents Sea is larger for the AO+ year than for the AO- year through Davis Strait and the intermediate layer in Fram Strait, but smaller when we consider the upper and deeper layers in Fram Strait. We show that an important fraction of the waters following the pathway from the Barents Sea to the deep layer in Fram Strait crosses the Lomonosov Ridge and enters the Canadian

Basin, where it recirculates following the topography. We do not know the influence of the AO state on the deep circulation, as the residence times in this layer are longer than the period over which the AO index keeps the same sign. However, our analysis gives evidences that, in the model, the deep circulation is also intensified in the Canadian Basin during a negative AO state, in a similar manner as the surface circulation. Concerning the surface layer export, the difference between the results of the two new Lagrangian experiments is probably due to the influence of the AO state on the circulation in the Barents Sea, as it cannot be explained by a difference in the circulation in the Arctic Basin along the Transpolar Drift. This would need to be studied in detail.

Rigor et al. (2002) and *Zhang et al.* (2003) also showed from observations and idealized modeling that the export of freshwater and sea ice increases on both sides of Greenland during a positive AO phase. In the model, the sum of the freshwater and sea-ice exports for the AO+ year though Fram Strait and Davis Strait are 130.5 mSv and 139.4 mSv respectively. These amounts fall to 106 mSv and 123.1 mSv for the AO- year. Our Lagrangian experiments show that the difference is completely due to a larger freshening of Atlantic Water for the AO+ year than the AO- year, whereas modifications of Pacific Water are roughly the same for the two experiments. In general, temperature as well as salinity modifications of the Atlantic Water are stronger for the AO+ year, even though differences are not very large. When we calculate freshwater and heat fluxes at the entrance and exit sections for the various pathways (not shown), the differences between the two sensitivity experiments in terms of freshwater and heat modifications are closely linked to the differences shown for the mass exports (Table 4.5). The modifications of heat and freshwater fluxes are thus larger for the intensified branches of circulation. It means that the AO state may have a bigger influence on the Arctic dynamics (the velocity field) than on specific water mass properties and transformations.

4.2.7 Conclusions.

In this paper, a quantitative Lagrangian analysis has been applied to the 3D output of a simulation using the global ocean/sea-ice high resolution DRAKKAR model (1/4° , which is about 12 km in the Arctic Ocean). We propose for the first time a quantitative scheme of the Arctic circulation and related water mass modifications, for a climatological year built over the 1980–2001 period. A validation of the model was carried out in the present paper as well as in *Lique et al.* (2009), comparing the model Eulerian fields with direct observations (when and where available) and with previous model studies (such as those published within the AOMIP project). Although the model Eulerian fields are shown to reproduce fairly well the Arctic Ocean circulation and water mass properties, which adds credibility to our Lagrangian analysis, the results are model and method dependent. The quantification of the water mass transformations might be affected by the the use a very

strong restoring to a climatological surface salinity. This study is only a first step toward a coherent scheme of the Arctic circulation.

The study mainly focuses on determining the origins of water masses exported from the Arctic Ocean along both sides of Greenland (through Davis Strait on the western side, and Fram Strait on the eastern side). At Davis Strait, the exports are composed of water of Pacific and Atlantic origins in equal part. On the other hand, in the model, the exports through Fram Strait are composed of water entering the Arctic within a Fram Strait Branch and a Barents Sea Branch, with only very small traces of pacific Water. Both branches export an equal amount of water in the upper and deep layer, whereas the exported intermediate water mainly comes from the Fram Strait Branch (80%).

The study reveals that, in the model, Pacific Water entering the Arctic exits on the western side of Greenland and is transferred quickly (O(10 years)) to the North Atlantic. It transits through the Beaufort Gyre in the upper layer, where gradual warming and salinification occur. Thus, we are unable to simulate a transfer of Pacific Water from Bering Strait to Fram Stait, though this transfer has been evidenced by several observers (*Jones et al.*, 1998, 2003; *Taylor et al.*, 2003). One could find this result a bit surprising, especially when one knows that the model inflow through Bering Strait is overestimated by about 20%, so we discussed the possible reasons for this model deficiency (also found for instance in the numerical study of *Karcher and Oberhuber* (2002)). The most likely explanation is the underestimation of the current on the shelf along the Canadian Coast, through which Pacific Water might be transferred to Fram Strait.

Atlantic Water exiting in the surface layer along both sides of Greenland remains about 10 years in the Arctic Basin, and undergoes a cooling and an important freshening (especially for the Barents Sea Branch). This transformation represents the most important source of salt for the Arctic Ocean. In the model, the fraction of these waters that exits through Davis Strait is found to enter the Canadian Basin in the Laptev Sea. Atlantic Water exiting through the intermediate and deep layers in Fram Strait follows different possible pathways in the Arctic, with trajectories being subject to topographic constraints. The intermediate layer is mainly composed of the Barents Sea Branch, and these waters need about 30 years to travel in the Arctic, where their temperature strongly decreases whilst their salinity remains roughly constant. As for the exports in the deeper layer, the travel time (from 1 year to 1000 years) depends strongly on the followed pathway and the transformations are less important (only the Barents Sea Branch undergoes an important cooling).

The role of the Barents Sea in the transformations of the Atlantic inflow has been under-

lined. The model results suggest that the Barents Sea Branch is almost fully transformed there in less than one year, due to exchanges with the very cold atmosphere. A fraction of the modifications of the Fram Strait Branch is due to turbulent mixing with the Barents Sea Branch, as both branches converge in the St. Anna Trough at the exit from the Barents Sea. As the Arctic is becoming more and more ice free, one can imagine that such strong and quick transformations could also occur over the other Arctic shelves.

Our study provides a picture of the mean circulation scheme, and this scheme is found to be relatively robust to a change in the AO state. Although this description of the Arctic mean state is prerequisite, thorough study of the variability of this scheme is needed to allow better understanding of the Arctic Ocean response to climate change. For instance, finer scales, both in time and space, have to be investigated, as our dynamic scheme might change if a higher resolution model with higher frequency outputs was used for the Lagrangian analysis. A complementary approach to this study could also be the simulation of passive tracers, taking into account both the advective and diffusive components of the water mass trajectories.

Acknowledgements : We thank Bruno Tremblay (editor), Greg Holloway and an anonymous reviewer for their great help and their important comments that have contributed to improve significantly our manuscript. We also thank C. Herbaut and J. Cuny for very helpful comments and suggestions on an earlier version. This study uses numerical experiments carried out within the DRAKKAR project. The simulation has been run at the IDRIS CNRS-GENCI computer centre in Orsay, France, by J.M. Molines. C. Lique is supported by CNES and IFREMER. A.M. Treguier, B. Blanke and N. Grima are supported by CNRS.

Chapitre 5

Variabilité des conditions de glace de mer.

5.1 Préambule

Au cours de l'exposé de l'état de l'art ainsi que dans les trois chapitres précédents, nous nous sommes principalement focalisés sur la composante océanique du bassin Arctique, dont la connaissance et la compréhension restent fragmentaires, de part la faible quantité d'observations en comparaison aux autres océans du globe, rendant difficile l'évaluation du réalisme des simulations numériques de cette région. Cela laisse peut être supposer, à tort, que la connaissance des conditions de glace dans la bassin Arctique est elle plus complète que celle des conditions océaniques.

Les mesures satellites donnent accès à une quantification de la concentration de la glace de mer dans les régions polaires depuis presque quatre décennies, ce qui nous permet de connaître la variabilité saisonnière à interannuelle de l'extension de glace dans le bassin Arctique, ainsi que sa tendance sur les 40 dernières années. Pourtant, tout comme l'altimétrie satellitale dans les autres régions du globe ne donne qu'une vision de la circulation océanique de surface, les mesures satellitales ne permettent pour le moment de n'avoir accès qu'à une vision en 2D de la glace de mer. De nouvelles techniques de mesures sont en cours de développement pour mesurer l'épaisseur de la glace de mer, avec les lancements des satellites *ICEsat* et *Cryosat2*, qui permettent d'avoir une vision 3D de la banquise Arctique (jusqu'à maintenant, les mesures d'épaisseur de glace restent rares et éparses, dans le temps et dans l'espace). Aujourd'hui encore, seuls les modèles numériques nous permettent donc d'étudier les conditions de glace de mer avec une vision 3D, ainsi que leur variabilité.

On conçoit pourtant aisément que c'est bien une connaissance et une compréhension de

la variabilité du volume de glace (et non simplement de son extension) qu'il nous faut avoir si l'on veut comprendre les mécanismes de variabilité du système d'eau douce dans le bassin polaire Arctique. Nous avons par exemple montré dans le chapitre 2 que les variations du flux glace-océan au Nord du Groenland étaient responsables d'environ la moitié de la variabilité interannuelle des exports d'eau douce liquide de l'Arctique vers l'Atlantique à travers le détroit de Fram (*Lique et al.*, 2009). On comprend bien ici que le système glace de mer-océan doit être étudié dans son ensemble, les deux composantes étant intrinsèquement liées.

Dans ce chapitre, nous allons donc nous concentrer sur la variabilité interannuelle et les éventuelles tendances du volume de glace dans le bassin Arctique. Le but principal de cette étude est de mettre en évidence, de manière systématique, le rôle des différents forçages atmosphériques (vent, flux de chaleur) dans cette variabilité. Pour ce faire, nous allons utiliser un modèle régional couplé glace/océan de la région Arctique et Atlantique Nord, au 1/2° . Le modèle ainsi que la simulation de référence sont ceux utilisés dans l'étude de *Herbaut and Houssais* (2009) pour comprendre l'influence de la NAO sur les régimes de circulation de la gyre subpolaire. Parallèlement à cela, nous avons réalisé des tests de sensibilité où les forçages atmosphériques sont tour à tour réduits artificiellement à un cycle climatologique annuel.

Les résultats sont présentés ici sous la forme d'un article encore en préparation.

5.2 Article en préparation : Atmospheric driving of the Arctic sea ice volume interannual variability.

5.2.1 Introduction.

The Arctic region has attracted much attention in recent years, as we expect an amplification of the climate change signature in the polar regions, primarily due to ice-albedo feedback associated with changes in snow and sea-ice coverage (the so-called "polar amplification", e.g. *Manabe and Stouffer* (1980); *Holland and Bitz* (2003)). Hence, monitoring the variability and the possible long term changes of the Arctic sea ice conditions, and underlying the mechanisms responsible for them are highly relevant for understanding the state of the present climate and for predicting future climate change. In this paper, we explore how the different components of the atmospheric forcing drive the interannual variability of the Arctic sea ice volume.

To estimate the sea ice volume and its variability directly from observations, one needs to measure the sea ice concentration and the sea ice thickness in the Arctic. The sea ice extent and area (which is the integral of the sea ice concentrations) are probably the only well-observed components of the Arctic sea ice conditions, as they are estimated from satellite observations since 1973. From these satellite records, *Parkinson et al.* (1999) and *Cavalieri et al.* (2003) reported on a large decline of the sea ice extent since the late 1970's, with a decreasing trend of about 3% per decade over the 1975–2000 period. More recent studies (*Comiso et al.*, 2008) have revealed that this trend strongly accelerates over the last decade (up to 10% per decade over 1996–2007 according to *Comiso et al.* (2008)). A large interannual variability is also superimposed on this long term trend, and each new minimum record has been largely commented in the literature (*Serreze et al.*, 2003; *Stroeve et al.*, 2005; *Comiso et al.*, 2008; *Zhang et al.*, 2008; *Drobot et al.*, 2008).

Sea ice thickness has been much more difficult to observe, and measurements over long time period remain very sparse. *Rothrock et al.* (1999) and *Wadhams and Davis* (2000) used observations made with submarine-based sonars to document a 40% decrease in sea ice thickness between 1958–1976 and the 1990's. However, *Holloway and Sou* (2002) used OGCM outputs to show that the subsampling of the observations used in these two studies lead to a large overestimation of the sea ice thickness decline. Recently, *Kwok et al.* (2009) provide us with one of the first estimate of the spatial distribution of sea ice thickness from 10 campaigns of the new ICEsat satellite from 2002 to 2008, and thus an estimation of the Arctic Sea ice volume over the recent period. However, the uncertainty remains huge on this quantity, and the sea ice volume time series presented in this study can not be used to get indications on the interannual variability.

The role of the large scale atmospheric circulation variability for the interannual variability of the Arctic sea ice conditions has been investigated in numerous studies (e.g., *Arfeuille et al.* (2000); *Deser et al.* (2000); *Holloway and Sou* (2002); *Köberle and Gerdes* (2003); *Makshtas et al.* (2003); *Rothrock and Zhang* (2005); *Ogi et al.* (2010)), and a response of the sea ice conditions and motion to the leading mode of variability in the atmosphere (AO for Arctic Oscillation, *Thompson and Wallace* (1998)) has been pointed out by different authors (*Deser et al.*, 2000; *Rigor et al.*, 2002).

Most of these studies have tried to consider separately the influence of the Surface Air Temperature (SAT) fluctuations and the wind anomalies to understand some aspects of the variability and long term trend of the sea ice extent, thickness and exports. However, as the AO index exhibit a large decadal variability, observational studies necessarily meet a limitation when trying to separate long term trend from variability, as the observation time series do not last more than about two decades. Longer time series are required to assess the long term trend robustness, and up to now such studies can only be conducted from model outputs. Moreover, also one can get evidence from observational dataset for similarity in mode of variability of some sea ice and atmospheric parameter, it remains really hard to clearly distinguish between dynamical and thermodynamical effects on the measured sea ice variability and long term changes.

Previous modeling studies have tried to answer similar question, that is to understand the role of the atmospheric forcing for the sea ice conditions variability and long term changes. *Köberle and Gerdes* (2003) and *Rothrock and Zhang* (2005) have looked into the respective role of thermal and wind forcing for the variations of the sea ice volume, that they link to an imbalance between sea ice production and sea ice exports from the Arctic. The two studies conclude that the production is mainly controlled by temperature over the Arctic basin, while local winds drive the sea ice export. However, no analysis of the different parameters that contribute the sea ice volume (concentration and thickness) is done in these paper, and such a decomposition might be interesting to understand how the variability of the sea ice volume is driven.

All these previous studies define the scope of the present paper. From model results, we further investigate and quantify the role of the different atmospheric forcing (wind and thermal flux) for the interannual variability and long term changes of the sea ice volume over the period 1958–2001. We also want to determine the spatial variations of the different atmospheric flux influence, as we examine separately the interannual and spatial variations, and long term changes of the sea ice thickness and concentration. To do so, we use a regional coupled ocean/sea-ice model of the Arctic Ocean and the North

Atlantic. A hindcast simulation is performed as well as perturbation experiments with restricted interannually varying forcing. The joint analysis of the three simulations allow us to better separate the influence of each atmospheric forcing. Here we aim at analyzing our set of three simulations in a systematic and comprehensive way, in order to clearly determine of the role of the different atmospheric forcing for the interannual variability and long term changes of the Arctic sea ice volume, and of each sea ice parameter that enter in the calculation of the sea ice volume.

The remainder of this paper is organized as follows. The model and the simulations used for the study are briefly described in section 2. The Arctic sea ice volume is examined in section 3. As the sea ice volume is dependent of the sea ice concentration and thickness, we examine each parameter separately (sections 4 and 5), and we try to understand the mechanisms at play for their variations and long term changes. In section 6, we make the link between the variations of the sea ice volume and the net sea ice production in the Arctic. A conclusion is given in section 7.

5.2.2 The numerical experiment.

The regional coupled ocean/sea-ice model configuration of *Herbaut and Houssais* (2009) is used to perform the simulations. It is based on the NEMO framework (*Madec*, 2008), including the LIM2 sea ice model which is a dynamic-thermodynamic model specifically designed for climate studies (*Timmermann et al.*, 2005). The domain encompasses the Arctic Ocean and the North Atlantic Ocean, with open boundaries at 30°S in the Atlantic Ocean and 50°N in the Pacific Ocean. The horizontal grid is 1/2° at the equator, leading to horizontal dimensions of 261x481 grid points, and the resolution is thus 50 km at the equator, 27.6 km at 60°N , and gets to 20 km in the Arctic Ocean. There is no singularity of the grid at the North Pole. There are 46 vertical levels with grid spacing ranging from 6 m near the surface to 250 m at the bottom. Along the boundaries, the oceanic velocity and tracer distributions are prescribed from the monthly climatology of a global simulation performed by the DRAKKAR project (*Barnier et al.*, 2006). The configuration uses a partial step representation of the bottom topography and a momentum advection scheme that both yielded a better representation of the ocean dynamics (*Penduff et al.*, 2007; *Le Sommer et al.*, 2009). Parameterizations include a laplacian mixing of temperature and salinity along isopycnals, a horizontal biharmonic viscosity, and a turbulence closure scheme (TKE) for vertical mixing. The bathymetry is derived from the 2-minute resolution Etopo2 bathymetry file of NGDC (National Geophysical Data Center).

The ocean is initialized from rest with temperature and salinity distributions from the Polar Science Center Hydrographic T/S Climatology (PHC 3.0 ; see *Steele et al.* (2001a)

for details). The surface forcing is based on daily atmospheric fields from the ERA40 reanalysis (1958–2001) with some regional corrections to improve the radiation flux over the North Atlantic and the precipitation and surface air temperature over the Arctic. Turbulent fluxes (wind stress, latent and sensible heat flux) are estimated using the CORE bulk formula (*Large and Yeager*, 2004). The river runoff is prescribed from a monthly climatology (http ://www.R-ArcticNET.sr.unh.edu). To avoid an excessive model drift, we add a relaxation of sea surface salinity to the PHC climatology. The coefficient (0.2 m/day) amounts to a decay time of 30 days for 6 m of water depth.

The model is first spun up for 23 years from 1979 to 2001. After that, several 44-year simulations are performed, starting from the last time step of this cycle (31^{th} of December, 2001). The reference simulation (REF) used the complete 44-year cycle of the reanalysis and ran from 1958 to 2001 with interannual daily forcing. To elucidate the relative effects of the variability in wind and heat flux forcing, REF was complemented by a set of perturbation experiments, in which the interannually varying forcing for 1958–2001 was artificially restricted to the heat flux (HEAT) or to the wind forcing (WIND). A fourth experiment has been carried out (CLIM) in which both the heat fluxes and the wind forcing were climatological. Note that the climatological forcing (heat flux or wind stress) were obtained by averaging day by day the daily forcing fields from 1958 to 2001. Interannual variability as well as high frequency variability (smaller than one season) are thus excluded from the climatological forcing fields. For the HEAT simulation, the meridional and zonal wind stress are averaged, while for the WIND simulation, all the forcing field that enter into the CORE bulk calculation of the atmospheric heat flux (Surface Atmospheric Temperature, Sea Level Pressure, dew point, Downward Long-Wave and Short Wave Radiation Flux and wind modulus) are averaged. However, in the latter experiment, small interannual variations of the atmospheric heat flux remain, as the model calculated Sea Surface Temperature (SST) also enters in the bulk calculation.

5.2.3 Variability of the Arctic sea ice volume.

In this section, we examine the variability of the Arctic sea ice volume. We aim at understanding long term changes and interannual variability of the different aspects of the Arctic sea ice. Hence, results presented here are averaged over calendar years. As we want to consider the complete sea ice pack, we thus refer to the Arctic sea ice as the sea ice encompassed in the Northern Hemisphere (NH) (unless specified).

The time series of the annual anomalies of the Arctic sea ice volume calculated from our four simulations are shown in Fig. 5.1. Mean values, standard deviations and linear trends are listed in Table 5.1. Linear trend are calculated from annual mean anomalies and the significance is calculated following *Santer et al.* (2000), based on a two-tailed

	Mean (km^3)	**Std** (km^3)	**Trend 1963–2001** (%/decade)	**Trend 1980–2001** (%/decade)
REF	19200	1600	**-2.5**	**-10.4**
HEAT	17300	800	**-2.3**	**-4.9**
WIND	20100	1200	0.3	-3.2
CLIM	19400	100	**0.1**	**0.4**

TAB. *5.1: Arctic sea ice volume in the four simulations : mean values, standard deviations (from annual mean) and linear trends calculated from annual mean anomalies (the trends that reach up the 95% significance level are indicated in bold). Remember that "Arctic" refer to all the Northern Hemisphere.*

Student t-test, assuming 2 degree of freedom less than the number of year used for the trend computation. Thus the significance calculated here is an upper bound of the real significance, as the effective degree of freedom is probably smaller. All the trends presented in the paper reach up the 95% significance level, unless specified.

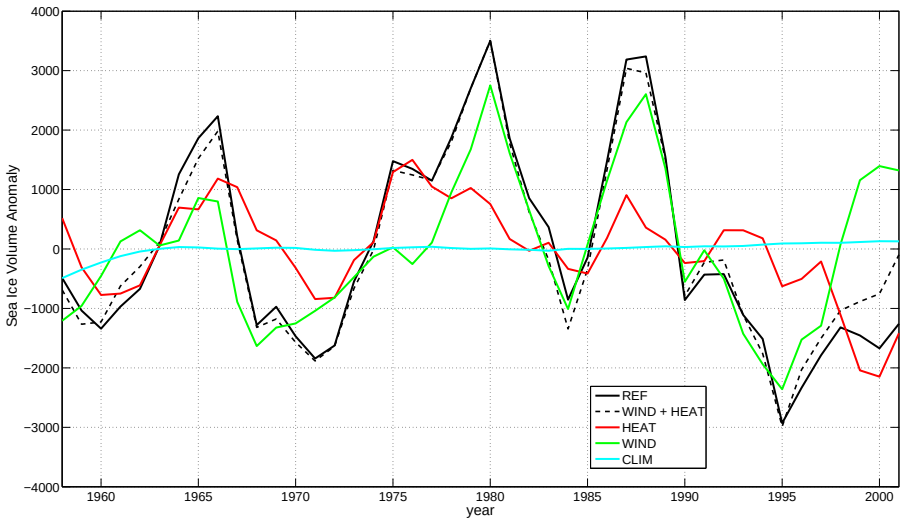

FIG. *5.1: Annual anomaly (in km^3) of the Arctic sea ice volume for the different simulations.*

From Fig. 5.1, it can be seen that the computed sea ice volume from the REF experiment exhibits large decadal variability, with a standard deviation of 1600 km^3, i.e. 9% of the long term mean. The first 4 or 5 years can be considered as a period of adjustment to the initial conditions, as the simulation has been initialized from the last day of December 2001 when the sea ice extent was lower than in the 1960's. In addition to these fluctuations, a least squares regression analysis of the yearly mean anomalies reveals a linear decrease of 2.5%/decade (-49 km^3/year) over 1963–2001 (excluding this way the period when the model adjustment is the largest). This is consistent with results from some previous modeling studies. For instance, *Fichefet et al.* (2003) found a 1.8%/decade decrease

over 1955–2001 or *Lique et al.* (2009) obtained a -2%/decade trend over 1965–2002. However, this figure has to be considered with caution, because of the relative shortness of the time series and the high amplitude decadal fluctuations, so that this result could be model and period dependent. For instance, in their model, *Köberle and Gerdes* (2003) found no significant trend in the sea ice volume over 1948–1998. Linear trend computed over 1980–2001 period is 4 times larger than over 1963–2001, showing that the decreasing trend accelerates strongly during the second part of the simulation. Our time series of Arctic sea ice volume is qualitatively similar to these of *Hilmer and Lemke* (2000), *Arfeuille et al.* (2000) or *Köberle and Gerdes* (2003), with the same periods of positive and negative anomalies. In particular, the local maximum in 1966 and 1987 are similar to what *Rothrock et al.* (2003) found when looking at the published mean ice thickness (i.e. the sea ice volume divided by the Arctic area) from eight different sea ice models. Similarly to the model results of *Lindsay and Zhang* (2006), our times series exhibits a rapid decreasing trend after its maximum in 1987-1988 that lasts until the recent years.

We now turn our attention to the Arctic sea ice volume variability simulated by the other simulations than REF. First, one can notice that the time series for CLIM exhibits almost no interannual variability, and a very small linear trend after 1963. This suggests that the interannual variability due to internal model variability is negligible, and that the model drift is small as well compared to forced long term changes. Second, Fig. 5.1 shows that the anomalies of sea ice volume in WIND (V_W) and HEAT (V_H) experiments linearly sum up to almost the value of the REF experiment. We can thus attribute partial sea ice volume changes to thermal and wind forcing respectively. This properties has been previously emphasized by *Köberle and Gerdes* (2003), and used afterward by *Rothrock and Zhang* (2005) who defined the sea ice volume change due to interannually varying thermal forcing as the residual between the total volume change and the wind-forced change. Note that, as our model spatial resolution is five (*Köberle and Gerdes*, 2003) and two (*Rothrock and Zhang*, 2005) times higher than in these previous studies, the linearity of the responses to the different forcing could have vanished in our simulation, and needed to be checked here.
The anomaly time series of both V_W and V_H present large decadal variability and thus contribute significantly to the variability of the total sea ice volume (V_R) (Fig. 5.1). As noted by *Köberle and Gerdes* (2003) and *Rothrock and Zhang* (2005), large events of sea ice accumulation or depletion can be explained by either V_W anomaly (e.g., the volume maximum in 1987-1988), or V_H anomaly (e.g., the volume minimum in 1975), or both (e.g., the volume maximum in 1965). The long term trend over 1963–2001 are similar in REF and HEAT, while the trend found in WIND is negligible. This suggest that the long term depletion of the sea ice volume might be related to long term changes of the atmospheric heat fluxes. The role of the SAT long term changes for the sea ice volume

decrease has been pointed out by *Hilmer and Lemke* (2000), and the SAT changes are probably the dominant parameter responsible for the atmospheric heat flux changes in our simulation.
To quantify the relative influence of wind and heat forcing on the interannual variability of the Arctic sea ice, we calculate the part of the variance of V_R explained by each components V_W and V_H, as done by *Rothrock and Zhang* (2005). As previously said, we neglect the contribution of the model internal variability. Thus, when we only consider their anomalies, we have : $V_R \approx V_W + V_H$. The variance of V_R can be calculated as :

$$var(V_R) \approx var(V_W + V_H) = var(V_W) + var(V_H) + 2cov(V_W, V_H)$$

We evaluate each term of this equation, and we find :

$$\begin{aligned} var(V_R) &= 2.5(10^3.km^3)^2 \\ var(V_W + V_H) &= 2.4(10^3.km^3)^2 \\ var(V_W) &= 1.5(10^3.km^3)^2 \\ var(V_H) &= 0.7(10^3.km^3)^2 \\ cov(V_W, V_H) &= 0.1(10^3.km^3)^2 \end{aligned}$$

The term of covariance is small : V_W and V_H do not tend to vary together. We also conclude from this calculation that the variability of wind and heat fluxes contributes respectively for 2/3 and 1/3 of the interannual variability of the Arctic sea ice volume. This result differ from what *Rothrock and Zhang* (2005) found, as, in their simulation, the three terms contribute almost equally to the total variance, and thus they found a significant correlation between V_H and V_W. This difference can probably be explained by the difference in the way we have simulated V_H : *Rothrock and Zhang* (2005) have just replaced the interannually varying SAT by an averaged annual cycle of SAT, whilst we have averaged all the variables that enter in the calculation of heat flux through the bulk formulae. Thus the varying winds are still entering in their calculation of the climatological heat flux, and probably explain the in-phase varying behavior of V_H and V_W.

In order to understand the mechanisms at play for the interannual variability and the long term changes of the sea ice volume, and specially the respective roles of the different atmospheric forcing, examining the sea ice volume time series is clearly insufficient. In fact, the sea ice volume is calculated from the sea ice concentration and thickness, which are 3D fields (two dimensions in space and one dimension in time), and the approach of reducing these fields to one single 1D dimensions is necessarily limited. Thus, to further understand the contributions of wind and heat flux variability, we will now examine the variability and changes of the thickness and concentration separately.

5.2.4 Variability of the sea ice concentration.

This section is devoted to examining the interannual variability and long term change of the sea ice concentration in the NH. To asses the model behavior regarding this sea ice parameter, we first examine the sea ice area time series. Then we examine the spatial variations of the sea ice concentration.

5.2.4.1 Arctic sea ice area

The time series of the sea ice area is commonly used to assess the basin-scale integrated variability of the sea ice conditions (*Comiso et al.*, 2008; *Parkinson and Cavalieri*, 2008). Sea ice area consists of the sum of the grid cell areas multiplied by the ice concentration for all cells with ice concentrations of at least 15% and thus provides the total area over which the ice is directly insulating the ocean from the atmosphere and reflecting solar radiation.

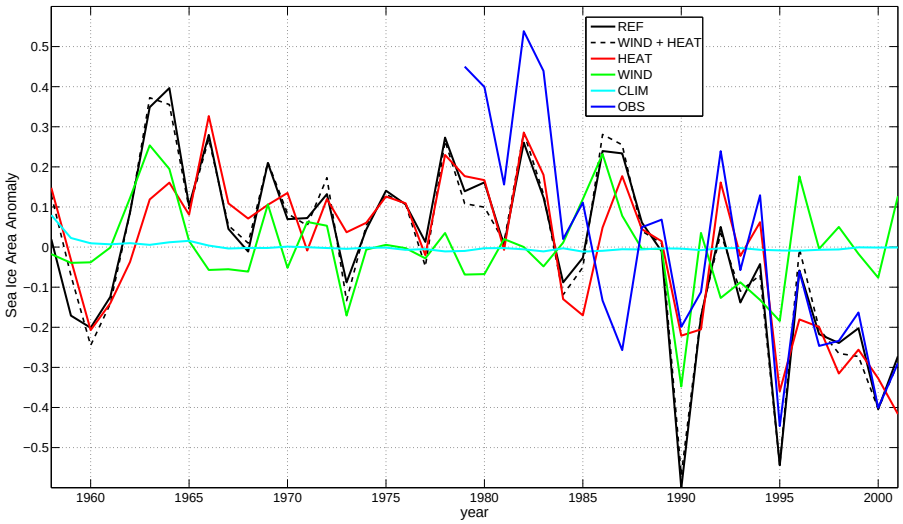

FIG. *5.2: Annual anomaly of the Arctic sea ice area ($10^6 km^2$) for the different simulations. Satellite observations are also shown for comparison (Fetterer et al., 2002, updated 2009).*

The time series of the annual anomalies of the Arctic sea ice area calculated from our four simulation are shown in Fig. 5.2. Variations calculated from REF outputs have to be compared to NSIDC observations (*Fetterer et al.*, 2002, updated 2009) after 1979. Overall the two time series compare well, with similar means ($9.4 \times 10^6 km^2$ versus $10.0 \times 10^6 km^2$ for REF and the observations respectively) and standard deviations ($0.25 \times 10^6 km^2$ versus $0.3 \times 10^6 km^2$). The two time series also correlate well (the correlation of the two time series is r=0.72). However, the simulated time series matches better the observation one after 1987 than before (note that the sea ice sensor has been changed in 1987 from SSM/R to SSM/I, what might explain at least a part of this mismatch). The smaller variations

of the REF sea ice area anomalies in the early 1980's lead to a weaker trend of decrease over the period 1979–2001 (-2.4%/decade for REF versus -2.9%/decade for the NSIDC observations). If we consider a longer time period (1963–2001, excluding this way the first year of model adjustment), the linear trend for the REF simulation is about -1.4%/decade. The time series of the REF sea ice area presents higher frequency fluctuations than the sea ice volume, with small decadal variability. However, the correlation between the variations of the Arctic sea ice volume and the fluctuations of the sea ice area is equal to 0.61 for REF, and thus the variations of the sea ice concentration explain a significant part (about 40%) of the sea ice volume interannual variations.

As for the sea ice volume anomalies, the anomalies of sea ice area in WIND (A_W) and HEAT (A_H) experiments linearly sum up to almost the value of the REF experiment (A_R), the variations of A_R and $A_W + A_H$ being very significantly correlated (r=0.98). Moreover, anomalies of the CLIM simulation are again negligible compared to the REF anomalies. We now consider the individual contributions of the anomalies of A_H and A_W to the ones of A_R. Considering the long term trend (over 1963–2001), we can note that A_W does not present any trend, whilst A_H presents the same trend than A_R (-1.2%/decade versus -1.4%/decade). This suggests that the long term trend of decrease of the sea ice area is due to interannual variability and changes of the atmospheric heat flux, although we have again to consider these results with caution due to the shortness of the period.

Regarding the interannual variability, time series of both A_H and A_W exhibit large year-to-year variability to the same order of magnitude than the fluctuations of A_R. The fluctuations of the HEAT experiments account for a more important part of the REF variability than the WIND fluctuations (r=0.85 between A_R and A_H while r=0.55 between A_R and A_W). We want to quantify the contribution of each atmospheric forcing to the variability of the sea ice area by doing the same analysis than for the sea ice volume. We find :

$$\begin{aligned} var(A_R) &= 4.6(10^5.km^2)^2 \\ var(A_W + A_H) &= 4.7(10^5.km^2)^2 \\ var(A_W) &= 1.2(10^5.km^2)^2 \\ var(A_H) &= 3.3(10^5.km^2)^2 \\ cov(A_W, A_H) &= 0.1(10^5.km^2)^2 \end{aligned}$$

The interannual variability of the atmospheric heat fluxes is thus responsible for 70 % of the interannual variability of the sea ice area, while the variability of the wind account for only 25%.

To get an idea of the spatial dependency of the the wind and heat forcing influence, we examine the spatial distribution of the sea ice concentration, as well as its variations and long term trends.

5.2.4.2 Spatial pattern of the Arctic sea ice concentration

Different observational datasets provide multidecadal estimates of sea ice concentration since 1972 and the interannual variability as well as the long term trend have been examined in numerous studies (e.g., *Walsh and Johnson* (1979); *Deser et al.* (2000); *Singarayer and Bamber* (2003); *Partington et al.* (2003)). However, it can not be deduced from observations whether the thermodynamical effect or the dynamic effect (wind stress) dominates the observed sea ice variations and long term trend (*Deser et al.*, 2000). Here we aim at using the idealized simulations HEAT and WIND to gain insight on these questions. Moreover, several studies highlighted the seasonal dependence of both the long term trend and the interannual variability of the sea ice extent, suggesting that different mechanisms could be at play during the different periods of the year. For instance, *Parkinson et al.* (1999) show that the Arctic sea ice cover as a whole has decreased by 2.9 % per decade over 1979–1996, with the largest reduction occurring in summer (6%/dec.) while the trend is negligible in winter. The winter and summer sea ice area time series have also been shown to not necessarily vary together (*Walsh and Johnson*, 1979). Thus, in the subsequent analysis we will follow the methodology of *Deser et al.* (2000) and *Deser and Teng* (2008), that is to analyze separately the summer and winter variability and trend of the sea ice concentration. Seasons are defined consistently with *Parkinson and Cavalieri* (2008) : Winter is defined as January - February - March and Summer is defined as July - August - September.

Long term trend :

First we examine the long term trend (from 1963 to 2001, excluding this way the first years of the simulations when the adjustment is the largest). Compared to observational studies (e.g., *Partington et al.* (2003); *Deser and Teng* (2008); *Stroeve et al.* (2008)), the time series presented here are longer and, as the trends are period dependent, our results might be more robust. In fact, the simulations cover about four decades. As a decadal period signature is visible in the sea ice volume variations, it might lead to a bias for the observational studies that just cover 20 to 25 years.
Fig. 5.3 show the long term trend at grid points with significant trends of the summer (JAS) and winter (JFM) sea ice concentration for the three simulations.

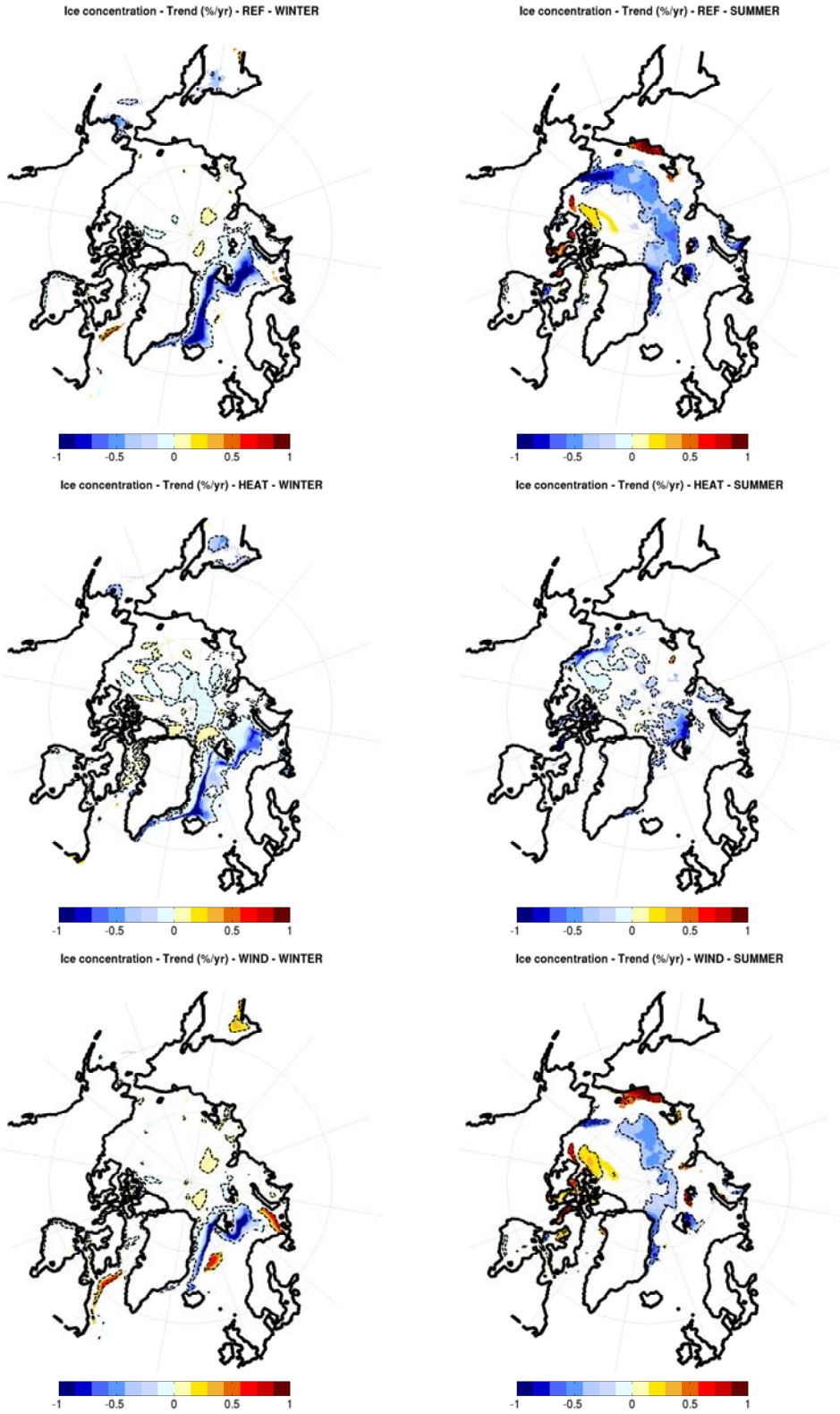

FIG. *5.3: Linear trends over 1963–2001 of the winter (left) and summer (right) mean sea ice concentration for the REF (top), HEAT (middle) and WIND (bottom) experiments. Only trends that reach a 90% significance level are shown and the black dotted line indicates the 95% significance level.*

In winter, important long term trends are visible only in the marginal zones (mainly East of Greenland), as the sea ice concentration amounts to 100% every year during winter in the Arctic interior. Thus we can logically infer that the trend are due (at least partly) to a change of the sea ice edge location and not only to a trend in the sea ice concentrations. In detail, we found downward trends in the Greenland and Barents Seas, as well as, to a lesser extent, in the Pacific sector (Bering Sea and Sea of Okhotsk) and upward trends in the Labrador Sea. Overall, the pattern is similar to the one found by *Partington et al.* (2003) for the 1972–1994 period, and those found by *Deser and Teng* (2008) (over 1979–2007) and *Stroeve et al.* (2008) (for March over 1979–2006) except in the Labrador Sea where the two latter studies reveals downward trends. In this region, *Deser and Teng* (2008) show that the sign of the trend is reversed when they consider two subperiods, and thus the difference probably comes from the difference in the period considered. *Deser and Teng* (2008) or *Stroeve et al.* (2008) suggest that part of this trend could be explained by trend in the temperature in the atmosphere, and an other part by the interannual to decadal changes in the atmospheric circulation (to which the AO index is a good proxy). Logically, the second part might become smaller as the time series becomes longer, as no long term trend is visible for the AO index. We examine the contributions of HEAT and WIND to the REF trends. Overall, except in the Labrador Sea, the HEAT and the REF simulations show similar trend. The contribution from the WIND simulation to the total trend is only significant in part of the Barents Sea (East of the Spitsbergen Island) and close to the Greenland coast in the Greenland Sea. It also accounts for the whole upward trend in a small part of the Labrador Sea.

During summer, the pattern of the REF long term trend is completely different, with large trends in the interior of the ice pack. Overall, we find negative trends in the interior and positive trends along the coastal regions. The largest positive trends can be found in and north of the CAA and in East Siberian Sea. Contrary to what happens in winter, the WIND experiment reproduces almost the same pattern of the summer sea ice concentration trend as the REF simulation, while the trend simulated by HEAT has small negative values, and is significant only in the northern Barents Sea and along the Alaskan coast. Thus, the summer trend is likely due to the long term changes of the wind stress. As the pattern exhibits large trend values both close to the sea ice edge and over the Arctic interior, the changes in the wind field might lead to changes in both the location of the sea ice edge and the sea ice concentration values themselves. Our results are consistent with the recent study of *Ogi et al.* (2010) that show that a decreasing trend found for the summer minimum sea ice extent can be related for a large part to the change in the wind stress that leads to a increasing sea ice export through Fram Strait.

Interannual variability

Here we follow again the methodology of *Deser et al.* (2000) : we extract the leading modes of the interannual variability of both winter and summer mean sea ice concentration by EOF decomposition. As we want to focus on the interannual variability, we check that the results are not dominated by the long term trend of the sea ice concentration, and we find that the EOF analysis results are similar when the long term trend is or is not subtracted from the seasonal mean anomalies. To be consistent with *Deser et al.* (2000), we choose to keep the sea ice concentration time series undetrended. Here the study of *Deser et al.* (2000) based on observations helps us to validate our own results (from REF) and we aim at using the sensitivity experiments to better understand the mechanisms behind the modes of variability.

Winter : Fig. 5.4 shows the leading EOF of the simulated winter sea ice concentration anomalies for the 3 experiments and the corresponding PC time series. The leading mode of variability accounts for 25% of the variability, while the following modes account for about or less than 10%. We thus focus our analysis on the first EOF.

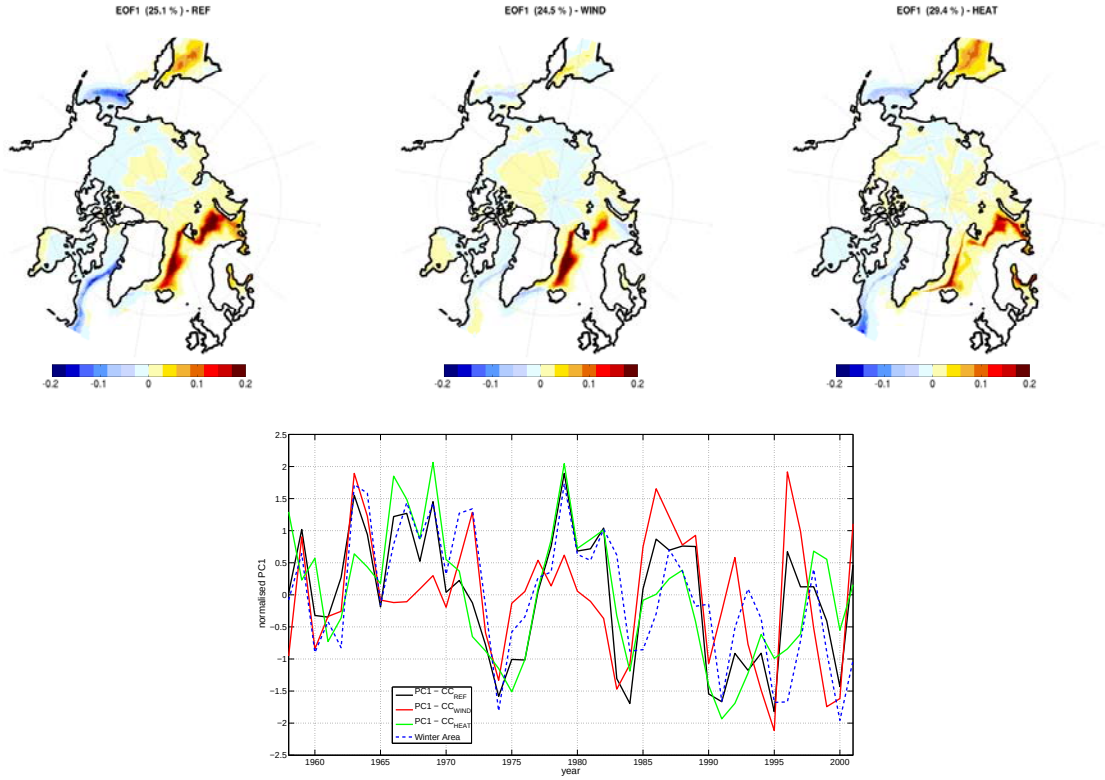

FIG. *5.4: First dominant mode of winter sea ice concentration variability based on EOF analyses of the REF, WIND and HEAT experiments, and time series of the principal components (PC) of the EOF. The t normalized time series of the winter sea ice area in the NH calculated from REF outputs is indicated along with the PC1.*

The leading mode spatial pattern and its associated PC time series are very similar to these found from observations (*Deser et al.*, 2000). It exhibits largest amplitude in the Atlantic sector, with opposite anomalies in the Greenland/Barents Sea and in the Baffin Bay/Labrador Sea. A similar but weaker out-of-phase behavior is also visible in the Pacific sector, between the Bering Sea and the Sea of Okhotsk. The PC of the leading EOF exhibits low frequency behavior, with decadal variations. In the early 1970's, 1980's and 1990's, the PC is strongly negative which means that the ice concentrations were anomalously high during winter West of Greenland and in the Bering Sea, and low in the Eastern Atlantic and in the Sea of Okhotsk. Note that the large values of the EOF are concentrated along the sea ice edge, while their value are negligible in the Arctic interior where the sea ice edge is constrained by land boundaries. Moreover, the PC time series is highly correlated with the winter sea ice area time series (r=0.68), suggesting that this mode of variability is primarily driven by the variations of the sea ice edge location.

This idea is supported by the results from HEAT and WIND. The leading mode of the simulated winter sea ice concentration anomalies in these two simulations are largely similar to the one found in REF, with the same out-of phase behaviors in both the Atlantic and Pacific sectors. The PC times series are also well correlated with those of REF (r=0.68 and 0.80 for WIND and HEAT respectively). As we find the same leading mode of interannual variability in the three simulations, this suggests that the wind stress and atmospheric heat flux fluctuate together over the sea ice edge regions during winter. This finding differ from the conclusions of *Deser et al.* (2000) and *Stroeve et al.* (2008), who found that the first winter EOF of the sea ice concentration (their EOF exhibit the same spatial pattern) is related to the AO variations. *Stroeve et al.* (2008) find a correlation of 0.88 between 9 year running means of the AO index and the first EOF of the March sea ice concentration. A comparable relation exists in our REF simulation (r=0.82 between the 9 years running means of the AO and the PC1). However, as the HEAT simulation reproduces the same leading mode of variability, this mode can not be completely related to the atmospheric circulation variations.

Summer : Fig. 5.5 shows the two leading EOF of the simulated summer sea ice concentration anomalies for the REF and WIND experiments and the corresponding PC time series. During summertime, the two leading modes of variability of the sea ice concentration account for a similar part of the total variance (17.6% and 15.2% for EOF1 and EOF2 respectively) : thus we examine the first two modes. The WIND simulation exhibits very similar modes of variability with comparable percentage of explained variance, PC times series and spatial pattern. This is not surprising as the variability of the summer sea ice concentration is very small in the HEAT simulation when compared to REF, and consequently both REF and WIND exhibit similar interannual anomalies of the summer

sea ice concentration.

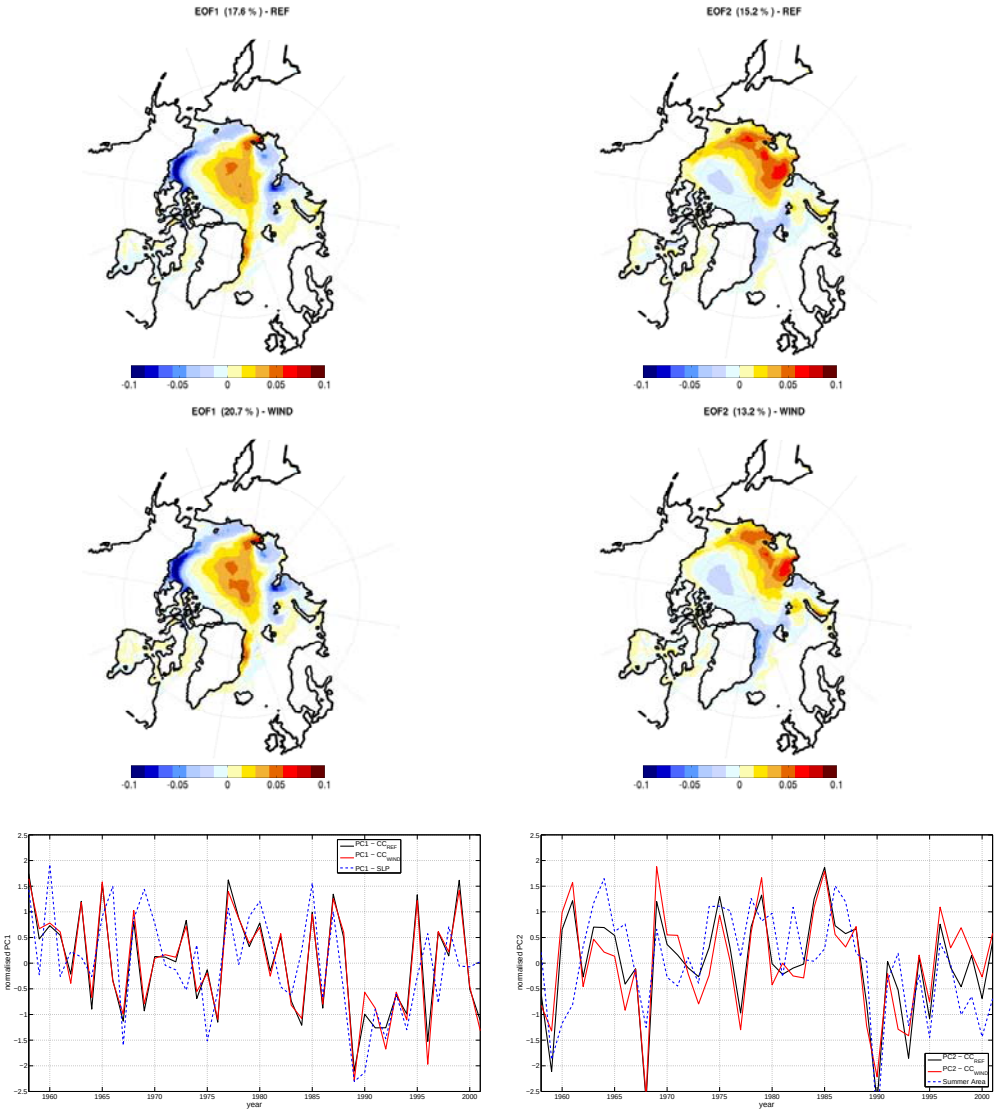

FIG. *5.5: First two dominant modes of summer sea ice concentration variability based on EOF analysis of the REF and WIND experiments, and time series of the principal components (PC) of the EOF. The time series of the principal component of the first EOF of the annual mean SLP variations north of 60 °N is also indicated along with the PC1, and the normalized time series of the summer sea ice area in the NH calculated from REF outputs is indicated along with the PC2.*

The leading mode of variability does not correspond to the one found in the observations (*Stroeve et al.*, 2008). It is surprisingly similar to the one found for the sea ice thickness (see following section), their spatial pattern and PC time series being similar (r=0.65 between the two time series). Thus we attribute the mode of variations to the numerical dependency between the sea ice concentration and thickness, as the determination of the sea ice concentration in the model is related to the freezing and melting rates and to the actual thickness of the sea ice floes.

The second mode of variability has, to our sense, more physical meaning and is similar to the first mode found in the observations by *Stroeve et al.* (2008). It consists on large opposite anomalies between the Laptev, East Siberian, Chukchi and Beaufort Seas and the remainder of the sea ice packs. We find a large correlation between the PC2 time series and this of the summer sea ice area (r=0.65 in the REF simulation), suggesting that this mode is dominant for explaining the fluctuations of the sea ice coverage during summer. We can attribute this mode to the variations of the wind stress, which are primarily responsible for the variations of the summer opening in the regions where the anomalies of the EOF2 are the highest. This explanation is consistent with those of *Stroeve et al.* (2008), even though they suggest that the emerging warming signal in the Arctic might become dominant for the summer sea ice concentration variability in the recent years (after 1995).

In summary, our modeling results bring in light a striking contrast between the interannual variability and the trend found during summer and winter. On the one hand, during summer, the sea ice concentration trend and variability are almost completely due to changes of the atmospheric circulation. On the other hand, taking into account the variations of the atmospheric heat flux is sufficient to reproduce most of the trend and interannual variability of the sea ice concentrations during wintertime, even though a similar variability can be found in the WIND simulation, likely due to the covariance of the heat flux and the wind forcing during winter.

5.2.5 Variability of the sea ice thickness.

We now consider the interannual variability and long term changes of the Arctic sea ice thickness. Few observations of this quantity is still available, and it is worse if we consider the variations about the mean state. For this parameter of the sea ice pack, the variations show lower frequency than the sea ice concentration ones, and exhibits a general in-phase variability all over the seasons. Thus, we will examine the interannual variability of the sea ice thickness from annual mean, as done by previous modeling studies on this topic (e.g., *Holloway and Sou* (2002); *Lindsay and Zhang* (2006)). The analysis of the sensitivity experiment should help to determine the role of the different atmospheric forcing for the interannual variability and trends.
The mean sea ice thickness, the standard deviation of the annual mean thickness for the 44 year simulation and the linear trend for the REF, HEAT and WIND experiments are shown in Fig. 5.6.

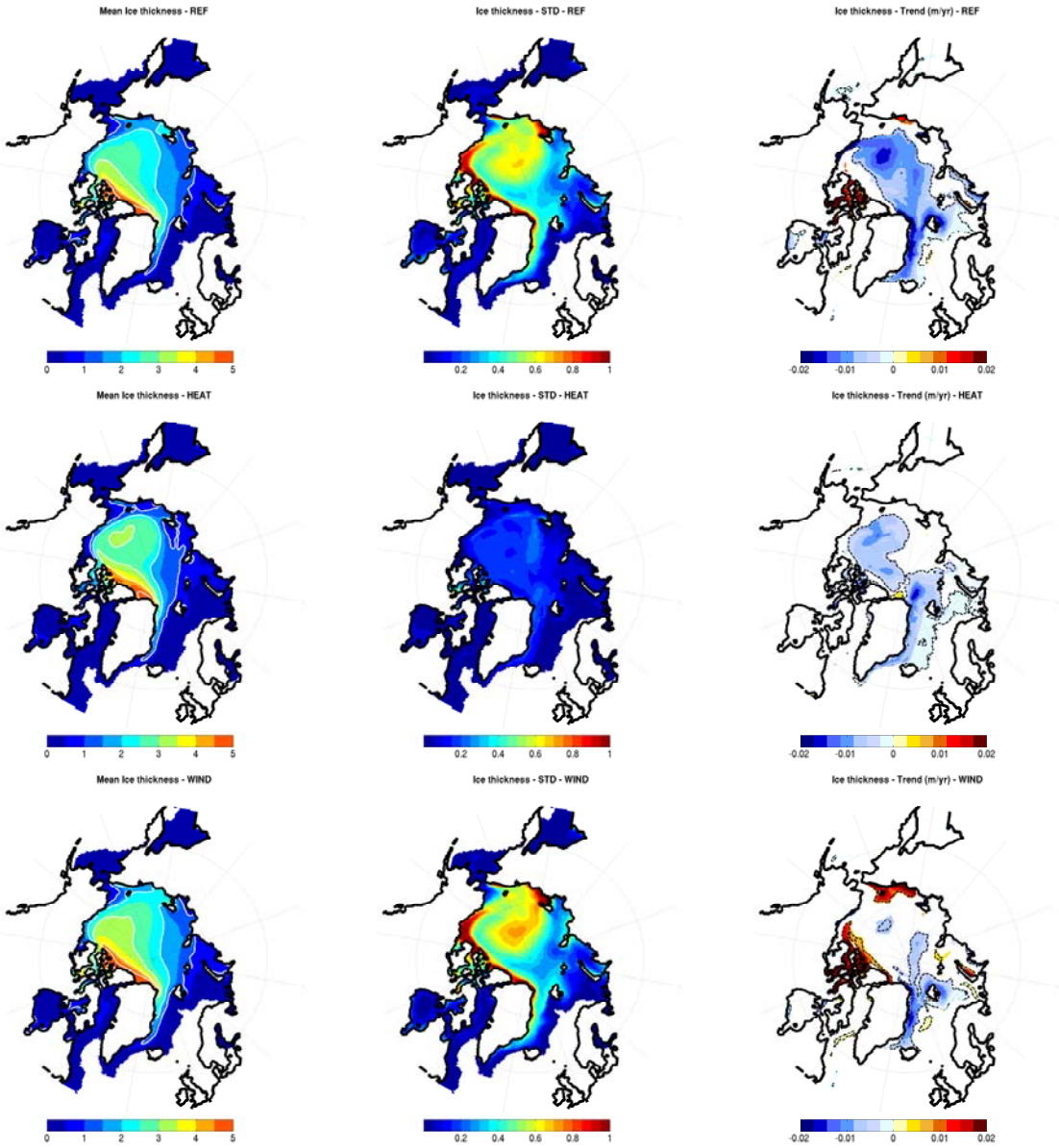

FIG. *5.6: Average over 1963–2001, standard deviations and linear trends of the sea ice thickness for the REF (top), HEAT (middle) and WIND (bottom) experiments. Only trends that reach a 90% significance level are shown and the black dotted line indicates the 95% significance level.*

The mean sea ice thickness is greater north of the CAA (around 5 m), and fairly uniform in the central Arctic (near 3m). The general pattern of the REF sea ice thickness is similar to the one simulated by *Holloway and Sou* (2002) or *Lindsay and Zhang* (2006). The mean sea ice thickness simulated by WIND and HEAT is roughly similar to this simulated by REF, despite a slightly thicker ice in the central Arctic (and in the East Siberian Sea for WIND).

Long term trend : The linear trend is calculated by taking the linear least square fit for the yearly mean anomalies. The main signal in the REF simulation is a large thinning in the central Arctic (up to -0.02 m/yr), which extends in a broad band to Fram Strait and along the eastern Greenland Coast. A thickening is also visible in and north of the CAA and in the East Siberian Sea (up to 0.013 m/yr). This pattern is consistent with the hypothesis of *Holloway and Sou* (2002) (and their own finding) that the sea ice thinning of almost 40% measured by *Rothrock et al.* (1999) or *Cavalieri et al.* (2003) is just representative of what happened in the central Arctic (the locations of the measurement used by *Rothrock et al.* (1999) shown in Fig. 2 of *Holloway and Sou* (2002) are located where we find the most negative trend).
Although the HEAT and WIND linear trends do not exactly sum up to the REF linear trend, one can see from Fig. 5.6 that the WIND trend and the HEAT trend both contributes to the REF trend, also the contributions differ in the different regions. In the central Arctic, the HEAT contribution to the decreasing trend is dominant, while the WIND contribution is dominant for the upward trend along the coast. North of Fram Strait and in the Greenland and Barents Seas, the WIND and HEAT contributions to the decreasing trend are similar.
The thinning visible in HEAT can be linked to enhanced anticyclonic circulation of the sea ice in the central Arctic (Fig. 5.7) that will help to export thicker ice through Fram Strait and thus lead to a thinning of the sea ice in the Beaufort Gyre.

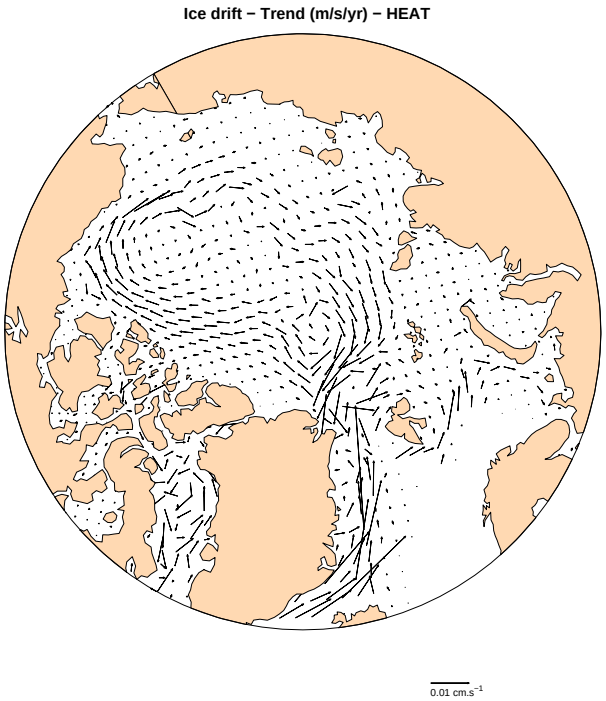

FIG. *5.7: Long term trend of simulated sea ice drift in HEAT over 1963–2001.*

At the same time, the interannual variability and long term changes of the wind forcing contributes to a thinning of the sea ice in the central Arctic and along the East Greenland Coast, and a thickening of the sea ice along the coastal Arctic regions. The spatial pattern of the long term trend in WIND (as well as the pattern of the sea ice drift trend, not shown) suggests that the long term changes of the wind forcing lead to a spatial redistribution of the sea ice, with an accumulation of thicker sea ice along the coast. Thus, in the model, the effects of long term changes of the Arctic wind field somehow damp the long-term decrease of the sea ice thickness and thus the total sea ice volume, which would be stronger if it was induced by heat flux trend only.

Interannual variability : The pattern for the REF experiment of the standard deviation from the annual mean (Fig. 5.6) is similar to the one found in the simulations of *Lindsay and Zhang* (2006), with a maximum (up to 1m) along the northern Canadian Coast, the Alaskan Coast and in the East Siberian Sea. In the central Arctic, the standard deviation is about 0.6 m.
To elucidate the role of the different atmospheric fluxes for the variability of the sea ice thickness, we examine the sea ice thickness simulated by the WIND and HEAT simulations. The standard deviation for HEAT is very small everywhere (less than 0.3 m) whilst the WIND standard deviation pattern and amplitude are very similar to those of REF. As we have done previously for the different sea ice variables, we verify that the WIND and HEAT sea ice thickness anomalies linearly sum up to the REF sea ice thickness anomalies. At each grid point, the time series of H_R and $H_W + H_H$ correlate well (more than 0.9) and the variance of H_R is very close to the variance of $H_W + H_H$ (the difference is close to zero almost everywhere ans always smaller than 20% where there is sea ice in both WIND and HEAT). Thus we can examine the contributions of HEAT and WIND to the REF sea ice thickness variations.
To do so, we have broken down the total variance at each model grid point (as done previously for the total volume). Results (not shown) show that in most of the Arctic interior where the sea ice is the thickest, the variance of the sea ice thickness in WIND accounts for most of the total variance and up to 100 % in the central Arctic (in this part of the basin, the variance from HEAT and the covariance between HEAT and WIND tend to compensate each other). Everywhere, the variance in HEAT remains very small compared to the total, while the covariance term contributes up to 20% in the regions where the sea ice is melting during summer.

In order to identify preferential modes of interannal variability, we perform an EOF analysis of the annual mean sea ice thickness anomalies. For the REF simulation, the first EOF explains 33.8% of the total variance, while the second and third modes explain only about 10%. Thus we focus our analysis on the first mode of variability shown in

Fig. 5.8, along with the time series of its amplitude coefficient.

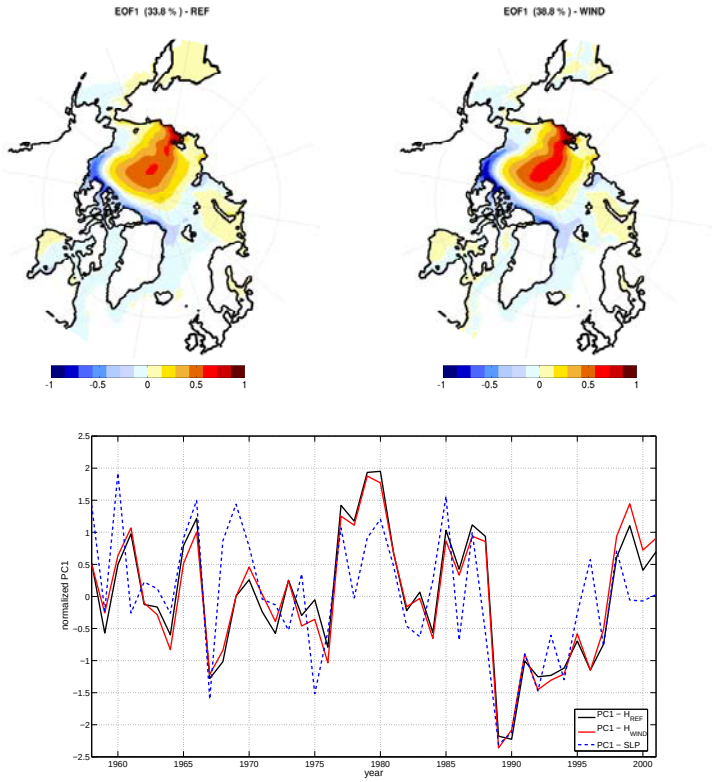

FIG. *5.8: First dominant mode of sea ice thickness variability based on EOF analyses of the REF and WIND experiments, and time series of the principal component (PC) of the EOF. The time series of the principal component of the first EOF of the annual mean SLP variations north of 60 °N is also indicated.*

Notably, the pattern of the first EOF and the PC in REF are similar to the results of *Holloway and Sou* (2002), suggesting that the mode extracted here is robust and has a physical meaning. In details, the spatial pattern is characterized by large anomalies in the East Siberian Sea (up to 1m) that decrease toward the Beaufort Gyre and the Fram Strait. Anomalies of opposite sign can be found along the coast north of the CAA and Greenland up to Fram Strait, and the anomalies outside the central Arctic are negligible. *Holloway and Sou* (2002) suggests that this mode of variability is likely linked to the variations of the AO. The large correlation found between the PC of the first sea ice thickness EOF and the PC of the first EOF of the SLP north of 60° (r=0.68, see Fig. 5.8) supports this finding.

The first EOF of the variations of the WIND sea ice thickness accounts for 41% of the variance, and both the spatial pattern and the PC times series are similar to the REF ones (Fig. 5.8). Meanwhile, we could not find any correspondence between the 5 first EOF of HEAT and WIND (remember also that the standard deviations in HEAT are very small compared to REF).

Thus, we find that the wind stress variations are responsible for an important part of the sea ice thickness variations. A possible mechanism associated to the first EOF is the advection of sea ice thickness anomalies from the East Siberian Sea or the North of the CAA due to the wind toward Fram Strait.

In summary, our finding back up the model results of *Holloway and Sou* (2002), that is that the leading mode of variability of the sea ice thickness can be linked with the AO variations, and that the long term decrease of the sea ice thickness observed by *Rothrock et al.* (1999) probably overestimates the bassin-scale thinning, due to the large spatial dependence of the long term trend on this parameter. Our sensitivity experiments allows us to separate the effect of the dynamical and thermodynamical forcing on the sea ice thickness variability and changes. We find that the interannual variations of the sea ice thickness are mostly due to the variations of the wind stress, the variations of the heat flux playing a minor role. On the opposite, the long term decreasing trend found in the central Arctic is mostly driven by the increasing trend of the air temperature over the Arctic Basin, even though the variability of the wind stress tends to redistribute the sea ice into the Arctic and thus to damp the decreasing trend of the sea ice volume.

5.2.6 Arctic sea ice production

Usually, the sea ice volume changes in the Arctic basin are related to an imbalance between ice production and ice export, and each term can be examined separately from numerical modeling outputs (*Köberle and Gerdes*, 2003; *Rothrock and Zhang*, 2005). This analysis helps to understand which phenomena are responsible for the changes in the sea ice volume. Moreover, the production term can be related to changes in the sea surface salinity changes in the Arctic interior, while the export term represents the quantity of freshwater exported from the Arctic to the Subpolar region, where it will represent a transfer of freshwater to the ocean.
In this study, we have chosen to consider the total sea ice pack encompassed in the Northern Hemisphere, and thus the calculated Arctic ice volume changes have to equal the sea ice production, the export being zero. Thus the balance reads :

$$\partial_t V = P$$

V being the total annual mean sea ice volume and P the annual averaged net production. Note that the export term in *Köberle and Gerdes* (2003) and *Rothrock and Zhang* (2005) is somehow the equivalent for us of the sea ice melting in the marginal sea ice zone (outside the Arctic interior). Thus, looking at the spatial distribution of the production term will help to determine the region that influence the most the volume changes. Again, the sensitivity experiments will allow us to elucidate the role of the different atmospheric

forcing on the sea ice volume variations.

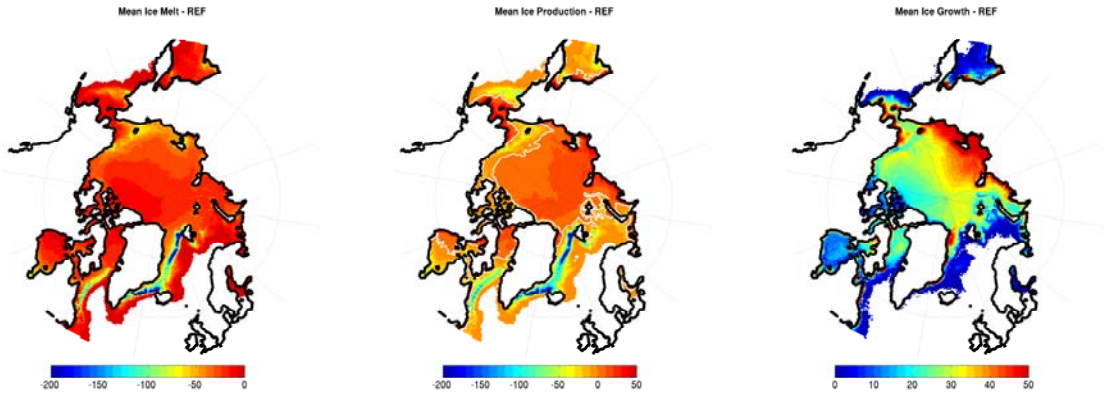

FIG. *5.9: Average over 1963–2001 of the sea ice melt (left), net production (middle) and growth (right) for the REF experiment. Unit is* m^3/s.

Fig. 5.9 shows the spatial distribution of the mean net sea ice production, and Fig. 5.10 the time series of the integrated net sea ice production. To further understand the net production, we also distinguish between sea ice melt and growth and the mean spatial pattern as well as their variations are also shown (the distinction is made on the monthly means). The largest values for the sea ice growth are visible in the Arctic interior, along the Siberian Coast, and in the western Fram Strait, while the largest values of the sea ice melt are logically visible in the marginal zones, with the largest contributions in the Greenland/Irminger and Labrador Seas. The integrated values of the sea ice growth and melt are of similar amplitude (their averaged values are $631\times10^3 m^3/s$ and -$646\times10^3 m^3/s$ respectively for the REF simulation, and their standard deviations are $20.4\times10^3 m^3/s$ and $37.9\times10^3 m^3/s$). However, the variability of the net production is largely dominated by the sea ice melt variability, their time series being well correlated (r=0.85) while no correlation could be found between the growth and net production time series.

In previous studies, *Köberle and Gerdes* (2003) found that both the sea ice production and export variations contribute equally to the volume changes, while *Zhang et al.* (2000) suggest that the sea ice export is dominating the volume changes. To explain this contrast, *Köberle and Gerdes* (2003) argue that the simulation used by *Zhang et al.* (2000) was too short to properly reproduce more than one phase of the AO, which might lead to biased results.

Our own finding supports the conclusions of *Zhang et al.* (2000), as we find that the sea ice melt variations (which occurs mainly outside of the Arctic interior, in the Greenland/Irminger Sea) are responsible for most of the sea ice volume changes (equal to the total net production) over 44 years. Hence we suggest that the difference between our findings and those of *Köberle and Gerdes* (2003) might be due to model dependency of the results.

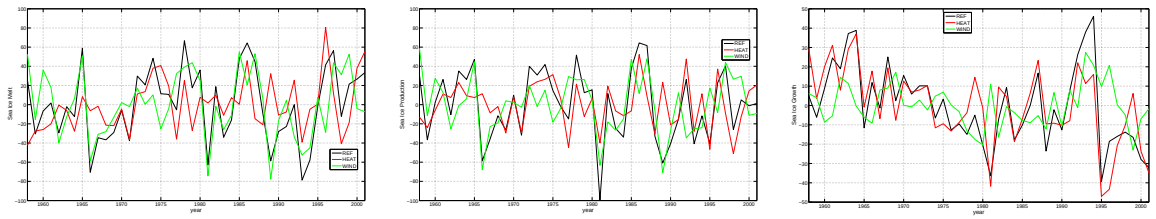

FIG. *5.10: Time series of the integrated sea ice melt (left), net production (middle) and growth (right) anomalies for the three experiments. Unit is* m^3/s.

The HEAT and WIND contributions to the REF sea ice growth, melt and net production are also indicated in Fig. 5.10. The behaviors of the sensitivity experiments present a striking contrast regarding the sea ice melt and growth time series : the HEAT anomalies dominate the REF sea ice growth anomalies (r=0.82) while the WIND anomalies dominate the REF sea ice melt anomalies (r=0.75). Note that for the melt and growth time series, the 3 simulations have comparable means and standard deviations.
Zhang et al. (2000), *Köberle and Gerdes* (2003) and *Rothrock and Zhang* (2005) found that the interannual variability of the sea ice net production is mainly thermodynamically forced, while the variations of the sea ice export are mostly explained by the wind stress fluctuations that modulate the sea ice export through Fram Strait. Our results are consistent with this conclusion, as the sea ice melt in the marginal zone can be linked to the sea ice export out of the Arctic basin.

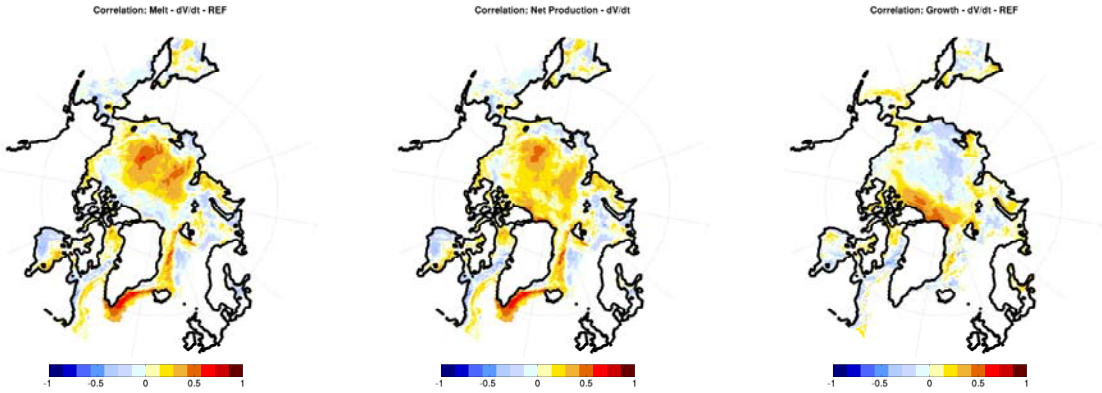

FIG. *5.11: Correlation between the sea ice volume derivative time series and the sea ice melt (left), net production (middle) and growth (right) for the REF simulation.*

Last, as we want to determine where the sea ice production variations have the strongest impact for the sea ice volume changes, we calculate at each model grid point the correlation between the total sea ice volume derivative time series and the local sea ice net

production, melt and growth. Results are shown in Fig. 5.11.

We find large correlations between the sea ice growth and the volume changes north of the CAA and Greenland. However, in this region, the standard deviation of the sea ice growth is small, which explains the smaller contribution of the sea ice growth to the total sea ice production despite these correlations. Regarding the sea ice melt, high correlations are visible in the Irminger/Greenland Seas (where the sea ice melt standard deviation is the largest) and in the Arctic interior. This spatial pattern could give insights on where measurements should be taken in order to approximate the total NH sea ice volume changes. We find that sea ice melt in the Irminger/Greenland Seas explains an important part of the sea ice volume changes. As the quantity of sea ice that melts in these regions can be directly related to the quantity of sea ice exported through Fram Strait, the measurement of the sea ice export through Fram Strait appears to be crucial.

5.2.7 Summary and concluding remarks.

Direct observations of the Arctic sea ice conditions are still limited and insufficient to understand the mechanisms responsible for their variability. Here we have investigated the time and spatial variability of the Arctic sea ice properties in a hindcast simulation using a regional ocean/sea-ice coupled model of the Arctic and North Atlantic forced with the 44 years ERA40 reanalysis, as well as in perturbation experiments forced with modified surface forcing. The hindcast simulation is found to reproduce the mean quantities of the Arctic sea ice cover but also some of the observed features of its interannual variability with reasonable accuracy.

We first examine the sea ice volume : the long term decreasing trend is found to be small over the period 1963–2001 (-2.5%/decade), but the decrease accelerates recently (-10.4%/decade over 1980–2001). Even though this decline is consistent with estimates based on observations (*Rothrock et al.*, 1999), it remains difficult to distinguish between physical and more or less arbitrary trends, as large decadal variations are superimposed on the long term changes. To better understand the physical mechanisms responsible for this long term trend, we use the model output to decompose the sea ice volume into the different parameters that enter in its calculation (concentration and thickness), and we look at their respective variability and the long term trend.

The sea ice area variations (which is the integral of the sea ice concentration) explains about 40% of the interannual fluctuations of the sea ice volume, and shows a linear decrease of -1.4%/decade. Looking into the spatial field of the sea ice concentration reveals that this parameter exhibits different variability and trends in the different regions, and during the different seasons. In winter, most of the variability and the largest decreasing

trend are located in the marginal sea ice zone, especially in the Greenland and Barents Seas. In summer, the decreasing trends are the largest in the central Arctic, while the main structure of variability is located along the Russian Coast. All these results regarding the sea ice concentrations are consistent with observational results (*Stroeve et al.*, 2008; *Deser and Teng*, 2008). As we analyze longer time series than those available from observations, our modeling results add robustness to the long term trend and variability of the sea ice concentration as described from direct measurements.

Regarding the sea ice thickness, our model results back up the finding of *Holloway and Sou* (2002) that the 40% thinning observed in the central Arctic (*Rothrock et al.*, 1999) is probably the upper bound of the total sea ice cap thinning, as we find reversed trend in the central Arctic and in the coastal regions. These results emphasize the crucial need for basin-wide ice thickness observations. We also confirm that the AO variations are responsible for the leading mode of the sea ice thickness variability, as suggest by *Holloway and Sou* (2002).

Our sensitivity experiments allow us to look at the respective roles of the dynamical and thermodynamical forcing in a systematic way, contrary to what has been done in previous studies where the long term trend were examined with shorter time series or no such decomposition of the sea ice volume and its variations were done. Regarding the sea ice volume, the thermal forced component explains completely the long term trend, while the wind forced component is responsible for 2/3 of the interannual variability. Again, we examine the sea ice concentration and thickness separately. Overall, the long term trend and variability of the sea ice concentration are almost completely due to changes and variability in the wind forcing fields during summer, while taking into account the variations of the atmospheric heat flux is sufficient to reproduce most of the trend and interannual variability of the sea ice concentrations during wintertime. Regarding the sea ice thickness, the increasing SAT over the Arctic is responsible for the thinning all over the Arctic interior, while the changes and variability of the wind stress tend to damp this trend and to cause a redistribution of the sea ice thickness in the Arctic basin. The variability of the wind stress is also responsible for most of the sea ice thickness variability, the thermal forcing playing a minor role. It underlines the crucial need to improve the wind forcing fields in the Arctic basin, as their variations play probably a more important role for the sea ice cover changes and variability than just the air temperature changes and variations.

Finally, the sea ice volume changes in the Northern Hemisphere are related to the sea ice net production, the latter being dominated by the variations of the sea ice melt. This results is similar to the findings of *Zhang et al.* (2000), but in contradiction with those of *Köberle and Gerdes* (2003) who find that both the sea ice melt and growth contribute

equally to the sea ice volume changes. No obvious reason could be found to explain this contradiction, and more investigation on the model dependency of our results would be required here. We find that the heat forcing dominates the sea ice growth, that is large in the Siberian part of the Arctic basin, while the variations of the wind stress explains most of the sea ice melt variance. This is consistent with the general idea that the sea ice export through Fram Strait is mainly wind driven (*Vinje*, 2001; *Tsukernik et al.*, 2010), as the largest values of the sea ice melt can be found in the Greenland/Irminger, and the integral value over this region is roughly equal to the sea ice export through Fram Strait. Thus monitoring the sea ice volume export through Fram Strait give indications on the total Arctic sea ice volume changes.

Conclusion

Une kyrielle de changements affectant toutes les composantes du système Arctique (atmosphère, océan et glace de mer) a été largement décrite ces dernières années dans la littérature. Mais si ces toutes transformations profondes du bassin polaire Arctique préoccupent autant la communauté scientifique, c'est sans doute parce que l'on s'attend à ce que ces modifications n'aient pas seulement un impact sur les populations et les écosystèmes locaux, mais également sur le reste de la planète, étant donné que l'Arctique joue un rôle particulier dans le climat mondial. L'objectif de cette thèse est donc de mieux comprendre comment le signal d'un changement local dans le bassin Arctique peut avoir un impact sur la circulation océanique globale et sur le climat. Nous visons ici plus particulièrement à comprendre les mécanismes de variabilité des échanges d'eau douce et de glace de l'océan Arctique vers l'Atlantique Nord, et notamment le lien entre ces échanges et la dynamique océanique et le bilan d'eau douce dans le bassin Arctique. Cette problématique est abordée à l'aide de plusieurs simulations et outils numériques, les observations ne permettant à l'heure d'actuelle que d'apporter une réponse très parcellaire à ce problème.

Nous nous intéressons tout d'abord au contenu halin du bassin Arctique, et au lien entre ses variations et celles des exports d'eau douce vers les mers Subarctiques. Deux approches complémentaires sont présentées ici : dans le chapitre 2, nous examinons de manière systématique la variabilité interannuelle de tous les termes du bilan d'eau douce de l'Arctique au cours de quatre décennies (1965–2002), alors que le chapitre 3 est focalisé sur un événement en particulier, à savoir les conséquences possibles pour le contenu halin Arctique du minimum de l'extension de glace sans précédent qui a eu lieu à la fin de l'été 2007.

La première étude permet de montrer que, dans notre simulation tout au moins, la variabilité interannuelle du contenu en douce de l'Arctique (stockée sous forme liquide ou de glace) est contrôlée principalement par quatre termes advectifs : l'apport d'eau douce liquide d'origine pacifique à travers le détroit de Bering, l'export de glace à travers le détroit de Fram et les exports sous forme liquide des deux côtés du Groenland, à travers les détroits de Fram et de Davis. Ce résultat n'est pas surprenant au vue des déficiences connues de notre simulation que nous forçons avec des apports fluviaux et des

précipitations en Arctique qui ne comprennent pas de variabilité interannuelle. La variabilité de ces deux termes joue sans doute en réalité un rôle important pour les variations du contenu halin. Mais les résultats de cette étude mettent principalement en lumière la nécessité de considérer les échanges d'eau douce entre l'Arctique et l'Atlantique à la fois sous forme liquide et de glace, mais également des deux côtés du Groenland. En effet, jusqu'aux années 1990, la vision communément répandue du fonctionnement du système Arctique est que la contribution principale des échanges d'eau douce entre l'Arctique et l'Atlantique est l'export de glace à travers le détroit de Fram, les exports d'eau douce liquide à l'Est et à l'Ouest du Groenland étant, à tort, considérés comme étant environ trois fois plus faibles que l'export de glace à Fram (e.g., *Aagaard and Carmack* (1989)). Ceci explique le nombre important d'études à base d'observations ou de modélisation s'intéressant à la variabilité du flux de glace à travers le détroit de Fram (e.g., *Vinje* (2001); *Kwok et al.* (2004); *Spreen et al.* (2009); *Tsukernik et al.* (2010)). Pourtant, plus récemment, des mesures plus complètes ont révélé que les flux d'eau douce liquide exportés de l'Arctique étaient sans doute largement sous estimés. Ainsi, *Meredith et al.* (2001) montrent que le flux d'eau douce liquide à travers le détroit de Fram est en moyenne aussi important que le flux de glace, tandis que *Cuny et al.* (2005) mettent en évidence que la contribution liquide à l'Ouest du Groenland est elle deux fois plus grande que le flux de glace à Fram. Notre étude confirme la nécessité d'améliorer notre connaissance des exports d'eau douce sous forme liquide provenant de l'Arctique, à la fois en intensifiant les mesures, mais aussi en améliorant le réalisme des simulations numériques sur ces aspects.

Nous montrons également dans ce chapitre que les mécanismes de variabilité des trois termes contribuant à l'export total d'eau douce diffèrent. Tandis que des études antérieures ont montré que la variabilité du flux de glace à travers le détroit de Fram est due aux vents locaux et/ou à la circulation atmosphérique à plus grande échelle (*Vinje*, 2001; *Tsukernik et al.*, 2010), nous suggérons ici que la variabilité des flux d'eau douce liquide est contrôlée différemment de part et d'autre du Groenland. A l'Ouest, à travers le détroit de Davis, les variations du flux de volume expliquent complètement les variations du flux d'eau douce liquide. A l'Est, ce sont à la fois les variations du flux de volume et celles de la salinité qui influent, à parts égales, sur la variabilité interannuelle du flux d'eau douce liquide. Ces variations de salinité peuvent être reliées à celles de la fonte et formation de glace de mer au Nord du Groenland. Les variations des flux de volume, fortement anti-corrélées entre l'Est et l'Ouest du Groenland, sont elles plus compliquées à comprendre et nécessiteront à l'avenir de nouvelles investigations. Il semble que le mécanisme proposé par exemple par *Proshutinsky and Johnson* (1997) qui consiste en une alternance entre des phases d'accumulation puis de relâchement d'eau douce liquide dans la gyre de Beaufort n'explique pas les variations ni des flux de volume ni des flux d'eau douce liquide exportés vers l'Atlantique Nord, puisque nous n'avons pu trouvé aucun lien entre

les variations de SSH dans la gyre de Beaufort et celles des différents exports.
Une piste à suivre pourrait être celle proposée récemment par *Marsh et al.* (2010) qui suggèrent l'existence d'une onde piégée à la côte qui se propagerait anticycloniquement autour du Groenland, et qui serait un réajustement de la circulation cyclonique forcée par le vent autour du Groenland trouvée par *Joyce and Proshutinsky* (2007) en appliquant au Groenland la règle des îles (*Godfrey*, 1989). Nous pensons que l'explication dynamique de l'anticorrélation entre les variations des transports de part et d'autre du Groenland pourrait se trouver ici.

La chapitre 3 aborde un autre aspect des variations du contenu halin du bassin Arctique, à partir de l'analyse d'une réanalyse océanique des années récentes. Alors que de nombreuses études se sont intéressées aux causes du minimum de glace record de septembre 2007 (e.g., *Comiso et al.* (2008); *Drobot et al.* (2008); *Zhang et al.* (2008)), les conséquences de cet épisode pour la salinité de l'Océan Arctique sont encore à explorer. A première vue, on s'attendrait à ce que l'événement de 2007 s'accompagne soit d'une augmentation du contenu d'eau douce liquide en Arctique, soit d'une augmentation de la quantité d'eau douce transférée aux mers Subarctiques, sous forme liquide ou de glace. En réalité, notre étude suggère que c'est plus compliqué que cela, et nous soulignons ici la nécessité de considérer le bassin Arctique dans son ensemble, et non pas seulement quelques régions comme la gyre de Beaufort où des mesures de la salinité ont été effectuée intensivement depuis 2003 (*Proshutinsky et al.*, 2009; *McPhee et al.*, 2009). En comparant le contenu en eau douce en 2007 et 2008 à celui moyenné sur la période 2002-2006, nous montrons que la salinité dans les bassins Canadien et Eurasien n'a pas évolué de la même façon. La fonte de glace se fait principalement dans le bassin Canadien, et la quantité d'eau douce correspondant à cette fonde est transférée à l'océan. La distribution spatiale de l'eau douce est également modifiée durant les années 2007 et 2008, avec une accumulation dans la gyre de Beaufort due à une circulation atmosphérique anticyclonique intensifiée au dessus du bassin Canadien. Au total, en considérant la glace et l'océan, la quantité d'eau douce reste quasiment constante dans ce bassin.
Contrairement à cela, notre simulation suggère que le bassin Eurasien s'est lui salinisé en 2007 et 2008, à cause d'une anomalie dynamique de la branche entrant d'eau Atlantique au Nord du détroit de Fram. Le manque de mesure dans cette région de permet pas de valider le comportement du modèle, et il serait sans doute intéressant de comparer la solution donnée par notre simulation avec des résultats d'autres modèles.
L'utilisation d'une simulation numérique nous permet ici de quantifier à la fois l'anomalie de volume de glace correspondant à l'épisode de 2007 (la connaissance de l'épaisseur de glace n'est pas suffisante pour pouvoir le faire à partir des observations), mais aussi la quantité d'eau douce liquide accumulée dans le bassin Canadien. Cette quantité est d'un ordre de grandeur similaire à celle supposée être à l'origine de l'épisode de GSA observé

en Atlantique Nord dans les années 1970 (*Dickson et al.*, 1988). On peut donc penser que si dans les années à venir, cette quantité d'eau douce est exportée vers l'Atlantique Nord, d'un côté ou de l'autre du Groenland, des modifications importantes de la salinité dans les mers Nordiques ou la gyre Subpolaire pourraient avoir lieu.

Connaître et comprendre le fonctionnement du système d'eau douce en Arctique (dans sa globalité ou simplement une de ses composantes) est probablement un des thèmes de recherche qui agite le plus la communauté scientifique Arctique à l'heure actuelle, et les études des chapitres 2 et 3 suivent finalement chacun une approche assez classique. Une analyse similaire à celle du chapitre 2 est par exemple en cours dans plusieurs simulations et modèles différents dans le cadre du projet AOMIP, et nous pouvons espérer tester la robustesse des résultats présentés ici et ainsi s'affranchir pas à pas de la dépendance des solutions au modèle utilisé.
Mais les conclusions des chapitres 2 et 3 révèlent aussi les insuffisances des démarches utilisées, et suggèrent que la compréhension du système d'eau douce dans le bassin Arctique ne peut se faire indépendamment de celle de la dynamique océanique du bassin. En effet, on montre par exemple que la salinité des eaux exportées à travers le détroit de Fram est modifiée au cours de leur parcours en Arctique, et la connaissance du trajet de ces masses d'eau dans le bassin est donc nécessaire. De même, on montre que ce sont des anomalies de la dynamique qui sont à l'origine des anomalies du contenu en eau douce en 2007 et 2008, même si l'origine de ces anomalies de circulation n'est pas forcément bien comprise. L'étude présentée au chapitre 4 a donc pour but de combler, en partie tout au moins, les lacunes concernant notre connaissance de la circulation en Arctique, et des transformations de masse d'eau associées à cette circulation.
Une année climatologique mensuelle est construite à partir des champs 3D de la simulation numérique utilisée au chapitre 2, puis une analyse lagrangienne est appliquée à ces champs moyens en utilisant l'outil ARIANE. L'étude permet de montrer que les masses d'eau exportées à travers le détroit de Davis sont constituées à parts égales d'eau d'origine pacifique et atlantique, tandis que seules des masses d'eau d'origine atlantique sont exportées à l'Est du Groenland. Ce résultat confirme là encore la nécessité de considérer les contributions aux exports vers les mers Subarctiques des deux côtés du Groenland, puisque, dans les couches de surface, l'eau atlantique est exportée pour moitié d'un côté et de l'autre du Groenland. Les observations de traceurs chimiques ont mis en évidence la présence de traces d'eau pacifique à Fram (*Jones et al.*, 1998; *Falck et al.*, 2005) et il semble que notre simulation ne parvienne pas à reproduire le transfert de masses d'eau entre Bering et Fram, qui se fait probablement par un courant côtier sur le plateau le long des côtes de la Sibérie, du Canada puis du Groenland (*Steele et al.*, 2004). L'implémentation d'une paramétrisation de l'effet Neptune (*Holloway and Wang*, 2009) pourrait sans doute permettre de corriger cette déficience. On peut supposer également

qu'une telle paramétrisation pourrait aider à représenter le Courant Côtier Est Groenland (EGCC) plus au sud, courant par lequel l'eau Pacifique pourrait être transférée à la gyre Subpolaire mais qui est mal représenté dans les simulations actuelles (*Treguier et al.*, 2006).

Ce travail nous a permis de proposer un schéma complet moyen de la circulation dans le bassin Arctique, de quantifier l'importance des différentes branches contribuant aux exports vers l'Atlantique ainsi que les transformations de masses d'eau et les temps de résidence associés à chaque branche. Un des résultats frappant concerne les transformations de masse d'eau en mer de Barents. Nous montrons que, dans notre simulation, la branche d'eau atlantique entrant par le Barents Sea Opening est modifiée complètement en mer de Barents en moins d'un an. Cela tient au fait que la position du front de glace permet des échanges entre les couches océaniques de surface et l'atmosphère, ce qui provoque une densification des eaux de surface qui pénètrent ensuite en Arctique par la fosse de Saint Anna. Il serait sans doute intéressant d'étudier plus en détails le lien entre la position du front de glace en mer de Barents et la quantité d'eau dense formée dans cette région.

Le schéma de circulation présenté ici est représentatif d'une climatologie mensuelle construite sur 20 années de simulation. Afin de tester la robustesse de nos résultats, la même analyse lagrangienne est appliquée à deux années climatologiques idéalisées représentatives de deux états contrastés de l'Oscillation Arctique, et il semble que le schéma de circulation reste cohérent entre les différentes climatologies. Mais il est évident qu'une étude plus approfondie de la variabilité du schéma de circulation serait intéressante, même si elle nécessiterait la mise en place de moyens numériques lourds.

Il nous semble également que la stratégie d'étude originale suivie ici pourrait, en étant appliquée à d'autres modèles, permettre de comprendre un peu mieux à la fois le fonctionnement du bassin Arctique mais aussi de mettre en évidence les forces et les faiblesses des simulations numériques. De plus, alors que les mesures chimiques ou de contaminants s'intensifient dans la région polaire Arctique, cette approche permettrait sans doute de développer une nouvelle synergie entre les communautés d'observations et de modélisation.

La dernière partie de ce manuscrit est consacrée à l'étude de la variabilité interannuelle des conditions de glace dans le bassin Arctique, et plus particulièrement au rôle des différents forçages atmosphériques pour cette variabilité. Les résultats des chapitres précédents suggèrent que la formation et la fonte de glace peuvent influencer les propriétés des masses d'eau exportées vers l'Atlantique Nord (chapitre 2), les propriétés hydrologiques à l'intérieur du bassin Arctique (chapitre 3) ou la formation d'eau dense en mer de Barents et les transformations des masses d'eau des couches de surface durant leur trajet en Arctique (chapitre 4). Il nous a donc semblé opportun d'essayer de comprendre un peu

plus en détails les mécanismes de variabilité du volume de glace de mer en Arctique.
Nous nous appuyons ici sur l'analyse d'une simulation de référence utilisant un modèle régional au 1/2° et représentant les années 1958 à 2001 (soit la période de la réanalyse ERA40 qui est utilisée pour forcée notre simulation). Cette simulation est complétée par des tests de sensibilité pour lesquels les différentes composantes des forçages atmosphériques sont réduites tour à tour à un cycle climatologique. Des jeux de simulations similaires ont été utilisés dans des études antérieures, que ce soit pour étudier les variations des conditions de glace en Arctique (*Köberle and Gerdes*, 2003; *Rothrock and Zhang*, 2005) ou les variations de la MOC en Atlantique Nord (*Eden and Willebrand*, 2001; *Biastoch et al.*, 2008). Mais contrairement aux études précédentes sur la glace de mer, nous présentons ici une étude systématique dans ce jeu de simulation de la variabilité interannuelle et de la tendance à long terme des différents paramètres (concentration et épaisseur) qui contribuent au calcul du volume de glace total. En général, on montre que les variations du vent contrôlent 2/3 de la variabilité interannuelle du volume de glace et quasiment toute celle de l'épaisseur de glace. Mais nous suggérons également que les variations et la tendance des champs de vent jouent un rôle potentiellement important pour les tendances des différents paramètres considérés, et ce n'est donc pas simplement l'augmentation des températures de l'atmosphère au dessus du bassin Arctique qui suffit à expliquer la tendance décroissante de l'extension et du volume de glace ces dernières années.
En examinant la production nette de glace (qui peut être reliée aux variations du volume de glace), on montre que ce sont les variations de la fonte de glace (et non celles de la formation) qui dominent les fluctuations de la production nette, la fonte étant importante dans les zones marginales de glace et particulièrement à l'Est du Groenland où toute la quantité de glace exportée à travers le détroit de Fram finit par fondre. Les variations de la fonte de glace (et donc également celles de la production nette) peuvent être reliée à la variabilité des vents, ce qui est cohérent avec les mécanismes de variabilité des exports de glace à Fram. Ces résultats suggèrent que la connaissance du flux de glace exporté à travers le détroit de Fram est un bon indicateur des variations temporelles du volume de glace en Arctique, et mettent donc en évidence la nécessité de mesurer avec plus de fiabilité l'épaisseur de glace, au niveau du détroit de Fram mais également dans tout le bassin puisque nous montrons que les tendances sur cette quantité sont fortement variables dans l'espace.
Les simulations utilisées dans cette étude constituent un jeu de données simulées intéressant qui pourra également par la suite être utilisé pour comprendre le rôle des différents forçages atmosphériques pour la variabilité de la dynamique océanique en Arctique et celle des échanges océaniques entre l'Arctique et l'Atlantique Nord.

Dans tout ce travail de thèse, nous nous sommes attachés à considérer l'Arctique à

l'échelle du bassin, et à plusieurs reprises nos analyses montrent que les observations, plus locales par nature, ne permettent souvent que de décrire une partie des phénomènes : le monitoring des changements de salinité dans la gyre de Beaufort ne permet pas de connaître les changements du contenu halin à l'échelle du bassin, la connaissance des variations du flux de glace exporté au détroit de Fram est très insuffisante pour connaître la quantité d'eau douce exportée vers l'Atlantique Nord, ou encore les mesures satellite de l'extension de glace ne permettent de décrire qu'une mince part des variations du volume de glace en Arctique. Nous soulignons ici la nécessité à la fois d'intensifier les mesures dans le bassin polaire Arctique, mais aussi peut être de cibler un peu plus les paramètres qui doivent être mesurés afin de coordonner plus intelligemment les campagnes de mesures futures, mais également de maintenir les systèmes d'observations sur des périodes plus longues afin d'avoir accès à la connaissance de la variabilité interannuelle et la tendance à long terme des différents observables (c'est ce que *Dickson* (2009) appelle *« Securing the legacy of the IPY »*).

Les résultats présentés dans cette thèse mettent également en évidence la présence de certaines zones clés, qui mériteraient sans doute par la suite des études plus locales. La mer de Barents en est un exemple, et il sera intéressant d'étudier dans le détail les processus de formations d'eau dense dans cette région, afin notamment de quantifier la contribution de la convection dans cette région au flux d'eau dense exporté de l'Arctique à travers le détroit de Fram. *Aksenov et al.* (2010) suggèrent que les variations de la localisation du front de glace sont liées à celle du volume d'eau dense formée. On peut penser que, avec l'accélération de la diminution de l'extension de glace observée ces dernières années (*Comiso et al.*, 2008), de plus en plus de zones peu profondes au dessus des plateaux seront découvertes de glace durant une partie importante de l'année, et que les échanges entre la surface de l'océan et l'atmosphère pourront engendrer de la convection plus importante dans ces régions. Ceci constitue une piste de réflexion intéressante pour nos futurs travaux.

Une autre perspective de cette thèse consisterait en une étude du devenir des masses d'eau exportées de l'Arctique vers l'Atlantique Nord, afin notamment d'essayer de mieux comprendre comment la variabilité de ces exports peut être liée à l'intensité de la convection profonde dans les mers Nordiques et du Labrador, et par conséquent avec l'intensité de la MOC. En effectuant un suivi lagrangien des masses d'eau exportées des deux côtés du Groenland, il serait par exemple possible de quantifier la part de ces masses d'eau qui atteignent les zones de convection profonde, ou encore de mieux comprendre si il existe un lien entre la variabilité des exports d'eau douce de l'Arctique avec les épisodes de GSA. Une des raisons pour laquelle ce travail n'a pas été effectué durant cette thèse est que la convection profonde, particulièrement en mer du Labrador, n'est pas représentée correctement dans les simulations disponibles (*Treguier et al.*, 2005).

De manière plus générale, l'amélioration des simulations numériques de la région Arc-

tique devrait ouvrir de nouvelles pistes de réflexion. Nous avons souligné plusieurs fois la nécessité d'améliorer les forçages atmosphériques, de réduire, supprimer ou paramétriser autrement le rappel en surface à une salinité climatologique (e.g., *Gerdes et al.* (2008)). De même, l'introduction de paramétrisations de la marée (*Holloway and Proshutinsky*, 2007b) ou encore des interactions entre les tourbillons et la topographie (effet Neptune, e.g., *Holloway and Wang* (2009)) devrait permettre d'améliorer significativement le réalisme des simulations. Enfin, l'amélioration de la résolution spatiale des modèles permettra de représenter les structures de petites échelles qui jouent sans doute un rôle pour la dynamique grande échelle de l'Arctique. L'existence d'un projet tel qu'AOMIP laisse espérer des progrès rapides et des développements intéressants pour les modèles numériques du bassin Arctique dans les années à venir.

Bibliographie

Aagaard, K., and E. Carmack (1989), The role of sea ice and other fresh water in the Arctic circulation., *Journal of Geophysical Research*, *94*, 14,485–14,498.

Aagaard, K., and P. Greisman (1975), Toward new mass and heat budgets for the Arctic Ocean., *Journal of Geophysical Research*, *80(27)*, 3,821–3,827.

ACIA (2005), Arctic climate impact assessment – scientific report, p. 1042, Cambridge University Press, Cambridge, United Kingdom and New York, NY, USA, available online at http ://www.acia.uaf.edu/pages/scientific.html.

Aksenov, Y., S. Bacon, A. C. Coward, and A. J. G. Nurser (2010), The North Atlantic inflow to the Arctic Ocean : High-resolution model study, *Journal of Marine Systems*, *79*, 1–22.

Arfeuille, G., L. A. Mysak, and L. Tremblay (2000), Simulation of the interannual variability of the wind-driven Arctic sea-ice cover during 1958-1998, *Climate Dynamics*, *16*, 107–121.

Barnier, B., G. Madec, T. Penduff, J. M. Molines, A. M. Treguier, J. Le Sommer, A. Beckmann, A. Biastoch, C. Böning, J. Dengg, C. Derval, E. Durand, S. Gulev, E. Remy, C. Talandier, S. Theetten, M. Maltrud, J. McClean, and B. De Cuevas (2006), Impact of partial steps and momentum advection schemes in a global ocean circulation model at eddy permitting resolution., *Ocean Dynamics*, *56*, 543–567, doi :10.1007/s10236-006-0082-1.

Belkin, I. M. (2004), Propagation of the "Great Salinity Anomaly" of the 1990s around the northern North Atlantic, *Geophysical Research Letter*, *31*(L08306), doi : 10.1029/2003GL019334.

Belkin, I. M., S. Levitus, J. Antonov, and S. A. Malmberg (1998), "Great Salinity Anomalies" in the North Atlantic., *Progress in Oceanography*, *41*.

Biastoch, A., C. W. Böning, J. Getzlaff, J. Molines, and G. Madec (2008), Causes of Interannual-Decadal Variability in the Meridional Overturning Circulation of the Midlatitude North Atlantic Ocean, *Journal of Climate*, *21*, 6599–6615.

Blanke, B., and S. Raynaud (1997), Kinematics of the Pacific Equatorial Undercurrent : an Eulerian and Lagrangian approach from GCM results., *Journal of Physical Oceanography*, *27*, 1038–1053.

Blanke, B., M. Arhan, G. Madec, and S. Roche (1999), Warm water paths in the Equatorial Atlantic as diagnosed with a general circulation model., *Journal of Physical Oceanography*, *29*, 2753–2768.

Blanke, B., S. Speich, G. Madec, and K. Döös (2001), A global diagnostic of interocean mass transfers., *Journal of Physical Oceanography*, *31*, 1623–1632.

Blanke, B., M. Arhan, S. Speich, and K. Pailler (2002), Diagnosing and picturing the North Atlantic segment of the global conveyor belt by means of an ocean general circulation model., *Journal of Physical Oceanography*, *32*, 1430–1451.

Blanke, B., M. Arhan, and S. Speich (2006), Salinity changes along the upper limb of the Atlantic thermohaline circulation., *Geophysical Research Letter*, *33(6)*, doi : 10.1029/2005GL024938.

Bloom, S. C., L. L. Takacs, A. M. Da Silva, and D. Ledvina (1996), Data Assimilation Using Incremental Analysis Updates, *Monthly Weather Review*, *124*, 1256–1271.

Brauch, J. P., and R. Gerdes (2005), Response of the northern North Atlantic and Arctic Oceans to a sudden change of the North Atlantic Oscillation., *Journal of Geophysical Research*, *110*, doi :10.1029/2004JC002436.

Brodeau, L., B. Barnier, T. Penduff, A. M. Treguier, and S. Gulev (2010), An ERA40-based atmospheric forcing for global ocean circulation models, *Ocean Modelling*, *31*, 88–104.

Cavalieri, D. J., C. L. Parkinson, and K. Y. Vinnikov (2003), 30-Year satellite record reveals contrasting Arctic and Antarctic decadal sea ice variability., *Geophysical Research Letters*, *30(18)*, doi :10.1029/2003GL018031.

Coachman, L. K., and K. Aagaard (1974), Physical Oceanography of Arctic and Subarctic Seas., in *Marine Geology and Oceanography*, edited by Y. Herman, pp. 1–72, Springer.

Comiso, J. C., C. L. Parkinson, R. Gersten, and L. Stock (2008), Accelerated decline in the Arctic sea ice cover, *Geophysical Research Letter*, *35*(L01703), doi : 10.1029/2007GL031972.

Condron, A., P. Winsor, C. Hill, and D. Menemenlis (2009), Simulated Response of the Arctic Freshwater Budget to Extreme NAO Wind Forcing, *Journal of Climate*, *22*, doi :10.1175/2008JCLI2626.1.

Cuny, J., P. B. Rhines, and R. Kwok (2005), Davis Strait volume, freshwater and heat fluxes., *Deep-sea research, Part 1*, *52*, 519–542.

Curry, R., and C. Mauritzen (2005), Dilution of the northern North Atlantic Ocean in recent decades., *Nature*, *308*, 1772–1774.

Dai, A., and K. Trenberth (2002), Estimates of freshwater discharge from continents : latitudinal and seasonal variations., *Journal of hydrometeorology*, *3*, 660–687.

De Steur, L., E. Hansen, R. Gerdes, M. Karcher, E. Fahrbach, and J. Holfort (2009), Freshwater fluxes in the East Greenland Current : A decade of observations, *Geophysical Research Letter*, *36*(L23611), doi :10.1029/2009GL041278.

DeBoer, A. M., and D. Nof (2004), The exhaust valve of the North Atlantic., *Journal of Climate*, *17(3)*, 417–422.

Delworth, T. L., and T. R. Knutson (2000), Simulation of early 20th century global warming., *Science*, *287*, 2246–2250.

Deser, C., and H. Teng (2008), Evolution of Arctic sea ice concentration trends and the role of atmospheric circulation forcing, 1979-2007, *Geophysical Research Letter*, *35*.

Deser, C., J. E. Walsh, and M. S. Timlin (2000), Arctic Sea Ice Variability in the Context of Recent Atmospheric Circulation Trends., *Journal of Climate*, *13*, 617–633.

Dickson, B. (2009), Securing the legacy of the IPY, *Nature Geoscience*, *2*, 374–376.

Dickson, R., B. Rudels, S. Dye, M. Karcher, J. Meinck, and I. Yashayaev (2007), Current estimates of freshwater flux through Arctic and subarctic seas., *Progress in Oceanography*, *73*, 210–230.

Dickson, R. R., J. Meincke, S. A. Malmberg, and A. J. Lee (1988), The Great Salinity Anomaly in the North Atlantic., *Nature*, *256(5517)*, 479–482.

Dickson, R. R., T. J. Osborn, J. W. Hurrell, J. Meincke, J. Blindheim, B. Adlandsvik, T. Vinje, G. Alekseev, and W. Maslowski (2000), The Arctic Ocean Response to the North Atlantic Oscillation., *Journal of Climate*, *13(15)*, 2671–2696.

Dickson, R. R., J. Meincke, and P. Rhines (2008), Arctic–subarctic Ocean fluxes : Defining the role of the northern seas in climate. A general introduction., in *Arctic–Subarctic Ocean Fluxes*, edited by R. R. Dickson, J. Meincke, and P. Rhines, pp. 1–12, Springer.

Döös, K. (1995), Inter–Ocean exchange of water masses., *Journal of Geophysical Research*, *100*, 13,499–13,514.

Drobot, S., J. Stroeve, J. Maslanik, W. Emery, C. Fowler, and J. Kay (2008), Evolution of the 2007–2008 Arctic sea ice cover and prospects for a new record in 2008, *Geophysical Research Letter*, *35*(L19501), doi :10.1029/2008GL035316.

Eden, C., and J. Willebrand (2001), Mechanism of Interannual to Decadal Variability of the North Atlantic Circulation., *Journal of Climate*, *14*, 2266–2280.

Ekwurzel, B., P. Schlosser, R. A. Mortlock, R. G. Fairbanks, and J. H. Swift (2001), River runoff, sea ice meltwater, and Pacific water distribution and mean residence times in the Arctic Ocean., *Journal of Geophysical Research*, *106(C5)*, 9075–9092.

Ezraty, R., F. Girard–Ardhuin, J. F. Piolle, and L. K. G. Heygster (February 2007), Arctic and Antarctic sea-ice concentration and Arctic sea ice drift estimated from Special Sensor Microwave Imager data. version 2.1, *Tech. rep.*, IFREMER/CERSAT.

Fahrbach, E., J. Meincke, S. Osterhus, G. Rohardt, U. Schauer, V. Tverberg, and J. Verduin (2001), Direct measurements of volume transports through Fram Strait., *Polar Research*, *20(2)*, 217–224.

Falck, E., G. Kattner, and G. Budeus (2005), Disappearance of Pacific water in the northwestern Fram Strait., *Geophysical Research Letter*, *32*, doi :10.1029/2005GL023400.

Ferry, N., L. Parent, G. Garric, B. Barnier, N. C. Jourdain, and the MERCATOR Ocean Team (2010), Mercator Global Eddy Permitting Ocean Reanalysis GLORYS1V1 : Description and results., *Mercator Ocean Quarterly Newsletter*, *36*.

Fetterer, F., K. Knowles, W. Meier, and M. Savoie (2002, updated 2009), Sea ice index., Boulder, CO : National Snow and Ice Data Center.

Fichefet, T., and M. A. Morales Maqueda (1997), Sensitivity of a global sea ice model to the treatment of ice thermodynamics and dynamics, *Journal of Geophysical Research*, *102*, 12,609–12,646.

Fichefet, T., H. Goosse, and M. A. Morales Maqueda (2003), A hindcast simulation of Arctic and Antarctic sea ice variability, 1955–2001., *Polar Research*, *22(1)*, 91–98.

Fieg, K., R. Gerdes, E. Fahrbach, A. Beszczynska-Möller, and U. Schauer (2010), Simulation of oceanic volume transports through Fram Strait 1995–2005, *Ocean Dynamics*, doi :10.1007/s10236-010-0263-9.

Friocourt, Y., S. Drijfhout, B. Blanke, and S. Speich (2005), Water mass export from Drake passage to the Atlantic, Indian and Pacific Oceans : A Lagrangian model analysis., *Journal of Physical Oceanography*, *35*, 1206–1222.

Gaillard, F., and R. Charraudeau (2008), New climatology and statistics over the global ocean.del 5.4.7, *Mersea Project report CNRS-STR-001 Del 5.4.7*.

Garric, G. (2006), News : Surface freshwater balance for global Mercator-Ocean analysis purposes., *Mercator Ocean Quarterly Newsletter*, *21*.

Gent, P. R. (2001), Will the North Atlantic Ocean thermohaline circulation weaken during the 21st century ?, *Geophysical Research Letter*, *28*(6), 1023–1026.

Gerdes, R., and U. Schauer (1997), Large-scale circulation and water mass distribution in the Arctic Ocean from model results and observations., *Journal of Geophysical Research*, *102(C4)*, 8467–8483.

Gerdes, R., M. Karcher, C. Köberle, and K. Fieg (2008), Simulating the long term variability of liquid freshwater export from the Arctic Ocean, in *Arctic–Subarctic Ocean Fluxes*, edited by R. R. Dickson, J. Meincke, and P. Rhines, pp. 405–425, Springer.

Godfrey, J. S. (1989), A Sverdrup model to the depth-integrated flow from the world ocean allowing for island circulations., *Geophys. Astrophys. Fluid Dyn.*, *45*, 89–112.

Golubeva, E. N., and G. A. Platov (2007), On improving the simulation of Atlantic Water circulation in the Arctic Ocean, *Journal of Geophysical Research*, *112*(C11), doi :10.1029/2006JC003734.

Goosse, H., T. Fichefet, and J. Campin (1997), The effects of the water flow through the Canadian Archipelago in a global ice-ocean model, *Geophysical Research Letter*, *24*, 1507–1510.

Goosse, H., J. M. Campin, E. Deleersnijder, T. Fichefet, P. P. Mathieu, M. A. Morales Maqueda, and B. Tartinville (2001), Description of the CLIO model Version 3.0., *Institut d'Astronomie et de Geophysique George Lemaître.*, Catholic University of Louvain-la-Neuve, Belgium, available online at http ://www.astr.ucl.ac.be/index.php ?page=CLIO

Haak, H., J. Jungclaus, U. Mikolajewicz, and M. Latif (2003), Formation and propagation of Great Salinity Anomalies., *Geophysical Research Letters*, *30(9)*, 1473–1476.

Häkkinen, S., and A. Proshutinsky (2004), Freshwater content variability in the Arctic Ocean., *Journal of Geophysical Research*, *73*, 210–230, doi :10.1029/2003JC001940.

Harder, M., P. Lemke, and M. Hilmer (1998), Simulation of sea ice transport through Fram Strait : Natural variability and sensitivity to forcing., *Journal of Geophysical Research*, *103*, 5595–5606.

Herbaut, C., and M. N. Houssais (2009), Response of the eastern North Atlantic subpolar gyre to the North Atlantic Oscillation, *Geophysical Research Letter*, *36*.

Hilmer, M., and P. Lemke (2000), On the decrease of Arctic sea ice volume., *Geophysical Research Letters*, *27*, 3751–3754.

Holland, M., J. Finnis, and M. C. Serreze (2006), Simulated Arctic Ocean freshwater budgets in the twentieth and twenty-first centuries., *Journal of Climate*, *19*, 6221–6242.

Holland, M. M., and C. M. Bitz (2003), Polar amplification of climate change in coupled models., *Journal of Climate*, *21*, 221–232, doi :10.1007/s00382-003-0332-6.

Holliday, N. P., S. L. Hughes, and A. Beszczynska-Möller (2009), ICES report on Ocean Climate 2008., *ICES Cooperative research report 298*.

Holloway, G. (1992), Representing topographic stress for large scale ocean models., *Journal of Physical Oceanography*, *22*, 1033–1046.

Holloway, G., and A. Proshutinsky (2007b), Role of tides in Arctic ocean/ice climate., *Journal of Geophysical Research*, *112*, doi :10.1029/2006JC003643.

Holloway, G., and T. Sou (2002), Has Arctic Sea Ice Rapidly Thinned ?, *Journal of Climate*, *15*, 1691–1701.

Holloway, G., and Z. Wang (2009), Representing eddy stress in an Arctic Ocean model, *Journal of Geophysical Research*, *114* (C13), doi :10.1029/2008JC005169.

Holloway, G., F. Dupont, E. Golubeva, S. Häkkinen, E. Hunke, M. Jin, M. Karcher, F. Kauker, M. Maltrud, M. A. Morales Maqueda, W. Maslowski, G. Platov, D. Stark, M. Steele, T. Suzuki, J. Wang, and J. K. Zhang (2007), Water properties and circulation in Arctic Ocean models., *Journal of Geophysical Research*, *112*, doi : 10.1029/2006JC003642.

Houghton, R., and M. Visbeck (2002), Quasi-decanal salinity fluctuations in the Labrador Sea., *Journal of Physical Oceanography*, *32*, 687–701.

Houssais, M. N., and C. Herbaut (2003), Variability of the ice export through Fram Strait in 1993–98 : the winter 1994/95 anomaly., *Polar Research*, *22(1)*, 99–106.

Hunke, E. C., and J. K. Dukowicz (1997), An Elastic Viscous Plastic Model for Sea Ice Dynamics, *Journal of Physical Oceanography*, *27*(6).

Ingvaldsen, R. B., L. Asplin, and H. Loeng (2004), Velocity field of the western entrance to the Barents Sea, *Journal of Geophysical Research*, *109*(C18).

IPCC (2007), Climate change 2007 - The Physical Science Basis. Contribution of Working Group I to the Fourth Assessment Report of the Intergovernmental Panel on Climate Change., p. 996, Cambridge University Press, Cambridge, United Kingdom and New York, NY, USA.

Jones, E. P., and L. G. Anderson (2008), Is the global conveyor belt threatened by Arctic Ocean fresh water outflow ?, in *Arctic–Subarctic Ocean Fluxes*, edited by R. R. Dickson, J. Meincke, and P. Rhines, pp. 385–404, Springer.

Jones, E. P., B. Rudels, and L. G. Anderson (1995), Deep waters of the Arctic Ocean : origins and circulation., *Deep Sea Research Part I*, *42*, 737–760.

Jones, E. P., L. G. Anderson, and J. H. Swift (1998), Distribution of Atlantic and Pacific waters in the upper Arctic Ocean : Implications for circulation., *Geophysical Research Letter*, *25(6)*, 765–768.

Jones, E. P., J. H. Swift, L. G. Anderson, M. Lipizer, G. Civitarese, K. K. Falkner, G. Kattner, and F. McLaughlin (2003), Tracing Pacific water in the North Atlantic., *Journal of Geophysical Research*, *108*, doi :10.1029/2001JC001141.

Joyce, T. M., and A. Proshutinsky (2007), Greenland's Island Rule and the Arctic Ocean circulation., *Journal of Marine Research*, *65*, 639–653.

Jungclaus, J., M. Haak, H. Latif, and U. Mikolajewicz (2005), Arctic–North Atlantic interactions and multidecadal variability of the meridional overturning circulation., *Journal of Climate*, *18*, 4013–4031.

Karcher, M., F. Kauker, R. Gerdes, E. Hunke, and J. Zhang (2007), On the dynamics of Atlantic Water circulation in the Arctic Ocean, *Journal of Geophysical Research*, *112*(C11), doi :10.1029/2006JC003630.

Karcher, M. J., and J. M. Oberhuber (2002), Pathways and modification of the upper and intermediate waters of the Arctic Ocean., *Journal of Geophysical Research*, *107*, doi :10.1029/2000JC000530.

Köberle, C., and R. Gerdes (2003), Mechanisms determining the variability of Arctic sea ice conditions and export., *Journal of Climate*, *16*, 2843–2858.

Köberle, C., and R. Gerdes (2007), Simulated variability of the Arctic Ocean Freshwater Balance 1948–2001., *Journal of Physical Oceanography*, *37*, 1628–1644.

Koch-Larrouy, A., G. Madec, B. Blanke, and R. Molcard (2008), Water mass transformation along the indonesian throughflow in an OGCM., *Ocean Dynamics*, *58*, 289–309, doi :10.1007/s10236-008-0155-4.

Kwok, R., and D. A. Rothrock (1999), Variability of Fram ice flux and North Atlantic Oscillation., *Journal of Geophysical Research*, *104*, 5177–5189.

Kwok, R., G. F. Cunningham, and S. S. Pang (2004), Fram Strait sea ice outflow, *Journal of Geophysical Research*, *109*(C01009).

Kwok, R., W. Maslowski, and S. W. Laxon (2005b), On large outflows of Arctic sea ice into the Barents Sea., *Geophysical Research Letters*, *32*, L22503, doi : 10.1029/2005GL024485.

Kwok, R., G. F. Cunningham, M. Wensnahan, I. Rigor, H. J. Zwally, and D. Yi (2009), Thinning and volume loss of the Arctic Ocean sea ice cover : 2003–2008., *Journal of Geophysical Research*, *114*(C07005), doi :10.1029/2009JC005312.

Lammers, R. B., A. I. Shiklomanov, C. J. Vorosmarty, B. M. Fekete, and B. J. Peterson (2001), Assessment of contemporary Arctic river runoff based on observational discharge records., *Journal of Geophysical Research*, *106*, 3321–3334.

Large, W., and S. Yeager (2004), Diurnal to decadal global forcing for ocean and sea-ice models : the datasets and flux climatologies., *NCAR technical note NCAR/TN-460+STR*, CGD division of the National Center for Atmospheric Research, available on the GFDL CORE web site.

Latif, M., E. Roeckner, U. Mikolajewicz, and R. Voss (2000), Tropical stabilization of the thermohaline circulation in a greenhouse warming simulation., *Journal of Climate*, *13*, 1809–1813.

Le Sommer, J., T. Penduff, S. Theetten, G. Madec, and B. Barnier (2009), How momentum advection schemes influence currenttopography interactions at eddy permitting resolution, *Ocean Modelling*, *29(1)*, 1–14.

Levitus, S., G. Matishov, D. Seidov, and I. Smolyar (2009), Barents Sea multidecadal variability, *Geophysical Research Letter*, *36*(L19604), doi :10.1029/2009GL039847.

Lietaer, O., T. Fichefet, and V. Legat (2008), The effects of resolving the Canadian Arctic Archipelago in a finite element sea ice model, *Ocean Modelling*, *24*(3-4), 140–152.

Lindsay, R. W., and J. Zhang (2005), The Thinning of Arctic Sea Ice, 1988 2003 : Have We Passed a Tipping Point ?, *Journal of Climate*, *18*, 4879–4894.

Lindsay, R. W., and J. Zhang (2006), Arctic Ocean Ice Thickness : Modes of Variability and the Best Locations from Which to Monitor Them*, *Journal of Physical Oceanography*, *36*, 496–506, doi :10.1175/JPO2861.1.

Lique, C., A. M. Treguier, M. Scheinert, and T. Penduff (2009), A model-based study of ice and freshwater transport variability along both sides of Greenland., *Climate Dynamics*, *33*, doi :10.1007/s0038200805107.

Lique, C., A. M. Treguier, B. Blanke, and N. Grima (2010), On the origins of water masses exported along both sides of Greenland : A Lagrangian Model Analysis., *Journal of Geophysical Research*, *115(C05019)*, doi :10.1029/2009JC005316.

Loder, J. W., B. Petrie, and G. D. Gawarkiewicz (1998), The coastal Ocean off North-Eastern North America : A large-scale view., in *The Sea, vol. 11.*, pp. 105–133, Wiley, New York.

Loeng, H., V. Ozhigin, and B. Adlandsvik (1997), Water fluxes trough the Barents Sea., *ICES Journal of Marine Science*, *54*, 310–317.

Madec, G. (2008), NEMO Ocean engine, *Note du pôle modélisation 27*, Institut Pierre-Simon Laplace (IPSL).

Madec, G., P. Delecluse, M. Imbard, and C. Levy (1998), OPA 8.1 Ocean General Circulation Model reference manual, *Note du pôle modélisation 11*, Institut Pierre-Simon Laplace.

Makshtas, A. P., S. V. Shoutilin, and E. L. Andreas (2003), Possible dynamic and thermal causes for the recent decrease in sea ice in the Arctic Basin, *Journal of Geophysical Research*, *108*(3232).

Manabe, S., and R. J. Stouffer (1980), Sensitivity of a global climate model to an increase of CO2 concentration in the atmosphere, *Journal of Geophysical Research*, *85*, 5529–5554, doi :10.1029/JC085iC10p05529.

Marsh, R., D. DesbruyÃ¨res, J. L. Bamber, B. A. De Cuevas, A. C. Coward, and Y. Aksenov (2010), Short-term impacts of enhanced Greenland freshwater fluxes in an eddy-permitting ocean model, *Ocean Science*, *6*, 749–760.

Maslowski, W., D. Marble, W. Walczowski, U. Schauer, J. L. Clement, and A. J. Semtner (2004), On climatological mass, heat, and salt transports trough the Barents Sea and Fram Strait from a pan-Arctic coupled ice-ocean model simulation., *Journal of Geophysical Research*, *109*, C03032, doi :10.1029/2001JC001039.

Mauritzen, C. (1996), Production of dense overflows waters feeding the North Atlantic across the Greenland–Scotland Ridge. Part 1 : Evidence for a revised circulation scheme., *Deep Sea Research Part I*, *43*, 769–806.

McPhee, M. G., A. Proshutinsky, J. H. Morison, M. Steele, and M. B. Alkire (2009), Rapid change in freshwater content of the Arctic Ocean, *Geophysical Research Letter*, *36*(L10602), doi :10.1029/2009GL037525.

Melling, H., T. A. Agnew, K. K. Falkner, D. A. Greenberg, C. M. Lee, A. Münchow, B. Petrie, S. J. Prinsenberg, R. M. Samelson, and R. A. Woodgate (2008), Freshwater fluxes via Pacific and Arctic outflows across the Canadian Polar shelf, in *Arctic–Subarctic Ocean Fluxes*, edited by R. R. Dickson, J. Meincke, and P. Rhines, pp. 193–247, Springer.

Meredith, M., K. Heywood, P. Dennis, L. Goldso, R. White, E. Fahrbach, U. Schauer, and S. Osterhus (2001), Freshwater fluxes through the western Fram Strait., *Geophysical Research Letters*, *28*, 1615–1618.

Molines, J. M., B. Barnier, T. Penduff, L. Brodeau, A. M. Treguier, S. Theetten, and G. Madec (2006), Definition of the interannual experiment ORCA025-G70, 1958-2004., *LEGI report LEGI-DRA-2-11-2006*, available at www.ifremer.fr/lpo/drakkar.

Nansen, F. (1902), The Norwegian North Polar Expedition 1893–1896, Scientific results., *Oceanography of the north polar basin.*, Longmans, Green, Toronto, Canada.

Nazarenko, L., G. Holloway, and N. Tausnev (1998), Dynamics of transport of 'Atlantique signature' in the Arctic Ocean., *Journal of Geophysical Research*, *103*, 31,003–31,015.

Ogi, M., I. G. Rigor, M. G. McPhee, and J. M. Wallace (2008), Summer retreat of Arctic sea ice : Role of summer winds, *Geophysical Research Letter*, *35*, doi : 10.1029/2008GL035672.

Ogi, M., K. Yamazaki, and J. M. Wallace (2010), Influence of winter and summer surface wind anomalies on summer Arctic sea ice extent, *Geophysical Research Letter*, *37*(L07701).

Orvik, K. A., and P. Niiler (2002), Major pathways of Atlantic water in the northern North Atlantic and Nordic Seas toward Arctic, *Geophysical Research Letter*, *29*(19).

Ostlund, H. G., and G. Hut (1984), Arctic Ocean water mass balance from isotope data., *Journal of Geophysical Research*, *89*, 6373–6381.

Ostlund, H. G., G. Possnert, and J. H. Swift (1987), Ventilation rate of the deep Arctic Ocean from Carbon 14 data., *Journal of Geophysical Research*, *92*, 3769–3777.

Parkinson, C. L., and D. J. Cavalieri (2008), Arctic sea ice variability and trends, 1979-2006, *Journal of Geophysical Research*, *113*(C12).

Parkinson, C. L., D. J. Cavalieri, P. Gloersen, H. J. Zwally, and J. C. Comiso (1999), Arctic sea ice extents, areas, and trends, 1978–1996., *Journal of Geophysical Research*, *104(C9)*, 20,837–20,856.

Partington, K., T. Flynn, D. Lamb, C. Bertoia, and K. Dedrick (2003), Late twentieth century Northern Hemisphere sea-ice record from U.S. National Ice Center ice charts, *Journal of Geophysical Research*, *108*, doi :10.1029/2002JC001623.

Penduff, T., J. Le Sommer, B. Barnier, A.-M. Treguier, J.-M. Molines, and G. Madec (2007), Influence of numerical schemes on current-topography interactions in 1/4 global Ocean simulations., *Ocean Science*, *3*, 509–524.

Perovich, D. K., J. A. Richter-Menge, K. F. Jones, and B. Light (2008), Sunlight, water, and ice : Extreme Arctic sea ice melt during the summer of 2007, *Geophysical Research Letter*, *35*, doi :10.1029/2008GL034007.

Peterson, B. J., R. M. Holmes, J. W. McClelland, C. J. Vorosmarty, R. B. Lammers, A. I. Shiklomanov, and S. Rahmstorf (2002), Increasing river discharge to the Arctic Ocean., *Science*, *298*, 2171–2173.

Peterson, B. J., J. McClelland, R. Curry, R. M. Holmes, J. E. Walsh, and K. Aagaard (2006), Trajectory shifts in the Arctic and Subarctic freshwater cycle, *Science*, pp. 1061–1066, doi :10.1126/science.1122593.

Pham, D. T., J. Verron, and M. C. Roubaud (1998), A singular evolutive extended Kalman filter for data assimilation in oceanography., *Journal of Marine Systems*, *16*, 323–340.

Pickard, G. L., and W. J. Emery (1990), Arctic sea, in *Descriptive Physical Oceanography : An Introduction.*, pp. 219–235, Elsevier.

Polyakov, I., L. Timokhov, I. Dmitrenko, V. Ivanov, H. Simmons, A. Beszczynska-Möller, R. Dickson, E. Fahrbach, L. Fortier, J.-C. Gascard, J. Hölemann, N. P. Holliday, E. Hansen, C. Mauritzen, J. Piechura, R. Pickart, U. Schauer, M. Steele, and W. Walczowski (2007), Observational Program Tracks Arctic Ocean Transition to a Warmer State, *Eos Trans. AGU*, *88*, 398–399.

Polyakov, I. V., A. Beszczynska, E. C. Carmack, I. A. Dmitrenko, E. Fahrbach, I. E. Frolov, R. Gerdes, E. Hansen, J. Holfort, V. V. Ivanov, M. A. Johnson, M. Karcher, F. Kauker, J. Morison, K. A. Orvik, U. Schauer, H. L. Simmons, O. Skagseth, V. T. Sokolov, M. Steele, L. A. Timokhov, D. Walsh, and J. E. Walsh (2005), One more step toward a warmer Arctic., *Geophysical Research Letter*, *32*, doi :10.1029/2005GL023740.

Polyakov, I. V., V. A. Alexeev, G. I. Belchansky, I. A. Dmitrenko, V. V. Ivanov, S. A. Kirillov, A. A. Korablev, M. Steele, L. A. Timokhov, and I. Yashayaev (2008), Arctic Ocean Freshwater Changes over the Past 100 Years and Their Causes, *Journal of Climate*, *21*, 364–384, doi :10.1175/2007JCLI1748.1.

Proshutinsky, A., M. Steele, J. Zhang, G. Holloway, N. Steiner, S. Häkkinen, D. Holland, R. Gerdes, C. Köberle, M. Karcher, M. Johnson, W. Maslowski, W. Walczowski, W. Hibler, and J. Wang (2001), Multinational effort studies differences among Arctic Ocean models., *Eos Trans. AGU*, *82(51)*, 643–644.

Proshutinsky, A., J. Yang, R. Krishfield, R. Gerdes, M. Karcher, F. Kauker, C. Köberle, S. Häkkinen, W. Hibler, D. Holland, M. Maqueda, G. Holloway, E. Hunke, W. Maslowski, M. Steele, and J. Zhang (2005), Arctic Ocean Study : Synthesis of Model Results and Observations., *Eos Trans. AGU*, *86(40)*, 368.

Proshutinsky, A., R. Krishfield, M.-L. Timmermans, J. Toole, E. Carmack, F. McLaughlin, W. J. Williams, S. Zimmermann, M. Itoh, and K. Shimada (2009), Beaufort Gyre freshwater reservoir : State and variability from observations., *Journal of Geophysical Research*, *114* (C00A10), doi :10.1029/2008JC005104.

Proshutinsky, A. Y., and M. A. Johnson (1997), Two circulation regimes of the wind-driven Arctic Ocean, *Journal of Geophysical Research*, *102*, 12,493–12,514.

Proshutinsky, A. Y., R. H. Bourke, and F. A. McLaughlin (2002), The role of the Beaufort Gyre in Arctic climate variability : seasonal to decadal limate scales, *Geophysical Research Letters*, *29(23)*, doi :10.1029/2002GL015847.

Rigor, I. G., R. L. Colony, and S. Martin (2000), Variations in Surface Air Temperature Observations in the Arctic, 1979-97., *Journal of Climate*, *13*, 896–914.

Rigor, I. G., J. M. Wallace, and R. L. Colony (2002), Response of sea ice to the Arctic Oscillation., *Journal of Climate*, *15*, 2648–2663.

Rothrock, D. A., and J. Zhang (2005), Arctic Ocean sea ice volume : What explains its recent depletion ?, *Journal of Geophysical Research*, *110*(C9).

Rothrock, D. A., Y. Yu, and G. Maykut (1999), Thinning of the Arctic sea-ice cover., *Geophysical Research Letters*, *26*, 3469–3472.

Rothrock, D. A., R. Kwok, and D. Groves (2000), Satellite views of the Arctic Ocean freshwater balance., in *The freshwater budget of the Arctic Ocean*, edited by E. L. Lewis, pp. 533–588, Kluwer Academics.

Rothrock, D. A., J. Zhang, and Y. Yu (2003), The Arctic ice thickness anomaly of the 1990s : A consistent view from observations and models, *Journal of Geophysical Research*, *108*.

Rudels, B., E. P. Jones, L. G. Anderson, and G. Kattner (1994), On the intermediate depth waters of the Arctic Ocean., in *The Polar Oceans and their role in shaping the global environment*, edited by O. M. Johannessen, R. Muench, and J. Overland, pp. 33–46, Geophysical Monograph 85.

Santer, B. D., T. M. L. Wigley, J. S. Boyle, D. J. Gaffen, J. J. Hnilo, D. Nychka, D. E. Parker, and K. E. Taylor (2000), Statistical significance of trends and trend differences in layer-average atmospheric temperature time series, *Journal of Geophysical Research*, *105*, 7337–7356, doi :10.1029/1999JD901105.

Schauer, U., H. Loeng, B. Rudels, V. K. Ozhigin, and W. Dieck (2002), Atlantic Water flow through the Barents and Kara Seas., *Deep Sea Research Part I*, *49*, 2281–2298.

Schauer, U., E. Fahrbach, S. Osterhus, and G. Rohardt (2004), Arctic warming through the Fram Strait : Oceanic heat transport from 3 years of measurements., *Journal of Geophysical Research*, *109*, doi :10.1029/2003JC001823.

Schauer, U., A. Beszczynska-Möller, W. Walczowski, E. Fahrbach, J. Piechura, and E. Hansen (2008), Variation of measured heat flow through the Fram Strait between 1997 and 2006., in *Arctic–Subarctic Ocean Fluxes*, edited by R. R. Dickson, J. Meincke, and P. Rhines, pp. 385–404, Springer.

Schlichtholz, P., and M. N. Houssais (1999), An inverse modelling study in Fram Strait. part 1 : dynamics and circulation., *Deep Sea Research Part II*, *46*, 1083–1135.

Schlosser, P., D. Bauch, R. Fairbanks, and G. Bönisch (1994), Arctic river runoff : mean residence time on the shelves and in the halocline., *Deep Sea Research Part I*, *41*, 1053–1068.

Schlosser, P., J. H. Swift, D. Lewis, and S. L. Pfirman (1995), The role of the large-scale Arctic Ocean circulation in the transport of contaminants., *Deep Sea Research Part II*, *42(6)*, 1341–1367.

Schweiger, A. J., J. Zhang, R. W. Lindsay, and M. Steele (2008), Did unusually sunny skies help drive the record sea ice minimum of 2007 ?, *Geophysical Research Letter*, *35*, doi :10.1029/2008GL033463.

Sciremammano, F. (1979), A suggestion for the presentation of correlations and their significance levels., *Journal of Physical Oceanography*, *9*, 1273–1276.

Serreze, M. C., and J. A. Francis (2006), The Arctic on the fast track of change, *Weather*, *61*, 65–69.

Serreze, M. C., J. A. Maslanik, T. A. Scambos, F. Fetterer, J. Stroeve, K. Knowles, C. Fowler, S. Drobot, R. G. Barry, and T. M. Haran (2003), A record minimum Arctic sea ice extent and area in 2002, *Geophysical Research Letter*, *30*(3), doi : 10.1029/2002GL016406.

Serreze, M. C., A. P. Barrett, A. G. Slater, R. A. Woodgate, R. B. Lammers, M. Steele, R. Moritz, M. Meredith, and C. M. Lee (2006), The large-scale freshwater cycle of the Arctic, *Journal of Geophysical Research*, *111*, C11010, doi :10.1029/2005JC003424.

Simonsen, K., and P. Haugan (1996), Heat budgets of the Arctic mediterranean and sea surface heat flux parameterizations for the Nordic Seas., *Journal of Geophysical Research*, *101*, 6553–6576.

Singarayer, J. S., and J. L. Bamber (2003), EOF analysis of three records of sea-ice concentration spanning the last 30 years, *Geophysical Research Letter*, *30*(5), doi : 10.1029/2002GL016640.

Skagseth, Ø. (2008), Recirculation of Atlantic Water in the western Barents Sea, *Geophysical Research Letter*, *35*, doi :10.1029/2008GL033785.

Smethie, W. M., P. Schlosser, G. Bönisch, and T. S. Hopkins (2000), Renewal and circulation of intermediate waters in the Canadian Basin observed on the SCICEX 96 cruise., *Journal of Geophysical Research*, *105*, 1105–1121.

Spall, M. A., R. S. Pickart, P. S. Fratantoni, and A. J. Plueddemann (2008), Western Arctic shelbreak eddies : Formation and transport., *Journal of Physical Oceanography*, *38(8)*, 1644–1668.

Speich, S., B. Blanke, and G. Madec (2001), Warm and cold routes of an OGCM thermohaline conveyor belt., *Geophysical Research Letter*, *28(2)*, 311–314.

Spreen, G., S. Kern, D. Stammer, and E. Hansen (2009), Fram Strait sea ice volume export estimated between 2003 and 2008 from satellite data, *Geophysical Research Letter*, *36*(L19502), doi :10.1029/2009GL039591.

Steele, M., and T. Boyd (1998), Retreat of the cold halocline layer in the Arctic Ocean., *Journal of Geophysical Research*, *103*, 10,419–10,436, doi :10.1029/98JC00580.

Steele, M., and W. Ermold (2004), Salinity trends on the Siberian shelves., *Geophysical Research Letter*, *31*(L24308), doi :10.1029/2004GL021302.

Steele, M., D. Thomas, and D. Rothrock (1996), A simple model study of the Arctic Ocean freshwater balance, 1979–1985., *Journal of Geophysical Research*, *101*, 20,833–20,848.

Steele, M., R. Morley, and W. Ermold (2001a), PHC : a global ocean hydrography with a high quality Arctic Ocean., *Journal of Climate*, *14*, 2079–2087.

Steele, M., W. Ermold, S. Häkkinen, D. Holland, G. Holloway, M. Karcher, F. Kauker, W. Maslowski, N. Steiner, and J. Zhang (2001b), Adrift in the Beaufort Gyre : A Model Intercomparison., *Geophysical Research Letters*, *28*, 2935–2938.

Steele, M., J. Morison, W. Ermold, I. Rigor, M. Ortmeyer, and K. Shimada (2004), Circulation of summer Pacific halocline water in the Arctic Ocean., *Journal of Geophysical Research*, *109*, doi :10.1029/2003JC002009.

Steele, M., W. Ermold, and J. Zhang (2008), Arctic Ocean surface warming trends over the past 100 years, *Geophysical Research Letter*, *35*(L02614).

Steiner, N., G. Holloway, R. Gerdes, S. Häkkinen, D. Holland, M. Karcher, F. Kauker, W. Maslowski, A. Proshutinsky, M. Steele, and J. Zhang (2004), Comparing modeled streamfunction, heat and freshwater content in the Arctic Ocean., *Ocean Modelling*, *6*, 265–284.

Stroeve, J., M. M. Holland, W. Meier, T. Scambos, and M. Serreze (2007), Arctic sea ice decline : Faster than forecast., *Geophysical Research Letter*, *34*, doi : 10.1029/2007GL029703.

Stroeve, J., A. Frei, J. McCreight, and D. Ghatak (2008), Arctic sea-ice variability revisited, *Annals of Glaciology*, *48*, 71–81.

Stroeve, J. C., M. C. Serreze, F. Fetterer, T. Arbetter, W. Meier, J. Maslanik, and K. Knowles (2005), Tracking the Arctic's shrinking ice cover : Another extreme September minimum in 2004, *Geophysical Research Letter*, *32*, doi :10.1029/2004GL021810.

Swift, J. H., K. Aagaard, L. Timokhov, and E. G. Nikiforov (2005), Long-term variability of Arctic Ocean waters : Evidence from a reanalysis of the EWG data set., *Journal of Geophysical Research*, *110*, C03012, doi :10.1029/2004JC002312.

Taylor, J. R., K. K. Falkner, U. Schauer, and M. Meredith (2003), Quantitative considerations of dissolved Barium as a tracer in the Arctic Ocean., *Journal of Geophysical Research*, *108*, doi :10.1029/2002JC001635.

Testut, C., P. Brasseur, J. Brankart, and J. Verron (2003), Assimilation of sea-surface temperature and altimetric observations during 1992–1993 into an eddy permitting primitive equation model of the North Atlantic Ocean, *Journal of Marine Systems*, *40*, 291–316.

The DRAKKAR group (2007), Eddy-permitting Ocean circulation hindcasts of past decades., *CLIVAR exchanges*, *42*.

Thiebaux, J., E. Rogers, W. Wang, and B. Katz (2003), A New High-Resolution Blended Real-Time Global Sea Surface Temperature Analysis, *Bull. Am. Met. Soc.*, *84*, 645–656.

Thomas, D., S. Martin, D. Rothrock, and M. Steele (1996), Assimilating satellite concentration data into an Arctic sea ice mass balance model, 1979–1985., *Journal of Geophysical Research*, *101*, 20,849–20,868.

Thompson, D. W. J., and J. M. Wallace (1998), The Arctic Oscillation signature in the wintertime geopotential height and temperature fields., *Geophysical Research Letter*, *25*, 1297–1300.

Timmermann, R., H. Goosse, G. Madec, T. Fichefet, C. Ethe, and V. Duliere (2005), On the representation of high latitude processes in the ORCA-LIM global coupled sea ice-ocean model., *Ocean Modelling*, *8*, 175–201.

Tranchant, B., C.-E. Testut, L. Renault, N. Ferry, F. Birol, and P. Brasseur (2008), Expected impact of the future SMOS and Aquarius Ocean surface salinity missions in the Mercator Ocean operational systems : New perspectives to monitor ocean circulation., *Remote Sensing of Environment*, *112*, 1476–1487.

Treguier, A. M., S. Theetten, E. P. Chassignet, T. Penduff, R. Smith, L. Talley, J. O. Beismann, and C. Boning (2005), The North Atlantic subpolar gyre in four high-resolution models., *Journal of Physical Oceanography*, *35*, 757–774.

Treguier, A. M., C. Gourcuff, P. Lherminier, H. Mercier, B. Barnier, G. Madec, J. Molines, T. Penduff, L. Czeschel, and C. Böning (2006), Internal and forced variability along a section between Greenland and Portugal in the CLIPPER Atlantic model., *Ocean Dynamics*, *56*, 568–580.

Trenberth, K. E., and J. M. Caron (2001), Estimates of Meridional Atmosphere and Ocean Heat Transports., *Journal of Climate*, *14*, 3433–3443.

Troccoli, A., and P. Kallberg (2004), Precipitation correction in the ERA–40 reanalysis., *ERA-40 Project Report Series 13*.

Tsukernik, M., C. Deser, M. Alexander, and R. Tomas (2010), Atmospheric forcing of Fram Strait sea ice export : a closer look, *Climate Dynamics*, doi :10.1007/s00382-009-0647-z.

Våge, K., R. S. Pickart, V. Thierry, G. Reverdin, C. M. Lee, B. Petrie, T. A. Agnew, A. Wong, and M. H. Ribergaard (2009), Surprising return of deep convection to the subpolar North Atlantic Ocean in winter 2007–2008., *Nature Geoscience*, *2*, doi : 10.1038/NGEO382.

Valdivieso Da Costa, M., and B. Blanke (2004), Lagrangian methods for flow climatologies and trajectory error assessment., *Ocean Modelling*, *6*, 335–358.

Vinje, T. (2001), Fram Strait ice fluxes and atmospheric circulation : 1950–2000, *Journal of Climate*, *14*, 3508–3517.

Wadhams, P., and N. R. Davis (2000), Further evidence of ice thinning in the Arctic Ocean, *Geophysical Research Letter*, *27*, 3973–3976.

Wadley, M. R., and G. R. Bigg (2002), Impact of flow through the Canadian Archipelago and Bering Strait on the North Atlantic and Arctic circulation : An ocean modelling study., *Quarterly Journal of the Royal Meteorological Society*, *128*(585), 2187–2203.

Walsh, J. E., and C. M. Johnson (1979), An Analysis of Arctic Sea Ice Fluctuations, 1953–77., *Journal of Physical Oceanography*, *9*(3).

White, D., L. Hinzman, L. Alessa, J. Cassano, M. Chambers, K. Falkner, J. Francis, W. J. Gutowski, M. Holland, R. M. Holmes, H. Huntington, D. Kane, A. Kliskey, C. Lee, J. McClelland, B. Peterson, T. S. Rupp, F. Straneo, M. Steele, R. Woodgate, D. Yang, K. Yoshikawa, and T. Zhang (2007), The Arctic freshwater system : Changes and impacts, *Journal of Geophysical Research*, *112*(G04S54), doi :10.1029/2006JG000353.

Woodgate, R. A., and K. Aagaard (2005), Revising the Bering Strait freshwater flux into the Arctic Ocean., *Geophysical Research Letters*, *32*, L02602, doi : 10.1029/2004GL021747.

Woodgate, R. A., E. Fahrbach, and G. Rohardt (1999), Structure and transports of the East Greenland Current at 75 N from moored current meters., *Journal of Geophysical Research*, *104*, 18,059–18,072.

Woodgate, R. A., K. Aagaard, and T. J. Weingartner (2005), Monthly temperature, salinity, and transport variability of the Bering Strait through flow., *Geophysical Research Letters*, *32*, L04601, doi :10.1029/2004GL021880.

Woodgate, R. A., K. Aagaard, and T. J. Weingartner (2006), Interannual changes in the Bering Strait fluxes of volume, heat and freshwater between 1991 and 2004., *Geophysical Research Letters*, *33*, L15609, doi :10.1029/2006GL026931.

Wu, P., R. Wood, and P. Stott (2004), Does the recent freshening trend in the North Atlantic indicate a weakening circulation ?, *Geophysical Research Letter*, *31*(L02301), doi :10.1029/2003GL018584.

Wunsch, C. (2005), The total Meridional Heat Flux and Its Oceanic and Atmospheric Partition., *Journal of Climate*, *18*, 4374–4380.

Yashayaev, I., and J. W. Loder (2009), Enhanced production of Labrador Sea Water in 2008, *Geophysical Research Letter*, *36*(L01606), doi :10.1029/2008GL036162.

Zhang, J., D. Rothrock, and M. Steele (2000), Recent Changes in Arctic Sea Ice : The Interplay between Ice Dynamics and Thermodynamics., *Journal of Climate*, *13*, 3099–3114.

Zhang, J., R. Lindsay, M. Steele, and A. Schweiger (2008), What drove the dramatic retreat of Arctic sea ice during summer 2007, *Geophysical Research Letter*, *35*(L11505), doi :10.1029/2008GL034005.

Zhang, X., M. Ikeda, and J. E. Walsh (2003), Arctic sea ice and freshwater changes driven by the atmospheric leading mode in a coupled sea ice-ocean model., *Journal of Climate*, *16(13)*, 2159–2177.

Thèse de Doctorat
de l'Université de Bretagne Occidentale

Étude des échanges entre l'Océan Arctique et l'Atlantique Nord : Origine, Variabilité et Impact sur les mers Nordiques.

Camille Lique

RESUME

C'est sans doute en Arctique que le changement climatique est le plus visible, et semble affecter toutes les composantes du système Arctique, et notamment ses bilans d'eau douce et de chaleur. Alors que l'on s'attend à ce que le signal d'un changement local en Arctique ait son impact climatique le plus important lorsqu'il est exporté au sud d'un coté ou de l'autre du Groenland vers les mers subarctiques, où il peut moduler l'intensité de la circulation thermohaline, l'objectif de cette thèse est donc d'étudier les échanges de volume, de chaleur, d'eau douce et de glace de l'Océan Arctique vers l'Atlantique Nord.

Tout d'abord, une simulation réaliste des années 1958 à 2002 basée sur un modèle global couplé glace/océan est utilisée pour étudier la variabilité du bilan d'eau douce en Arctique, afin de comprendre quelle composante de ce bilan contrôle les variations du contenu halin du bassin. On s'intéresse également à la variabilité des exports d'eau douce vers l'Atlantique Nord, et on montre que les exports d'eau douce vers l'Atlantique sont contrôlés par des mécanismes différents de part et d'autre du Groenland : dans les détroits canadiens, le transport de volume domine la variabilité, alors que salinité et courants contribuent à la variabilité dans le détroit de Fram. Par la suite, une réanalyse océanique des années récentes nous permet d'explorer les conséquences pour le contenu halin de l'Arctique du minimum record de l'extension de glace de l'été 2007.

Une méthode numérique originale est ensuite utilisée pour comprendre l'origine des masses d'eau qui sont exportées de l'Arctique vers l'Atlantique Nord. On effectue ainsi une analyse lagrangienne qualitative à partir des sorties 3D mensuelles climatologiques d'un modèle global couplé glace/océan à haute résolution, qui permet de quantifier les contributions relatives des différentes branches de circulation à ces exports, ainsi que les échelles de temps et les transformations de masses d'eau associées. Un schéma complet de la circulation dans le bassin Arctique est ainsi proposé, et nous soulignons le rôle clé de la mer de Barents pour les transformations des eaux d'origine Atlantique.

Enfin, nous examinons l'influence relative des différents forçages atmosphériques (vent, flux de chaleur et halins) sur les variations du volume de glace en Arctique. Des expériences de sensibilité sont réalisées à l'aide d'un modèle régional de l'Arctique et l'Atlantique Nord, permettant de mieux comprendre les distributions spatiales et temporelles des contributions des différents forçages atmosphériques.

MOTS-CLES

Océan Arctique - Bilan d'eau douce - Flux d'eau douce - Glace de mer - Modèle numérique - Analyse Lagrangienne - Forçages atmosphériques.

Echanges between the Arctic and the North Atlantic : Origin, Variability and Impact on the Nordic Seas.

Camille Lique

ABSTRACT

While perhaps the most obvious, ice retreat is just one aspect of a changing Arctic system. The Arctic Ocean is also undergoing unprecedented modifications, that mostly affect its heat and freshwater budgets. As the signal of Arctic change is expected to have its major climatic impact by reaching south the subarctic seas, on either side of Greenland, to modulate the Atlantic thermohaline circulation, the objective of this thesis is to investigate the variability of the exports of volume, heat, freshwater and sea-ice from the Arctic Ocean to the North Atlantic.

First, a realistic simulation from 1958 to 2002 run with a global ocean/sea-ice model is used to investigate some aspects of the variability of the Arctic freshwater budget, trying to understand which component of the balance is responsible for the variability of the Arctic freshwater content. We also examine the variability of the freshwater exports to the North Atlantic and we find that this variability is controlled differently on both sides of Greenland : whilst freshwater transport variations across Davis Strait are completely determined by the variations of the total volume flux, the salinity variations due to the ice ocean flux north of Greenland are responsible for a significant part of the freshwater export variability through Fram Strait. Afterward, a simulation run with a fully assimilated model of the very recent period is used to explore the possible consequences of the 2007 sea ice extent minimum on the Arctic Ocean freshwater content.

Then, the origins of the water masses exported from the Arctic to the North Atlantic along both sides of Greenland are investigated, using an original numerical method. A quantitative Lagrangian analysis is applied to the monthly climatological 3D output of a global ocean/sea-ice high resolution model. It allows quantification of the different branches of the export to the North Atlantic, as well as related timescales and water mass transformations. A complete and coherent scheme of circulation for the Arctic is proposed, and the role of the Barents Sea for the transformation of the Atlantic inflow is emphasized.

Last, we examine the relative influences of the different atmospheric fields (wind stress, heat and salt flux) on the variability of the Arctic sea ice volume. Sensitivity experiments run with a regional Arctic/North Atlantic model allow to investigate the spatial and temporal distributions of these influences.

KEY-WORDS

Arctic Ocean - Freshwater budget - Freshwater flux - Sea ice - Numerical model - Lagrangian analysis - Atmospheric forcing.